UNIVERSITÉ DE MONTRÉAL

PHOSPHORUS TREATMENT BY STEEL SLAG FILTERS MODELLING OF REMOVAL MECHANISMS AND APPLICATION FOR PHOSPHORUS REMOVAL FROM SEPTIC TANK EFFLUENTS

DOMINIQUE CLAVEAU-MALLET

DÉPARTEMENT DES GÉNIES CIVIL, GÉOLOGIQUE ET DES MINES

ÉCOLE POLYTECHNIQUE DE MONTRÉAL

THÈSE PRÉSENTÉE EN VUE DE L'OBTENTION

DU DIPLÔME DE PHILOSOPIAE DOCTOR

(GÉNIE CIVIL)

JUIN 2017

UNIVERSITÉ DE MONTRÉAL

ÉCOLE POLYTECHNIQUE DE MONTRÉAL

Cette thèse intitulée :

PHOSPHORUS TREATMENT BY STEEL SLAG FILTERS MODELLING OF REMOVAL MECHANISMS AND APPLICATION FOR PHOSPHORUS REMOVAL FROM SEPTIC TANK EFFLUENTS

présentée par : CLAVEAU-MALLET Dominique

en vue de l'obtention du diplôme de : Philosophiae Doctor

a été dûment acceptée par le jury d'examen constitué de :

M. BAUDRON Paul, Ph. D., président

M. COMEAU Yves, Ph. D., membre et directeur de recherche

M. COURCELLES Benoît, Doctorat, membre et codirecteur de recherche

M. CLÉMENT Bernard, Ph. D., membre et codirecteur de recherche

M. SMITH Scott, Ph. D., membre

M. PENN Chad J., Ph. D., membre externe

REMERCIEMENTS

Merci à mon directeur Yves Comeau pour m'avoir accueilli dans son équipe en 2009 et pour m'avoir permis de réaliser ce projet de doctorat. Merci plus particulièrement pour trois choses qui ont été importantes pour moi, d'abord la confiance qui m'a été portée et les opportunités de travailler sur des projets variés, ensuite la flexibilité parce que j'ai eu deux enfants durant mes études supérieures, et finalement l'opportunité d'aller au congrès WWTmod 2016. Ce congrès a eu une grande importance pour mon projet de doctorat et pour le développement de mon expertise.

Merci à mon codirecteur Benoît Courcelles d'avoir participé dans ce projet, plus particulièrement pour le développement des équations de précipitation dans le modèle. Mes réunions avec Benoît formaient des étapes de validation importantes, en plus de fournir de nouvelles stratégies de modélisation. Merci à mon codirecteur Bernard Clément qui a participé au projet pour la validation statistique des fonctions d'épuisement.

Merci à Philippe Pasquier, professeur en génie géologique, pour sa participation dans ce projet. En tant que membre de mon examen prédoctoral, Philippe a posé une question de modélisation géochimique pour une application de géothermie qui a grandement influencé le développement de mon modèle. De plus, sa participation dans l'élaboration de la méthode d'inversion pour la calibration des essais cinétiques s'est avérée essentielle. Merci à Fanny Eppner, étudiante au doctorat sous la supervision de Philippe Pasquier, avec qui j'ai eu plusieurs discussions sur la modélisation. Fanny a travaillé sur le développement d'un modèle thermo-hydro-géochimique pour la géothermie; son projet impliquait des défis qui étaient complémentaires au mien et c'était toujours intéressant et utile d'en discuter.

Merci à Étienne Boutet, Félix Lida et Serge Baillargeon, de la compagnie Bionest, pour leur participation dans ce projet. J'ai travaillé étroitement avec Bionest durant trois ans et le développement de mon modèle en a beaucoup profité. J'ai beaucoup apprécié l'ouverture d'esprit chez Bionest et la bonne collaboration entretenue, et c'était motivant de voir que mon travail pouvait mener au développement d'une technologie de traitement concrète.

Merci à Patricia Bove, étudiante à la maîtrise, avec qui j'ai travaillé étroitement de 2015 à 2017. J'ai partagé avec Patricia l'entretien et l'opération des essais de filtres à scories au laboratoire, puisqu'elle les utilisait pour son projet de neutralisation. J'ai également travaillé avec elle sur les

aspects de modélisation de son projet de maîtrise. Patricia est une collègue de travail agréable, intelligente et efficace. J'ai beaucoup apprécié travailler avec elle.

Merci aux techniciens de laboratoire qui ont contribué à ce projet. Merci à Denis Bouchard pour les analyses de phosphore et carbone, et pour son soutien technique dans toutes sortes de situations. Merci à Mélanie Bolduc et Jérôme Leroy pour leur soutien apporté au laboratoire. Merci à Manon Leduc pour les analyses de calcium et métaux. Merci aux étudiants et techniciens qui m'ont aidé à l'installation et au démantèlement de mes colonnes de scories : Sanaz Alizadeh, Xavier Lachapelle-Trouillard, Patricia Bove, Denis Bouchard, Sophie Levesque, Charles Élysée et Pierre-Antoine Maloin.

Merci aux collègues avec qui j'ai eu la chance de travailler de près ou de loin sur des projets de filtres à scories. Un merci spécial à Claire Dacquin, Simon Allaire, Simon Amiot, stagiaires de premier cycle, qui ont réalisé bon nombre d'essais cinétiques pour mon projet de doctorat. Merci également aux stagiaires qui ont réalisé des projets complémentaires à mon projet de doctorat; Brice Siroux (précipitation dans les champs d'infiltration), Aurore Bordier (précipitation dans les filtres à scories) et Alexandra Païs (précipitation dans les filtres à scories). Merci à Anna Staingart et Zakariae Anjab, étudiants à la maîtrise, qui ont réalisé des projets sur les filtres à scories qui m'ont aidé à développer mon modèle. Merci à Félix Lida et Patricia Bove, étudiants à la maîtrise, qui ont réalisé les travaux expérimentaux présentés dans l'article #1 et dans la section sur la neutralisation, respectivement. Merci à Margit-Kõiv-Vainik, chercheure invitée, pour m'avoir invitée à participer aux projets des Bobines (article #4), et pour les nombreuses discussions sur les filtres à scories et matériaux réactifs. Merci à Marie Ferland pour les discussions et le développement de l'expertise sur les essais de traceur. Merci à Dominic Vallerand avec qui j'ai travaillé sur la rédaction d'un article de transfert sur les filtres à scories dans la revue Vecteur Environnement. Merci à Marc-André Labelle pour les discussions dans les réunions de laboratoire. Merci à Cristian Neagoe, Zhanna Grebenshchykova et Xavier Lachapelle-Trouillard pour les discussions sur le projet PhytoValP.

Merci à mes collègues étudiants qui ont rendu la vie à Polytechnique très agréable : Marie Ferland, Marie-Laure De Boutray, Catherine Brosseau, Sanaz Alizadeh et Sophie Lévesque. Merci plus particulièrement à Sophie, qui partageait mon bureau avec ses sujets de discussion variés, et Sanaz, avec les *coffee break* qui brisaient le rythme rapide du quotidien.

Merci aux professeurs et étudiants gradués du programme de génie géologique pour les discussions du midi : Félix Gervais, Denis Marcotte, Michel Chouteau, Philippe Pasquier, Pierre Bédard, Paul Baudron, Manon Leduc, Jérôme Leroy, Fanny Eppner, Éric Chou, Pascale Brunet et Bernard Dusseault. J'ai toujours passé mes heures de dîner en génie géologique, j'aimais discuter de projets de ce domaine, je trouvais que ça maintenait mon esprit élargi tout en changeant de la routine du traitement des eaux, avec des gens sympathiques.

Merci à Manon Latour, agente aux dossiers étudiants, pour son aide dans toutes les étapes administratives de ce doctorat.

Merci à Jalal Hawari qui m'a aidé à pratiquer ma soutenance de thèse.

Merci au CRSNG pour avoir financé ma bourse d'étude, et aussi pour avoir financé le projet.

Finalement, merci à mon conjoint Mathieu Bélisle, qui m'a donné un soutien inconditionnel durant toute la durée de mes études supérieures, et à mes enfants Rosanne et Antoine, qui sont deux petits soleils.

RÉSUMÉ

Le premier objectif de cette thèse était de proposer un système de traitement du P incluant un filtre à scories intégré à une chaîne de traitement de fosse septique et élément épurateur. L'utilisation d'un filtre à scories en recirculation dans la fosse septique a été étudiée (article #1). Deux modes de recirculation ont été testés. Le meilleur système a été la recirculation du 2^{e} compartiment vers le 1er compartiment à 50% de recirculation, avec 4.2 et 1.9 mg P/L à l'effluent en P total et ortho-phosphates, respectivement. La cible de 1 mg /L à l'effluent n'a pas été atteinte, mais l'ajout du filtre à scories a permis la rétention de 79% du phosphore, comparativement à 29% sans filtre.

Le deuxième objectif de cette thèse était de proposer un modèle d'enlèvement du P dans les filtres à scories qui permette la prédiction de la longévité et de l'efficacité d'enlèvement par simulations numériques. Un programme de recherche incluant quatre projets a été entrepris. Dans le premier projet (article #2), des filtres à scories ont été opérés au laboratoire afin de caractériser leur utilisation potentielle pour le traitement d'un lixiviat minier. Une méthode préliminaire de caractérisation expérimentale des scories a été développée. Les résultats ont montré que la précipitation en hydroxyapatite et la croissance de cristaux étaient les mécanismes responsables de l'enlèvement du P. Dans le deuxième projet, un modèle numérique préliminaire incluant des équations pour l'épuisement des scories et la précipitation de l'hydroxyapatite a été développé (article #3). Les fonctions d'épuisement des scories ont été mesurées à partir d'essais cinétiques en flacon et des simulations numériques avec le logiciel PHREEQC ont été réalisées. Les résultats de simulation ont montré un comportement typique d'un filtre à scories, avec l'arrivée d'une percée (sans calibration expérimentale). Dans le troisième projet (article #4), le modèle numérique préliminaire a été validé en reproduisant des données expérimentales réelles. Pour ce faire, des simulations PHREEQC ont été réalisées et comparées avec les données d'un essai pilote de traitement d'effluent piscicole. L'épuisement des scories et le changement d'affluent ont été reproduits. Dans le quatrième projet (article #5), le modèle numérique préliminaire a été raffiné avec une équation pour la diffusion dans une barrière de précipités et des équations pour séparer la précipitation homogène et hétérogène. Des essais cinétiques ont été réalisés afin de raffiner la méthode de mesure des fonctions d'épuisement. Un essai de filtre à scories en colonne a été réalisé au laboratoire pour calibrer le modèle. Les simulations numériques réalisées avec le logiciel PHREEQC ont reproduit avec précision les résultats expérimentaux de phosphore et pH. Le modèle proposé P-Hydroslag pourrait être utilisé pour la conception de filtre à scories.

ABSTRACT

The first objective of this thesis was to propose a phosphorus treatment system based on a steel slag filter integrated to a septic tank-infiltration bed system. The use of a recirculating steel slag filter was studied in an experimental program (paper #1). Two recirculation modes with various recirculation ratios were tested. The best system was the one with a recirculation from the end to the inlet of the second compartment of a septic tank with a 50% recirculation ratio in the slag filter, achieving 4.2 and 1.9 mg P/L at the effluent for TP and o-PO_4, respectively. The 1 mg P/L level goal was not reached, but 79% of phosphorus was kept in the system, compared to 29% without the slag filter.

The second objective of this thesis was to propose a phosphorus removal mechanism model for steel slag filters usable to predict its efficiency and longevity by numerical simulations. A research program including four projects was realized. In the first project (paper #2), steel slag filters were operated in the laboratory to characterize their potential utilization to a mine leachate. A preliminary experimental slag characterization method was developed. Results showed that precipitation into hydroxyapatite and crystal growth following pH rise and oversaturation were mechanisms responsible for phosphorus removal.

In the second project, a preliminary numerical model including equations for slag exhaustion and hydroxyapatite precipitation was developed (paper #3). Slag exhaustion functions were measured by batch kinetic tests and numerical simulations were performed with the PHREEQC software. Simulation results showed a typical steel slag filter behavior, with a breakthrough curve (without experimental calibration). In the third project, (paper #4), the preliminary numerical model was validated by reproducing real experimental data. Simulations were realized with PHREEQC and they were compared with data from a pilot test of fish farm effluent treatment with steel slag filters. Slag exhaustion and influent changes were correctly reproduced by simulations.

In the fourth project (paper #5), the preliminary numerical model was refined with an equation for diffusion through a crystal barrier and equations for separating homogeneous and heterogeneous precipitation. Batch kinetic tests were performed to refine the measurement method of exhaustion functions. A steel slag filter experiment was realized in laboratory for model calibration. Numerical simulations conducted with PHREEQC reproduced with precision pH and ortho-phosphate experimental results. The proposed P-Hydroslag model could be used for design of steel slag filters.

TABLE OF CONTENTS

LIST OF TABLES

LIST OF FIGURES

LIST OF SYMBOLS AND ABBREVIATIONS

ADM1	Anaerobic digestion model number 1
ADR	Advection-diffusion-reaction
AFB	Aerated filter bed
ASM1	Activated sludge model 1 (ASM2, ASM2d and ASM3 are subsequent versions)
BF	Blast furnace
BOD_5	Biochemical oxygen demand after 5 days
BOF	Basic oxygen furnace
CAL	Calcite
CFD	Computational fluid dynamic
COD	Chemical oxygen demand
$CBOD_5$	Carbonaceous biochemical oxygen demand after 5 days
CSTR	Completely stirred tank reactor
EAF	Electric arc furnace
HAP	Hydroxyapatite
HAP_HE	Heterogeneous hydroxyapatite
HAP_HO	Homogeneous hydroxyapatite
HRT	Hydraulic retention time
HRT_V	Hydraulic retention time of voids
HRTVe	Efficient hydraulic retention time of voids
MDDEP	*Ministère du développement durable, de l'environnement et des parcs* (Ministry of Environment, Sustainable Development and Parks)
MON	Monetite
n	Porosity

OLR	Organic loading rate
o-PO_4	Ortho-phosphates
P	Phosphorus
SC	Slag column
SEM	Scanning electronic microscopy
SF	Sacrificial slag filter
SI	Saturation index
SS	Suspended solids
TCLP	Toxicity characteristic leaching procedure
TEM	Transmission electronic microscopy
TIC	Total inorganic carbon
TIS	Tanks in series
TKN	Total Kjeldahl nitrogen
TP	Total phosphorus
TSS	Total suspended solids
TW	Treatment wetland
VSS	Volatile suspended solids
XRD	X-ray diffraction

CHAPTER 1 INTRODUCTION

Objectives of the thesis

Phosphorus in wastewater is a major environmental concern. Very small phosphorus inputs in the environment is enough for perturbation of ecosystems and occurrence of eutrophication. One important consequence of phosphorus discharge is the formation of cyanobacteria in summer periods, as observed in Quebec's lakes in the last years (Blais, 2008). Phosphorus discharge in the environment originates from various sources, including agriculture, industry and domestic wastewater. In this project, focus is given to phosphorus in domestic wastewater from isolated or a few houses (autonomous or decentralized treatment, as opposed to centralized treatment with sewers and treatment plants). In Quebec, this type of effluent is typically treated with a septic tank followed by an infiltration bed. The number of septic tanks in Quebec province was estimated at 700 000 in 2002 (Radio-Canada, 2002).

Phosphorus removal in a septic-tank-infiltration-bed system is not regulated and this type of system was not initially designed or intended to remove phosphorus. Septic tanks and infiltration beds are not efficient for long term phosphorus removal, as high concentration (up to 5 mg P/L) were observed in the water table below an infiltration bed (Robertson, Schiff & Ptacek, 1998). Improving the phosphorus retention of such systems is the challenge addressed in this thesis. The proposed solution is through the use of steel slag filters.

Slag is a by-product from iron and steel mills (National Slag Association, 2009) available in various types, size or composition. Electric arc furnace (EAF) steel slag, a particular type of granular alkaline slag, can be used as reactive media for phosphorus capture. This principle was successfully applied in many studies (Barca *et al.*, 2013; Chazarenc *et al.*, 2008; Claveau-Mallet, Wallace, & Comeau, 2013; Drizo *et al.*, 2006; Kõiv *et al.*, 2016; Vohla *et al.*, 2011). For example, total phosphorus concentration as low as 0.1 mg P/L were reached for a fish farm effluent (Kõiv *et al.*, 2016). The main advantages of steel slag filters are their low capital and operating costs and their simplicity. Therefore, it would be interesting to use steel slag filters for septic tank effluent treatment. This technological challenge brings us to the first objective of this thesis.

OBJECTIVE 1: Propose a phosphorus treatment system based on a steel slag filter integrated to a septic-tank-infiltration-bed system. The system must fulfill the following criteria:

- Maximum total phosphorus effluent concentration of 1 mg P/L. This value was set from the Quebec discharge criteria for tertiary treatment systems (MDDEP, 2009b).
- Effluent total suspended solids (TSS) and carbonaceous biochemical oxygen demand ($CBOD_5$) must meet discharge criteria for a secondary treatment system (30 and 25 mg/L, respectively).
- Two-year longevity without any human intervention for septic tank and steel slag filter. This period corresponds to the required maintenance frequency for a septic tank receiving less than 3240 L/d of domestic wastewater in Quebec (MDDEP, 2009a).
- Low capital and operating costs. 500 $ (2017 CAD) per two years is the target cost.

As mentioned previously, steel slag filters were largely used in research studies for phosphorus treatment, but they are rarely used in full-scale projects. There are no regulations nor certifications regarding their utilization. One important issue preventing this is the wide efficiency variability reported by different teams who studied them (Vohla *et al.*, 2011). There is no clear consistent estimated P removal capacity of steel slag filter within studies and it is not possible to predict longevity and removal efficiency of the filter. A better understanding of phosphorus removal mechanisms in steel slag filters would help to elucidate this problem. The second objective of this thesis is related to this issue.

OBJECTIVE 2: Propose a phosphorus removal mechanism model for steel slag filters, including the following properties:

- The model must be compatible with a simulation software including features for transport in porous media, kinetic reactions and chemical equilibrium.
- The model should be based on slag dissolution and precipitation of phosphorus minerals, and on the evolution of filter hydraulic properties following the accumulation of precipitates. A preliminary model proposed by the candidate (Claveau-Mallet, Wallace, & Comeau, 2012) will be the starting point.
- The model must be usable for predictions by numerical simulations.

Content of this thesis

This paper-based thesis includes one published paper related to objective 1 and four papers related to objective 2 (three published and one submitted). The first chapter presents a literature review including one section for each objective. Literature review for objective 1 is focused on potential applications of steel slag filters in autonomous and decentralized treatment while that for objective 2 presents relevant modeling concepts for hydraulics and physicochemical treatment. Two chapters are focused on objective 1. Paper #1, presented in chapter 2, presents a complete study of septic tank upgrade with recirculating steel slag filters, followed by a general discussion on objective 1 in chapter 3. The complete reference for paper #1 is:

Claveau-Mallet, D., Lida, F. & Comeau, Y. (2015). Improving phosphorus removal of conventional septic tanks by a recirculating steel slag filter. *Water Quality Research Journal of Canada*, 50(3), 211-218.

Modeling of steel slag filters is the central point of this thesis from all points of view (experimental work, modeling work and original scientific contribution). Consequently, five chapters (5 to 9) are related to objective 2. Each chapter presents a significant step in the development of the P-Hydroslag model (summarized in Table 1.1). The modeling work of the thesis started from a previous modeling study including the description of involved phenomena. This work (not part of this thesis) was published previously:

Claveau-Mallet, D., Wallace, S. & Comeau, Yves. (2012). Model of phosphorus precipitation and crystal formation in electric arc furnace steel slag filters. *Environmental Science & Technology,* 46(3), p. 1465-1470.

A study of a mining leachate treatment by steel slag filter is presented as paper #2. Essential experimental observations and conclusions related to crystal growth, an important feature in this thesis progression, are presented. A first short-term batch test experimental procedure was developed for characterization of slag reactivity. Crystal growth observations and batch test protocol from this paper lead directly to the development of a formal model in subsequent papers. Understanding phosphorus removal mechanisms in steel slag filters was widened by consideration of metals and fluoride removal. The complete reference for paper #2 is:

Claveau-Mallet, D., Wallace, S. & Comeau, Y. (2013). Removal of phosphorus, metals and fluoride from a gypsum mining leachate using steel slag filters. *Water Research*, 47(4), 1512-1520.

A prototype model was developed and is presented as paper #3. This model version represents a significant advance compared to previous modeling work (article 2012) as numerical simulations were made possible by the translation of observed phenomena into equations. A critical part of this paper was the development of an experimental method for the characterization of slag kinetic parameters. This simple prototype model included precipitation rates for calcium phosphate and did not consider calcite precipitation. The complete reference for paper #3 is:

Claveau-Mallet, D., Courcelles, B. & Comeau, Y. (2014). Phosphorus removal by steel slag filters : modeling dissolution and precipitation kinetics to predict longevity. *Environmental Science & Technology*, 48(13), 7486-7493.

The prototype model presented in paper #3 was a promising step for steel slag filter modeling, but it did not present any calibration or validation with real data. Validation of the prototype model was realised by approximately reproducing experimental data from a pilot-scale steel slag filter, presented in a complementary paper (Chapter 7). Simulation results were not perfect but realistic enough to stimulate further model development work. The complete reference for the complementary paper is:

Kõiv, M., Mahadeo, K., Brient, S., **Claveau-Mallet, D**. & Comeau, Y. Treatment of fish farm sludge supernatant by aerated filter beds and steel slag filters – Effect of organic loading rate. Ecological Engineering, 94, p. 190-199.

Paper #4 presents the first version of the P-Hydroslag model in chapter 7. While paper #3 presented the development of a modeling tool, paper #4 presents the refinement of this modeling tool, its calibration and the demonstration of its prediction capacity. Paper #4 was submitted at the beginning of 2017:

Claveau-Mallet, D., Courcelles, B., Pasquier, P. & Comeau, Y. Numerical simulations with the P-Hydroslag model to predict phosphorus removal by steel slag filters. Submitted to Water Research on March 9th 2017 (manuscript number WR38848).

Table 1.1 : Content of chapters 5 to 9

Chapter	Involved model	Main outcomes
-	Preliminary modeling work	Conceptual model. Qualitative description of involved phenomena. **Work published prior to the Ph.D. program in Claveau-Mallet et al (2012).**
5	Preliminary modeling work	Important observations related to crystal growth. Development of a preliminary experimental procedure for slag behavior characterization. Practical application for mining leachate treatment. **Work presented as paper #2 in this thesis.**
6	Presentation of prototype model	Translation of conceptual model into mathematical equations. Development of a lab test for characterization of slag. Running numerical simulations and longevity prediction (without experimental calibration or validation). **Work presented as paper #3 in this thesis.**
7	Validation of prototype model	Approximate reproduction of experimental data using the prototype model. **Work presented as complementary paper in this thesis.**
8	Presentation and calibration of P-Hydroslag model	Refinement of the model's equations (diffusion barrier and precipitation into homogeneous and heterogeneous crystals). Translation of mathematical equations into a format compatible with general modeling frameworks in wastewater treatment. In-depth study of slag characterization method and precipitation constant calibration. Calibration of the model with experimental data of a filter. **Work presented as paper #4 in this thesis.**
9	General discussion	Critical view on objective 2 and accomplished work regarding model development steps, complementary studies. Next steps for the P-Hydroslag model development.

The General discussion chapter is focused on a critical view of work conducted regarding the development of a new model; and presents complementary studies related to industrial R&D process optimization and steel slag filter effluent neutralization. Several recommendations for further development steps are provided. The contribution of the Ph.D. candidate in each step leading to the five presented papers is shown in Table 1.2. All papers were written by the candidate, except the complementary paper in which the contribution was for the writing of sections related to modeling, reviewing, synthetizing work (important reduction of word count), and re-melting of Table 7.3, which presents preliminary full-scale design parameters for the treatment of supernatant of a freshwater fish farm sludge settling tank.

Table 1.2 : Relative contribution of the Ph.D. candidate in each paper

Paper	1	2	3	Complementary	4
Project and objectives definition	60%	40%	80%	10%	80%
Experimental work	10%	85%	75%	5%	75%
Simulation and modeling work	80%	75%	90%	95%	80%
Interpretation and literature review	60%	80%	90%	30%	90%
Paper writing	90%	90%	90%	30%	90%

CHAPTER 2 CONTEXT AND LITERATURE REVIEW

2.1 Applications of steel slag filters for phosphorus removal in autonomous decentralized treatment

2.1.1 Established scientific knowledge in steel slag filtration

Steel slag filters are passive systems formed of slag, a waste product from the iron and steel industry. Several types of slag are available and scientists started to use their reactive properties for water treatment applications in the 1980 (Yamada *et al.*, 1986). Slag size ranges from powder to big pebbles, but coarse sand and small gravel size offers a compromise between higher surface area and reduced clogging (Abderraja Anjab, 2009). Alkaline slag is a particular type of slag that allows high phosphorus removal. Electric arc furnace (EAF), blast furnace (BF) and basic oxygen furnace (BOF) slag are types of alkaline slag commonly used in steel slag filters. In this thesis, focus will be given to alkaline steel slag filters (phosphorus removal mainly by precipitation), in opposition with neutral slag filters (phosphorus removal mainly by adsorption).

Three types of alkaline slag study were conducted: short-term batch tests, column filter-tests and full-scale tests. Batch tests remain the more frequent and numerous type of reported studies (Chazarenc *et al.*, 2008). Column or full-scale tests, however, are more reliable and representative of the real behavior of a filter, mainly because of incorrect extrapolation of traditional batch-test interpretation methods to full-scale design. A selected list of recent column, pilot or full-scale studies is summarized in the next lines.

Column tests were conducted during four years by Baker *et al.* (1998), resulting in 90% phosphorus removal from a reconstituted wastewater with 3.3 mg P/L o-PO_4. The hydraulic retention time of voids of their columns was 0.9 day. Slag were also used directly in the ground for capture of contaminants from a septic tank (Smyth *et al.*, 2002). Buried filters were monitored for two years with achieved phosphorus concentration of 0.05 mg P/L. These authors also conducted column tests during eight years with still a 0.3 mg P/L effluent concentration at the end of operation. Steel slag filters were used for treatment of constructed wetlands effluent with a 75% phosphorus removal in one year (Chazarenc, Brisson, & Comeau, 2007). Slag columns were used in a pilot test for the treatment of a fish farm sludge supernatant with a 97% removal (Kõiv *et al.*, 2016). In

Estonia, hydrated oil shale ash (an alkaline material similar to slag) had not reached any sign of saturation in one year of operation and achieved 99% phosphorus removal over that period (Kõiv *et al*., 2010). In France, EAF and BOF slag were used in horizontal flow filters with HRT_V of 1 to 2 days for the treatment of a constructed wetland effluent with concentrations of total phosphorus of 8.5 mg P/L, o-PO_4 of 7.8 mg P/L and pH of 7.2 (Barca *et al.*, 2013).

Studies cited in the previous paragraph showed high phosphorus removal efficiency of steel slag filters, with effluent concentration generally below 1 mg P/L. For alkaline slag filters, phosphorus concentration is low when pH is above 10 (Vohla *et al.*, 2011). The main problems associated to steel slag filters are efficiency decrease after an unknown period of time (this period may be less than one year) and clogging (Chazarenc *et al.*, 2008). For our specific application (autonomous and decentralized domestic wastewater treatment with low influent flow rate), issues that must be addressed are a poor understanding and control of filter longevity, large required volumes for processes (also including safety factors that could be lowered if the system was better understood), clogging (and short-circuiting), high pH of the filter effluent and replacement/handling logistics.

2.1.2 Regulatory context of autonomous and decentralized treatment in Quebec

Wastewater treatment units are commonly classified in categories following general treatment steps: preliminary treatment (mainly trash and grit removal), primary treatment (septic tanks or primary settling), secondary treatment (various biological processes for organic matter removal), advanced secondary treatment (various biological processes for improved organic matter and suspended solids removal), tertiary treatment (various chemical and physical processes for nitrogen, phosphorus and fecal coliforms) (MDDEP, 2009a). For autonomous and decentralized treatment in Quebec, a septic tank is always installed as a primary treatment unit. Following units can be secondary, advanced secondary or tertiary treatment units, according to applicable regulations. Target concentrations at effluent related to their respective treatment level in Quebec is presented in Table 2.1.

Combinations of treatment units following a septic tank are numerous. The most frequent treatment lines met in Quebec are shown in Figure 2.1. Two options are considered for effluent management: infiltration or discharge in the environment. Regulation asks for prioritization of infiltration in cases

where it is possible to do so. An infiltration bed following the septic tank is the most common and simple option, widely encountered in Quebec (Figure 2.1A). In the case where *in situ* soil is not suitable for installation of an infiltration bed, an advanced secondary treatment unit is added to the line before infiltration in a polishing bed, a thinner version of the infiltration bed (Figure 2.1B).

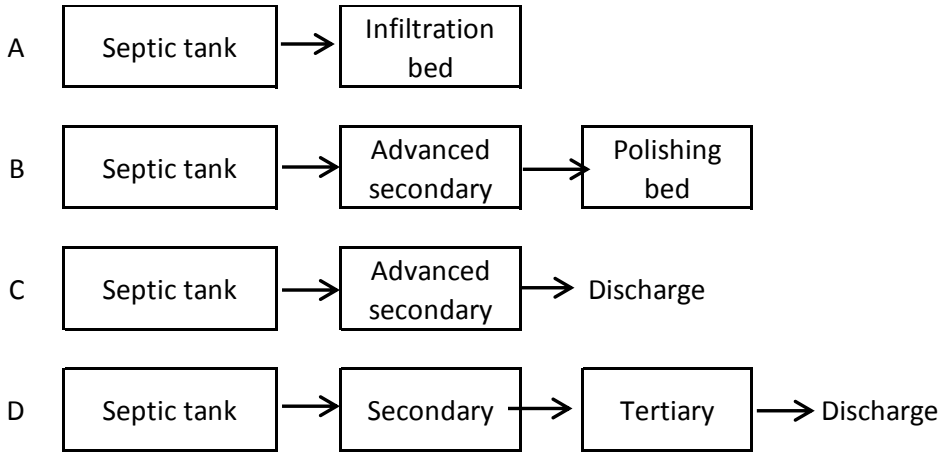

Figure 2.1: Common treatment systems in autonomous and decentralized treatment. A and B: effluent management by infiltration, C and D: effluent management by discharge

Table 2.1 : Discharge criteria for five treatment categories applicable in Quebec regulation (MDDEP, 2009a)

		Discharge criteria			
		TSS	BOD_5-C	Fecal coliforms	TP
		mg/L	mg/L	UFC/ 100 mL	mg P/L
Treatment type	Primary	100	-	-	-
	Secondary	30	25	-	-
	Advanced secondary	15	15	50 000 after reactivation	-
	Tertiary (phosphorus removal)	15	15	50 000 after reactivation	1
	Tertiary (desinfection)	15	15	200 after reactivation	-

When infiltration is not possible, the effluent has to be discharged to the environment. The minimum treatment level required for discharge is advanced secondary (MDDEP, 2009a). This option is shown in Figure 2.1C. If discharge is made in a sensitive ecosystem, a tertiary unit has to be added to the treatment system (Figure 2.1D).

Conventional technologies used in autonomous and decentralized treatment include infiltration trenches and beds, and various filters considered as advanced secondary treatment units (*hors sol* sand filter, classical sand filter, recirculating sand filter). Several non-conventional technologies certified as secondary, advanced secondary or tertiary units are available. Non-conventional technologies are certified by the *Bureau de normalisation du Québec* (*BNQ)*. Only two systems are currently available for tertiary treatment: the electrocoagulation DpEC unit from Premier Tech Aqua and the activated alumina filter from Norweco.

For influent flowrates smaller than 3240 L/d, discharge criteria are set by considering the receiving environment capacity, mainly from the dilution factor in low flow period and from the proximity of a sensitive lake. Phosphorus is the critical factor that limits discharge into lakes. However, discharge in a lake is allowed under specific conditions (Bernier, 2001). In Quebec, the environment ministry sets discharge criteria for influent flowrates over 3240 L/d. Phosphorus discharge criteria are based on the *Position ministérielle de réduction du phosphore*. For influent flowrates over 20 m^3/d, the target range is 0.5 to 1 mg P/L if the discharge point is in a critical ecosystem.

One important aspect of autonomous and decentralized wastewater treatment regulation is the legal uncertainty related to infiltration. Infiltration beds and polishing beds are not associated to treatment levels (secondary, advanced secondary or tertiary), these units are simply accepted as is. For isolated dwellings, infiltration is always accepted even if the discharge point is located in a phosphorus-sensitive receiving environment. However, the infiltration bed capacity for phosphorus retention is not well known, and studies showed the presence of phosphorus plumes reaching water table under infiltration beds (Robertson, Schiff & Ptacek, 1998).

2.1.3 Two approaches for upgrading phosphorus retention with slag filters in isolated dwellings systems

2.1.3.1 Tertiary treatment unit for new wastewater treatment systems

The first approach is to solve phosphorus problems by developing a tertiary treatment unit based on steel slag filters, as shown in Figure 2.1D. This option concerns new constructions that cannot use infiltration for technical reasons and when phosphorus discharge criteria are set. This option involves a criteria of 1 mg P/L at effluent and a point discharge. Neutralization of the slag filter

effluent is mandatory prior to discharge as the effluent pH must be between 6.5 and 9.5. This approach was chosen by *Bionest*, a Quebec company specialised in the development of autonomous and decentralized wastewater treatment units. A collaboration was formed between *Bionest* and Polytechnique Montreal for the development of this product. During her Ph.D., the candidate contributed to *Bionest* product development with slag filter modeling studies, ideas for slag filter design and neutralization modeling studies that led to a patent application (Boutet *et al.*, 2017). A discussion comparing approaches 1 and 2 is provided in Chapter 4.

2.1.3.2 Upgrading phosphorus retention capacity of existing systems

The second approach is to develop a treatment unit based on steel slag filters that would be added to existing septic tank-infiltration bed systems. This option involves a diffuse discharge (infiltration in the water table) without regulation for phosphorus and thus, no specific target concentration. Effluent pH is not submitted to discharge regulations. To this day, the second approach concerns a voluntary market, or near-lake residents who want to improve the lake water quality by retaining more phosphorus in their wastewater treatment system.

One simple implementation of a slag filter is to add it between the septic tank and the infiltration bed (Figure 2.2). Preliminary studies of septic tank effluent treatment with slag filter following this configuration were conducted at Polytechnique (Staingart, 2012). Removals of 91% for total phosphorus and 99% for ortho-phosphates were observed for a period of 90 days using an HRT_V of 12 hours and 10-30 mm slag size. This scenario, however, is probably not directly applicable in the treatment system because of the excessive pH of 10 to 11 coming to the infiltration bed which could affect biological treatment and may favor chemical precipitation clogging in the bed.

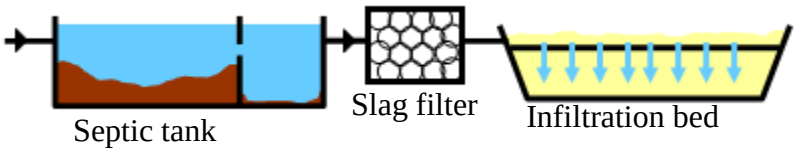

Figure 2.2: Slag filter configuration with 100% septic tank effluent is sent to a slag filter prior to the infiltration bed

The high pH issue could be overcome by using a recirculating filter in which only a fraction of the flowrate would pass (Figure 2.3). pH in the septic tank would be slightly increased (8 to 9) and would likely not affect biological treatment in the infiltration bed. This strategy would also reduce

the slag filter volume. Phosphorus is expected to be captured in three compartments: septic tank, slag filter and infiltration bed.

2.1.4 Phosphorus retention in steel slag filter

A 95% or higher phosphorus removal is expected in the filter, with a pH at effluent above 11 (Claveau-Mallet *et al.*, 2012).

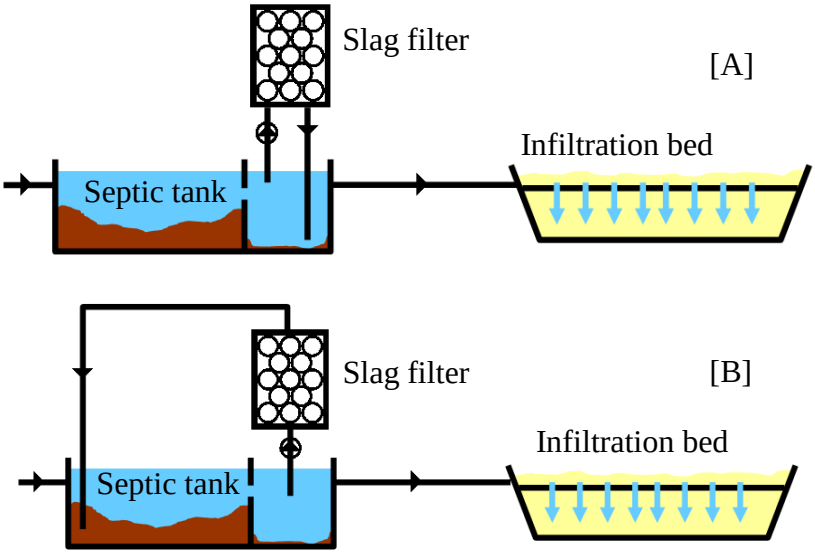

Figure 2.3 : Possible recirculating configurations. A : recirculation withing second compartment, B : recirculation from second to first compartment

2.1.5 Phosphorus retention in septic tank

Ortho-phosphate concentration in a steel slag filter effluent is related to pH (Figure 2.4). Assuming that this relationship is applicable in a septic tank, if the pH in the septic tank is increased from 7 to 8 or 9, a fraction of ortho-phosphates will be precipitated and settled in the tank. This approach is similar to conventional phosphorus removal by lime (Metcalf & Eddy *et al.*, 2014).

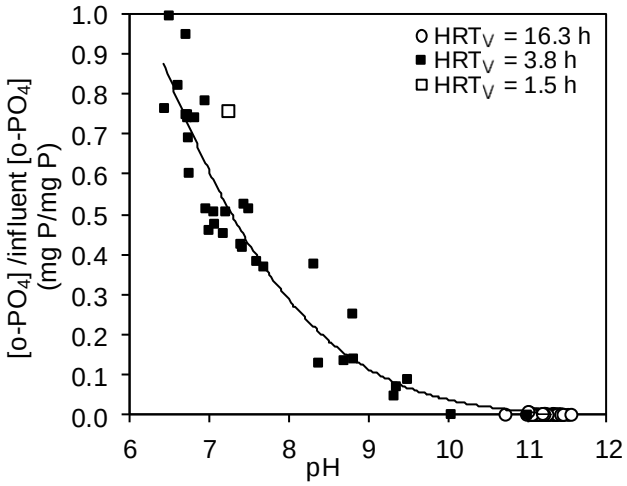

Figure 2.4: Relationship between ortho-phosphates and pH at a steel slag filter effluent (Claveau-Mallet *et al.*, 2012)

2.1.6 Phosphorus retention in an infiltration bed

Phosphorus retention mechanisms in a conventional infiltration bed are adsorption and precipitation (Chambers *et al.*, 2001) which are affected by pH and pe. These mechanisms are insufficient for ensuring a consistent and long term phosphorus concentration below 1 mg P/L for the effluent leaching into the groundwater, as concentrations of up to 5 mg P/L were observed below infiltration beds (Robertson, Schiff & Ptacek, 1998). pH in infiltration beds is typically between 6 to 7. At those pH value, iron phosphate minerals such as vivianite, strengite and variscite may form (Robertson, Schiff & Ptacek, 1998) but such a pH is too low for hydroxyapatite precipitation. Slag filter leachates may favor hydroxyapatite precipitation via increased pH (9) and increased calcium. Struvite ($MgNH_4PO_4$ $6H_2O$) precipitation would also be favored by a pH increase, but it occurs only above a critical Mg/P ratio (Jaffer *et al.*, 2002).

2.2 Modeling concepts relevant for steel slag modeling

This section presents modeling concepts that were used in Chapter 5 to 8. To avoid redundancy, only concepts that are not already presented in paper presented in these Chapters are presented. The literature review from papers 2 to 4 and section 2.1.1 presented briefly steel slag, past applications of steel slag for water treatment, technical aspects and issues associated with steel slag

filters and modeling needs. The next section will emphasize fundamental modeling concepts that were used in this thesis modeling work.

2.2.1 Hydraulic models for porous media

In a porous media reactor, as well as in any kind of reactor, hydraulics should be known and correctly modelled before conducting simulation work. Two useful models for hydraulics modeling of porous media reactors such as constructed wetlands or reactive filters, will be presented in this section. Modeling of porous media rectors involves important aspects:

- As the reactor volume is partly filled with media, the empty bed hydraulic retention time (*HRT*) of the reactor is not fully available for water flow and treatment. The hydraulic retention time of voids (HRT_V) should be used for analysis and design, following equation 2.1, with *n* being the reactor porosity. *n* is defined as the total volume fraction occupied by water, including both mobile and immobile water. *n* can be calculated from simple mass-volume relationship. Typically, porosity is 30% in sand (Domenico & Schwartz, 1998) and 50% in steel slag filters (Claveau-Mallet, Courcelles, & Comeau, 2014).

$$HRT_V = nHRT \tag{2.1}$$

- The effective hydraulic retention time of void (HRT_{Ve}) is defined from effective porosity (n_e) as the real retention time of the reactor, considering that only a fraction of porosity is available for water flow (equation 2.2). HRT_{Ve} cannot be calculated from mass-volume relationship, it has to be calibrated from tracer tests. HRT_V is used for design, while HRT_{Ve} is used for modeling.

$$HRT_{Ve} = n_e HRT \tag{2.2}$$

- The hydraulic model should be calibrated (or validated) with tracer tests.

2.2.1.1 The advection-diffusion-reaction model

The advection-diffusion-reaction (ADR) equation (equation 2.3) was developed for groundwater flow in hydrogeology applications (Fetter, 1999). In this equation, a solute (its concentration is represented by *C*) migrates by both convection ($\vec{v}C$ term) and mechanical dispersion ($D \cdot \nabla C$ term)

in a porous media, in which reactions occur ($\left(\frac{\partial C}{\partial t}\right)_{rx}$ term). *D* is the dispersion coefficient (m^2/s) of the porous media.

$$div(D \cdot \nabla C - \vec{v}C) + \left(\frac{\partial C}{\partial t}\right)_{rx} = \frac{\partial C}{\partial t} \quad (2.3)$$

For 1D simple flow of a conservative solute (without reactions), analytical solutions are available. For example, a 1D continuous-flow pulse-injection tracer test response curve can be modeled with equation 2.4 (Fetter, 1999). In this equation, C_0 is the initial concentration of the tracer (mol/m^3), erfc is the complementary error function, *x* is the position from the injection point (m), v_x is the water velocity (m/s), *D* is the dispersion coefficient (m^2/s) and *t* is time (s).

$$C(x,t) = \frac{C_0}{2}\left(erfc\left(\frac{x-v_x t}{2\sqrt{Dt}}\right) + exp\left(\frac{xv_x}{D}\right) erfc\left(\frac{x+v_x t}{2\sqrt{Dt}}\right)\right) \quad (2.4)$$

Tailing typically found in tracer tests can be modeled in the ADR model as retardation. The ADR equation including an additional term for retardation is shown in equation 2.5. In this equation, B_d is the soil volumetric mass (g/m^3) and *C** is the solute concentration sorbed onto soil (g solute / g soil).

$$div(D \cdot \nabla C - \vec{v}C) - \frac{B_d}{\theta}\frac{\partial C^*}{\partial t} + \left(\frac{\partial C}{\partial t}\right)_{rx} = \frac{\partial C}{\partial t} \quad (2.5)$$

It is possible to solve the ADR equation by finite elements, using hydraulic parameters that were calibrated in simple tracer tests. The ADR model was the one used in this thesis modeling work. The ADR model was implemented in the PHREEQC software for 1D flow.

ADR model in PHREEQC

In PHREEQC, the 1D flow ADR model is represented by a column divided into cells. Numerically, the ADR model is solved in three steps (Parkhurst & Appelo, 1999): first cells and their water content are shifted from one to the other, second dispersion is modeled by mixing between adjacent cells, and third kinetic or equilibrium reactions are performed. Retardation (and tailing of a tracer test) can be modeled by the double porosity module which consists of parallel cells along the column. Each column cell is connected to an immobile cell in which mixing with the mobile cell is possible via a mixing factor (Figure 2.5). Tracer test response curve can be directly calibrated with a numerical tracer test by trial and errors or numerical optimization.

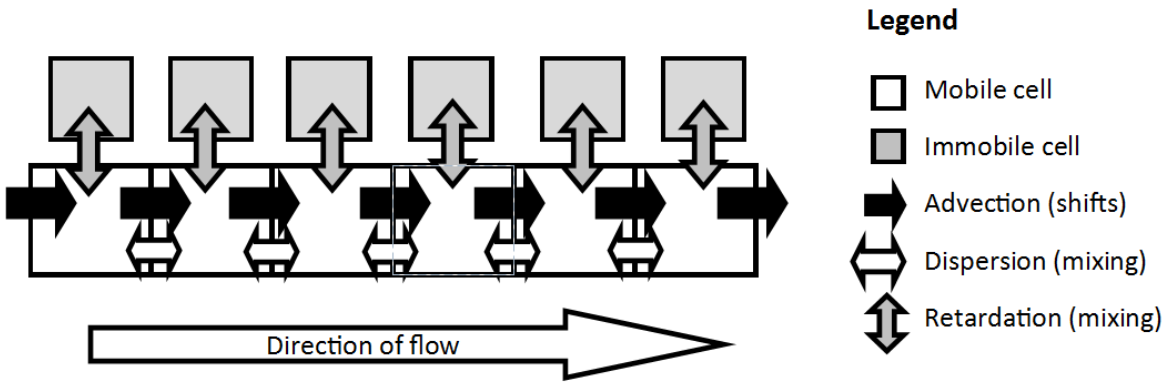

Figure 2.5 : Schematic representation of the PHREEQC double porosity module for ID transport in a 6-cell column

2.2.1.2 The tanks-in-series (TIS) flow model

This model is used for constructed wetlands and is described in Kadlec and Wallace (2009). Migration of solute in the porous media is represented by a succession of completely stirred tank reactors (CSTR). This model can be represented by a gamma distribution (equation 2.6), in which *N* is the number of tanks and *t* time. Note that *N* does not have to be an integer in this equation. As the gamma distribution is a probability density function, the tracer response curve should be transformed into a *f(t)* function by normalization with the total tracer mass (equation 2.7). Calibration of the model can be done by minimizing the error between equations 2.6 and 2.7.

$$f(t) = \frac{N^N {HRT_{Ve}}^{N-1}}{{HRT_{Ve}}^N \Gamma(N)} exp\left(\frac{-Nt}{HRT_{Ve}}\right) \quad (2.6)$$

$$f(t) = \frac{C(t)}{\int_0^\infty C(t)dt} \quad (2.7)$$

2.2.1.3 Comparison of hydraulic models

Calibration of a tracer test using both models is presented in Figure 2.6. This tracer test was performed on a steel slag column; this column test will be presented in Chapter 8. Two tanks-in-series (TIS) calibration are presented using partial data ($t \leq 11$ h or $t \leq 25$ h) in the optimization step. The PHREEQC ADR model was calibrated visually by heuristic optimization. Calibrated parameters were N = 28.2 and TRH_{Ve} = 8.5 h for TIS-11 h; N = *12.9* and TRH_{Ve} = 9.8 h for TIS-25 h; D^*=5 cm, D_n = 5e-6 s^{-1} and HRT_{Ve} = 9.4 h for the PHREEQC ADR model. Note that the TIS-

11 h calibration is very close to a plug flow, with high *N* and symmetrical curve, and TRH_{Ve} close to the peak.

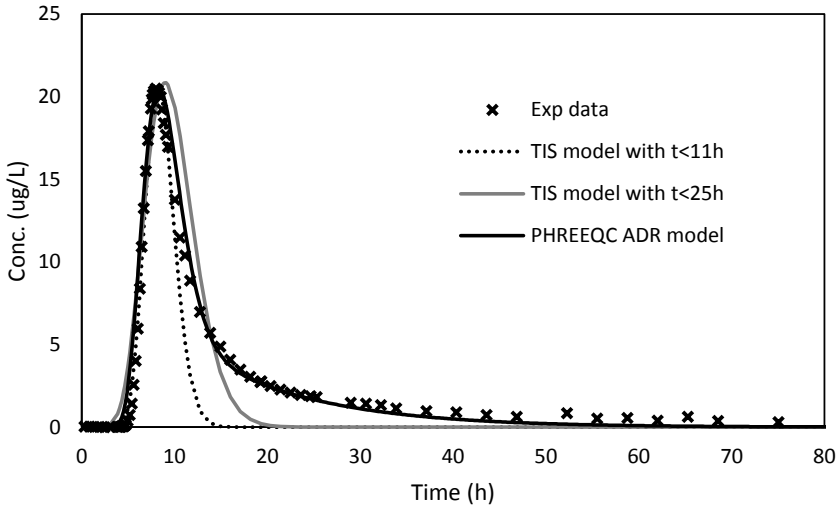

Figure 2.6 : Calibration of a tracer test using the TIS and the PHREEQC ADR models

Table 2.2 : Hydraulic parameters for the TIS and PHREEQC ADR models

Parameter	Description
TIS model	
N	Number of tanks in series
HRT_{Ve} (h)	HRT_{Ve}/N is the theoretical *HRT* of a CSTR
PHREEQC ADR model	
*D** (cm)	Dispersivity
D_n (s^{-1})	Exchange factor between mobile and immobile cells
HRT_{Ve} (h)	HRT_{Ve}/(number of cells) is the duration of a shift

The PHREEQC ADR model resulted in a better calibration than the TIS model. The TIS model can either calibrate the peak or part of the tail, depending on the number of data considered in optimization. Adding data to the optimization step improved slightly the tail, but the peak was shifted. The better accuracy of the PHREEQC ADR model can be explained by its higher complexity, which involves three calibrated parameters for effective volume, dispersion and retardation, compared to the TIS model which involves only two parameters for effective volume and dispersion (Table 2.2). For simple 1D cases with no or small tails, both models may be equivalent. Note that both models do not consider media at all. CSTR are assumed to be empty and

completely stirred, with an *HRT* that represents effective porosity. In the PHREEQC ADR model, column cells contain only water with a shift duration that considers effective porosity.

The ARD model is definitely more suitable for complex flow systems such as 2D-3D flow or reactors with evolving hydraulic properties. While ADR can be solved with finite elements and has flexibility in attributing properties to each element, the TIS model is fixed into a given configuration of completely stirred tank reactors (CSTR). For example, a reactive media wetland in which progressive clogging occurs has evolving hydraulic properties and should be modeled as a 2D flow. This strategy was employed by Samsó *et al.* (2015), who modeled bioclogging in a constructed wetland using the Richard's equation for unsaturated flow in the COMSOL software. In this study, biomass growth was affecting the hydraulic conductivity of the media and bioclogging effect was changing following operation mode. Another example is a reactive filter implemented in the ground in which hydraulics is affected by progressive carbonate and metal hydroxides precipitation (de Repentigny & Courcelles, 2014).

2.2.2 Physicochemical models in wastewater treatment

For the purpose of this thesis, a model will be defined as a combination of equations that represent correctly and globally mechanisms occurring in a process. The required level of complexity and number of equations for reaching a "correct" and "global" representation of a process operation is not fixed, it depends on the modeller's objectives. Models involving numerous equations have to be solved numerically, but analytical resolution is possible for simple models with one or few equations and simple systems. In most cases, two models have to be superimposed for considering both hydraulics and chemical reactions. In wastewater treatment models, hydraulics is often simplified and focus is given to chemical models. Examples of well-known models in wastewater treatment are ASM1, ASM2, ASM2d and ASM3 for activated sludge; and ADM1 for anaerobic digestion (Corominas *et al.*, 2010).

These kinetic-based models are concisely represented in a Gujer matrix (Henze *et al.*, 2000). In this matrix, each biological or physicochemical process is written in a single line. The matrix includes 5 columns: 1) rate name, 2) stoichiometric coefficients of state variables in solution affected by the rate, 3) stoichiometric coefficients of state variables of other phases (mineral phases, gaseous phases or biomass) affected by the rate, 4) rate equation and 5) equilibrium constant. A simple example of construction of the Gujer matrix is shown in Table 2.3 for calcite precipitation.

The matrix includes two important equations: one for stoichiometry (column 1) and one for rate (column 4). Ca^{2+} and ${CO_3}^{2-}$ are the aqueous state variables involved while $CaCO_3$ is the mineral phase state variable. Stoichiometric coefficients of columns 2 and 3 are determined following the stoichiometric equation in column 1. Note that coefficients of column 2 and 3 have opposite signs: what is removed from water (negative sign) is used for solid phase formation (positive sign). At each solving step, the rate of column 4 is first calculated (mol/L); second it is multiplied with coefficients from column 2 to determine which amounts of state variables are removed from the solution. Similarly, the rate is multiplied with coefficients from column 3 to determine the amount of newly formed minerals. The Gujer format is useful for numerical resolution as columns 2 to 4 form a matrix that is directly used for mathematical resolution. An example of a full Gujer matrix is provided in section 8.4.

Table 2.3 : Example of Gujer matrix construction for calcite precipitation

Col 1 Rate name and stoichiometric equation	Col 2 Stochio – aqueous phase		Col 3 Stochio – mineral phase	Col 4 Rate expression	Col 5 Solubility product
	Ca^{2+}	${CO_3}^{2-}$	$CaCO_{3(s)}$		
Calcite precipitation $Ca^{2+} + CO_3^{2-}$ $\leftrightarrow CaCO_{3(s)}$	-1	-1	+1	r_{CAL} $= k_{CAL} log\left(\frac{\{Ca^{2+}\}\{{CO_3}^{2-}\}}{K_{spCAL}}\right)$	K_{spCAL} $= 10^{-8.48}$

2.2.2.1 Motivation for physicochemical model development

In the early development of wastewater treatment models, focus was given to biological models, as processes were optimized for organic matter removal. The emerging preoccupation for nutrient and resource recovery made these traditional models deficient for answering these new challenges. Traditional biological models did not consider important physicochemical phenomena (Lizarralde *et al.*, 2015). There is a need for improved physicochemical modeling in various applications as nutrient recovery (Ping *et al.*, 2016; Seckler, Bruinsma, & van Rosmalen, 1991), anaerobic digestion (Solon *et al.*, 2015), chemical P removal (Hauduc *et al.*, 2015; Maher *et al.*, 2015) and also activated sludge and plant-wide modeling (Flores-Alsina *et al.*, 2015). As an example, the

ASM2D model includes precipitation without pH prediction (Mbamba *et al.*, 2015); and the ADM1 model does not consider ionic strength and ion pairings (Solon *et al.*, 2015). Benefits that would be obtained from these physicochemical models include more accurate pH control and improved process stability (especially for high strength influent processes as anaerobic digestion), reduction of scaling problems, reduction of needed chemicals, improvement of recovered nutrient pellets purity and others. The consideration of physicochemical processes in wastewater treatment models necessitates to integrate chemical and geochemical equilibrium models.

2.2.2.2 Chemical and geochemical equilibrium models

Equilibrium chemical models assume that all reactions are instantaneous. Important equilibrium reactions that are typically included in water chemistry models are acid-base reactions, ion pairing, equilibrium with a solid or gas phase, and calculation of species activity (Parkhurst & Appolo, 1999). For any species i, the activity a_i is calculated by equations 2.8 and 2.9 where m_i is the molality, A a constant, z_i the ionic charge of specie, and μ the ionic strength of the solution. An example of chemical model with equilibrium equations is provided in Table 2.4 for the closed (no contact with atmosphere) carbonate system (Eppner *et al.*, 2015). Acid/base and ion pairing processes are generally assumed to be at equilibrium, but it is not always the case for processes involving mineral (or gaseous) phases. The modeller can assume either equilibrium or kinetic for those depending on his modelling assumptions.

Table 2.4 : Equilibrium reactions in the closed carbonate system

Reactions	Equilibrium constants (log)	Type of reaction
$H^+ + OH^- \leftrightarrow H_2O$	-14	acid/base
$H^+ + {CO_3}^{2-} \leftrightarrow {HCO_3}^-$	-10.329	acid/base
$Ca^{2+} + {HCO_3}^- \leftrightarrow {CaHCO_3}^+$	-1.106	ion pairing
$2H^+ + {CO_3}^{2-} \leftrightarrow H_2CO_3$	-16.7	acid/base
$Ca^{2+} + {CO_3}^{2-} \leftrightarrow {CaCO_3}_{(aq)}$	-3.224	ion pairing
$Ca^{2+} + H_2O = H^+ + CaOH^+$	12.78	ion pairing
$Ca^{2+} + {CO_3}^{2-} \leftrightarrow {CaCO_3}_{(s)}$	-8.48	equilibrium with mineral phase

$$a_i = \gamma_i m_i \quad (2.8)$$

$$log\gamma_i = -Az_i^2 \left(\frac{\sqrt{\mu}}{1+\sqrt{\mu}} - 0.3\mu\right) \quad (2.9)$$

2.2.2.3 Recent work on physicochemical modeling

Modeling needs presented below lead to the creation in 2010 of a Task Group on a generalized physicochemical framework at the International Water Association (IWA, 2017). This task group's objective was to propose a general modeling strategy that would be applicable for physicochemical models. It is admitted that most fundamental principles of chemical and physicochemical reactions are already known, what is unknown is the best way to consider them for wastewater treatment modeling. This task group resulted in the proposal of a rigorous mathematical approach for incorporating existing biological and physicochemical models (Lizarralde *et al.*, 2015). Important outcomes of this approach were the multiphase extension of the Gujer compact model representation, separating gas hold-up (bubbles within aqueous phase) and off-gas (gas above the aqueous phase) transfer processes and separating "k_L" and "a" in the mass transfer coefficients. Solon *et al.* (2015) added ionic strength and ion pairing to the ADM1 model for anaerobic digestion. She showed that anaerobic digestion performance and gas production is affected by these physicochemical reactions.

Precipitation modeling works

Precipitation of calcite was studied more deeply by Mbamba *et al.* (2015), who proposed correction factors for temperature and impurity presence in calcite. In general, the precipitation rate for a given phase considers saturation index and specific surface of the mineral phase (Lizarralde *et al.*, 2015; Mbamba *et al.*, 2015; Mbamba *et al.*, 2015; Stumm & Morgan, 1996). Several strategies were proposed for modeling homogeneous precipitation (also called self-seeding or spontaneous nucleation), as setting an arbitrary initial seed concentration of crystals (Mbamba *et al.*, 2015). In this model, homogeneous precipitation is considered the same as heterogeneous precipitation by "forcing" an initial mineral specific surface. A second possible strategy is the definition of activation terms for surfaces from suspended solids or precipitated phase, as well as supersaturation to represent homogeneous precipitation (Lizarralde *et al.*, 2015). In both cases, homogeneous and heterogeneous precipitates are considered the same state variable, and a constant crystal size is assumed.

Crystal morphology is especially important for struvite recovery. Total suspended solids (TSS) was found to affect struvite pellet morphology and purity precipitated from a sludge dewatering liquor, which affects harvesting and economic value of pellets (Ping *et al.*, 2016). This author studied the content of various organic compounds in struvite pellets formed under various TSS concentrations. He concluded that suspended solids should be removed prior to the precipitation process to improve the pellet purity.

Modeling of phosphorus removal by chemical coagulation was recently studied by Hauduc *et al.* (2015). This author proposed a new model including hydrous ferric oxides precipitation, phosphorus adsorption onto flocs and coprecipitation. Involved reactions in this model were basic equilibrium reactions, ion pairing, precipitation of ferric oxides and ferric phosphate, surface complexation onto hydrous ferric oxides and aging processes of oxides. An important feature of this model was the translation of floc aggregation phenomenon and reduction of adsorption sites into four aging processes that were related to mixing conditions. This model resulted in good predictions of coagulation experimental results.

2.2.2.4 Modeling issues in wastewater physicochemical treatment modeling

Issues in hydraulic modeling

The CSTR model presented in section 2.2.1.2 is traditionally used for modeling of various wastewater treatment process. This model's strength is its simplicity and low computational costs, but it involves restricting hypothesis on reactors: they are assumed to be completely mixed. Modellers have to choose between two options: keep the widely accepted CSTR model, or consider non-uniformity in reactors using discretization of reactor volume and computational fluid dynamic (CFD). This issue is important for physicochemical modeling applications as well as biological modeling applications. Recent studies have outlined the necessity to consider complex hydraulic in wastewater treatment processes. Terashima *et al.* (2009) used CFD to show that anaerobic digesters are non-homogeneous even under mixing conditions. This author proposed a new parameter, the uniformity index, to describe mixing dynamics. CFD was used in another study for modeling of a mainstream facultative aerobic/anoxic reactor, resulting in heterogeneous distribution of oxygen concentration and water velocity in the reactor (Rehman *et al.*, 2016).

The utilization of such complex hydraulic models need heavy calculation times compared to the CSTR model. An alternative method for consideration of complex hydraulics, the compartmental

model, was used by Rehman *et al.* (2016). The compartment model consists in using several completely mixed compartments connected by convection or exchanges. This model looks like two or more parallel CSTR lines connected by exchanges and no convection, in a way similar to the PHREEQC double porosity module (described in section 0). The compartmental model has to be calibrated with CFD, but once calibrated, it can represent complex hydraulics with lower computational requirements. The disadvantage of this method is its non-flexibility as the calibration has to be redone if operation conditions are changed.

Issues in numerical resolution of physicochemical models

Resolution of complex systems involving numerous equilibrium and kinetic reactions requires heavy computational power. There is not yet a consensus on the best numerical strategy to employ for physicochemical model resolution (Claveau-Mallet, 2016). Two main approaches are possible. In the ordinary differential equation approach, both equilibrium and kinetic reactions are expressed as kinetic rates and are solved simultaneously. In that case, kinetic constants of equilibrium reactions are set at very high values, much higher than those for kinetic reactions, resulting in instantaneous reactions. This method was employed by Hauduc *et al.* (2015) in a model for chemical phosphorus removal. Second, the differential algebraic equation approach solves kinetic reactions by differential equations and equilibrium reactions are calculated at each iteration step with algebraic equations. Equilibrium reactions can be solved by coupling the kinetic model with existing speciation software as PHREEQC, or implement selected equilibrium from existing database into the model. Possible methods for solving algebraic equations include gradient search methods as proposed by Solon *et al.* (2015) for an anaerobic digestion application. Calculation time for complex problems can be reduced by using a transformation matrix for kinetic rates, as proposed by Eppner *et al.* (2015). This author modelled physicochemical reactions for geothermal applications, which involve complex modeling (superposition of groundwater flow, solute transport and heat exchanges).

Issues in steel slag filter modeling

The physicochemical modeling approach presented previously is suitable for steel slag modeling, however, steel slag have their own modeling specificities and issues, listed below.

- Steel slag filter influents are generally secondary effluents containing little organic matter. In that case, biological treatment is not required nor intended. If organic matter were present

in the influent, the high pH in the alkaline steel slag filter would strongly inhibit biological reactions. Consequently, a model for tertiary steel slag filtration can completely neglect biological reactions and consider only physicochemical reactions. If the steel slag filter is used after primary treatment, biological model may be considered, but it should be revised to consider correctly the effect of high pH and long-term sludge retention time (no sludge wastage).

- While struvite is a major mineral phase to consider in nutrient recovery, hydroxyapatite and calcite are the main mineral phases precipitated in steel slag filters. Coprecipitation and adsorption into iron oxides is not expected in steel slag filters because of the high pH (Baker *et al.*, 1998; Valsami-Jones, 2001). Redox transformations with iron can be neglected because of assumption of oxic conditions (high oxygen concentration at the effluent of the biological treatment process and no oxygen consumption in the slag filter).
- Precipitation rates are already studied and understood in other physicochemical processes, but this is not the case for slag itself. Modeling slag particle behavior (leaching, adsorption, etc.) is the challenge of steel slag filters.
- Nucleation issues and modeling choices encountered in physicochemical modeling remain important for steel slag filters.
- Hydraulic is an important aspect of steel slag filtration modeling because of long-term clogging.

2.2.3 Existing design tools for steel slag filters

To the author's knowledge, no modeling tool following the approach presented in preceding paragraphs exist for steel slag filter. Three design tools that were proposed in other studies are presented in this section.

2.2.3.1 Adsorption isotherms

An adsorption isotherm is the simplest and fastest design tool, as design parameters can be determined very easily with simple batch tests. Adsorption isotherms are already used for other wastewater or drinking water granular processes such as activated carbon filters (Metcalf & Eddy *et al.*, 2014). Several adsorption isotherm equations exist, but they all have the same basis

assumption: there is an equilibrium between the amount of sorbed substance at the solid surface and substance concentration in water. An adsorption isotherm describes the relationship between sorbed and soluble component. The Langmuir isotherm (equation 2.10) is an example of commonly used isotherm (Fetter, 1999), in which *C* is the concentration of the solute in water at equilibrium (g/L), *C** the solute mass sorbed on the surface (g solute / kg solid), *a* a constant (L/mg) and *b* the maximum solute amount that can be sorbed on the surface (mg solute /kg solid).

$$\frac{C}{C^*} = \frac{1}{\alpha\beta} + \frac{C}{\beta} \qquad (2.10)$$

Sorption isotherms were largely studied for P removal by slag (Vohla *et al.*, 2011), but they were found to be unreliable for prediction of full-scale filter behavior. The main problem related to adsorption isotherms is the surface hypothesis. Slag is not only a surface, it is also a source of CaO leaching in bulk water. Sorption isotherms are not suitable for representing precipitation occurring in bulk water, nor slag aging.

2.2.3.2 The kC* model

The kC* model is usually utilized for organic matter removal in constructed wetlands (Kadlec & Wallace, 2009). This model was proposed for the design of steel slag filters by Barca, who calibrated this model on horizontal subsurface flow filters using EAF or BOF slag (Barca *et al.*, 2013). He expressed the kC* model into equation 2.11, in which *C* is the Total phosphorus (TP) concentration (mg P/L) at the distance *x* (m) from inlet, *L* is the length of the filter (m), k_V a constant, C_0 is the inlet TP concentration (mg P/L) and *C** is the background outlet TP concentration. This model's assumptions are plug flow and constancy of k_V and *C**. In the study, *C** was taken as 0.1 mg P/L from observed experimental data, and the calibrated model fitted well the data within the filter. k_V was not constant within the experiment. This model's strength is its simplicity, as it simplifies both slag dissolution and P precipitation into a single first-order kinetic model. Its weaknesses are uncertainty associated with the empirical determination of *C**, considering that target P concentration at effluent is generally low (1 mg P/L or below), and assumption that k_V is constant (impossible to predict slag exhaustion).

$$\frac{C - C^*}{C_0 - C^*} = exp\left(-k_V HRT_V \frac{x}{L}\right) \qquad (2.11)$$

2.2.3.3 Prediction models in agricultural applications

Modeling work has been conducted in the field of agricultural for predicting P removal efficiency of steel slag filters. In agriculture runoff management, steel slag filters are implemented in P removal structures as ditch filters, confined bed runoff filter, riparian runoff filter, surface inlets, pond filters or subsurface drainage filters operated at HRT_V smaller than 10 minutes (Penn *et al.*, 2016). An empirical model based on an exponential function was proposed for these structures (Penn *et al.*, 2016):

$$DP_{rem}(\%) = be^{m*CP_{add}} \quad (2.12)$$

CP_{add} is the cumulative phosphorus added (mg P/ kg media), DP_{rem} (%) discrete phosphorus removal, *b* and *m* empirical coefficients related to retention time, inlet phosphorus concentration and material properties (pH, buffer index, amorphous Fe and Al, particle size, total Al, Ca and Fe). Strengths of this empirical model were to consider indirectly both precipitation kinetics (by P inlet concentration and retention time) and slag behavior. Slag behavior modeling followed a global approach, as key parameters (pH and buffer capacity) were considered in the model, and not only the total calcium content. The authors of this study distinguished reactive media based on Al/Fe sorption and those based on calcium phosphate precipitation. In this model, slag exhaustion is represented by the exponential function. Finally, the model was calibrated and validated on field experiments, which proved its efficiency in real-life design. One weakness of this model is its non-flexibility for wastewater treatment modeling applications. It could not be easily interfaced with other wastewater treatment models if used in whole-plant modeling, and it would have to be recalibrated if additional mechanisms such as metal precipitation were considered.

CHAPTER 3 ARTICLE 1: IMPROVING PHOSPHORUS REMOVAL OF CONVENTIONAL SEPTIC TANKS BY A RECIRCULATING STEEL SLAG FILTER

Claveau-Mallet, D., Lida, F. & Comeau, Y. (2015). Improving phosphorus removal of conventional septic tanks by a recirculating steel slag filter. *Water Quality Research Journal of Canada*, 50(3), 211-218.

ABSTRACT

The objective of this project was to increase the P retention capacity of a conventional septic tank by adding a recirculating slag filter. Two recirculation modes and recirculation ratios from 5 to 50% were tested in the laboratory with reconstituted domestic wastewater. The best system was recirculation from the end to the inlet of the second compartment of a septic tank with a 50% recirculation ratio in the slag filter, achieving 4.2 and 1.9 mg P/L at the effluent for TP and o-PO_4, respectively, and a pH of 8.8. The calculated size of the slag filter for a 2-bedroom house application was 1875 kg for an expected lifetime of 2 years. The 1 mg P/L level goal was not reached, but P precipitation may be favoured by the relatively high effluent pH reaching the infiltration bed.

Keywords: phosphorus removal, septic tank, steel slag, onsite wastewater treatment

3.1 Introduction

In Quebec, the conventional wastewater treatment system for an isolated dwelling consists of a septic tank followed by an infiltration bed (MDDEP, 2009a). Septic tanks are designed for primary treatment of SS and BOD_5, which are controlled in Quebec regulations. The infiltration bed acts as a secondary treatment system, after which water joins the natural water table. To this day, conventional septic tanks and infiltration beds are not controlled for phosphorus (P), but such systems discharge excess P to the environment via infiltrating water (Robertson, Schiff & Ptacek, 1998), contributing to the eutrophication of freshwaters.

The objective of this project was to improve the P removal capacity of the conventional septic tank - infiltration bed system with a simple and extensive technology. The target total P (TP) concentration of the infiltration water was 1 mg P/L. The selected technology was a steel slag filter

fed with the supernatant of the downstream end of the septic tank and recirculating into either the first or the second part of the septic tank. Experimental septic tanks with slag filters were constructed and operated in the laboratory. In this project, focus was given to septic tanks without considering infiltration beds.

Phosphorus removal from wastewater is commonly achieved using intensive processes, as biological treatment (Metcalf & Eddy., 2003), coagulation/floculation (Szabó *et al.*, 2008; Evoqua, 2014) or membrane filtration (Metcalf & Eddy., 2003). Passive technologies for P removal exist, but they are either not reaching 1 mg P/L at effluent (for example constructed wetlands are rapidly saturated, (Chazarenc *et al.*, 2007)); or very expensive (electrocoagulation system for isolated dwelling, (Premier Tech Aqua, 2014)). Slag was selected for its low cost and its potential high P removal capacity.

Slag is a by-product of the steel industry that is known to capture P (Vohla *et al.*, 2011; Yamada *et al.*, 1986). Several metallurgic processes result in different slag types and size (National Slag Association, 2009). Slag filters are currently operated as tertiary treatment units in research projects for P removal (Chazarenc *et al.*, 2008), but long-term full-scale units are limited to a unique process operated in New-Zealand (Shilton *et al.*, 2006), to the authors' knowledge. A particular application of slag for wastewater treatment is the alkaline slag filter, containing alkaline gravel-size slag. This type of filter raises the wastewater pH to 10-11 and induces P precipitation and filtration (Claveau-Mallet *et al.*, 2012). As a passive and highly efficient P-removal technology, the slag filter is a promising and economical unit to upgrade septic tanks for P removal. However, its high effluent pH complicates its direct application, as a pH of 11 is not suitable for discharge or infiltration. It is also possible that the required filter size and replacement cost for a 2-year longevity (MDDEP, 2009a) may be uneconomical. Recirculation in the slag filter is a strategy that represents a compromise between P removal, effluent pH and filter size. Moreover, addition of a slag filter in the septic tank may favour P precipitation and stabilization in the infiltration bed (Robertson, Schiff & Ptacek, 1998).

3.2 Materials and Methods

3.2.1 Experimental Unit

A schematic of the experimental pilot unit is shown in Figure 3.1. Septic tank compartments were represented by two covered 26 L plastic boxes. The water volumes in compartments 1 and 2 were 20 L and 10 L, respectively. The outlet of compartments was controlled by overflow tubing. Septic tanks were fed with reconstituted domestic wastewater using a peristaltic pump with intermittent operation (8 feedings per day, for an average flowrate of 14.2 L/d). The total *HRT* of the septic tank was 2.1 d, according to Quebec requirements (MDDEP, 2009a). Two slag filter recirculation modes were tested: recirculation from compartment 2 back to compartment 1inlet, and recirculation within compartment 2. Slag filters were fed from the bottom with intermittent operation. Filters had a diameter of 15 cm and a length of 39 cm. The experimental unit was sampled at different points (see Figure 3.1) and samples were analyzed for *COD* (chemical oxygen demand), *TSS* (total suspended solids), *VSS* (volatile suspended solids), *TP*, orthophosphate (o-PO_4), calcium, alkalinity, pH and conductivity. Tests were divided into 6 phases with varying recirculation ratio, as shown in Table 3.1. They were conducted from June to November 2013.

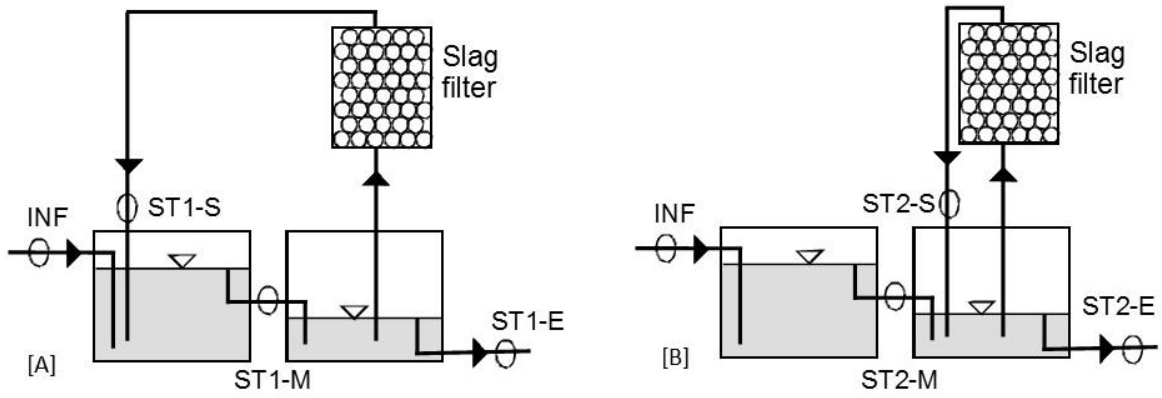

Figure 3.1 : Schematic of the experimental unit showing recirculation from compartment 2 to 1 (a) and from compartment 2 to 2 (b). Sampling points and their label are identified on the schematic by circles

At the end of all phases, each compartment was homogeneously mixed and sampled in triplicates. Slag filters were emptied, sampled and analyzed for a P mass balance.

Table 3.1 : Experimental program

Phase	Wastewater type[a]	Duration	Slag filter recirculation ratio	Slag filter influent flowrate	Slag filter HRT_V
		d	%	L/d	h
1	1	20	5	0.71	118
2	1	20	10	1.42	59
3	1	19	25	3.55	24
4	2	9	25	3.55	24
5	2	19	50	7.11	12
6	2	20	10	1.42	59

a: see Table 3.2 for Wastewater composition

3.2.2 Slag Media and Wastewater Characteristics

The slag used in this study was 5-10 mm electric arc furnace slag produced by Arcelor Mittal, Contrecoeur, Quebec. This slag was previously used for P removal filter applications (Abderraja Anjab, 2009; Chazarenc *et al.*, 2007; Claveau-Mallet *et al.*, 2012; Lospied, 2003; Mahadeo, 2013; Chapter 6). The chemical composition of slag was (% w/w): 40.6 CaO, 18.2 Fe_2O_3, 16.3 SiO_2, 10.2 MgO, 5.1 Al_2O_3, 3.9 MnO, 0.47 P_2O_5, 0.44 TiO_2, 0.41 Cr_2O_3, 0.05 Na_2O and 0.03 K_2O.

Septic tanks were fed with reconstituted wastewater. Primary sludge, KH_2PO_4, K_2HPO_4 and $NaHCO_3$ were added to tap water, resulting in wastewater characteristics presented in Table 3.2. Two wastewater sludges were used, with a higher suspended solids content for wastewater 2. Feeding was done from a continuously mixed barrel kept at 4°C which was renewed and analysed every 6 days.

Table 3.2 : Reconstituted water composition

Parameters	Units	Wastewater 1	Wastewater 2
Sludge origin (wastewater treatment plant)		Auteuil (Laval)	St-Hyacinthe
pH	-	7.6±0.2	7.3±0.1
o-PO_4	mg P/L	10.5±0.6	9.7±1
TP	mg P/L	14±4	22.7±4.5
Calcium	mg/L	30±2	30±2
Alkalinity	mg $CaCO_3$/L	228±3	235±7
Conductivity	µS/cm	598±20	594±5
COD	mg/L	44±6	567±200
TSS	mg/L	16±5	441±190
VSS	mg/L	14±3	283±130

3.2.3 Analytical Determinations

Slag composition was determined by Acmelabs (Vancouver) by ICP-emission spectrometry. Analyses for *COD*, *TSS*, *VSS*, *TP*, o-PO_4, calcium and alkalinity were conducted following standard procedures: methods 5220-D, 2540-D, 2540-E, 4500-P-F, 3500 and 2320-B (APHA *et al.*, 2005).

3.2.4 Calculations for Full-Scale Application

The full-scale size of a slag filter (mass and volume) was calculated according to equations 3.1 and 3.2, that were developed by the authors. These equations are based on the P retention capacity (r_{max}) and P mass balance of the slag filter. The equation parameters are defined in Table 3.3.

$$m_{slag} = \frac{Q_{slag}\left(c_{i-slag} - c_{o-slag}\right)T_{life}}{r_{max}} \times \frac{(365\ d/year)}{(1000\ g/kg)} \tag{3.1}$$

$$V_{slag} = \frac{m_{slag}}{\rho_{slag}} \tag{3.2}$$

Equations 3.1 and 3.2 were used to design a full-scale application. Q_{slag} was chosen based on experimental results.

Table 3.3 : Parameters for equations 3.1 and 3.2

Description	Symbol	Units
Required lifetime	T_{life}	year
Dry density of slag filter	ρ_{slag}	kg slag/m^3
Total influent flowrate in septic tank	Q	L/d
Influent flowrate in the slag filter	Q_{slag}	L/d
Influent conc. of the slag filter	$c_{i\text{-}slag}$	mg P/L
Effluent conc. of the slag filter	$c_{o\text{-}slag}$	mg P/L
P retention capacity of slag filter	r_{max}	g P/kg slag
Mass of slag filter	m_{slag}	kg slag
Volume of slag filter (including porosity)	V_{slag}	m^3

3.3 Results

3.3.1 Wastewater composition monitoring

COD, *TSS* and *VSS* results are presented in Figure 3.2. Both systems were efficient for settling, as shown in Figure 3.2. *TSS* were reduced below 70 mg/L after the first compartment. The settling

efficiency was not changed by the drastic increase of influent *TSS* related to the change of wastewater. *VSS* and *COD* curves were similar to *TSS* curves.

The effect of the slag filter on P removal is shown in Figure 3.3. The slag filter had a negligible effect on the total P and o-PO_4 removal at recirculation ratio of 5 and 10%, while recirculation ratio of 25 and 50% reduced the P concentration at effluent. pH at the outlet of the slag filter was kept at 11 for the whole test duration. The slag filter increased pH in the first and second compartments from 7.5 to up to 9. pH 9 represents a discharge target in the infiltration bed suitable for P precipitation (Robertson, Schiff & Ptacek, 1998; Valsami-Jones, 2001). The system was stable, as concentrations of the second 10% phase were similar to concentrations of the first 10% phase. Low o-PO_4 concentrations were related to high pH, as reported in past studies (Claveau-Mallet *et al.*, 2012; Vohla *et al.*, 2011). High pH increases OH^- and PO_3^{4-} concentrations, which could result in hydroxyapatite ($Ca_{5(}PO_4)_3OH$) supersaturation and precipitation (Article 3 - Chapter 6; Valsami-Jones, 2001). P concentration at the outlet of slag filter were below 1 mg P/L for TP and below 0.1 mg P/L for o-PO_4.

The slag exhaustion behavior is shown in Figure 3.4. Alkalinity, calcium and conductivity curves were similar: the slag effluent concentration was high at the beginning and it slowly decreased. High calcium, alkalinity and conductivity were related to high pH. Concentrations in the other sampling points were constant and similar to the influent concentration. The concentration of the slag filter effluent of system 1 was higher and decreasing faster than the one of system 2. This difference was probably related to the variability of the slag. The slag filter of system 1 may have contained several reactive slag particles. Previous work conducted by the authors showed that slag behavior can be variable (results not shown). In a full-scale application, slag reactivity and its variability should be characterized to ensure a sufficient filter longevity.

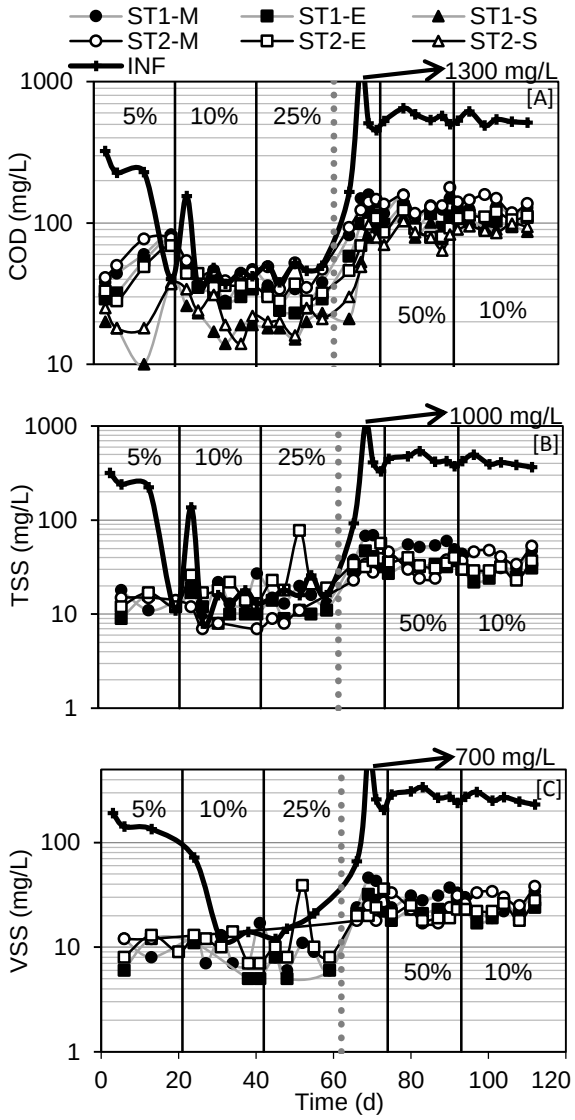

Figure 3.2 : COD (a), TSS (b) and VSS (c) monitoring of the pilot unit

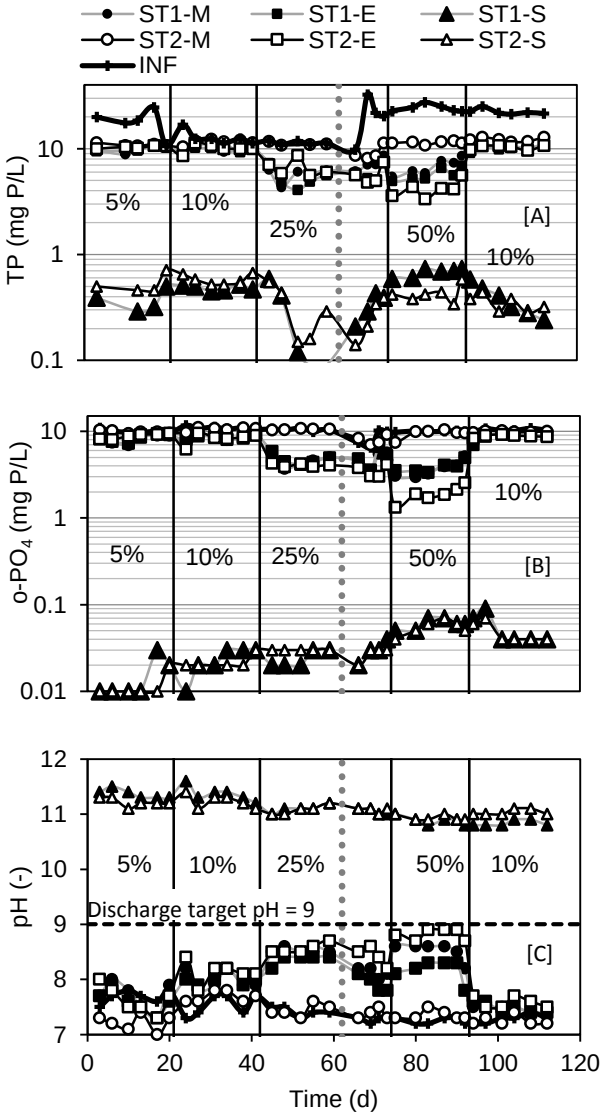

Figure 3.3 : TP (a), o-PO_4 (b) and pH (c) monitoring of the pilot unit

Recirculation phases (5, 10, 25, 50 and 10%) are indicated with vertical lines. The transition from wastewater 1 to wastewater 2 is indicated by the grey dotted line

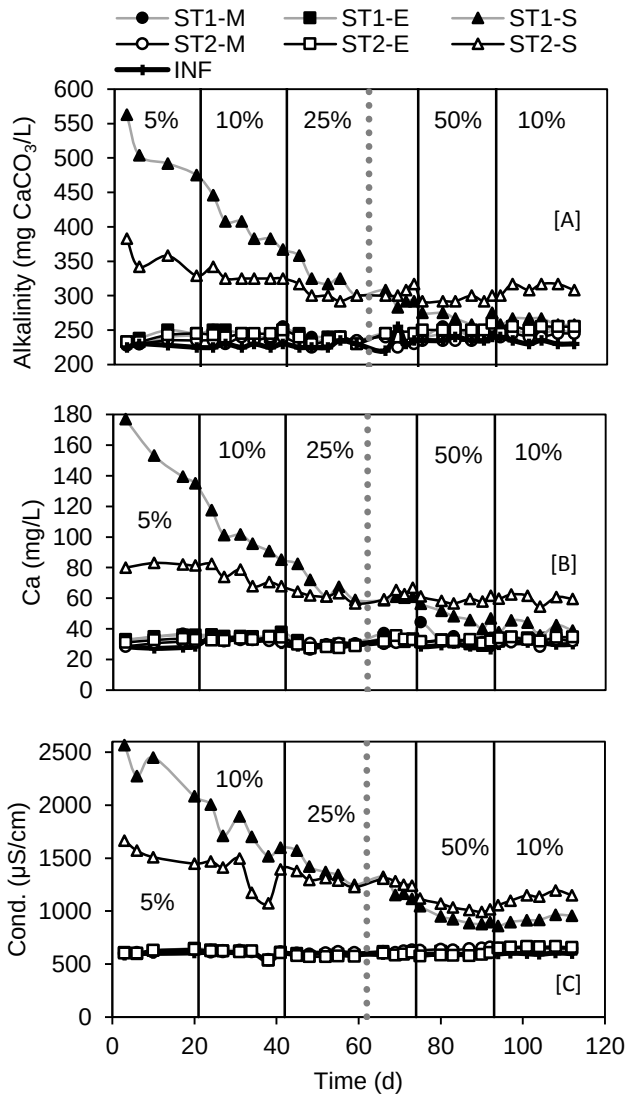

Figure 3.4 : Alkalinity (a), calcium (b) and conductivity (c) monitoring of the pilot unit. Recirculation phases (5, 10, 25, 50 and 10%) are indicated with vertical lines. The transition from wastewater 1 to wastewater 2 is indicated by the grey dotted line

3.3.2 Phosphorus mass balance

A mass balance of TP was performed on both systems at the end of the experiment. The amount of P accumulated in the first compartment, second compartment and slag filter was determined by experimental measurement at the end of the experiment. The amount of total P that passed each tubing section was calculated according to equation 3.3.

$$AP_z = \sum Q c_i \Delta t_i \tag{3.3}$$

where AP_z is the amount of P in tubing section z (g P), Q the influent flowrate (L/d), c_i is the concentration of P in interval i (mg P/L) and Δt_i is the duration of interval i (d). Accumulated amounts of P in each unit or tubing section are shown in Figure 3.5. The mass balance was calculated according to the following equation:

$$Mass\ balance\ (\%) = \frac{Accumulated\ P + Outlet\ P}{Inlet\ P} \tag{3.4}$$

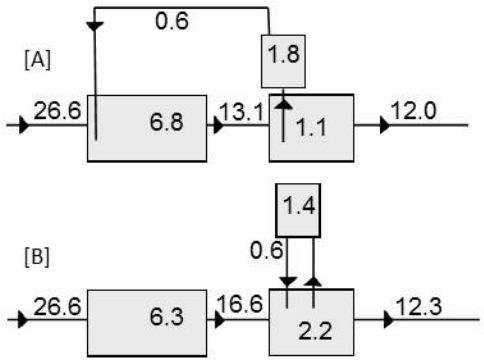

Figure 3.5 : TP fluxes (units in g) for the whole duration of the experiment in system 1(a) and 2 (b). Fluxes are indicated next to arrows. Accumulated P measured at the end of the experiment is indicated in each compartment

The global mass balances were 82% and 83% for systems 1 and 2, respectively. Mass balances for each unit are less accurate but they remain satisfying considering the technical challenges for representative sampling of coarse media. Amounts of accumulated P were similar in both systems, except for the second compartment, where P was more retained in system 2, which is advantageous (Figure 3.5). Accumulated P is divided in two fractions: stabilized organic matter in septic tanks (~84%), and precipitates of calcium phosphate in the slag filter (~16%). In a full-scale application, P from the slag filter could be recovered in agricultural uses (Bankole, Rezan, & Sharif, 2011), while P from the septic tank would be sent to subsequent treatment facilities according to the routine emptying of the tank.

3.4 Discussion

3.4.1 P Removal Performance and Selection of the Best System

A comparison of TP and o-PO_4 concentration at the effluent of the pilot unit for all recirculation phases and both systems is presented in Figure 3.6. Recirculation ratio of 5 and 10% did not result in satisfying P removal, with concentration at effluent of ~8 mg P/L o-PO_4 and ~10 mg P/L TP. The 25% and 50% recirculation ratio were better with ~5 and ~6 mg P/L at effluent, but they did not achieve the objective of 1 mg P/L. The 50% ratio for system 2 resulted in the lowest P concentrations of ~3 and ~4 mg P/L for o-PO_4 and TP and it was the recommended system (Figure 3.7).

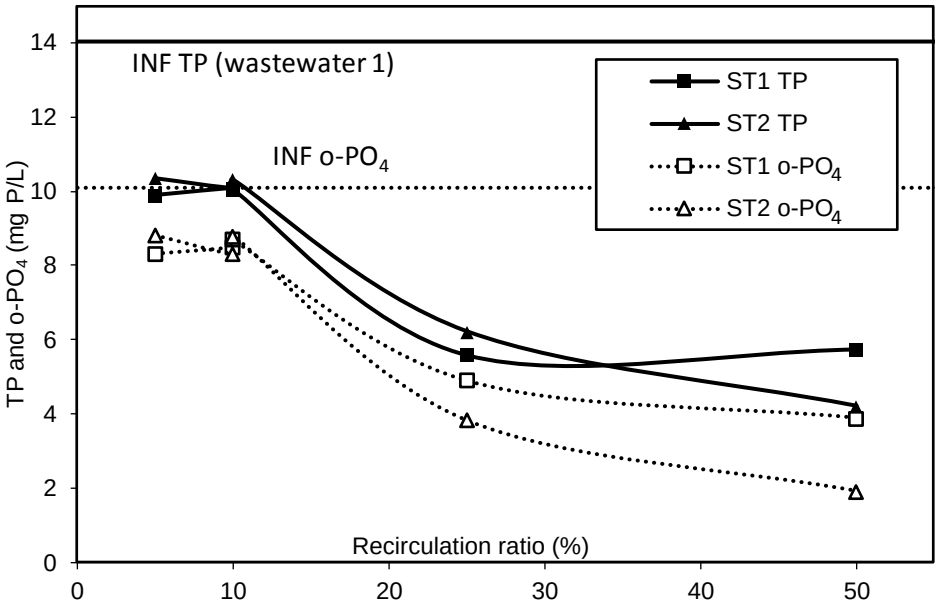

Figure 3.6 : Relationship between mean P concentration at the effluent of the pilot unit and recirculation ratio

The recommended system achieved 4.2 mg P/L and 1.9 at effluent for TP and o-PO_4, compared to 10 and 9 mg P/L with a 5% recirculation ratio. This result represents a significant amount of P removal, but it did not reach the initial objective of 1 mg P/L TP. The objective may be reached by the following infiltration bed, where filtration and precipitation should occur (Robertson, Schiff & Ptacek, 1998). As the pH entering the infiltration bed is raised by the slag filter to 8.8, calcium phosphate precipitation could be favoured in the infiltration bed (Metcalf & Eddy., 2003). Stable

calcium phosphates as hydroxyapatite could form and stop P migration (Valsami-Jones, 2001). Thus, the combination of the recommended system with the infiltration bed could result in water infiltrating in the natural soil with less than 1 mg P/L of TP. The subsequent step of this project would be to install the system in a real septic tank and monitor water properties in the infiltration bed.

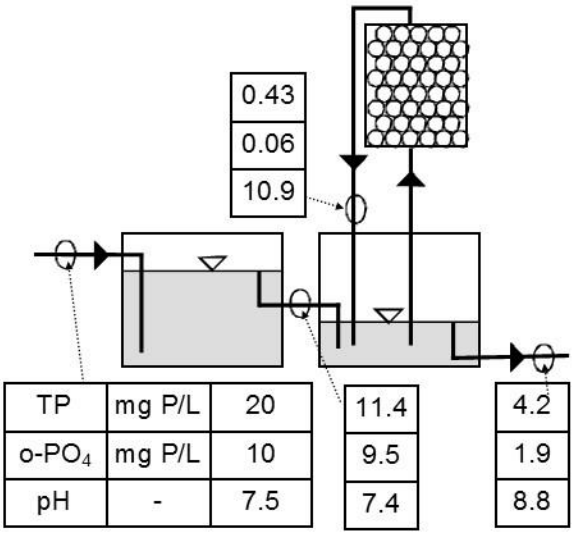

Figure 3.7 : Recommended system (system 2 with 50% recirculation in the slag filter) and selected wastewater characteristics

3.4.2 Application to a Full-Scale System

The application of the recommended system to an isolated two-bedroom dwelling is presented in Table 3.4.

Calculations presented in Table 3.4 illustrate an iterative process: 1- choice of r_{max}, 2- calculation using equations 3.1 and 3.2, and 3- validation of the HRT_V and filter longevity. If the HRT_V is too low or the longevity too high, then r_{max} is not realistic and a lower value must be used. Criteria values for longevity and HRT_V can be determined following past experimental work or modeling. The choice of r_{max} is critical, as it influences directly the filter mass. r_{max} has to be estimated according previous studies (c. f. Table 3.5). r_{max} is influenced by the HRT_V, influent P concentration and presence of buffers in the water to treat (Article 3 – Chapter 6). The authors recommend to use the *P-Hydroslag* model (Article 3 – Chapter 6) for the determination of r_{max}. This model considers the specific influent composition of each wastewater and the HRT_V of the filter. It also facilitates

the validation step, as the model uses a known HRT_V and it calculates the filter longevity. According previous work using the P-hydroslag model with similar conditions, the authors recommend r_{max} = 2 g P/kg slag (second line of Table 3.5: the model results in r_{max} = 2.3 g P/kg slag, HRT_V = 16 h and longevity = 820 pore volumes). The validation criterion provided by the model is respected: 23.1 h > 16 h and 760 pore volumes < 820 pore volumes. The corresponding filter mass is 1875 kg. The *P-Hydroslag* model is a useful tool, as it considers the specific composition of the wastewater and of the slag. It is also possible to evaluate the sensitivity of given parameters (HRT_V, P concentration, etc.) on r_{max} and longevity.

Table 3.4 : Application of the proposed system to an isolated two-bedromm dwelling

Description	Parameters	Units	Value			Comments
Input						
Required lifetime	T_{life}	years	2			From Quebec requirements (MDDEP, 2009a)
Dry density of slag filter	ρ_{slag}	kg slag/m^3	1800			Estimated assuming 50% porosity
Total influent flowrate	Q	L/d	1080			For a 2-bedroom house
Influent flowrate in the slag filter	Q_{slag}	L/d	540			50% recirculation
TP concentration at the inlet of the slag filter	$c_{i\text{-}slag}$	mg P/L	10			From this study
TP concentration at the outlet of the slag filter	$c_{o\text{-}slag}$	mg P/L	0.5			From this study
Scenarios for 3 assumptions						
P retention capacity of the slag filter	r_{max}	g P/kg slag	2	3	4	see Table 3.5
Calculation						
Slag filter mass	m_{slag}	kg slag	1875	1250	938	From Equation 3.1
Slag filter volume	V_{slag}	m^3	1.04	0.69	0.52	From Equation 3.2
Validation						
Voids hydraulic retention time of the slag filter	HRT_V	H	23.1	15.4	11.6	Ok if HRT_V high enough (see text)
Filter longevity	FL	pore volumes	758	1143	1516	Ok if longevity low enough (see text)
Similar calculations for a 6-bedroom house						
Slag filter mass	m_{slag}	Kg	5610	3740	2805	Corresponds to Q = 3240 L/d (MDDEP, 2009a)

The recommended value for r_{max} (2 g P/kg slag) may seem prudent when compared to other past experimental values (up to 6 g P/kg slag, (Claveau-Mallet *et al.*, 2012)). However, these slag filters were fed with synthetic solutions containing only o-PO_4 salts. If inorganic carbon, particulate matter or other buffers were added to the influent, r_{max} would probably be lower. Past work showed that the presence of inorganic carbon reduces r_{max} (Article 3 – Chapter 6). Ideally, the *P-Hydroslag* model should be run with data obtained from a representative wastewater sample.

Table 3.5 : P retention capacity obtained in previous studies conducted with the same slag

Influent o-PO_4	HRT_V of slag	Retention capacity[a]	Longevity[a]	Type of water	Ref	Notes
mg P/L	h	mg P/g slag	pore volumes			
10	16	3.2	1200	Num. simulations	Article 3 - Chapter 6	P as o-PO_4 only in distilled water
10	16	2.3	820	Num. simulations	Article 3 - Chapter 6	P as o-PO_4 only, water contained 0.5 mM $NaHCO_3$
10	?	>2	?	Fishfarm effluent	(Chazarenc *et al.*, 2007)	On-site pilot unit
26	16.3	>6.3	>911	Synthetic	(Claveau-Mallet *et al.*, 2012)	P as o-PO_4 only in distilled water
27	3.8	1.1	200	Synthetic	(Claveau-Mallet *et al.*, 2012)	P as o-PO_4 only in distilled water
2-8	15	>0.5	>677	Fishfarm effluent	(Brient, 2012; Mahadeo, 2013)	On-site pilot unit preceded by slag filter
2-8	6	0.9	1722	Fishfarm effluent	(Brient, 2012; Mahadeo, 2013)	On-site pilot unit preceded by slag filter
20 to 120	24	2.2	113	Synthetic	(Lospied, 2003)	P as o-PO_4 only in distilled water
26 to 130 TP	31	>3.6 (for TP)	>209 (for TP)	Reconstituted fishfarm effluent	(Abderraja Anjab, 2009)	Preceded by 93 void volumes of tap water feeding

[a]: Retention capacity and longevity reached when the effluent concentration exceeds 1 mg P/L o-PO_4

On a full-scale application, the slag filter effluent composition should be monitored to insure that pH is kept above 10. pH monitoring as a control method is a challenge, as pH may drop suddenly with a corresponding decrease in P removal efficiency as have been observed with slag filters (Article 3 – Chapter 6; Claveau-Mallet *et al.*, 2012). One way to overcome this problem would be to monitor slag filter by conductivity. As the conductivity decrease is regular (Figure 3.4) and is

related to high pH, it would be possible to define a conductivity criteria after which the filter is not any more efficient. The development of such a methodology will be part of future work.

3.5 Conclusion

The objective of this project was to improve the P retention capacity of a conventional septic tank by adding a recirculating slag filter. The best tested system at bench scale with a reconstituted wastewater influent was by recirculating within compartment 2 with a 50% recirculation ratio in the slag filter, achieving 4.2 and 1.9 mg P/L at the effluent for TP and o-PO_4, respectively, and pH 8.8. The calculated mass of the slag filter for a 2-bedroom house application was 1875 kg. The 1 mg P/L goal was not reached, but P precipitation should be favoured by the relatively high effluent pH reaching the infiltration bed. This study will be followed by a full-scale project in a septic tank, including monitoring of the infiltration water.

3.6 Acknowledgements

The authors warmly thank Denis Bouchard for P analysis and Manon Leduc for calcium analysis. This project was funded by the Natural Sciences and Engineering Research Council of Canada.

3.7 References

Abderraja Anjab, Z. (2009). *Development of a steel slag bed for phosphorus removal from fishfarm wastewater (In French).* (M.A.Sc. thesis, Polytechnique Montreal, Canada).

APHA, AWWA & WEF. (2012). Standard methods for the examination of water and wastewater (22nd ed.). Washington, D. C: American Public Health Association, American Water Works Association & Water Environment Federation.

Bankole, L. K., Rezan, S. A., & Sharif, N. M. (2011). Thermodynamic modeling of mineral phases formation in EAF slag system and its application as agricultural fertilizer. *SEAISI Quarterly (South East Asia Iron and Steel Institute), 40*(4), 26-32.

Brient, S. (2012). *Dephosphatation of a fish farm wastewater with extensive steel slag fiters (in French).* (M.A.Sc. thesis, Polytechnique Montreal, Canada).

Chazarenc, F., Brisson, J., & Comeau, Y. (2007). Slag columns for upgrading phosphorus removal from constructed wetland effluents. *Water Science and Technology, 56*, 109-115.

Chazarenc, F., Kacem, M., Gérente, C., & Andrès, Y. (2008). *'Active' filters: a mini-review on the use of industrial by-products for upgrading phosphorus removal from treatment wetlands.* Paper presented at the 11th Int. Conf. on Wetland Systems for Water Pollution Control, Indore, India, November 1 – November 7.

Claveau-Mallet, D., Courcelles, B., & Comeau, Y. (2014). Phosphorus removal by steel slag filters: Modeling dissolution and precipitation kinetics to predict longevity. *Environmental Science and Technology, 48*(13), 7486-7493.

Claveau-Mallet, D., Wallace, S., & Comeau, Y. (2012). Model of phosphorus precipitation and crystal formation in electric arc furnace steel slag filters. *Environmental Science and Technology, 46*(3), 1465-1470. doi:10.1021/es2024884

Evoqua Water Technologies. (2014). Biomag system for enhanced secondary treatment. Retrieved from www.evoqua.com/en/products/separation_clarification/ballasted-clarifiers/Pages/biomag-system.aspx, accessed on December 26, 2014.

Lospied, C. (2003). *Evaluation of steel slag capacity and removal conditions for dissolved phosphorus (In French).* (M.A.Sc. thesis, Polytechnique Montreal, Canada).

Mahadeo, K. (2013). *Treatment of fish farm sludge supernatant with aerated filter beds and steel slag filters - Effect of organic matter and nutrient loading rates.* (M.Eng. thesis, Polytechnique Montreal, Canada).

MDDEP. (2009a). *Guide technique - traitement des eaux usées des résidences isolées*. Québec: Ministère du développement durable, de l'environnement et des parcs.

Metcalf & Eddy. (2014). *Wastewater engineering: treatment and reuse* (5th ed.). New York: McGraw-Hill.

National Slag Association. (2009). General Information about National Slag Association (NSA). Retrieved from http://www.nationalslag.org/nsageneral.htm, accessed on March 16, 2012.

Premier Tech Aqua. (2014). Premier Tech Aqua products. Retrieved from http://premiertechaqua.com/assainissement-traitement-eaux-usees/biofiltre-entrepreneur-desinfection#1389, accessed December 26, 2014.

Robertson, W. D., Schiff, S. L., & Ptacek, C. J. (1998). Review of phosphate mobility and persistence in 10 septic system plumes. *Groundwater, 36*(6), 1000-1010.

Shilton, A. N., Elmetri, I., Drizo, A., Pratt, S., Haverkamp, R. G., & Bilby, S. C. (2006). Phosphorus removal by an 'active' slag filter-a decade of full scale experience. *Water Research, 40*(1), 113-118.

Szabó, A., Takács, I., Murthy, S., Daigger, G. T., Licskó, I., & Smith, S. (2008). Significance of design and operational variables in chemical phosphorus removal. *Water Environment Research, 80*(5), 407- 416.

Valsami-Jones, E. (2001). Mineralogical controls on phosphorus recovery from wastewaters. *Mineralogical Magazine, 65*(5), 611-620.

Vohla, C., Kõiv, M., Bavor, H. J., Chazarenc, F., & Mander, Ü. (2011). Filter materials for phosphorus removal from wastewater in treatment wetlands-A review. *Ecological Engineering, 37*(1), 70-89.

Yamada, H., Kayama, M., Saito, K., & Hara, M. (1986). A fundamental research on phosphate removal by using slag. *Water Research, 20*(5), 547-557.

CHAPTER 4 GENERAL DISCUSSION AND RECOMMENDATIONS RELATED TO STEEL SLAG FILTERS APPLICATIONS IN AUTONOMOUS AND DECENTRALIZED TREATMENT

This chapter is a synthesis related to Objective 1 which was "propose a phosphorus treatment system based on a steel slag filter integrated to a septic-tank-infiltration-bed system". Firstly, each design criterion is discussed regarding fulfillment or not. Secondly, an additional discussion and synthesis related to Paper #1 is provided. Finally, both design approaches presented in Chapter 2 are compared, and recommendations are presented.

4.1 Critical discussion regarding the thesis objective

Objective 1 was fulfilled with the proposition of a slag filter system as presented in Paper #1. This system includes a slag filter operated in a recirculation mode at 50% influent flowrate within the second compartment of the septic tank. The resulting total P concentration at effluent was 4.2 mg P/L. The 1 mg P/L total phosphorus target was not reached, however, a significant P retention improvement was observed. With this slag filter configuration, 79% of total P was kept in slag filter and septic tank before being discharged in the infiltration bed. Without slag filter, only 29% of total P was kept in the septic tank. The o-PO_4 removal efficiency was especially improved, with 1.9 mg P/L at effluent, compared to 8.5 mg P/L without slag filter. While particulate phosphorus may be filtrated and kept in the infiltration bed, o-PO_4 migrate more easily from the infiltration bed to the water table. Thus, focus should be given to o-PO_4 removal more than total phosphorus removal.

Results from Paper #1 are considered promising regarding the 1 mg P/L discharge criteria, but more work is needed to evaluate the final phosphorus concentration in discharge water (reaching water table after infiltration bed). The proposed recirculating slag filter increased the o-PO_4 retention of the septic tank, which is a crucial improvement, considering high migration potential of o-PO_4 in the water table (Robertson, Schiff & Ptacek, 1998). The full characterization of the system P retention capacity would need additional studies regarding P retention in infiltration bed. Important aspects that should be considered are precipitation potential in the infiltration bed, filtration and stability of particulate P, and P leaching risks from septic tank if the slag filter is exhausted.

The discharge criteria defined in this thesis also included secondary treatment criteria for BOD_5 (25 mg/L) and TSS (30 mg/L). As explained in Chapter 2, a conventional infiltration bed is assumed to meet secondary treatment criteria. This assumption is safe, as design loading rate for infiltration bed is much smaller then ones for comparable (but more intensive) effective processes as tricking filters (Metcalf & Eddy *et al.*, 2014) or wetlands (Kadlec & Wallace, 2009). The effect of pH rise of septic tank effluent on biological removal of the infiltration bed was not studied, but it was assumed to be small, as pH 6-9 is tolerable for biological treatment (Metcalf & Eddy *et al.*, 2014).

In the presented study, longevity was not directly assessed as the slag filter was oversized. The required HRT_V (and filter size) for insuring a two-year longevity could be evaluated using numerical simulations (as presented in section 9.3.1). Costs of the proposed system were not directly evaluated. Transportation of slag and easiness of replacement will be important aspects to consider in costs analysis.

4.2 Phosphorus fractionation in the system

In the proposed system, phosphorus is trapped and accumulated in three compartments: steel slag filter, septic tank and infiltration bed. Phosphorus removal in the steel slag filter observed in paper #1 was high, and relatively easy to predict, as shown in Figure 2.4.

It would be interesting to understand removal mechanisms in the septic tank, as it is the only compartment where phosphorus could be easily recovered in maintenance operations (enriched sludge eventually sent to a nutrient recovery process). One important issue is to assess if calcium-phosphate-based mechanisms are controlling P removal in the septic tanks, as it is the case in a steel slag filter. In order to answer this question, data from paper #1 was superimposed to Figure 2.4 (Figure 4.1). Slag filter effluent data had a pH around 11, and was following the 0.01-0.1 mg P/L range, as observed in previous study. Septic tank effluent data was located between pH 7.5 and 9, and it followed the general decreasing tendency observed in previous steel slag filter studies. This observation suggests that in a 'slag-leachate-doped' septic tank, o-PO_4 is removed via calcium-phosphate precipitation in the same way then in steel slag filter. This conclusion has important implication for design: it is therefore possible to predict o-PO_4 retention in the septic tank for a known pH. Note that the increasing data spread following pH may be attributed by the

logarithmic scale that emphasis o-PO_4 uncertainty at low o-PO_4, and also to HRT_V not being high enough to achieve a low pH. The o-PO_4 decreasing slope is greater after pH of 10.5; it may be explained by the increasing PO_4^{3-} concentration after pH 10.5 (PO_4^{3-} is the specie that contributes to hydroxyapatite saturation). Following the decreasing tendency, it is possible to predict that o-PO_4 concentration at the septic tank effluent would be close to 1 mg P/L if pH was raised at 9.5 in the septic tank. Recommendation from paper #1 was 50% recirculation flowrate with pH = 9 at the septic tank effluent, but it would be promising to increase slightly the recirculation rate to achieve pH = 9.5 and improve P retention.

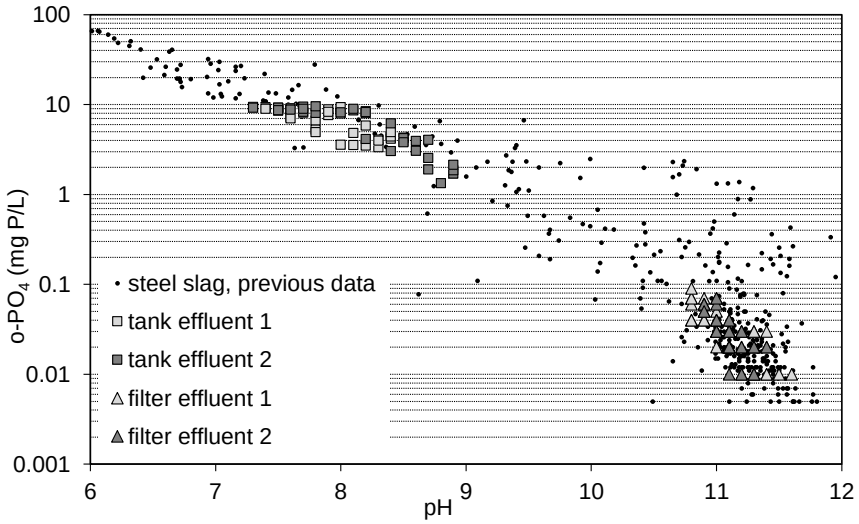

Figure 4.1 : o-PO_4-pH relationship in the septic tank compared to previous steel slag filter data

In the infiltration bed, calcium-phosphate precipitation may not be the only removal mechanism, as reported by Robertson *et al.* (1998). This author studied several o-PO_4 plumes under mature conventional septic systems. Using saturation index calculation for several phosphate mineral phases, he concluded that phosphorus removal is controlled by iron, as o-PO_4 plumes were equilibrated with iron phases as variscite and strengite. At high pH (pH=8), o-PO_4 concentrations increased, and HAP supersaturation was observed. Saturation index calculations were done considering the standard bulk solubility of HAP from PHREEQC database (10^{-55} M^9). In the modeling work presented in this thesis, it was shown that HAP solubility product is much higher because of crystal size (explained in section 8.2.4.1). HAP equilibrium lines were simulated using PHREEQC considering a solubility of 10^{-46} M^9 to account for fine-particle solubility. Different possible calcium concentrations were tested and initial o-PO_4 of the groundwater was set at 3 mg/L.

Results are shown in Figure 4.2A. At pH 8, no phosphorus reduction was observed. At pH 8.5, o-PO_4 reduction was possible only under high calcium concentration (50 mg /L or higher). At low calcium concentration (25 mg/L), o-PO_4 concentration remained unchanged until pH 8.6. Hydroxyapatite equilibrium lines shown in Figure 4.2 are more realistic then these presented by Robertson *et al.* (1998), who observed relatively high o-PO_4 concentration in pH = 8 plumes.

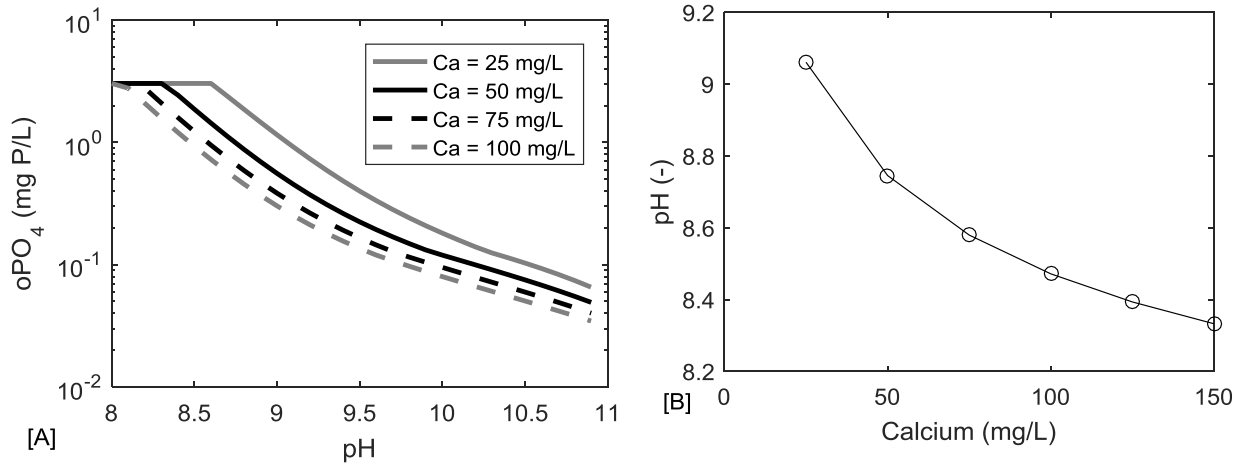

Figure 4.2 : theoretical o-PO_4 concentration in a groundwater in equilibrium with hydroxyapatite (A) and theoretical needed pH for achieving 1 mg P/L o-PO_4 in a groundwater in equilibrium with hydroxyapatite (B)

Theoretical needed pH for reaching 1 mg P/L o-PO_4 (Figure 4.2B) shows that water in the infiltration bed should have a pH higher than 8 to achieve satisfactory phosphorus removal. Calcium concentration plays an important role as it is involved in hydroxyapatite solubility. At low calcium concentration, pH has to be much higher to achieve efficient phosphorus removal (at calcium = 25 mg/L, needed pH is 9). Steel slag may contribute to increase the calcium concentration of infiltration water, as it leaches CaO. Results from paper #1 showed, however, that calcium concentration at the septic tank effluent was not increased by the presence of slag filter, even at 50% recirculation rate. This could be explained a calcium consumption in the septic tank for phosphorus precipitation.

One important aspect of P precipitation in infiltration bed is the buffering effect of atmospheric CO_2. High pH infiltration water may be rapidly equilibrated by atmospheric CO_2 input. If the CO_2 transfer rate is higher than the hydroxyapatite precipitation rate, precipitation may not happen.

One question to evaluate is the possible solubility reduction of hydroxyapatite following long-term crystal growth, as infiltration beds are typically operated for 25-30 years. This crystal growth and solubility reduction seems to not take place, as mature septic systems infiltration water reported by Robertson *et al.* (1998) was more likely equilibrated with fine hydroxyapatite (Figure 4.2A).

4.3 Comparison of all-inflow (tertiary treatment unit) and recirculating (filters added to existing tanks) approaches

Two possible answers to this thesis first objective were presented in section 2.1.3: development of a new tertiary treatment unit (currently under development at *Bionest* industrial partner) or upgrading of existing tanks (paper #1). These two systems are compared in Table 4.1 following several criteria. In this table, longevity is assumed to be two years for both options.

Table 4.1 : Development and operational issues related to new tertiary treatment slag filter units VS improved existing tanks with recirculating slag filters

Criteria	Option 1 New tertiary treatment unit	Option 2 Improved existing tanks
Regulation context	Implementation of systems motivated by applicable discharge criteria for phosphorus and lack of affordable technologies	Implementation of systems driven by voluntary motivation only (no regulation)
Required filter volume	2.43 m^3 for 3-bedroom houses (assuming HRT_V = 18 h)	1.62 m^3 for 3-bedroom houses (assuming HRT_V = 24 h and 50% recirculation)
Clogging of slag filter	Low risk (slag filter fed with secondary effluent)	High risk (slag filter fed with primary effluent)
Target P concentration	Accurate control of effluent P concentration needed	No control needed
Expected TP at effluent	0.5 mg/L (at steel slag filter effluent)	1-2 mg P/L (at septic tank effluent)
P recovery potential	70% (See Table 4.2)	76.5%
Construction effort	Low (primary and secondary units have to be built anyway)	High (digging in existing sites not wished)

From a regulation point of view, option 1 is the more realistic scenario. In Quebec, there is a lack of affordable tertiary treatment technologies suitable for autonomous and decentralized

applications, and steel slag filters represent a potential solution with their simplicity and low cost. Concerning option 2, even if regulations change for phosphorus, it is reasonable to believe that existing conventional septic tanks would be replaced to meet tertiary treatment requirements, and we go back to option 1.

Recirculation is interesting because it decreases the needed volume for the reactor. Assuming HRT_V = 18 for option 1 and 24 h for option 2, the needed volume for option 2 is 33 % smaller than the needed one for option 1. Note that a higher HRT_V was assumed for option 2 to consider the effect of influent type. While steel slag filter is fed with a secondary effluent in option 1, it is fed directly from the septic tank in option 2. The steel slag filter in option 2 would therefore be more subject to clogging, explaining why design HRT_V was increased to 24 h. In practice, it may be more interesting to implement option 1 with a bigger reactor in a project that already involves the construction of primary and secondary units, compared to an existing tank where digging and installation of a new reactor is not wished. For option 2, it would have been interesting to install the steel slag filter within the existing tank to limit construction perturbations, but the needed filter volume is too big to allow it.

Table 4.2 : o-PO_4 mass balance comparison between options 1 and 2

	Option 1 New tertiary treatment unit	Option 2 Improved existing tanks
effluent o-PO_4 (mg P/L)	0.5 (slag filter effluent)	1.9 (septic tank effluent)
P mass in effluent (%)	10	19
P mass in primary (and secondary for option 1) reactors (%)	70	76.5
P mass in slag filter (%)	20	4.5

From a nutrient recovery point of view, option 2 is slightly better than option 1. Nutrient recovery from steel slag filter is not easy, or even impossible, as steel slag filter at the end of lifetime is cemented into a block, and phosphorus precipitates are part of the cement in a stable form. It would be therefore preferable to accumulate phosphorus in biological or primary reactors in which sludge can be sent to a subsequent nutrient recovery unit. P mass balance (o-PO_4 only) for both options is

presented in Table 4.2, assuming 10 mg P/L at influent and 1 mg/L at slag filter effluent (for both options). A 50% recirculation rate was assumed and o-PO_4 concentrations in this system were chosen following Figure 3.7. While option 2 involves a higher o-PO_4 concentration at effluent, the recoverable P fraction is slightly higher (76.5% instead of 70%).

For both options, installation and replacement logistics is a real challenge. Accurate longevity prediction of steel slag filters and choose of design HRT_V is also a concern for both options. Longevity prediction is critical for option 1, as a target phosphorus concentration is required by regulations. The expected TP concentration at effluent for option 1 is known from previous studies (Kõiv *et al.*, 2016) and from *Bionest* R&D results. In option 2, there is no accurate target to meet, but the steel slag longevity may be affected by clogging. In option 2, the expected TP concentration at the effluent of septic tank was postulated following results from paper #1 (Chapter 3), assuming that P retention would be slightly improved by increasing the recirculation rate.

4.4 Recommendations

It is recommended to evaluate precisely the effect of influent type (primary of secondary) on steel slag filter efficiency and longevity. Steel slag filters are efficient for secondary effluent treatment (as project presented in complementary paper) or inorganic effluent treatment (as project presented in paper #2), but their efficiency for primary effluent treatment is not clearly established. A design HRT_V of 24 h was proposed (Table 4.1), but it was not demonstrated that this HRT_V would insure a two-year longevity. Additional studies should be conducted to evaluate the exact needed HRT_V for primary effluents.

It is recommended to validate the P-Hydroslag model (presented in Chapter 8) as a longevity prediction modeling tool in first experimental applications of both options. More precisely, the model should be adapted to consider the organic matter effect from primary effluents (modeling recommendations are discussed in section 9.5). If validated, the P-Hydroslag model could be used for design optimization of these systems. For steel slag filters, optimization means finding a compromise between slag filter size and replacement frequency.

It is recommended to test the system proposed in paper #1 (recirculation within the second compartment at 50% flowrate) in a pilot-scale study. This study would validate the efficiency of this system in real conditions. Testing of higher recirculation rates (50 to 75%) should be

considered in order to reduce P concentration at the effluent of the septic tank and favor P removal within the infiltration bed. Water at different depths of the infiltration bed should be sampled and monitored to assess P removal within the infiltration bed. Study of P removal in infiltration beds could be refined by a more controlled lab-scale test. Aspects to consider in a future study are:

- Find an optimal HRT_V of the slag filter regarding filter longevity and resulting outlet pH going to the septic tank,
- Evaluate the stability of the removal efficiency,
- Optimize the recirculation piping positions in the septic tank to minimize sludge pumping in the slag filter,
- Assess the behavior and stability of particulate P in the system,
- Evaluate potential P leaching from the septic tank if the slag filter exhausts,
- Validate P removal mechanisms in the bed soil by sampling mineral phases,
- Evaluate the effect of competing precipitation of calcite and redox chemistry,
- Evaluate the effect of high pH on biological treatment in the infiltration bed,
- Evaluate the effect of type of soil on P retention in the infiltration bed,
- Evaluate the buffering effect by atmospheric CO_2 on P removal in the infiltration bed.

CHAPTER 5 ARTICLE 2: REMOVAL OF PHOSPHORUS, FLUORIDE AND METALS FROM A GYPSUM MINING LEACHATE USING STEEL SLAG FILTERS

Claveau-Mallet, D., Wallace, S. & Comeau, Y. (2013). Removal of phosphorus, metals and fluoride from a gypsum mining leachate using steel slag filters. *Water Research*, 47(4), 1512-1520.

ABSTRACT

The objective of this work was to evaluate the capacity of steel slag filters to treat a gypsum mining leachate containing 11-107 mg P/L ortho-phosphates, 9-37 mg/L fluoride, 0.24-0.83 mg/L manganese, 0.20-3.3 zinc and 1.7-8.2 mg/L aluminum. Column tests fed with reconstituted leachates were conducted for 145 to 222 days and sampled twice a week. Two types of electric arc furnace (EAF) slags and three filter sequences were tested. The voids hydraulic retention time (HRT_v) of columns ranged between 4.3 and 19.2 h. Precipitates of contaminants present in columns were sampled and analyzed with X-ray diffraction at the end of tests. The best removal efficiencies over a period of 179 days were obtained with sequential filters that were composed of Fort Smith EAF slag operated at a total HRT_v of 34 h which removed 99.9% of phosphorus, 85.3% of fluoride, 98.0% of manganese and 99.3% of zinc. Mean concentration at this system's effluent was 0.04 mg P/L ortho-phosphates, 4 mg/L fluoride, 0.02 mg/L manganese, 0.02 zinc and 0.5 mg/L aluminum. Thus, slag filters are promising passive and economical systems for the remediation of mining effluents. Phosphorus was removed by the formation of apatite (hydroxyapatite, $Ca_5(PO_4)_3OH$ or fluoroapatite, $Ca_5(PO_4)_3F$) as confirmed by visual and X-ray diffraction analyses. The growth rate of apatite was favored by a high phosphorus concentration. Calcite crystals were present in columns and appeared to be competing for calcium and volume needed for apatite formation. The calcite crystal growth rate was higher than that of apatite crystals. Fluoride was removed by precipitation of fluoroapatite and its removal was favored by a high ratio of phosphorus to fluoride in the wastewater.

Keywords: Wastewater treatment, slag filters, mining remediation, hydroxyapatite growth

5.1 Introduction

Mining operations can have major impacts on the environment and indirectly affect human health. The site closure is a determinant step to limit long-term damage caused by mining leachate. Mining residual tailings are stocked in piles that can reach large dimensions. If rain and surface water are not well controlled, they may become contaminated while flowing through piles and discharged in the environment. While many modern mining companies take responsibility to restore the site after the mine life, old orphan mining sites still exist and create contamination from mining leachates. Gypsum mining leachates may favor eutrophication and be toxic as they contain high concentration of phosphorus, fluoride and metals. The objective of this research was to assess the capacity of steel slag filters for the passive treatment of multi-component gypsum mining leachates.

Slag is a waste material produced in iron and steel mills. When the original ore is melted, metallic and non metallic components are separated. The artificial lava floating over melted iron is recovered and cooled, resulting in slag. Different varieties of slag exist, depending of the metallurgical process it comes from. Two main types of slag are identified by the American National Slag Association: blast furnace slag and steel slag (National Slag Association, 2009). Blast furnace slag is produced from iron mills, where iron ore, flux stone (calcium rich stone) and coke react in a blast furnace. Its main components are silica oxides, alumina, lime and magnesia. Steel slag is produced from basic oxygen furnace (BOF slag) or electric arc furnace (EAF slag), where iron and scrap are processed with lime. Its main components are calcium silicates, aluminoferrites and oxides of calcium, iron, magnesium and manganese. Three types of slag shapes are produced (air cooled, expanded or granulated). Cooling processes determine the porosity and crystalline fraction of slag. Finally, crushing and/or sieving results in different slag grain size, from powder to coarse aggregates.

Using slag for phosphorus removal from wastewater effluents has been studied with short term batch tests, column tests and field scale tests (Chazarenc *et al.*, 2008; Vohla *et al.*, 2011; Yamada *et al.*, 1986). Short-term batch tests remain the most documented approach (Chazarenc *et al.*, 2008), but focus will be given to column and field-scale filters in the next paragraphs. Various types of wastewaters were treated in recent field-scale studies: a contaminant plume from a septic tank (Smyth *et al.*, 2002), effluent of constructed wetlands (Chazarenc *et al.*, 2007), landfill leachates

(Kõiv *et al.*, 2010), effluent of domestic wastewater treatment ponds (Pratt & Shilton, 2010) and fish farm sludge supernatant (Brient, 2012).

Some specific properties of slag filters were addressed in recent studies. Regeneration of slag filters after drying was shown to be possible by Drizo *et al.* (2002), who increased her column retention capacity from 1.35 to 2.35 mg P / g of slag with this process. The hydraulic retention time of slag filters has a direct impact on their removal performances (Liira *et al.*, 2009; A. Shilton *et al.*, 2005). Some authors highlighted important differences between short term tests and pilot tests performance results. Shilton *et al.* (2005) reported that full-scale tests gave higher removal performances than similar tests conducted in columns, possibly because of the influence of algae. Pratt and Shilton (2010) suggested that short-term batch tests are not suitable to characterize performances of slag filters even if phosphorus is treated by adsorption, because long-term slag alteration creates new adsorption sites. The major difficulties related with slag filters are clogging and decline of efficiency after 6 months (Chazarenc *et al.*, 2008). Finally, the formation of hydroxyapatite was observed by many authors when the effluent pH of filters is high (Chazarenc *et al.*, 2008; Vohla *et al.*, 2011).

Fluoride and metals removal was previously studied by adsorption on slag (Huang, Shih, & Chang, 2011; Xu *et al.*, 2011; Zhou & Haynes, 2010). Precipitation of CaF_2 using chemical additives (Yang *et al.*, 2001) or fluidized bed (Aldaco, Irabien, & Luis, 2005) was also documented. Selective precipitation of phosphorus or fluoride from specific wastewaters containing both components was performed using staged chemical processes (Grzmil & Wronkowski, 2006; Warmadewanthi & Liu, 2009; Yang *et al.*, 2001). The utilization of passive slag filters for single-metal removal was documented in several studies (Renman *et al.*, 2009; Smyth *et al.*, 2002), but further work is needed to assess the capacity of such systems to treat wastewaters containing phosphorus, fluoride and metals.

5.2 Materials and Methods

5.2.1 Reconstituted leachates and tested media

Two reconstituted wastewaters were prepared, representing low (L1) and high (L2) concentration leachates from an orphan gypsum mine, located in Joplin, Missouri. Laboratory-grade salts ($CaCl_2$, $NaNO_3$, KH_2PO_4, etc.) were individually dissolved and mixed together in tap water. pH was

adjusted using 25 to 45 mL of H_2SO_4 6N. The resulting solution was settled for about 24 h and the supernatant was used for tests. Reconstituted wastewaters were sampled and analyzed at every new feeding barrel. The composition of reconstituted leachates is shown in Table 5.1.

Table 5.1 : Composition of reconstituted leachates

Component	Units	L1	L2	Component	Units	L1	L2
pH	-	6.92	5.67	Mn	mg/L	0.24	0.83
Na	mg/L	154	311	Zn	mg/L	0.20	3.3
Ca	mg/L	32	177	SO_4	mg S/L	201	317
K	mg/L	17	132	Cl	mg/L	25	265
Mg	mg/L	16	17	o-PO_4	mg P/L	11	107
Al	mg/L	1.7	8.2	F	mg/L	9	37

Two types of slags were used: EAF slag from Fort Smith, Arkansas (FS slag) and EAF slag from Blytheville, Arkansas (B slag). The chemical and mineralogical composition of the tested slags are given in Table 5.2 and Table 5.3. Chemical analyses were performed by Acme Analytical Laboratories (Vancouver, Canada) using $LiBO_2/Li_2B_4O_7$ fusion and dilute nitric digestion followed by ICP-emission spectrometry. Mineralogical composition was determined by X-ray diffraction analysis in the Geology Department of Tartu University, Estonia.

5.2.2 Column tests

Column tests were conducted using transparent Plexiglas columns (17 cm long and 15 cm in diameter) fed continuously with a peristaltic pump from the bottom center (upflow) with the effluent coming out from the top center. Columns were filled with washed and 105°C-dried 5-10 mm slag. The column tests setup is presented in Figure 5.1. Columns were continuously fed for the whole test duration (145 to 222 days, e. g. Figure 5.1) and no backwashing was needed. Feeding was stopped for very short periods to clean tubings. The HRT_V for each column was computed following a weight procedure utilized in permeability tests (ASTM, 2006; Chapuis, Baass, & Davenne, 1989). The effluent of each column was collected once or twice a week for pH, P, F, Ca, Mn, Zn and Al determination. At the end of tests, columns were opened and precipitates were sampled. White precipitates were considered inorganic as no biofilm formation was observed in columns. Precipitates were picked up using a metal spatula and were partly dried using absorbent

paper. The resulting precipitate (having a paste aspect) was dried at room temperature. 22 powder samples were taken.

Table 5.2 : Chemical composition of tested slags

		Slag ID				Slag ID	
Component	Units	B	FS	Component	Units	B	FS
CaO	%	31.7	28.8	Na_2O	%	0.06	0.06
Fe_2O_3	%	29.5	25.2	K_2O	%	0.03	<0.01
Al_2O_3	%	11.9	7.7	Ba	ppm	455	436
SiO_2	%	10.9	14.5	Sr	ppm	301	267
MgO	%	10.3	14.7	Zr	ppm	194	1011
MnO	%	3.29	7.96	Nb	ppm	182	180
Cr_2O_3	%	0.68	1.09	Y	ppm	27	8
TiO_2	%	0.50	0.37	Ni	ppm	<20	103
P_2O_5	%	0.48	0.31	Sc	ppm	6	2
				Total	%	99.4	100.8

B: Blytheville slag; FS: Fort Smith slag

5.2.3 Analytical determinations

pH was determined on water samples in the half-hour following sampling, using a 4-point pH calibration (pH = 4, 7, 10 and 12). Water samples were acidified with H_2SO_4 5N or HNO_3 6N prior to subsequent analyses. Orthophosphates were determined using a Lachat QuikChem 8500 flow injection analyser, using the ascorbic acid method (APHA *et al.*, 2005). Analyses of metals were conducted with an AAnalyst 200 flame atomic absorption apparatus, using a standard mass spectrometry method (MDDEP, 2006). Analyses of sulfates were conducted with the turbidimetric method (APHA *et al.*, 2005). Fluoride concentration was determined using a Cole-Parmer epoxy combined probe filled with KCl 3M.

Table 5.3 : Mineralogical composition of tested slags

			Slag ID	
Mineral phase	Chemical formula	Units	B	FS
Merwinite	$Ca_3Mg(SiO_4)_2$	%	9.2	3.9
Wuesitite	FeO	%	31	42
C2S, beta	Ca_2SiO_4	%	26	29
C4AF	$Ca_2Fe_{0.28}Al_{1.72}O_5$	%	3.5	3.5
Mayenite	$Ca_{12}Al_{14}O_{33}$	%	4.7	2.7
Gehlenite	$Ca_2Al(Si,Al)_2O_7$	%	2.1	0.9
Periclase	MgO	%	3.2	3.3
Akermanite	$Ca_2MgSi_2O_7$	%	2.0	1.7
Magnesioferrite	$MgFe_2O_4$	%	15	5.1
Bredigite	$Ca_{14}Mg_2(SiO_4)_8$	%	3.0	7.3
Spinel, submagnesian	$MgAl_2O_4$	%	0.5	0
Quartz	SiO_2	%	0	0.4
Total		%	99.9	100.0

B: Blytheville slag; FS: Fort Smith slag

Crystal powder samples were analyzed using the X-ray diffraction powder method. A Philipps X'Pert diffractometer operated at 50 kV and 40 mA and a Bragg-Brentano geometry with Cuk_α radiation were used. The Scherrer equation (Cullity, 2001) was used for the determination of the mean crystal size from diffractograms (peak at θ= 25.9° for apatite and θ = 29.5° for calcite). A new parameter was created to qualitatively compare the proportions of apatite and calcite ($CaCO_3$) within samples: the HAP/$CaCO_3$ ratio. It was defined as the ratio between the intensity of the apatite peak at position 2θ = 25.9° and that of the calcite peak at position 2θ = 29.5°.

5.2.4 Toxicity tests

Toxicity tests were performed to assess the environmental innocuity of slag. A 35 g slag sample was placed in a 1000 mL Erlenmeyer flask filled with 700 mL of extraction fluid. Two extraction fluids were tested: distilled water and acetic acid (Toxicity Characteristic Leaching Procedure (TCLP) extraction solution #2 (USEPA, 1992)). The Erlenmeyer was mixed for 24 h, after which

metal concentrations were determined. Samples were tested in duplicates and mean concentrations were reported.

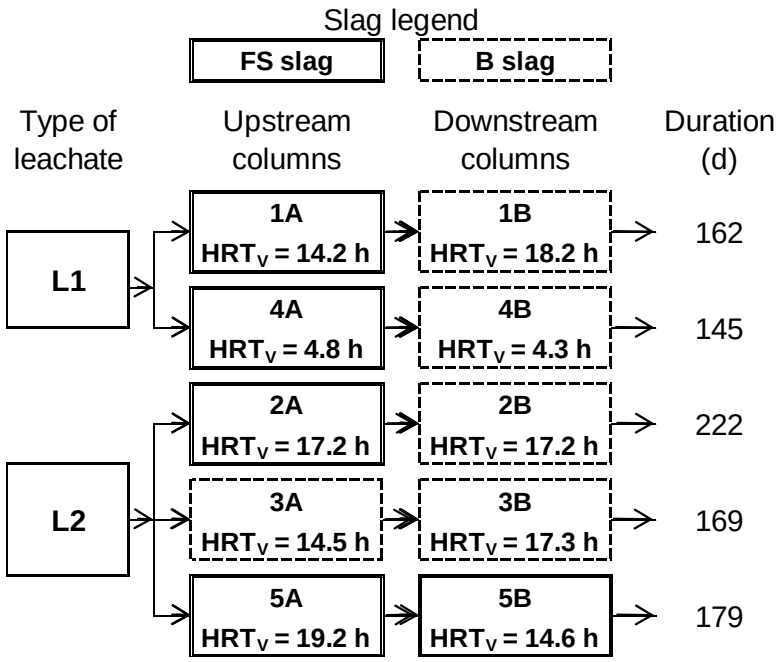

Figure 5.1 : Schematic of the column tests experimental setup and operational conditions

5.3 Results

Results of column tests are presented in Figure 5.2. Exhaustive data tables are presented as online supplementary data. In general, a better removal of contaminants was correlated to high pH and calcium concentrations. Several upstream columns displayed a pH drop during the experiment (Figure 5.2A). The pH drop of the B slag was observed sooner than that of the FS slag. Downstream columns all had an effluent pH over 11, except column 3B which had a pH drop after 70 days of operation (results not shown). Phosphorus concentration was between 0.01 and 1 mg P/L when the effluent pH was over 10 independently of the slag type (Figure 5.2C). In general, downstream filters polished the upstream filters' effluent to concentrations between 0.01 and 0.1 mg P/L (Figure 5.2D). P removal efficiency was greatly affected by a reduction in pH in columns 3A, 3B and 5A.

Fluoride removal (Figure 5.2E and F) performance was low from L1 (initial concentration of 10 mg/L, treated concentration of 7 mg/L) and high from L2 (initial concentration of 40 mg/L, treated concentration of 4 mg/L). B slag provided significant fluoride removal from L2 (<1 mg/L, column 3A) compared to FS slag (4 mg/L, column 2A). Fluoride removal was reduced when the pH became

less than about 7 in column 3A and 9 in column 5A. Downstream filters removed approximately another 1 mg/L of fluoride from the upstream filter effluent.

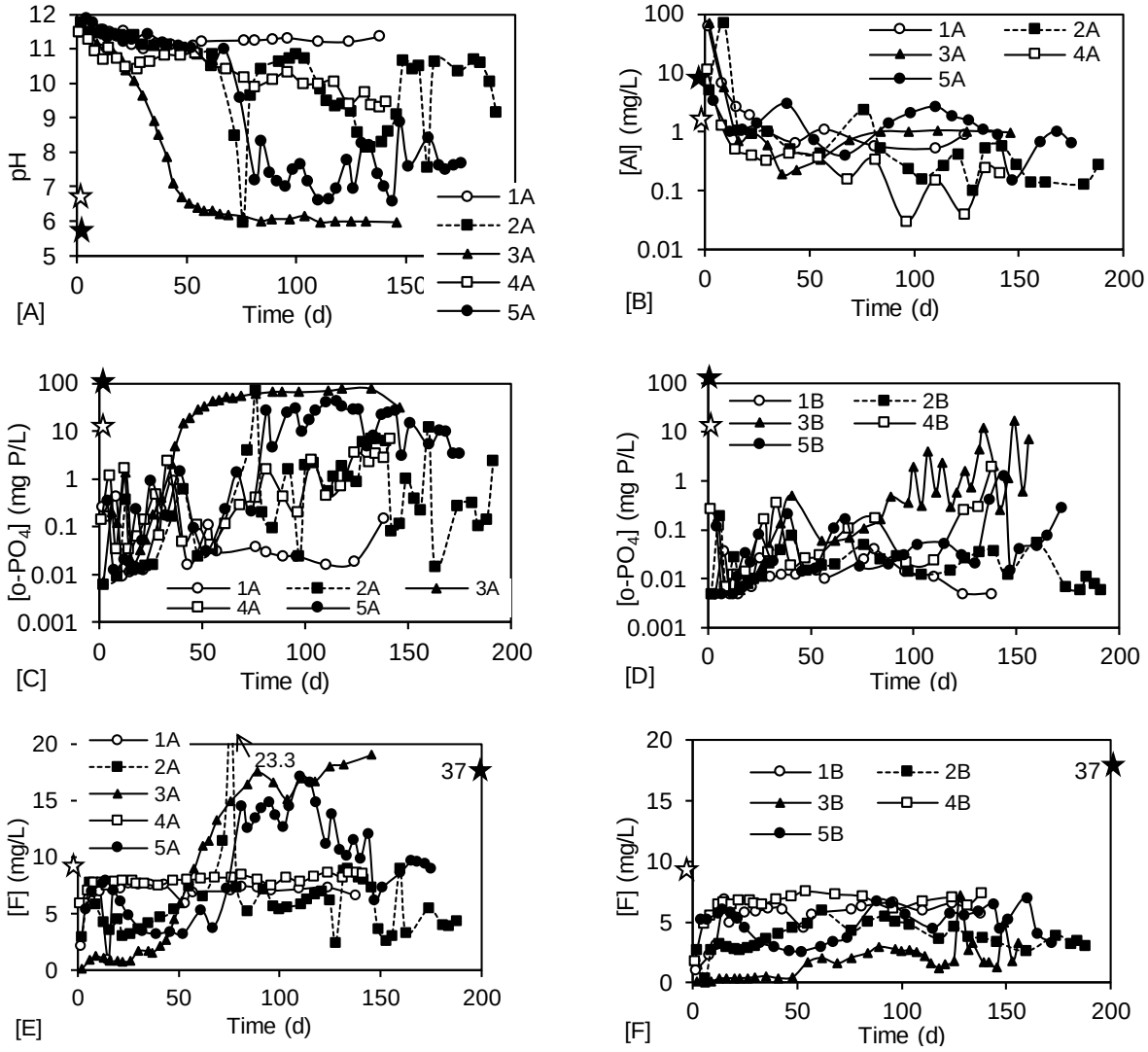

Figure 5.2 : Selected column tests results : pH (A), Al(B), o-PO_4 (C and D) and F (E and F). The letter A or B besides the column refers to upstream (A) or downstream (B) position of the series of columns. The average influent concentration is shown on the vertical axis for the L1 (empty star) and L2 (full star) leachates

Metals removal resulted in a manganese concentration below 0.1 mg/L and a zinc concentration below 0.5 mg/L when the pH was above 10 (results not shown). Manganese and zinc removal was affected by a reduction in pH in columns 3A and 5A. This relationship was not observed for

aluminum (Figure 5.2B), whose concentration was in general below 1 mg/L. Leaching of aluminum, however, was observed for all columns at the beginning of operation.

X-ray diffraction analysis confirmed the presence of apatite (hydroxyapatite or fluoroapatite) in all crystal samples. Calcite was present in 9 samples (columns 1A, 2A, 2B, 4A, 4B, 5B). Apatite mean crystal sizes of samples were between 16 and 65 nm while calcite mean crystal sizes were between 31 and 316 nm. The HAP/$CaCO_3$ ratio was between 0.18 and 0.64 for columns 1A, 1B, 4A and 4B and between 0,59 and 2.56 for columns 2A, 2B, 3A, 3B, 5A and 5B.

Toxicity test results are presented in Table 5.4. The TCLP criterion (Environmental Health and Satefy Online, 2008) for Ag, Cd and Pb were met in both the distilled water and the acetic acid extraction fluid.

Table 5.4 : Toxicity tests results using acetic acid (TCLP) and distilled water as extraction fluid

Contaminant (mg/L)	B slag		FS slag		TCLP criteria
	Distilled water	Acetic acid	Distilled water	Acetic acid	
Fe	0.05	101	0.03	99	
Mn	<0.01	14.8	<0.01	49	
Zn	0.024	6.6	0.014	2.9	
Cu	0.02	0.38	0.01	0.13	
Cd	<0.01	<0.01	<0.01	<0.01	1
Pb	<0.01	0.23	<0.01	0.36	5
Ni	<0.01	0.13	<0.01	0.26	
Ag	0.015	0.027	0.012	0.039	
Ca	159	903	116	1429	
Al	66.9	107	16.6	33	

Note : detection limit = 0.01 mg/L

5.4 Discussion

5.4.1 Efficiency and longevity of filters

Results of column tests showed that efficient treatment by reactive filters of a multi-component mining leachate is possible. The treatment performance of upstream columns is shown in Table

5.5. The best global removal efficiency in L2, which corresponded to a concentrated leachate, was obtained by the sequence B-B. This sequence achieved global removals of 98.8 %, 94.8 %, 94.4 % and 98.6 % for P, F, Mn and Zn, respectively, after 169 days of operation. However, a decrease in pH and removal efficiency was observed in the upstream column after 30 days, limiting its use as a long-term treatment system. The sequence FS-FS resulted in lower fluoride removal efficiency, but in a greater longevity as the pH decrease in the upstream column was observed after 70 days of operation. The global removal of sequence FS-FS after 179 days of operation was 99.9 %, 85.3 %, 98.0 % and 99.3 % for P, F, Mn and Zn, respectively. The highest retention capacity value obtained for phosphorus was 8.3 mg P/g media with FS slag. This value is higher than typical retention capacities obtained in column or field tests for EAF slag, which are between 1 and 2.5 mg P/g media (Chazarenc *et al.*, 2008; Vohla *et al.*, 2011).

Table 5.5 : Contaminants retention for column tests

Column ID	Type of wastewater	Type of slag	HRT_V (h)	Retention capacity reached (mg contaminant/g media)				
				P	F	Mn	Zn	Al
1A	L1	FS	14.2	0.737	0.16	0.010	0.011	0.050
2A	L2	FS	17.2	8.26	2.30	0.053	0.241	0.369
3A	L2	B	14.5	4.54	2.46	0.026	0.183	0.387
4A	L1	FS	4.8	2.62	0.30	0.035	0.048	0.227
5A	L2	FS	19.2	8.11	2.21	0.054	0.244	0.516

The different longevity of B and FS slags can be explained by their mineralogical composition. FS slag contained 7% of bredigite ($Ca_{14}Mg_2(SiO_4)_8$) while B slag contained only 3% of bredigite (Table 5.3). It was previously shown that bredigite is the first calcium oxide that dissolves, causing the pH to rise (Kostura *et al.*, 2005). Slag B started to exhaust its dissolution capacity before slag FS presumably because it did not contain enough readily soluble oxides.

Treatment results of the best tested sequence (two successive FS slag filters operated at total HRT_V of 34 h) are presented in boxplots and compared with effluent concentrations of the actual lime treatment plant of the Joplin mine in Figure 5.3. The tested slag filters were more efficient than the

lime treatment plant for most of the contaminants studied (phosphorus, manganese, zinc, aluminum). However, slag filters were less efficient than the lime treatment plant for fluoride. However, as slag filters are passive and efficient for removal of phosphorus and metals, they could replace the precipitation treatment plant which involves sludge disposal, constant chemical addition and maintenance. The proposed slag filter design for the Joplin mine leachate is presented in Figure 5.4. The system is composed of "*n*" successive FS slag filters operated at an HRT_V of at least 19 h. The utilization of successive filters would increase the efficiency and longevity of the system because upstream filters offer partial removal that extends the removal capacity of downstream filters.

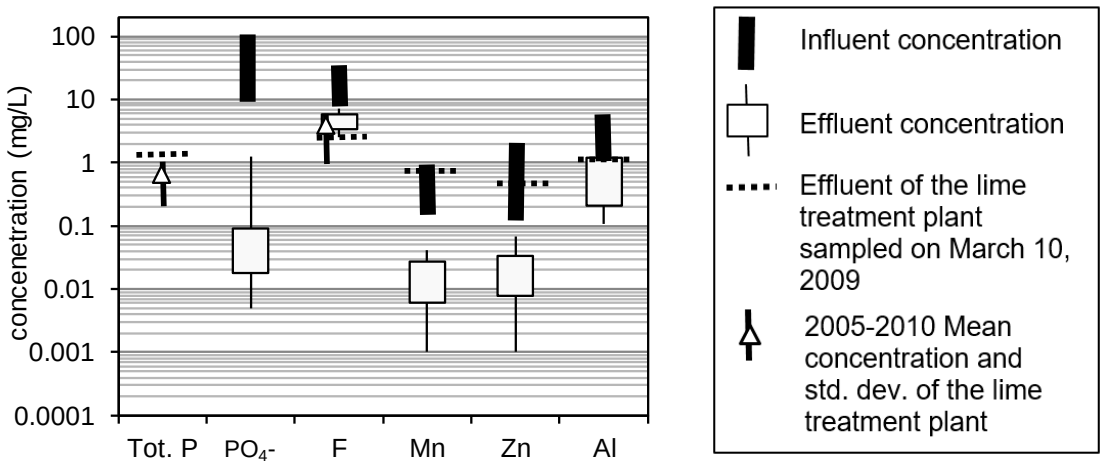

Figure 5.3 : Effluent concentrations of an efficient slag filter (two successive FS slag filters operated at a total HRT_V of 24) compared with the influent and actual effluent concentrations of the lime treatment plant

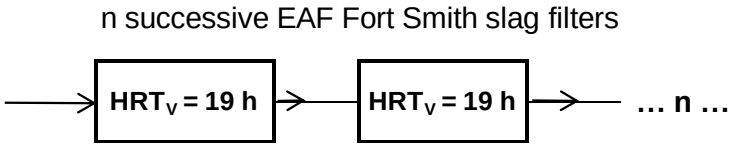

Figure 5.4 : Schematic of the proposed slag filter design for the Joplin mining leachate phosphorus removal

The environmental safety of tested slags was assessed from toxicity tests. Toxicity tests performed in distilled water resulted in low or below detection limit metal concentrations. This result may be representative of the leaching behavior of a full-scale filter at its maximum efficiency (high effluent

pH). On the other side, toxicity tests performed in acetic acid resulted in higher concentrations in the extraction fluid for several metals. This result illustrates the potential leaching problem of an acidic influent on a slag filter. When the filter's neutralizing capacity starts to extinguish, it will not be able any more to raise the pH of the acidic influent and leaching of metals may take place. Filters should be replaced before their treatment capacity is reached to minimize metal leaching. pH monitoring could be a reliable indicator of the filter performance.

A strong link between a high pH and a low effluent phosphorus concentration was observed (Figure 5.5). Different logarithmic regressions were obtained for the pH-o-PO_4 relation between pH 6 and pH 9. These variations may be caused by different initial water compositions. Initial leachates have different chemical equilibrium caused by different contaminant concentrations and the absence or presence of the carbonate system. Moreover, different precipitation behaviours could explain the different relationships between columns 3A and 5A that were fed with the same influent solution. Fluoride removal was more efficient in column 3A than in column 5A. The formation of fluoroapatite (and competition with the formation of hydroxyapatite) had an effect on pH and o-PO_4 concentration.

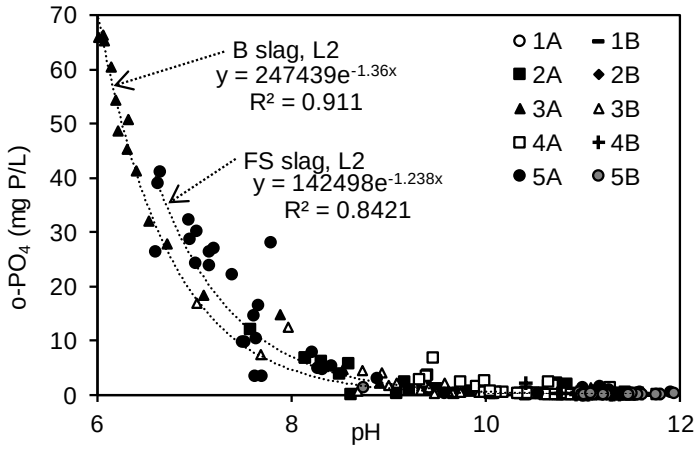

Figure 5.5 : Relationship between effluent o-PO_4 and pH

5.4.2 Fluoride and metals removal

Effluent fluoride concentration was related to effluent pH (Figure 5.6). A high pH always resulted in a lower fluoride concentration. The composition of the leachate also influenced the efficiency of fluoride removal as with the FS slag, the fluoride removal was 10% with L1 and 85% with L2 (the more concentrated leachate). The fluoride removal efficiency was increased when the

fluoride/phosphorus ratio of the wastewater was low, favouring the precipitation of fluoroapatite. Fluoroapatite has the same molecular structure as hydroxyapatite, but precipitation of hydroxyapatite is probably favoured by the constant dissolution of hydroxide ions from slag. The fluoride/phosphorus mass ratio was 0.88 in L1 and 0.33 in L2. In comparison, the stoichiometric fluoride/phosphorus mass ratio of fluoroapatite is 0.20. The requirement of phosphorus for fluoride precipitation in fluoroapatite may explain the poor fluoride removal capacity of downstream filters that were exposed to a low concentration of phosphorus, compared to upstream filters.

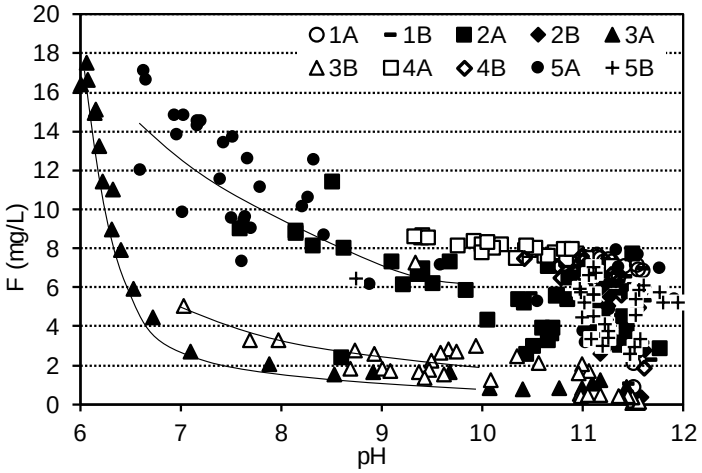

Figure 5.6 : Relationship between fluoride and pH in column effluent

Fluoride removal performance and mechanisms observed in this study were quite different from what was tested with other kinds of wastewaters containing both phosphorus and fluoride. Fluoride removal from electronics wastewater by CaF_2 precipitation was reported (Yang *et al.*, 2001). These authors noted that phosphorus competes with fluoride for precipitation and that the addition of CaF_2 seeds increases the selective precipitation of fluoride, which is optimized at a pH below 9. Grzmil and Wronkowski (2006) performed selective precipitation of phosphorus and fluoride by CaF_2 addition from a phosphoric acid production wastewater, using a sequence of different pH and chemical additives. These authors reached final concentrations of 5-10 mg P/L and 8-18 mg F/L from initial concentrations of 200 mg F/L and 200-400 mg P/L. Selective precipitation of phosphorus from semiconductor wastewater containing fluoride was performed using magnesium salts (Warmadewanthi and Liu, 2009). The initial wastewater contained 936 mg F/L, 118 mg P/L and other compounds. It seems that in the presence of a high fluoride concentration, the precipitation of CaF_2 is favoured. Yehia and Ezzat (2009) observed the precipitation of

fluoroapatite and CaF_2 at low and high concentrations on apatite media. Processes based on the selective precipitation of phosphorus or fluoride could allow the recovery of relatively pure phases, even if they involve the use of chemical additives and mechanical maintenance. Combined removal of phosphorus and fluoride by slag filters, however, offers the advantage of reaching a low fluoride concentration and of being relatively simple and economical.

The slag composition influenced the efficiency of fluoride removal. The mean fluoride removal at maximum efficiency was >90% with the B slag and 75% with the FS slag when columns were fed with the high concentration leachate L2. Hydroxyapatite and fluoroapatite have essentially the same molecular structure as they only differ by the OH or F ion that is located within the hexagonal pattern. It is possible that a solid solution of hydroxyapatite and fluoroapatite was precipitated and that the B slag had some specific characteristics that catalyzed the formation of fluoroapatite. The leaching of some trace metallic compounds, for example, or the presence of a specific mineralogical phase, may have affected the presence of fluoride in nucleation and growth processes.

Metals removal efficiency was linked with pH as was phosphorus removal (Figure 5.8 and Figure 5.9). The mean removal efficiency at maximum efficiency of B slag and FS slag was 75% for Mn and >90% for Zn. Mn was not removed if the pH was lower than 6. The B and FS slags showed an initial Al leaching (concentration at effluent up to 70 mg/L), but Al removal was >90% after that initial period.

5.4.3 Crystal growth

Crystal growth in filters was investigated using crystal size determination. A qualitative interpretation of apatite growth in upstream filters is presented in Figure 5.7. Crystal-size-time curves had fan shapes, suggesting that new crystal seeds are constantly formed while older seeds continue to grow. This process resulted in a distribution of crystal sizes, older seeds being larger and younger seeds being smaller. Crystal growth rates were dependent on the leachate composition. For the same slag media (FS slag), the crystal sizes was smaller in L1 than in L2, suggesting that a higher phosphorus concentration results in a higher apatite growth rate. As efficient crystal growth increases the retention capacity of slag filters (Claveau-Mallet *et al.*, 2012), the high initial phosphorus concentration of L2 may explain the high retention capacities obtained in the present study compared with typical low phosphorus concentration experiments. However, it was

previously shown that highly concentrated wastewater favours nucleation instead of crystal growth (Seckler *et al.*, 1991), resulting in an inefficient crystal organization.

Apatite crystal growth was also dependent on pH. With respect to saturation, hydroxyapatite has three stability zones related to phosphorus concentration and pH (Kim *et al.*, 2006). The first one (low pH and low phosphorus concentration) corresponds to soluble hydroxyapatite. The second one (high pH and high phosphorus concentration, up to 100 mg P/L) involves direct precipitation and crystal growth of hydroxyapatite. The last zone is an intermediary meta-stable zone (high phosphorus concentration and neutral pH) where hydroxyapatite may remain supersaturated. In that meta-stable zone, specific conditions such as hydroxyapatite crystal seeds are necessary for hydroxyapatite precipitation and crystallization, otherwise ions remain in solution. This phenomenon may have happened in column 3A, where crystal seeds were formed in the first 30 days of operation at a pH over 9. During the following period (pH near 6 between t = 50 and 150 d), crystal growth occurred. At these neutral-pH conditions apatite growth resulted in the biggest crystals observed (squares in Figure 5.7).

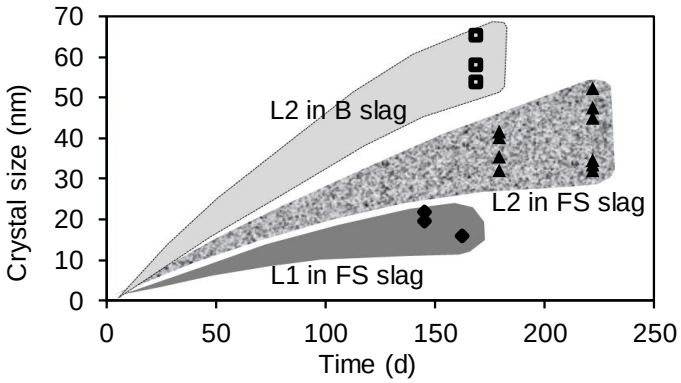

Figure 5.7 : Apatite growth in upstream filters

Results of this study highlight the importance of calcite formation in slag filters as a competitive reaction to apatite formation. For the same influent (L1), crystals in column with HRT_V of 14 h had a mean HAP/$CaCO_3$ ratio of 0.64 while crystals in column with HRT_V of 4.8 h had a mean HAP/$CaCO_3$ ratio of 0.33. Thus, calcite formation was favoured by a higher HRT_V, meaning that calcite grows faster than apatite. These observations, also reported by Liira *et al.* (2009), highlight the importance of the hydraulic retention time. A high hydraulic retention time favors compact precipitation and increases the crystal retention capacity, but considering that calcite grows faster

than apatite, this should result in a larger proportion of calcite. As calcite crystals occupy void spaces that are no longer available for apatite formation and growth, an efficient filter should be operated to minimize calcite formation. In summary, choosing the hydraulic retention time of a slag filter is a compromise between a high retention time for efficient crystal accumulation and a low retention time to limit calcite formation. Calcite formation may also be diminished by removing inorganic carbon from the wastewater in a preceding process and limiting contact between the atmosphere and the filter.

5.5 Conclusion

The objective of this work was to evaluate the capacity of steel slag filters to treat a gypsum mining leachate containing phosphorus, fluoride and metals. The proposed slag filter process was composed of two successive Fort Smith EAF slag operated at total hydraulic retention time of voids of 34 h. This system was still removing 99.9% of phosphorus, 85.3% of fluoride, 98.0% of manganese and 99.3% of zinc after 179 days of operation. Mean concentration at this system's effluent was 0.04 mg P/L phosphorus, 4 mg/L fluoride, 0.02 mg/L manganese, 0.02 zinc and 0.5 mg/L aluminum. Thus, slag filters are promising passive and economical systems for mining remediation. Technical aspects (filter geometry, contact of the filter with atmosphere, pH stabilization of the effluent) and economical considerations (transport cost, frequency of replacement) need to be considered for future full-scale applications.

Apatite growth was observed in filters. The apatite growth rate was favored by high phosphorus concentration in the influent. Calcite crystals were present in filters and were identified as competing with phosphorus removal. The growth rate of calcite crystals was higher than that of apatite crystals. Fluoride was removed by precipitation of fluoroapatite and its removal was favored by a high phosphorus/fluoride ratio in the influent. Fluoride removal was poor when no phosphorus was present in the influent.

5.6 Acknowledgements

The authors thank Kalle Kirsimäe, Riho Mõtlep and Martin Liira from the University of Tartu for the XRD analysis of slags, Denis Bouchard, Aurore Bordier and Marie Ferland from Polytechnique Montréal for technical assistance and Mark Finney from Shaw Environmental for scientific support and data concerning the mine. Tube City (Arkansas) and Harsco Minerals (Arkansas) provided

samples of Fort Smith slag and Blytheville slag respectively. This project was funded by the Natural Sciences and Engineering Research Council of Canada, the Missouri Remediation Trust and the *Fonds de recherche du Québec Nature et technologies.*

5.7 Appendix A

The relationship between Mn, Zn and pH is shown in Figure 5.8 and Figure 5.9.

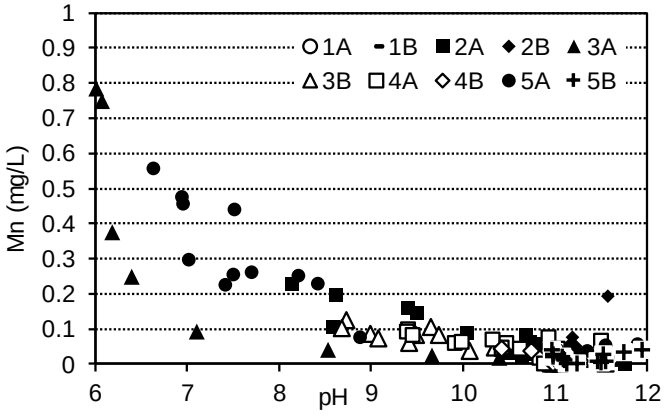

Figure 5.8 : Relationship between manganese and pH in column effluent

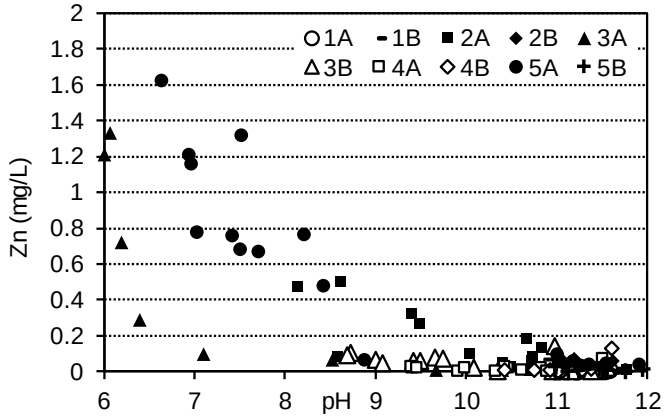

Figure 5.9 :Relationship between zinc and pH in column effluent

5.8 Appendix B

Supplementary data related to this article can be found online at doi:10.1016/j.watres.2012.11.048.

5.9 References

Aldaco, R., Irabien, A., & Luis, P. (2005). Fluidized bed reactor for fluoride removal. *Chemical Engineering Journal, 107*(1-3), 113-117.

APHA, AWWA & WEF. (2005). Standard methods for the examination of water and wastewater (21st ed.). Washington, D. C: American Public Health Association, American Water Works Association & Water Environment Federation.

ASTM. (2006). *Standard test method for permeability of granular soils (constant head).* ASTM D2434-68. West Conshohocken, PA: American Society for Testing Materals.

Brient, S. (2012). *Dephosphatation of a fish farm wastewater with extensive steel slag fiters (in French).* (M.A.Sc. thesis, Polytechnique Montreal, Canada).

Chapuis, R. P., Baass, K., & Davenne, L. (1989). Granular soils in rigid-wall permeameters. Method for determining the degree of saturation. *Canadian geotechnical journal, 26*(1), 71-79.

Chazarenc, F., Brisson, J., & Comeau, Y. (2007). Slag columns for upgrading phosphorus removal from constructed wetland effluents. *Water Science and Technology, 56*, 109-115.

Chazarenc, F., Kacem, M., Gérente, C., & Andrès, Y. (2008). *'Active' filters: a mini-review on the use of industrial by-products for upgrading phosphorus removal from treatment wetlands.* Paper presented at the 11th Int. Conf. on Wetland Systems for Water Pollution Control, Indore, India, November 1 – November 7.

Claveau-Mallet, D., Wallace, S., & Comeau, Y. (2012). Model of phosphorus precipitation and crystal formation in electric arc furnace steel slag filters. *Environmental Science and Technology, 46*(3), 1465-1470. doi:10.1021/es2024884

Cullity, B. D. (2001). *Elements of x-ray diffaction* (3rd ed.). Upper Saddle River, NJ: Prentice Hall.

Drizo, A., Comeau, Y., Forget, C., & Chapuis, R. P. (2002). Phosphorus saturation potential: A parameter for estimating the longevity of constructed wetland systems. *Environmental Science and Technology, 36*(21), 4642-4648.

Environmental Health and Safety Online. (2008). The EPA TCLP: Toxicity Characteristic Leaching Procedure and Characteristic Wastes (D-codes). Retrieved from http://ehso.com/cssepa/TCLP.htm, accessed on April 19, 2012.

Grzmil, B., & Wronkowski, J. (2006). Removal of phosphates and fluorides from industrial wastewater. *Desalination, 189*(1-3 SPEC. ISS.), 261-268.

Gy, P. (1979). *Developments in geomathematics. theory and practive 4, Sampling of particulate materials*. New York: Elsevier Scientific Publications.

Huang, Y.-H., Shih, Y.-J., & Chang, C.-C. (2011). Adsorption of fluoride by waste iron oxide: The effects of solution pH, major coexisting anions, and adsorbent calcination temperature. *Journal of Hazardous Materials, 186*(2-3), 1355-1359.

Kim, E.-H., Yim, S.-B., Jung, H.-C., & Lee, E.-J. (2006). Hydroxyapatite crystallization from a highly concentrated phosphate solution using powdered converter slag as a seed material. *Journal of Hazardous Materials, 136*(3), 690-697. doi:10.1016/j.jhazmat.2005.12.051

Kõiv, M., Liira, M., Mander, Ü., Mõtlep, R., Vohla, C., & Kirsimäe, K. (2010). Phosphorus removal using Ca-rich hydrated oil shale ash as filter material - The effect of different phosphorus loadings and wastewater compositions. *Water Research, 44*(18), 5232- 5239.

Kostura, B., Kulveitová, H., & Leško, J. (2005). Blast furnace slags as sorbents of phosphate from water solutions. *Water Research, 39*(9), 1795-1802.

Liira, M., Kõiv, M., Mander, Ü., Mõtlep, R., Vohla, C., & Kirsimäe, K. (2009). Active filtration of phosphorus on Ca-rich hydrated oil shale ash: Does longer retention time improve the process? *Environmental Science and Technology, 43*(10), 3809-3814.

MDDEP. (2006). Metals determination: method by mass spectrometry with argon plasma ionizing source (in French) (3rd ed.): Centre d'expertise en analyse environnementale, Ministère du développement durable, de l'environnement et des parcs. MA. 200 – Mét 1.1.

National Slag Association. (2009). General Information about National Slag Association (NSA). Retrieved from http://www.nationalslag.org/nsageneral.htm, accessed on March 16, 2012.

Pratt, C., & Shilton, A. (2010). Active slag filters-simple and sustainable phosphorus removal from wastewater using steel industry byproduct. *Water Science and Technology, 62*(8), 1713-1718.

Renman, A., Renman, G., Gustafsson, J. P., & Hylander, L. (2009). Metal removal by bed filter materials used in domestic wastewater treatment. *Journal of Hazardous Materials, 166*(2-3), 734-739.

Seckler, M. M., Bruinsma, O. S. L., & van Rosmalen, G. M. (1991). Crystallization of calcium and magnesium phosphates in a fluidized bed. *Crystal Properties and Preparation, 36*(38), 263-272.

Shilton, A., Pratt, S., Drizo, A., Mahmood, B., Banker, S., Billings, L., Glenny, S., & Luo, D. (2005). 'Active' filters for upgrading phosphorus removal from pond systems. *Water Science and Technology, 51*(12), 111-116.

Smyth, D. J. A., Blowes, D. W., Ptacek, C. J., Baker, M. J., & McRae, C. W. T. (2002). *Steel production wastes for use in permeable reactive barriers (PRBs).* Paper presented at the Third International Conference on Remediation of Chlorinated and Recalcitrant Compounds, Monterey, CA., May 20-23.

USEPA. (1992). Toxicity characteristic leaching procedure. United States Environment Protection Agency Test Method 1311, Washington (DC).

Vohla, C., Kõiv, M., Bavor, H. J., Chazarenc, F., & Mander, Ü. (2011). Filter materials for phosphorus removal from wastewater in treatment wetlands-A review. *Ecological Engineering, 37*(1), 70-89.

Warmadewanthi, & Liu, J. C. (2009). Selective precipitation of phosphate from semiconductor wastewater. *Journal of Environmental Engineering, 135*(10), 1063-1070.

Xu, X., Li, Q., Cui, H., Pang, J., Sun, L., An, H., & Zhai, J. (2011). Adsorption of fluoride from aqueous solution on magnesia-loaded fly ash cenospheres. *Desalination, 272*(1-3), 233-239.

Yamada, H., Kayama, M., Saito, K., & Hara, M. (1986). A fundamental research on phosphate removal by using slag. *Water Research, 20*(5), 547-557.

Yang, M., Zhang, Y., Shao, B., Qi, R., & Myoga, H. (2001). Precipitative removal of fluoride from electronics wastewater. *Journal of Environmental Engineering, 127*(10), 902-907.

Yehia, A., & Ezzat, K. (2009). Fluoride ion uptake by synthetic apatites. *Adsorption Science and Technology, 27*(3), 337-347.

Zhou, Y.-F., & Haynes, R. J. (2010). Sorption of heavy metals by inorganic and organic components of solid wastes: Significance to use of wastes as low-cost adsorbents and immobilizing agents. *Critical Reviews in Environmental Science and Technology, 40*(11), 909-977.

CHAPTER 6 ARTICLE 3: PHOSPHORUS REMOVAL BY STEEL SLAG FILTERS: MODELING DISSOLUTION AND PRECIPITATION KINETICS TO PREDICT LONGEVITY

Claveau-Mallet, D., Courcelles, B. & Comeau, Y. (2014). Phosphorus removal by steel slag filters : modeling dissolution and precipitation kinetics to predict longevity. *Environmental Science & Technology*, 48(13), 7486-7493.

ABSTRACT

This article presents an original numerical model suitable for longevity prediction of alkaline steel slag filters used for phosphorus removal. The model includes kinetic rates for slag dissolution, hydroxyapatite and monetite precipitation and for the transformation of monetite into hydroxyapatite. The model includes equations for slag exhaustion. Short-term batch tests using slag and continuous pH monitoring were conducted. The model parameters were calibrated on these batch tests and experimental results were correctly reproduced. The model was then transposed to long-term continuous flow simulations using the software PHREEQC. Column simulations were run to test the effect of influent P concentration, influent inorganic C concentration and void hydraulic retention time on filter longevity and P retention capacity. High influent concentration of P and inorganic C, and low hydraulic retention time of voids reduced the filter longevity. The model provided realistic P breakthrough at the column outlet. Results were comparable to previous column experiments with the same slag regarding longevity and P retention capacity. A filter design methodology based on a simple batch test and numerical simulations is proposed.

Keywords : slag, phosphorus, wastewater treatment, PHREEQC, hydroxyapatite, model

6.1 Introduction

Slag filters are a promising technology for phosphorus (P) removal from wastewater. In the last 20 years, these passive systems were tested with success in different countries (Vohla *et al.*, 2011). The large-scale utilization of slag filters, however, is inhibited by the limited number of full-scale implementations and the absence of mechanism based rather than empirical design methodology. Diverging results from various studies complicate the elaboration of a design strategy. The

objective of this paper is to propose a model of phosphorus removal in alkaline steel slag filters. This model considers both longevity and efficiency of reactive filters.

The main mechanism for P removal observed in alkaline steel slag filters is the formation of hydroxyapatite (HAP), a stable calcium phosphate. HAP formation was observed in many previous studies (Baker *et al.*, 1998; Claveau-Mallet *et al.*, 2012; Article 2 – Chapter 5; Drizo *et al.*, 2006; Kim *et al.*, 2006; Liira *et al.*, 2009). Several metastable calcium phosphates such as brushite, monetite (MON) and octacalcium phosphate are precursors of HAP (Lundager Madsen, 2008; Valsami-Jones, 2001) and they were observed in slag filters (Bowden *et al.*, 2009; Kim *et al.*, 2006). HAP formation was the basis of a conceptual model presented by Claveau-Mallet *et al.* (Claveau-Mallet *et al.*, 2012). This conceptual model comprises three steps: (1) slag dissolution, (2) phosphorus precipitation and crystal growth, and (3) P removal rate decrease caused by void filling particle accumulation and slag exhaustion. In the present project, this conceptual model is developed into a mathematical expression suitable for numerical simulations.

A challenge for the prediction of P removal is the disparity between batch test and continuous flow filter test results (Chazarenc *et al.*, 2008). The proposed strategy is to characterize a given slag in a batch test and define parameters that are realistic in a filter test.

6.2 Material and methods

The methodology involved two parts, batch test experiments with slag and numerical simulations.

6.2.1 Slag media

Electric arc furnace (EAF) slag from Arcelor Mittal located in Contrecoeur (QC) was used. The slag size was 5-10 mm and its density was 3.6 g/cm^3. The chemical composition of the slag was 33% Fe_2O_3, 30% CaO, 16% SiO_2 and 12% MgO. The same slag was used for phosphorus removal and mechanism studies in previous experiments (Chazarenc *et al.*, 2007; Claveau-Mallet *et al.*, 2012; Drizo *et al.*, 2002; Drizo *et al.*, 2006; Mahadeo, 2013).

6.2.2 Batch kinetic tests

A given amount of slag was placed in a 1L Erlenmeyer flask filled with 700 mL of solution (demineralised water or phosphorus solution). The Erlenmeyer was closed with a rubber cap

connected with a nitrogen gas filled balloon to avoid exposure to atmosphere oxygen when sampling. A pH probe was inserted in the cap to allow continuous monitoring during tests. A syringe was used for water sampling by connecting it to a plastic tubing with a pinched valve inserted in the cap. Water samples were filtered at 0.45 microns and analyzed for ortho-phosphates ($o\text{-}PO_4$) and calcium. The temperature was controlled at 20°C and the Erlenmeyer was mixed on a gyratory shaker at 160 rpm, which produced movement of the slag at the bottom of the Erlenmeyer without suspension of the slag. The test lasted 3 to 7 days. The effect of three parameters were tested in three experimental sets: initial phosphorus concentration, water/slag ratio and slag exhaustion.

$o\text{-}PO_4$ analyses were performed using a Lachat QuikChem 8500 flow injection analyzer using the ascorbic acid method (APHA *et al.*, 2005). Analyses of calcium were conducted with an AAnalyst 200 flame atomic absorption apparatus, using a standard mass spectrometry method (MDDEP, 2006).

6.2.2.1 Effect of initial phosphorus concentration

Initial phosphorus concentrations of 0, 10, 20 and 50 mg P/L were tested in the presence of a constant amount of slag of 35 g per flask. These concentrations were chosen as representative of concentrations met in real wastewaters. A fresh slag sample was used for each experiment. Phosphorus solutions were prepared using KH_2PO_4 and 30 mg/L of calcium added as $CaCl_2{\cdot}2H_2O$. Results obtained from these tests were used to calibrate the simulation model.

6.2.2.2 Effect of water/slag ratio

Slag masses of 35, 70, 350 and 700 g per flask were tested in distilled water. 700 g per flask was the highest amount of slag possible to add without affecting the probe. A fresh slag sample was used for each experiment. Test results were used to assess the effect of water/slag ratio on dissolution kinetics. The tested water/slag ratios were 1, 2, 10 and 20 mL/g. Reported water/slag ratio in various types of studies range from 0.33 mL/g in a slag filter with 50% porosity to 20 mL/g in leaching standard procedure tests (USEPA, 1992).

6.2.2.3 Slag exhaustion

Tests were conducted at a constant initial phosphorus concentration of 45 mg P/L. A fresh slag sample of 350 g was used in a first batch test. The sample was then placed in a 0.08N HNO_3 "bath" solution for 24 h after which the solution pH was measured. The slag sample was then drained and used in a second test, which was followed by a second HNO_3 bath. The slag sample was submitted to 5 successive batch tests each followed by a HNO_3 bath. The objective of this experimental set was to determine the effect of slag exhaustion (cumulative leached CaO, mol/g) on the rate of slag dissolution, a specific slag kinetic parameter.

6.2.3 PHREEQC modeling

PHREEQC is a free software commonly used for complex geochemical calculations (Parkhurst & Appelo, 1999). PHREEQC includes equilibrium calculations, irreversible reactions, kinetic rates and mineral phases. The default PHREEQC Interactive 3.0 database was used. The main feature of the proposed model is to consider the kinetic rates of slag dissolution and of phosphorus precipitation in mineral phases. Slag dissolution was modeled as a simple CaO dissolution (Claveau-Mallet *et al.*, 2012). Two phosphorus mineral phases were included: HAP and MON. MON was chosen in the model to represent several amorphous or crystalline precursors in a single and simple expression. MON was preferred to other calcium phosphate species for its simple expression.

The transformation rate of metastable MON to the final stable phase HAP was included in the model.

6.2.3.1 Slag dissolution and phosphorus precipitation model and equations

The slag dissolution rate is defined by equation 6.1, where r_{diss} is the CaO dissolution rate (M/s), pH is the pH of water at any time and pH_{sat} is the saturation pH of the slag. k_{diss} (M/s) is the dissolution constant. pH_{sat} is a function defined as the maximum pH reached (considered constant during a batch test) and k_{diss} is empirically determined by iterations (several simulations with various values of k_{diss} are run and the best fit is kept). The slag surface area is considered constant during the test.

$$r_{diss} = k_{diss}\left(\frac{pH_{sat}-pH}{pH_{sat}}\right) \qquad (6.1)$$

The equation of HAP precipitation is given in equation 6.2. The rate of HAP precipitation (r_{HAP}, M/s) is expressed by a simple precipitation rate equation (Lasaga, 1981), where k_{HAP} (M/s) is a constant and SI_{HAP} is the saturation index of HAP in water (equation 6.3). This rate equation assumes a constant temperature and specific surface area. SI_{HAP} is defined by equation 6.4, where K_{spHAP} is the solubility product of HAP.

$$5Ca^{2+} + 3PO_4^{3-} + OH^- \leftrightarrow Ca_5(PO_4)_3OH \quad (6.2)$$

$$r_{HAP} = k_{HAP}\, SI_{HAP} \quad (6.3)$$

$$SI_{HAP} = log\left(\frac{[Ca^{2+}]^5[PO_4^{3-}]^3[OH^-]}{K_{spHAP}}\right) \quad (6.4)$$

Equations of MON precipitation are similar to the ones for HAP (equations 6.5 to 6.7).

$$Ca^{2+} + HPO_4^{2-} \leftrightarrow CaHPO_4 \quad (6.5)$$

$$r_{MON} = k_{MON}\, SI_{MON} \quad (6.6)$$

$$SI_{MON} = log\left(\frac{[Ca^{2+}][HPO_4^{2-}]}{K_{spMON}}\right) \quad (6.7)$$

The transformation of MON to HAP is expressed in equation 6.8. The transformation rate ($r_{MONtoHAP}$, M/s) is a function of pH and of the remaining amount of MON (equation 6.9), and $k_{MONtoHAP}$ (M/s) is a constant determined by iterations. The transformation of MON to HAP was represented in PHREEQC by the addition of Ca^{2+} and OH^- to MON via the formation of the mineral phase $Ca(OH)_2$ (equation 6.10). Kinetic constants (k_{HAP}, k_{MON} and $k_{MONtoHAP}$) were determined empirically by iterations (several simulations with various values of k_{HAP}, k_{MON} and $k_{MONtoHAP}$ are run and the best fit is kept). Equilibrium constants (K_{spHAP}, 10^{-46} M^9 and K_{spMON}, 10^{-7} M^2) were chosen from the literature (Stumm & Morgan, 1996; Valsami-Jones, 2001). A discussion concerning the value of K_{spHAP} is provided in the result section.

$$3CaHPO_4 + 2Ca^{2+} + 4OH^- \rightarrow Ca_5(PO_4)_3OH + 3H_2O \quad (6.8)$$

$$r_{MON\ to\ HAP} = k_{MONtoHAP}\, pH\ MON \quad (6.9)$$

$$Ca^{2+} + 2OH^- \rightarrow Ca(OH)_2 \quad (6.10)$$

Precipitation phases included in the model are summarized in Table 6.1.

Table 6.1 : Precipitation phases included in the model

Phase	Formula	Log(k) (-)	Reference
HAP	$Ca_5(PO_4)_3OH$	-46	(Stumm & Morgan, 1996)
MON	$CaHPO_4$	-7	(Valsami-Jones, 2001)

6.2.3.2 Batch simulations

The KINETICS data block of PHREEQC was used to simulate batch experiments. The four rates described in the last section were added in the RATES data block and dissolution parameters of slag (k_{diss} and pH_{sat}) were kept constant. Experimental initial solutions were represented using KH_2PO_4, $CaCl_2$ and CaO put in a pH 7 pure water with the REACTION data block, followed by an equilibrium at saturation index zero with HAP and MON in the EQUILIBRIUM_PHASES data block. No equilibrium with atmospheric CO_2 was done. Small amounts of CaO were added before the initial simulated solutions to reproduce initial experimental pH at time zero and the evolution of water properties (pH, calcium, phosphorus, amount of mineral phases) over time was computed by PHREEQC. From an experimental point of view, it was technically impossible to impose ideal initial conditions, which would mean that there is an instantaneous and homogenous contact between slag and water at time zero. Therefore, for simulations, a little amount of slag had already reacted before time zero of the test.

6.2.3.3 Simulation of column tests

The TRANSPORT data block was used to simulate water flow in a 1D column. The KINETICS and RATES data blocks were used for the definition of the four model rates. Inlet solutions were simulated in a similar way to batch tests: KH_2PO_4, K_2HPO_4, $CaCl_2$ and $NaHCO_3$ were added to a pH 7 pure water thought the REACTION data block, after which solutions were put into equilibrium with HAP and MON using the EQUILIBRIUM_PHASES data block. The column was divided into 10 cells that were 11 cm thick each and a dispersivity of 1 cm (size of slag particles) was used (Domenico & Schwartz, 1998). A sensitivity analysis for dispersivity was performed with values of 0, 1, 2 and 5 cm (results presented as support information). The '-correct_disp' data block was set to true and flux boundary conditions were used at column's ends. Each cell had a total volume of 2 L with a porosity of 50%. The slag density was defined as 3.6 g/cm^3. The evolution of water properties over time within each column cell was computed by PHREEQC. The two

dissolution parameters of slag k_{diss} and pH_{sat}, which were kept constant in batch simulations, were modified to account for the evolution of the slag/water ratio and of slag exhaustion. Constant values were replaced by exhaustion equations that were defined according to batch test results. Column simulations were run for 2000 void volumes, which were long enough to determine the column longevity. The column longevity was defined as the time at which the effluent phosphorus concentration increased to reach a value of 1 mg P/L. Other longevity definitions are possible (e. g. reach a given percentage of the influent concentration), but 1 mg P/L was chosen to represent a possible concentration requirement. The studied parameters (and tested values) were voids hydraulic retention time (HRT_V) (4, 8 and 16 h), influent phosphorus concentration (5, 6, 8, 10, 12, 14, 16, 18, 20, 22, 24, 26, 28 and 30 mg P/L) and influent $NaHCO_3$ concentration (0.0 and 0.5 mM). A total of 84 simulations were run.

6.3 Results and discussion

6.3.1 Batch test results: model application

Experimental and numerical results of batch tests are compared in Figure 6.1 for pH, P and Ca. Calibrated parameters were $k_{spHAP} = 10^{-46}\ M^9$, $k_{spMON} = 10^{-7}\ M^2$, $k_{MON} = 10^{-7}\ M/s$, $k_{HAP} = 10^{-8.6}\ M/s$, $k_{MONtoHAP} = 10^{-6}\ pH^{-1}s^{-1}$, $pH_{sat} = 11.52$ and $k_{diss} = 10^{-6.9\ \mp\ 0.4}\ M/s$. Experimental pH and phosphorus were accurately reproduced by the model and calcium was in the same range except for t greater than 1000 seconds in which calcium concentration was overestimated. Complex waves present in the pH experimental curves (e. g. 400 to 2000 min, curve 50 mg P/L, Figure 6.1A) resulting from the cumulative effect of phosphoric acid buffers and phosphate calcium precipitations on hydroxide concentration were also accurately reproduced by the model.

The value of HAP solubility product used in the model ($k_{spHAP} = 10^{-46}\ M^9$) was higher then usual tabulated mineralogical data, which range from 10^{-55} to 10^{-63} M^9 (Oelkers, Bénézeth, & Pokrovski, 2009; Parkhurst & Appelo, 1999; Stumm & Morgan, 1996). The small size of freshly formed HAP crystals explains this difference. Surface energy influences solubility when the crystal size is smaller than 1 μm. The effect of specific surface on solubility product is given by the following equation (Stumm & Morgan, 1996):

$$logK_{sp\_at\_S} = logK_{sp\_at\_S0} + \frac{\frac{2}{3}\bar{\gamma}\, S}{2.3R\,T} \qquad (6.11)$$

where K_{sp} is the solubility product, S is the specific surface area (m^2/mol), $\bar{\gamma}$ is the mean free surface energy (87 mJ/m^2 for HAP), R is the ideal gas constant (8.31 J mol^{-1} K^{-1}) and T is the temperature (298 K). Using equation 6.11 and assuming a columnar crystal structure with a length/diameter ratio of 25/1, a crystal length of 0.016 µm and a bulk crystal solubility of 10^{-57} M^9, the solubility of finely grained HAP increased to 10^{-46} M^9. Such values for crystal size and morphology were reported in previous studies (Claveau-Mallet *et al.*, 2012; Article 2 – Chapter 5). Equation 6.11 explains why HAP supersaturation has been reported in alkaline slag filters (Baker *et al.*, 1998).

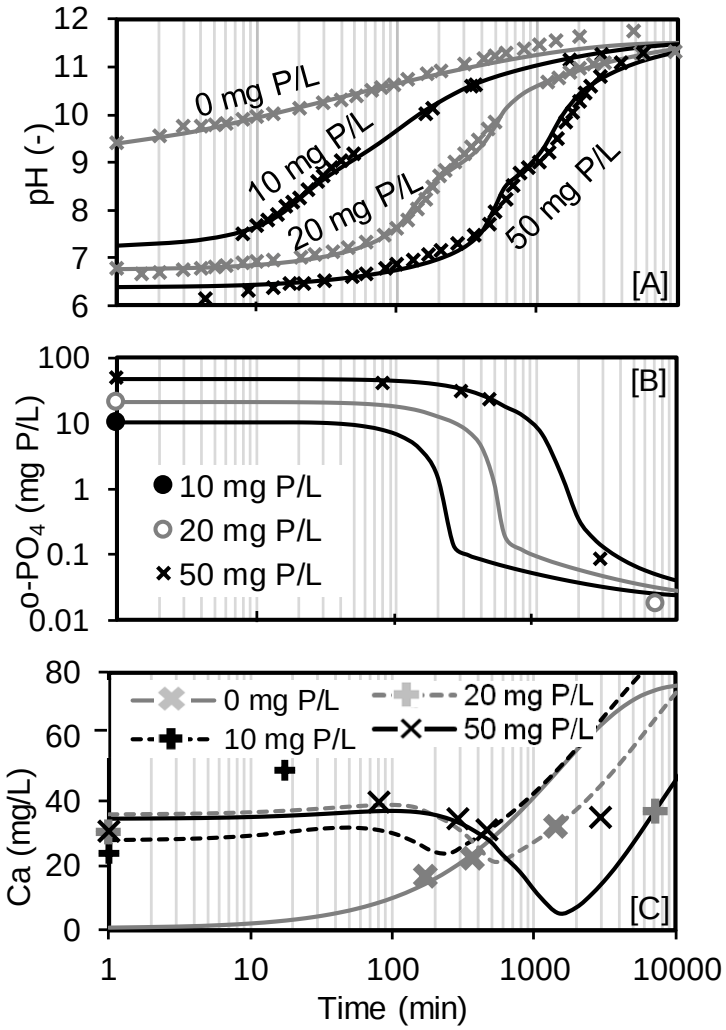

Figure 6.1 : Comparison of batch test experimental and simulated results for pH (A), phosphorus (B) and calcium (C). Simulated results are represented with lines and experimental results with circles, plus or X symbols

For all simulated batch tests, the precipitation parameters of the model (k_{spHAP}, k_{spMON}, k_{MON}, k_{HAP} and $k_{MONtoHAP}$) had constant values (0, 10, 20 and 50 mg P/L initial phosphorus concentration) while the slag dissolution kinetic constant k_{diss} varied slightly between $10^{-6.4}$ and $10^{-7.2}$ M/s. This variation can be explained by the intrinsic composition variability of the slag. The expected presence of readily available CaO at the surface of slag particles increased the CaO dissolution rate of a given slag sample. This effect is important when 35 g slag samples are used in a batch test, as there are less than fifty slag particles in a sample. Therefore, it is important to test several slag sample replicates to assess the k_{diss} mean value and variability. The slag composition variability would probably be smaller if slag samples containing more particles were used. For subsequent column simulations, the mean value was used for log(k_{diss}) to account for slag compositional variability.

6.3.2 Analysis of precipitation hypothesis

The model calibration presented in this study illustrates the importance of the precipitation hypothesis. Four simulations with different precipitation hypotheses were compared to experimental data (Figure 6.2A).

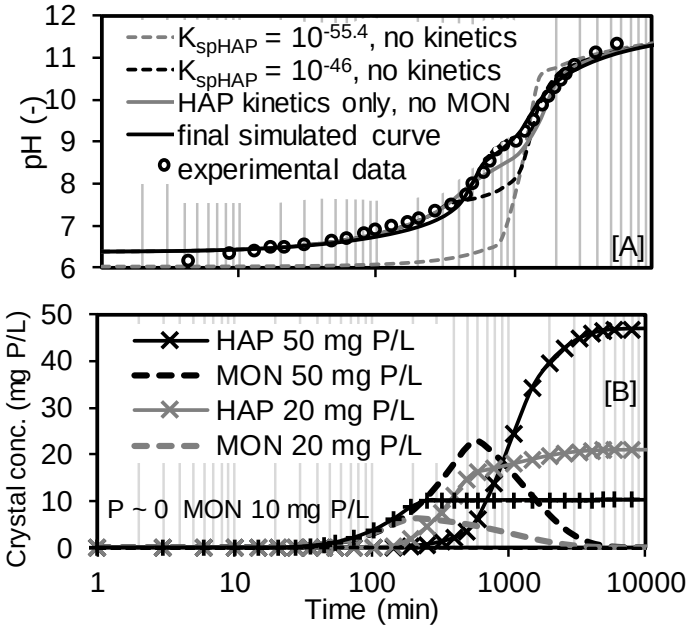

Figure 6.2 : Effect of different precipitation hypotheses on simulated batch test results at an initial P concentration of 50 mg P/L (A) and evolution of phosphorus precipitates concentration in simulated batch tests (B)

The first hypothesis was based on a simple model which considers only the precipitation of HAP at equilibrium with $k_{spHAP} = 10^{-55.4}M^9$ (the value provided in the PHREEQC database). Simulation results did not reproduce well the pH curve and the phosphorus concentration at the end of the simulation was too low (results not shown). The second model was similar to the first one, except for the value of k_{spHAP} which was increased to $10^{-46}M^9$. The resulting pH curve was closer to experimental data, but did not reproduce well the curve portion between 400 and 2000 minutes. The phosphorus simulated curve did not reproduce well the experimental data in the pH range of 7 to 9 (results not shown). In the third model, HAP precipitation kinetic was added, which improved the fit for both pH and phosphorus experimental curves. Finally, the fourth and complete model considering both HAP and MON formation fitted well for both pH and phosphorus (Figure 6.1). It was concluded that precipitation kinetics should be considered in a slag filter phosphorus removal model. A model based only on equilibrium phenomena is too simple and does not accurately represent reality.

Adding an intermediary precipitate as MON to the model improved its realism. Precipitation of HAP is significant only above pH 9, after which oversaturation rapidly increases. Thus, precipitation of HAP alone does not explain the reduction of phosphorus in solution at intermediary pH (7 to 9), which was observed in the present and previous studies (Baker *et al.*, 1998; Barca *et al.*, 2013; Brient, 2012; Claveau-Mallet *et al.*, 2012; Article 2 – Chapter 5). The addition of MON precipitation and transformation to HAP to the model was justified by previous studies. Several calcium phosphate precipitates are known to be metastable and to transform into HAP, which is stable (Valsami-Jones, 2001). This transformation phenomenon was qualitatively observed by scanning electronic microscopy and X-Ray diffraction in slag filter experiments (Bowden *et al.*, 2009) and bioceramic applications (Lundager Madsen, 2008). The evolution of HAP and MON concentration in simulations is shown in Figure 6.2B. MON had a lifetime of about 2000 minutes (33 hours), after which it was completely transformed into HAP. The simulated lifetime of MON is confirmed by Tsuru *et al.* (2001), who observed an amorphous precipitate 1 to 3 days before the appearance of HAP in crystal growth experiments under neutral conditions. However, HAP started to precipitate faster in this study (after about 100 minutes). This was probably the result of alkaline conditions which favored HAP formation. Results of simulations indicated that transformation of MON into HAP is controlled by pH. Similar results were obtained in bioceramics applications

under alkaline conditions with MON formation at neutral conditions. Le *et al.* (2012) and Ito *et al.* (2008) observed HAP at alkaline pH, and both HAP and MON at neutral conditions.

6.3.3 Using the model to predict filter longevity

6.3.3.1 Batch test results: adaptation of model parameters to continuous flow filters

The model that was used for batch test simulations could not be used directly for long term continuous flow column simulations as the behavior of slag dissolution differed between these two conditions. First, dissolution kinetics are faster in a column slag filter because its water to slag ratio is 0.3 mL/g (assuming a porosity of 50% and a slag grain density of 3.6), compared to 20 mL/g in batch tests. Second, slag is progressively exhausted in continuous flow slag column filters, a phenomenon that was not observed in batch tests. Consequently, the slag dissolution parameters of the model (k_{diss} and pH_{sat}) were modified to consider these two factors. The effect of water/slag ratio in batch tests is presented in Figure 6.3. k_{diss} and pH_{sat} presented in this Figure were determined by calibration of their respective pH experimental curves with the proposed model. Relationships were used to extrapolate k_{diss} and pH_{sat} values from a ratio of 20 to a ratio of 0.3, which is the ratio present in slag filters. The resulting dissolution parameters for column simulations were $k_{diss} = 10^{-5.5} M/s$ and $pH_{sat} = 12.44$ which represent the initial dissolution behavior of slag without exhaustion.

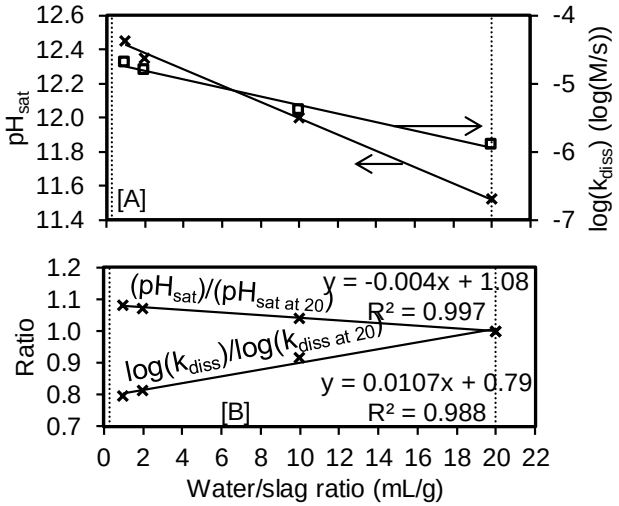

Figure 6.3 : Effect of water/slag ratio on slag dissolution kinetic parameters. Dotted lines represent typical ratio values in slag filters (0.3 mL1gl left line) and standard batch tests (20 mL/g; right line)

Results of slag exhaustion batch tests are presented in Figure 6.4. These results illustrate the expected exhaustion of slag as pH_{sat} and k_{diss} progressively decrease. The proposed batch test is a simple methodology that indirectly considers various and complex slag properties including size, composition and initial presence of reactive powder on the slag surface. Initial dissolution parameters determined previously ($k_{diss} = 10^{-5.5} M/s$ and $pH_{sat} = 12.44$) were multiplied by relationships presented in Figure 6.4 to take into account the decrease in dissolution rate caused by slag exhaustion. The resulting dissolution parameters used in column tests are presented in equations 6.12 and 6.13. The A parameter was computed by PHREEQC at each time step within the RATE modulus. The other precipitation parameters of the column slag filter model (k_{spHAP}, k_{spMON}, k_{MON}, k_{HAP} and $k_{MONtoHAP}$) remained identical to those of the batch test model.

$$\log(k_{diss}) = -5.5(365A + 1) \rightarrow k_{diss} = 10^{-1997A-5.5} \quad (6.12)$$

$$pH_{sat} = 12.44(4 \times 10^6 A^2 - 1670A + 1) \rightarrow pH_{sat} = 5.0 \times 10^7 A^2 - 20700A + 12.44 \quad (6.13)$$

where A is the cumulative amount of leached CaO (mol/g).

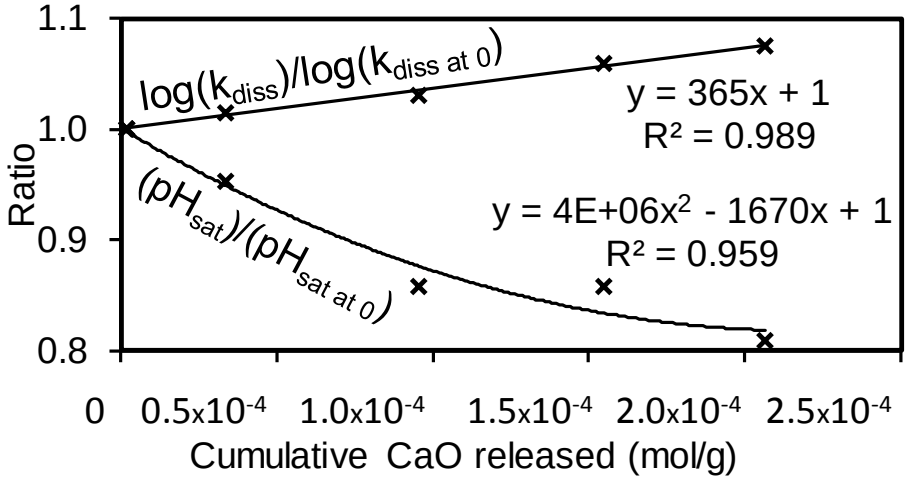

Figure 6.4 : Slag dissolution exhaustion relationships

6.3.3.2 Column modeling results

The simulated water composition at the column outlet is presented in Figure 6.5 for simulations with HRT_V = 16 h and influent $NaHCO_3$ concentration = 0. Results of all simulations are presented in a design graph in Figure 6.6.

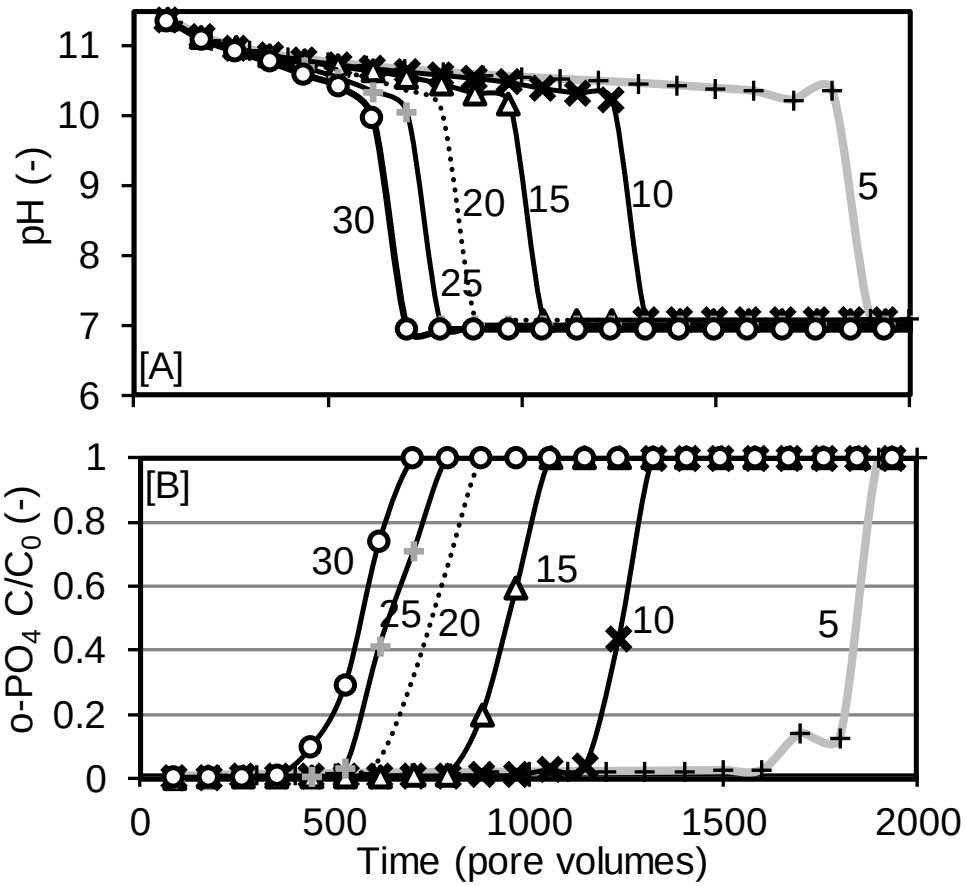

Figure 6.5 : pH (A) and orthophosphates concentration (B) at the outlet of simulated column tests at HRT_V = 16 h and influent $NaHCO_3$ = 0, under various influent P concentrations. The influent P concentration (mg P/L) of each simulation is indicated next to its curve

The same general trend was observed for all simulations. A good phosphorus removal efficiency at the beginning of operation was followed by a rapid decrease in efficiency. pH decreased slowly from 11 to 10, after which it rapidly dropped to 7 to 8, a trend that is typical of the behavior of real slag filters. A variation in inlet phosphorus concentration influenced the filter longevity, as shown in Figure 6.5. This result is explained by the buffer effect of phosphoric acid which exhausts slag. The addition of HCO_3 in the inlet water had a similar effect, reducing the filter longevity (Figure 6.6). The longevity reduction caused by influent HCO_3^- was more pronounced at low influent phosphorus concentration. A similar effect would be expected from the trapping of gaseous CO_2 if the liquid of the filter with its high pH were exposed to the atmosphere. A lower hydraulic retention time also reduced the filter longevity (Figure 6.6). A too short HRT_V resulted in an insufficient reaction time for slag dissolution and phosphorus precipitation. A high pH in the filter is a

necessary but not a sufficient condition for phosphorus precipitation. Once the pH is raised above 10, time is needed for phosphorus precipitation as HAP to take place. This result provides an explanation for the wide orthophosphates concentration range (0.01 to 1 mg P/L) observed at high pH in slag filter effluents (Article 2 – Chapter 5). In practice, with the type of slag studied, maintaining a high pH is an essential indicator of an efficient P removal. o-PO_4 must be also monitored to ensure a low effluent value. In summary, for a given slag, the filter longevity depends on the composition of the inlet water (its buffer capacity) and on the HRT_V.

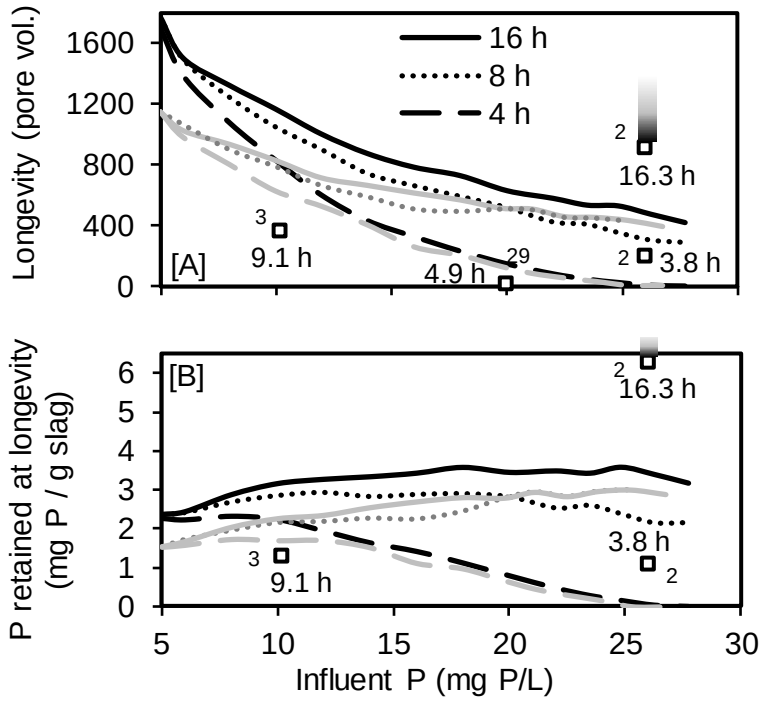

2: (Claveau-Mallet *et al.*, 2012)

3: Article 2 – Chapter 5

29: (Vallet, 2001)

Figure 6.6 : Design graph for prediction of longevity (A) and P retention at longevity (B) based on simulation results. Simulations with and without initial $NaHCO_3$ are presented in gray and black, respectively. The HRT_V is indicated in the legend. Experimental results from past studies are presented by squares or elongated squares to indicate that the longevity was greater than the value at the point. HRT_V and reference are indicated next to each point.

Previous experimental works conducted in the authors' laboratory are compared to simulated results in Figure 6.6. Tests from these past studies were performed in saturated vertical columns fed from the bottom with synthetic wastewater (ref. 2 and 3) or with a real aquatic park effluent (ref. 29). The proposed design graph does reproduce these experimental results: it overestimates (ref. 3 and 29) or underestimates (ref. 2) them. Several reasons explain this difference. First, the

slag used in ref. 3 was not the same batch as the one tested in the present study. The dissolution equations for that particular slag should be established following the proposed batch procedure to produce its own design graph. Second, the slag aging was not the same in ref. 2 and 29. Even if the slag was produced in the same steel mill using the same process, its reactivity can be greatly affected by weathering (Chazarenc *et al.*, 2007) and size (Abderraja Anjab, 2009). Thus, kinetic parameters for a given slag with a given weathering should not be used for the same slag with a different weathering. Third, the wastewater used in ref. 29 was a real wastewater containing salts, organic matter and inorganic carbon, which is not directly comparable with the design graph, that supposes a synthetic wastewater containing only inorganic phosphorus. Simulated results, nevertheless, remain in the same order of magnitude as those obtained experimentally for both longevity and retention capacity. Another factor that could explain the difference between simulations and experimental results is filter clogging, a factor discussed in a subsequent section.

This study proposes that the phosphorus removal performance of a slag filter is defined by two parameters: longevity and retention capacity at saturation. The proposed modeling strategy allows to calculate both values, which are important for design consideration. Longevity and retention capacity are not related by a simple and unique relationship. They are determined by the cumulative effect of the slag dissolution potential and precipitation kinetics, both of which are influenced by wastewater composition. As an example, a high influent phosphorus concentration increases the phosphorus retention capacity at saturation, but decreases longevity (Figure 6.5). A 70% reduction of HRT_V had a small influence on the retention capacity (decrease of only 7.5%) but a large effect on longevity (decrease of 26%). Finally, adding HCO_3 to the wastewater reduced the saturation capacity (Figure 6.5) because the pH-rise capacity of the slag was consumed by the carbonic acid.

6.3.4 Research needs

The proposed model needs to be improved and calibrated with experimental results before being used as a design tool. Its main shortcoming is the assumption that the contact between water and slag is never limited by the accumulation of particles, which is not realistic as clogging takes place due to particulate organic matter and various precipitates, notably HAP, other calcium phosphates and calcite. Particulate matter and precipitates prevent direct contact between slag surface and interstitial water, resulting in a reduced effective dissolution kinetic. They also reduce filter porosity and the available time for reaction (Courcelles *et al.*, 2011). As an example, the initial

porosity of 50% is reduced to 47% when longevity is reached for the base condition simulation (assuming an HAP density of 3.8 g/cm^3). Therefore, the proposed model effectively represents the maximum potential filter efficiency, a value that could not be reached in a real application. The proposed model needs to be completed to account for such clogging. A promising approach would be to couple a hydrodynamic code with a geochemical code, for example HYDRUS coupled with PHREEQC (PC Progress, 2014) or COMSOL coupled with PHREEQC (COMSOL, 2014). The model also has to consider recovery properties that were observed in a previous study (Drizo *et al.*, 2002). Recovery may be explained by our model as a reorganization of precipitates when the filter dries (Claveau-Mallet *et al.*, 2012). The more compact precipitate structure created increases contact between water and slag surface.

Specific recommendations are proposed to improve the model:

Define more precisely the kinetic parameters. Batch tests could be run under different conditions (real wastewater, influent cations, known HAP growth inhibitors, etc.) to assess their specific effect on dissolution and precipitation kinetics (Cucarella & Renman, 2009). The importance of MON in different stages of the filter operation could be assessed in batch tests containing HAP seeds. Statistical analyses should be conducted to evaluate the number of replicates that would be needed to correctly represent slag variability. The current proposed precipitation rates consider a constant specific surface which is unrealistic and additional work should be conducted to relate HAP growth rate to specific surface area (Lasaga, 1981).

Add calcite precipitation within the slag filter model considering that calcite precipitation acts as a competitor to HAP precipitation (Article 2 – Chapter 5; Liira *et al.*, 2009). Calcite formation can be a major concern in filters open to atmosphere.

Consider the evolution of hydraulic conductivity and porosity for column simulations (Courcelles *et al.*, 2011). The evolution of these hydraulic properties is related to the total amount of precipitates and other particulate matters present in the filter. Precipitates should also be considered as a diffusion barrier for ions moving from the slag surface to interstitial water.

The longitudinal and transverse dispersivity used in the model should be determined by tracer tests in experimental column tests. Several tracer tests should be conducted at different moments in the lifetime of the column to assess the effect of particle accumulation on dispersivity. Dispersivity could also be estimated from the media properties (Delgado, 2006; Jourak *et al.*, 2013).

Consider slag variability in a column simulation. In the present study, a constant k_{diss} was used. This constant value could be replaced by a distribution that would be determined by batch tests. The effect of different statistical distributions on simulation results should be assessed.

Implement the model in a 2D or a 3D model. The model proposed in this paper is a 1D model that is valid only for plug flow systems such as long columns.

6.3.5 Practical design strategy for the prediction of slag filter longevity

The main contribution of this paper was to propose a prediction tool for slag filter longevity based on dissolution and precipitation kinetics. The proposed methodology is summarized in three steps:

Experimental batch tests. Each type of slag with specific composition and aging should be calibrated with the proposed batch tests prior to column simulations. First, slag should be sampled according to a standard procedure (ASTM, 2011) to ensure representative sampling. Batch tests should be conducted in replicates with continuous pH monitoring and grab sampling for calcium and phosphorus analysis. Several tests should be conducted with different ratios of slag to water. Exhaustion tests should be conducted. These tests should be conducted with distilled water and the real wastewater to be treated. The resulting kinetic parameters of the slag would be more reliable.

Numerical calibration of batch tests. Calibration of pH-rise curves should be conducted using the dissolution and precipitation model. Dissolution and precipitation kinetic constants can then be determined from which the exhaustion equation is defined. Grab P and calcium analyses should be used for the validation of the pH curve calibration.

Numerical simulations of filter. The longevity and retention capacity of the filter can then be predicted. Several HRT_V should be tested to optimize longevity and filter size.

Design strategies that can be applied to increase the longevity and retention capacity of the filter include using fresh (non-weathered) slag, removing inorganic carbon upstream of the filter and increasing the HRT_V.

6.4 Associated content

6.4.1 Supporting Information

A sensivity analysis for dispersivity was run with the following conditions: influent o-PO_4 = 27.7 mg P/L, influent $NaHCO_3$ = 0 and HRT_V = 8 h. This material is available free of charge via the Internet at http://pubs.acs.org.

6.5 Author information

Corresponding Author

*dominique.claveau-mallet@polymtl.ca

6.6 Acknowledgements

The authors warmly thank Denis Bouchard and Manon Leduc for chemical analyses and technical support, Claire Dacquin who worked on this project as an undergraduate intern, Denis Marcotte for data analysis advices and Philippe Bouchard from Harsco for providing slag samples. This project was funded by the Natural Sciences and Engineering Research Council of Canada.

6.7 Abbreviations

HAP	Hydroxyapatite
HRT_V	Void hydraulic retention time (h)
k_{diss}	Slag dissolution kinetic constant (M CaO/s)
k_{HAP}	Hydroxyapatite precipitation kinetic constant (M HAP/s)
k_{MON}	Monetite precipitation kinetic constant (M MON/s)
$k_{MONtoHAP}$	Kinetic constant for the transformation of monetite to hydroxyapatite (M $Ca(OH)_2$(M MON s pH)$^{-1}$)
K_{spHAP}	Hydroxyapatite solubility product (M^9)
K_{spMON}	Monetite solubility product (M^2)
MON	Monetite

pH_{sat}	Slag saturation pH (-)
r_{diss}	Slag dissolution rate (M CaO/s)
r_{HAP}	Hydroxyapatite precipitation rate (M HAP/s)
r_{MON}	Monetite precipitation rate (M MON/s)
$r_{MONtoHAP}$	Monetite to hydroxyapatite transformation rate (M $Ca(OH)_2$/s)
SI_{HAP}	Saturation index of hydroxyapatite (-)
SI_{MON}	Saturation index of monetite (-)

6.8 References

Abderraja Anjab, Z. (2009). *Development of a steel slag bed for phosphorus removal from fishfarm wastewater (In French).* (M.A.Sc. thesis, Polytechnique Montreal, Canada).

APHA, AWWA & WEF. (2012). Standard methods for the examination of water and wastewater (22nd ed.). Washington, D. C: American Public Health Association, American Water Works Association & Water Environment Federation.

ASTM. (2011). *Standard Practice for Reducing Samples of Aggregate to Testing Size*. ASTM C 702 / C 702 M−11. West Conshohocken, PA: American Society for Testing Materals.

Baker, M. J., Blowes, D. W., & Ptacek, C. J. (1998). Laboratory developmentof permeable reactive mixtures for the removal of phosphorus from onsite wastewater disposal systems. *Environmental Science and Technology, 32*(15), 2308-2316.

Barca, C., Troesch, S., Meyer, D., Drissen, P., Andrès, Y., & Chazarenc, F. (2013). Steel slag filters to upgrade phosphorus removal in constructed wetlands: two years of field experiments. *Environmental Science and Technology, 47*(1), 549-556. doi:10.1021/es303778t

Bowden, L. I., Jarvis, A. P., Younger, P. L., & Johnson, K. L. (2009). Phosphorus removal from waste waters using basic oxygen steel slag. *Environmental Science and Technology, 43*(7), 2476-2481.

Brient, S. (2012). *Dephosphatation of a fish farm wastewater with extensive steel slag fiters (in French).* (M.A.Sc. thesis, Polytechnique Montreal, Canada).

Chazarenc, F., Brisson, J., & Comeau, Y. (2007). Slag columns for upgrading phosphorus removal from constructed wetland effluents. *Water Science and Technology, 56*, 109-115.

Chazarenc, F., Kacem, M., Gérente, C., & Andrès, Y. (2008). *'Active' filters: a mini-review on the use of industrial by-products for upgrading phosphorus removal from treatment wetlands.* Paper presented at the 11th Int. Conf. on Wetland Systems for Water Pollution Control, Indore, India, November 1 – November 7.

Claveau-Mallet, D., Wallace, S., & Comeau, Y. (2012). Model of phosphorus precipitation and crystal formation in electric arc furnace steel slag filters. *Environmental Science and Technology, 46*(3), 1465-1470. doi:10.1021/es2024884

Claveau-Mallet, D., Wallace, S., & Comeau, Y. (2013). Removal of phosphorus, fluoride and metals from a gypsum mining leachate using steel slag filters. *Water Research, 47*(4), 1512-1520.

COMSOL. (2014). Retrieved from http://www.comsol.com/, accessed on May 9, 2014.

Courcelles, B., Modaressi-Farahmand-Razavi, A., Gouvenot, D., & Esnault-Filet, A. (2011). Influence of precipitates on hydraulic performance of permeable reactive barrier filters. *International Journal of Geomechanics, 11*(2), 142-151.

Cucarella, V., & Renman, G. (2009). Phosphorus sorption capacity of filter materials used for on-site wastewater treatment determined in batch experiments - a comparative study. *Journal of Environmental Quality, 38*(2), 381-392.

Delgado, J. M. P. Q. (2006). A critical review of dispersion in packed beds. *Heat Mass Transfer, 42*(4), 279-310.

Domenico, P. A., & Schwartz, F. W. (1998). *Physical and Chemical Hydrogeology* (2nd ed.). New York: John Wiley & sons.

Drizo, A., Comeau, Y., Forget, C., & Chapuis, R. P. (2002). Phosphorus saturation potential: A parameter for estimating the longevity of constructed wetland systems. *Environmental Science and Technology, 36*(21), 4642-4648.

Drizo, A., Forget, C., Chapuis, R. P., & Comeau, Y. (2006). Phosphorus removal by electric arc furnace steel slag and serpentinite. *Water Research, 40*(8), 1547-1554.

Ito, H., Oaki, Y., & Imai, H. (2008). Selective synthesis of various nanoscale morphologies of hydroxyapatite via an intermediate phase. *Crystal Growth & Design, 8*(3), 1055-1059.

Jourak, A., Frishfelds, V., Hellström, J. G., Lundström, T. S., Herrmann, I., & Hedström, A. (2013). Longitudinal dispersion coefficient: effects of particle-size distribution. *Transport in Porous Media, 99*(1), 1-16.

Kim, E.-H., Yim, S.-B., Jung, H.-C., & Lee, E.-J. (2006). Hydroxyapatite crystallization from a highly concentrated phosphate solution using powdered converter slag as a seed material. *Journal of Hazardous Materials, 136*(3), 690-697. doi:10.1016/j.jhazmat.2005.12.051

Lasaga, A. C. (1981). Rate laws of chemical reactions, In *Kinetics of Geochemical Processes* (Vol. 8, pp. 1-68). Chelsea, MI: Mineralogical Society of America.

Le, H. R., Chen, K. Y., & Wang, C. A. (2012). Effect of pH and temperature on the morphology and phases of co-precipitated hydroxyapatite. *Journal of Sol-Gel Science and Technology, 61*(3), 592-599. doi:10.1007/s10971-011-2665-7

Liira, M., Kõiv, M., Mander, Ü., Mõtlep, R., Vohla, C., & Kirsimäe, K. (2009). Active filtration of phosphorus on Ca-rich hydrated oil shale ash: Does longer retention time improve the process? *Environmental Science and Technology, 43*(10), 3809-3814.

Lundager Madsen, H. E. (2008). Influence of foreign metal ions on crystal growth and morphology of brushite ($CaHPO_4$, $2H_2O$) and its transformation to octacalcium phosphate and apatite. *Journal of Crystal Growth, 310*(10), 2602-2612.

Mahadeo, K. (2013). *Treatment of fish farm sludge supernatant with aerated filter beds and steel slag filters - Effect of organic matter and nutrient loading rates.* (M.Eng. thesis, Polytechnique Montreal, Canada).

MDDEP. (2006). Metals determination: method by mass spectrometry with argon plasma ionizing source (in French) (3rd ed.): Centre d'expertise en analyse environnementale, Ministère du développement durable, de l'environnement et des parcs. MA. 200 – Mét 1.1.

Oelkers, E. H., Bénézeth, P., & Pokrovski, G. S. (2009). Thermodynamic Databases for Water-Rock Interaction. In Mineralogical Society of America & Geochemical Society (Eds.), *Thermodynamics and kinetics of water-rock interaction* (Vol. 70, pp. 1-46). Chantilly, VA.

Parkhurst, D. L., & Appelo, C. A. J. (1999). *User's guide to PHREEQC (Version 2) - A computer program for speciation, batch-reaction, one-dimensional transport, and inverse geochemical calculations*. (Water-Resources Investigations Report 99-4259). Denver: United States Geological Survey.

PC Progress. (2014). Hydrus-1D for Windows, Version 4.xx. Retrieved from PC Progress website, http://www.pc-progress.com/en/Default.aspx?hydrus-1d, accessed on May 9, 2014.

Stumm, W., & Morgan, J. J. (1996). *Aquatic Chemistry: Chemical Equilibria and Rates in Natural Waters* (3rd ed.). New York: John Wiley & Sons.

Tsuru, K., Kubo, M., Hayakawa, S., Ohtsuki, C., & Osaka, A. (2001). Kinetics of apatite deposition of silica gel dependent on the inorganic ion composition of simulated body fluids. *Nippon Seramikkusu Kyokai Gakujutsu Ronbunshi/Journal of the Ceramic Society of Japan, 109*(1269), 412-418.

USEPA. (1992). Toxicity characteristic leaching procedure. United States Environment Protection Agency Test Method 1311, Washington (DC).

Vallet, B. (2001). *Phosphorus removal of the Montreal Biodome Saint-Laurent Marin basin by steel slag (In French)*. Intern Report, Polytechnique Montreal, Montreal.

Valsami-Jones, E. (2001). Mineralogical controls on phosphorus recovery from wastewaters. *Mineralogical Magazine, 65*(5), 611-620.

Vohla, C., Kõiv, M., Bavor, H. J., Chazarenc, F., & Mander, Ü. (2011). Filter materials for phosphorus removal from wastewater in treatment wetlands-A review. *Ecological Engineering, 37*(1), 70-89.

CHAPTER 7 TREATMENT OF FISH FARM SLUDGE SUPERNATANT BY AERATED FILTER BEDS AND STEEL SLAG FILTERS - EFFECT OF ORGANIC LOADING RATE

7.1 Introduction

Fresh water trout farms discharge a significant amount of polluting nutrients, estimated to be for ammonium between 100-150 g N d^{-1} per ton of annual fish production and for orthophosphate (o-PO_4) between 20-60 g P d^{-1}per ton (Boaventura *et al.*, 1997). The main source of P in trout farms is raw sludge that is composed of fish excreta, uneaten food and fish carcass debris, and contains 30–84% of the total P discharged from fish farms (Lefrançois *et al.*, 2010). Fish farms in Quebec, Canada are required to limit their global P discharge to the environment to 4.2 kg P per ton of fish produced, according to the Sustainable Development Strategy for Freshwater Aquaculture in Quebec (i.e. STRADDAQ). The commonly used approach to reduce pollutants from the effluent of fish farms is by separating the solids from water through physical settling (Cripps and Bergheim, 2000). Once collected and settled, however, fish sludge still presents environmental problems mainly due to the management of the nutrient-rich sludge supernatant. Due to their remote location and relatively small volume of sludge supernatant (e.g. from 10 to 250 m^3 d^{-1} in the fish farm of this study) the use of conventional intensive treatment systems is not commonly used. Therefore, more ecological, economically beneficial and low maintenance treatment options have to be found with the main goal of reducing P discharge.

Several studies (Comeau *et al.*, 2001; Drizo *et al.*, 2006; Chazarenc *et al.*, 2010; Pratt & Shilton, 2010; Puigagut *et al.*, 2011) were conducted to find the best methods for organic matter and nutrient (especially P) removal from fish farm wastewater. One ecological option is to use treatment wetlands (TWs) with filter systems as has been done for various types of wastewater from mainly domestic but also industrial, mining, agricultural, landfill leachate origins (Kadlec and Wallace, 2009). Common TW technologies, however, require large land area that is not always available. Furthermore, there are several constraints that derive from using TWs in cold climate conditions. One key element for efficient organic matter and nitrogen removal in TWs is the supply of oxygen that is needed for aerobic microbial processes. To address this issue, several studies have been done

with intensified (i.e. engineered) TWs that use forced aeration (Muñoz *et al.*, 2006; Nivala *et al.*, 2013; Ouellet-Plamondon *et al.*, 2006; Vymazal, 2011).

In TWs, phosphorus is mainly precipitated in or sorbed onto filter media (Kadlec & Wallace, 2009). A sustainable solution could be to use reactive filter units containing replaceable material with a high P binding capacity (Brix *et al.*, 2001; Drizo *et al.*, 2006; Kõiv *et al.*, 2010; Shilton *et al.*, 2006). High P removal efficiency has been shown through calcium (Ca)-phosphate precipitation using reactive filtration in Ca-rich alkaline filter materials (Liira *et al.*, 2009; Claveau-Mallet *et al.*, 2012; Article 3 - Chapter 6). Potential materials for P precipitation include high Ca content industrial by-products such as metallurgical slags and ashes, in which Ca occurs in CaO form (lime) and/or Ca-silicates (Vohla *et al.*, 2011).

As determined by the toxicity characteristic leaching procedure TCLP (U.S. Environmental Protection Agency, 1992) only non-hazardous filter materials should be selected for wastewater applications. Slags from 58 mills in the U.S. were tested and it was shown that although the total concentration of some metals in slag may be elevated, they remained tightly bound to the slag matrix and were often not readily leachable (Proctor *et al.*, 2000). In current study electric arc furnace steel slag from Quebec, Canada was used and it has been considered as safe material according to TCLP procedure.

With reactive filter materials, appropriate biological pre-treatment for removing solids, organic matter and nutrients is crucial to provide a long lifetime of the reactive media by decreasing the risk of clogging and permitting the use of finer reactive filter media with higher P sorption capacity (Hedström, 2006). Phosphorus sorption sites may be blocked by organic matter or sorption may be reduced by competitive sorption of organic anions or by metal complexation (Nilsson *et al.*, 2013). Supersaturation of pore water with respect to Ca and o-PO_4 is essential for the precipitation of stable Ca-phosphate phases (House *et al.*, 1999; Liira *et al.*, 2009).

The goal of our study was to develop an on-site compact, cost-effective and environmentally friendly method for the treatment of the supernatant of fish farm sludge settling silos. The main objectives of this study : a) to determine the organic matter and nutrients removal efficiency of a pilot treatment system consisting of a series of aerated gravel filter beds (AFBs, as a replacement for an aerated TW) and electric arc furnace steel slag filters; b) to determine the effect of loading rate on performance; c) to determine the effect of void hydraulic retention time (HRT_V) on o-PO_4

removal in slag filters; d) to validate the P-Hydroslag model as a design tool for slag filters; and e) to propose preliminary design options for fish farms.

7.2 Material and Methods

7.2.1 Site description

An on-site pilot experiment (Figure 7.1) for the treatment of the supernatant from sludge settling silo (i.e. reservoir) was established in 2010 at the "Ferme Piscicole des Bobines", a fresh water trout farm in East Hereford, Quebec, Canada that ran for a total of 11.5 months. In the Bobines fish farm, there is a total 40 interior fish tanks. The water used (10 000 to 20 400 m^3 d^{-1}) originates from fresh groundwater (15%) and from microscreened recirculated water (85%).

In 2010 and 2011 (during P1), about 250 m^3 d^{-1} of screenings were collected and stored in a settling silo of 250 m^3 with an HRT of about one day (Figure 7.1). During the winter and spring of 2012 (just before P2), a sludge thickener, a new settling tank and a liming system for P removal were added. This new installation reduced the flowrate of concentrated sludge from 250 m^3 d^{-1} to about 10 m^3 d^{-1} and increased its pollutant concentration. The supernatant of the new sludge thickener (~240 m^3 d^{-1}) was returned to the microscreen and the thickened sludge (~10 m^3 d^{-1}) was sent to a newly built sludge silo with a volume of 370 m^3 providing an *HRT* of 37 days. After settling in the new sludge silo, the highly concentrated supernatant was limed for P removal and then stored in silo for limed sludge. Two times per year the thickened sludge from the new sludge silo and the limed sludge were spread on agricultural land for fertilization and land amendment (Figure 7.1).

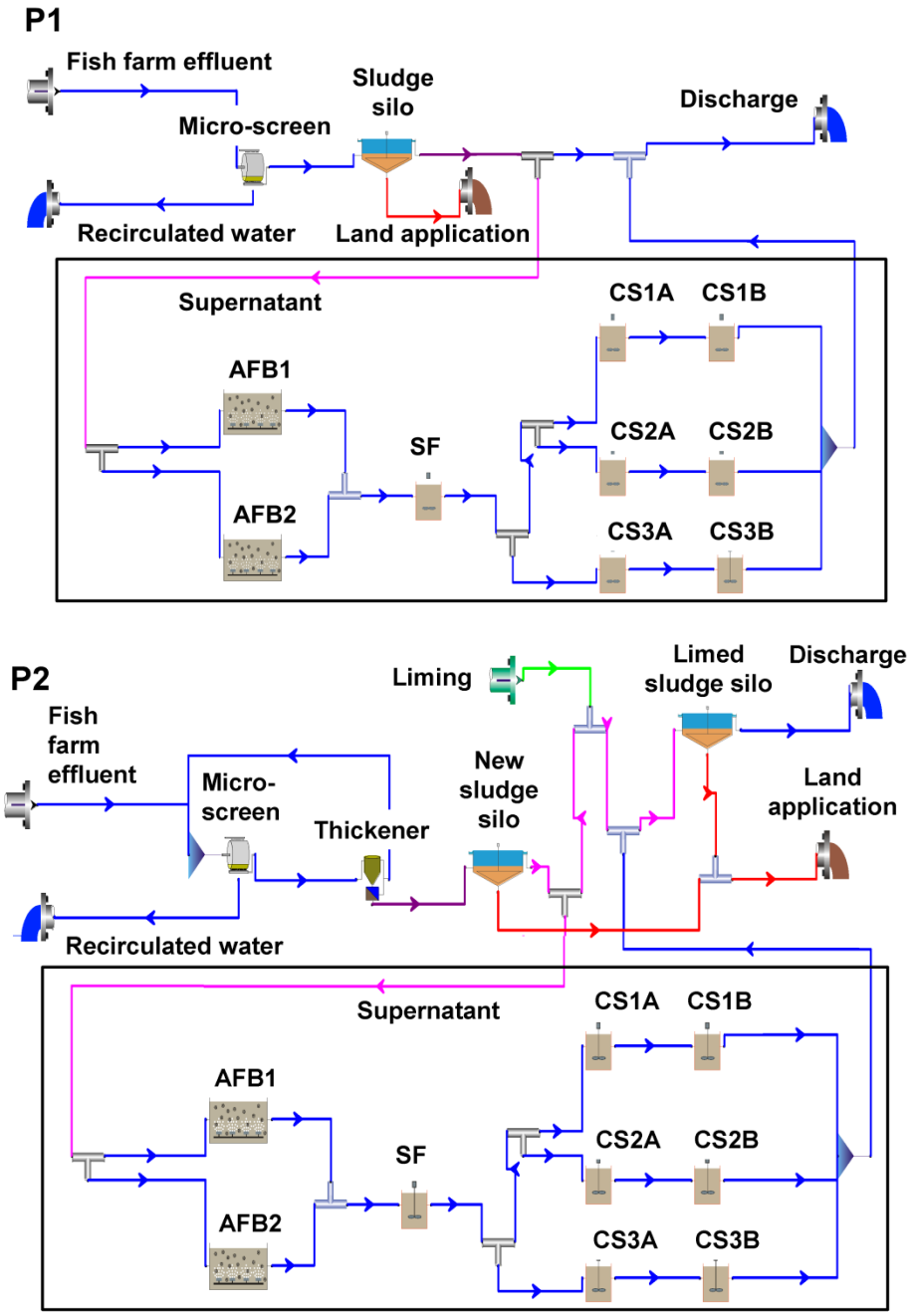

Figure 7.1 : Schematic diagram of the fish farm treatment system and experimental system during Phase 1 (P1) and Phase 2 (P2) when the sludge supernatant contained a low (P1) or a high pollutant (P2) concentration. Abbreviations: AFB1 and AFB2 – two parallel aerated filter beds; SF – sacrificial slag filter; SC1A+SC1B, SC2A+SC2B, SC3A+SC3B – three parallel dual-stage steel slag columns with different void hydraulic retention times

7.2.2 Experimental design

The experimental treatment system was composed of two parallel downflow saturated aerated filter beds (AFBs) followed by a sacrificial slag filter (SF) and three parallel dual-stage steel slag columns (SCs; Figure 7.1). An insulated truck trailer was used to install the experimental system to avoid freezing during winter periods.

The main design parameters of the experimental filter units are summarized in Table 7.1.

Table 7.1 : Summary of design parameters of the experimental filter units in Phase 1 (P1) and Phase 2 (P2). Abbreviations: AFB1 and AFB2 – two parallel aerated filter beds; SF – sacrificial slag filter; SC1, SC2, SC3 – three parallel dual-stage steel slag columns

Design parameters	**Units**	**AFB1, AFB2**	**SF**	**SC1, SC2, SC3**
Water flow conditions		saturated downflow	saturated upflow	saturated upflow
Filter size (diameter × height or *length × width × height)	m×m or *m×m×m	*1.0×1.0×1.0 (each AFB)	0.45×0.8	0.3×1.3 (each stage)
Water level in filter units	m	1.0	0.8	1.3
Volume of filter material	m^3 $filter^{-1}$ (*or $stage^{-1}$)	0.90	0.13	*0.095
Filter material		gravel	EAF steel slag	EAF steel slag
Particle size of material	mm	10-25	P1 SF1 = 20-40 P2 SF2 = 10-30 P2 SF3 = 10-30	5-10
Density of material	kg L^{-1}	2.6	3.6	3.6
Porosity of filter (estimated)	%	38	45	40
Initial void volume	m^3	0.36	0.052	0.038
Void hydraulic retention time (HRT_V)	h	P1 = 48 P2 = 65	P1 = 3.5 P2 = 4.8	P1: 20, 12, 4.5 P2: 30, 15, 6.0 (per stage)
Organic loading rate (OLR)	kg BOD_5 m^{-3} d^{-1}	P1 = 0.015 P2 = 0.50	–	–
Air flow direction		counter-current	–	–

Even though the aerated filter beds (AFBs) are aerated saturated downflow biofilters, the lower design values of trickling filters (Metcalf & Eddy *et al.*, 2014) were used to minimize maintenance of the AFBs. The design criterion chosen was based on a specific nitrogen removal rate per rock surface area (see also Table 7.3). The AFB effective volume was 0.36 m^3 each and they were periodically fed with sludge supernatant. The aeration system consisted of a porous diffuser that was connected to an air pump with a total air flow rate of 0.15 $m^3\ min^{-1}$. The supernatant treated in both AFBs was combined and then gravity flowed to the airtight upflow sacrificial filter with coarse steel slag (SF; Figure 7.1). The main functions of the SF were to capture some inorganic carbon and P to improve the efficiency of the subsequent SCs. During P1, the coarse steel slag in SF was changed after 184 days of utilization to smaller size slag material (see Table 7.1). For P2, a new and finer steel slag was used (Table 7.1). For the SF, three periods are used, SF1 (first 184 d) and SF2 (lasting 77 d) both during P1, and SF3 (lasting 77 d) during P2 (Table 7.1).

The effluent from the SF was pumped to three parallel dual-stage upflow EAF steel slag columns (SC1A+SC1B; SC2A+SC2B; SC3A+SC3B; Figure 7.1) which main function was o-PO_4 precipitation. The dual-stage SCs had different HRT_V (Table 7.1) to determine the effect of hydraulic and pollutant loading rates on the efficiency of the EAF filters. All steel slag units were closed airtight to prevent atmospheric CO_2 dissolution into the high pH water that would result in bicarbonate formation and calcium carbonate precipitation. Gravity flow was favored in the slag columns by installing a venting system connected to a siphon filled with mineral oil to minimize atmospheric CO_2 dissolution while allowing liquid flow.

The onsite pilot experiment was divided into two phases. Phase 1 (P1) lasted from the end of November 2010 to the middle of August 2011 for a duration of 8.5 months. During P1, the sludge supernatant was relatively diluted and the OLR of 0.015 kg $BOD_5\ m^{-3}\ d^{-1}$ to the experimental system was low. Phase 2 (P2) lasted from the end of May 2012 to the end of August for total duration of 3.0 months. During P2 the sludge supernatant was highly concentrated and the OLR was high (0.5 kg $BOD_5\ m^{-3}\ d^{-1}$). Between the two phases, during rebuilding of the fish farm sludge treatment system, the experimental system was at rest for 9 months with the filter units drained and all slag filters kept airtight.

7.2.3 Filter materials

Electric arc furnace (EAF) steel slag, a by-product of the steel industry, was used in the experimental filters and was produced by Arcelor Mittal of Contrecoeur, Quebec, Canada and obtained from "Minéraux Harsco", also of Contrecoeur. The tested steel slag has been used also in previous studies (Claveau-Mallet *et al.*, 2012; Article 3 - Chapter 6). Washed gravel (schist) used as a filter media in our aerated filter beds and as a bottom drainage layer in slag filters was obtained from a nearby quarry in East-Hereford, Quebec, Canada. The chemical composition of the EAF steel slag and gravel used in our experiment is presented as supplementary material in Supplementary Table 7.4.

7.2.4 Sampling and analytical methods

Samples from the influent and effluent of all filter units and from combined effluent of aerated filter beds (AFB_{cb}) were taken once a week during the whole period of the operation using standard procedures (APHA *et al.*, 2012). Extra samples were taken from the middle of the first slag columns ($SC1A_{mid}$; $SC2A_{mid}$; $SC3A_{mid}$). The chemical oxygen demand (*COD*), carbonaceous biochemical oxygen demand ($CBOD_5$), total suspended solids, (*TSS*), volatile suspended solids (*VSS*), total Kjeldahl nitrogen (*TKN*), ammonium (NH_4), nitrate plus nitrite (NO_x), total phosphorus (TP), orthophosphate ($o\text{-}PO_4$), calcium (Ca^{2+}), alkalinity and pH were determined according to Standard Methods (APHA *et al.*, 2012). The Statistica 7.0 software was used for data analyses for which a level of significance of α=0.05 was used in all cases. In the "Results and discussion" section, significant differences were outlined when $p < 0.05$ was obtained.

7.2.5 Numerical simulations

Slag column operation was simulated using the P-Hydroslag model written in the PHREEQC software, using slag exhaustion equations that were determined previously for the "Minéraux Harsco" EAF slag (Article 3 – Chapter 6). The exhaustion equations were adapted to consider 40% porosity, resulting in the following equations:

$$log(k_{diss}) = -0.3688B - 5.46 \quad (7.1)$$

$$pH_{sat} = 1.71B^2 - 3.835B + 12.44 \quad (7.2)$$

where k_{diss} is the slag dissolution kinetic constant (M Ca s^{-1}), pH_{sat} is the slag saturation pH and B is the total leached CaO in the slag filter (mol L^{-1}).

Slag column influent solutions were reproduced using chemicals ($CaCl_2$, KH_2PO_4, K_2HPO_4, CaO, NH_4Cl, $NaHCO_3$ and KCl) in the REACTION datablock. Solutions were equilibrated with hydroxyapatite, monetite and calcite in the EQUILIBRIUM_PHASES datablock. Resulting solutions are shown in Table 7.2. Simulations were conducted for both phases P1 and P2, and for the first columns SC1A, SC2A and SC3A. Simulated and experimental results were compared. Additional simulations using the AFB effluent as column influent were conducted to assess the effect of removing the SF.

Table 7.2 : Composition of simulated influent solutions of the slag columns (AFBs effluent feeding the SF and SF effluent feeding the SCs)

Phase	**pH**	**Ca^{2+}**	**TIC**	**o-PO_4**	**NH_4**	**Alkalinity**
	-	mg L^{-1}	mg C L^{-1}	mg P L^{-1}	mg N L^{-1}	mg $CaCO_3$ L^{-1}
AFB P1	7.19	24.6	13.4	2.42	-	51.6
SF P1	8.27	28.1	13.4	2.42	-	60.3
AFB P2	7.39	23.4	159.8	13.6	210	645.3
SF P2	8.07	30.7	145.2	13.6	210	663.4

7.3 Results and discussion

During P1, the supernatant from the sludge silo had a composition similar to typical low strength municipal wastewater while it was much more concentrated during P2 (Supplementary Table 7.5). Standard deviation (SD) values indicate that during both phases the influent concentration of most pollutants was quite variable over time (Supplementary Table 7.5). The variability was due to the varying amount of solids in the sludge silo with peak concentrations due to the silo being full of solids and in need of cleaning.

7.3.1 Removal of organic matter, solids and nitrogen

The main functions of the aerated filter beds were to remove solids and to oxidize organic matter and ammonium. During P1, the aerated filter beds (AFB_{cb} – shown as combined effluent) were very efficient in mineralizing organic matter and removing solids (Supplementary Table 7.5; Figure

7.2). Average reductions obtained in the AFBs were 95.3% for *COD*, 97.3% for BOD_5, 95.8% for *TSS* and 94.9% for *VSS* resulting in effluent values of less than 3 mg *TSS* L^{-1} (Figure 7.2). During P2, the degradation of organic matter in AFBs was quite good (Supplementary Table 7.5; Figure 7.2), with an average removal of 65% for *COD* and 71% for BOD_5 (Figure 7.2). However, the AFB effluent *COD* and BOD_5 values remained high at 1730 and 895 mg O_2 L^{-1}, respectively.

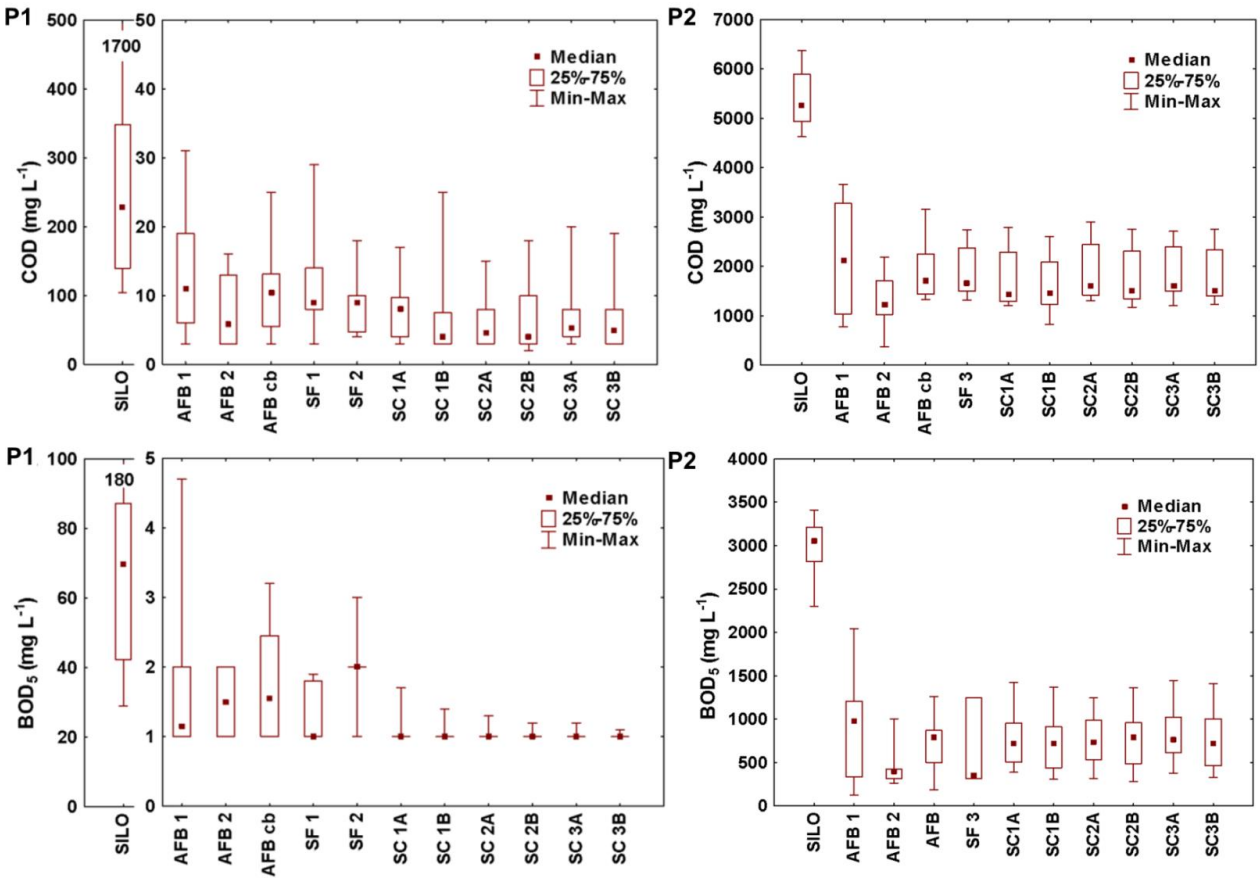

Figure 7.2 : Organic matter removal by the various treatment units (presented as changes in BOD_5 and *COD* values) during Phases 1 and 2 (P1 and P2) of the experiment. Note: The two AFBs and the three sets of two columns in series of SCs were operated in parallel

A rapid increase in *TSS* and *VSS* concentration from the sludge silo was observed after about 170 days of operation during P1 (Figure 7.3) indicating that the sludge silo needed to be emptied. During P2, the effluent from the AFBs had a higher *TSS* and *VSS* concentration than the influent, indicating that the AFBs should have been backwashed to prevent excessive solids accumulation. Backwashing could be achieved by sending AFB treated water and air at the bottom of the AFB to clean the bed of excess biosolids, as is typically done for biofilters (Metcalf & Eddy, 2014). The

recovered solids would then be sent to a settling tank for treatment. With low loaded AFBs, such an operation may have to be done once a month or less.

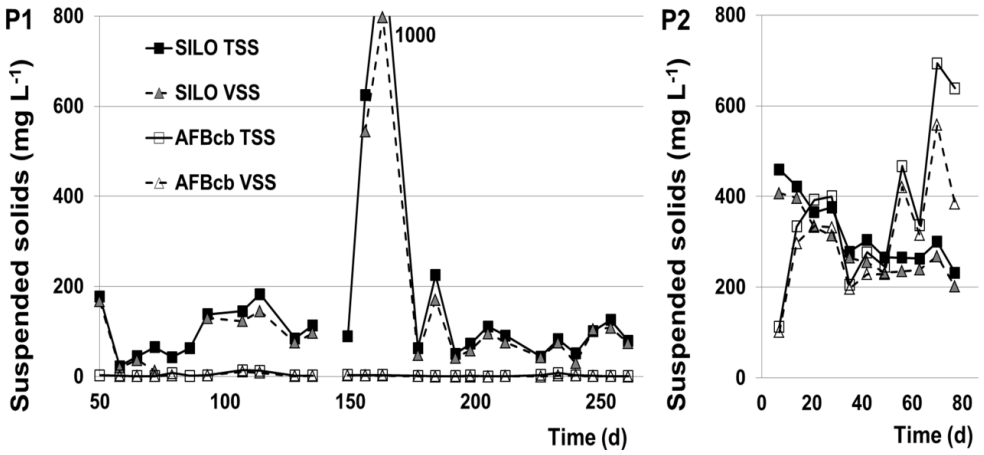

Figure 7.3 : Evolution of total suspended solids (*TSS*) and volatile suspended solids (*VSS*) concentration in the combined effluents of the aerated filter beds (AFB_{cb}) effluent during P1 and P2

Efficient ammonification of organic nitrogen (*TKN* minus NH_4) and nitrification were observed in the AFBs during P1 (average effluent *TKN* only 0.9 mg N L^{-1}) as confirmed by the increase of oxidized nitrogen concentration in the effluent (from 0.05 to 5.1 mg L^{-1}, Figure 7.4).

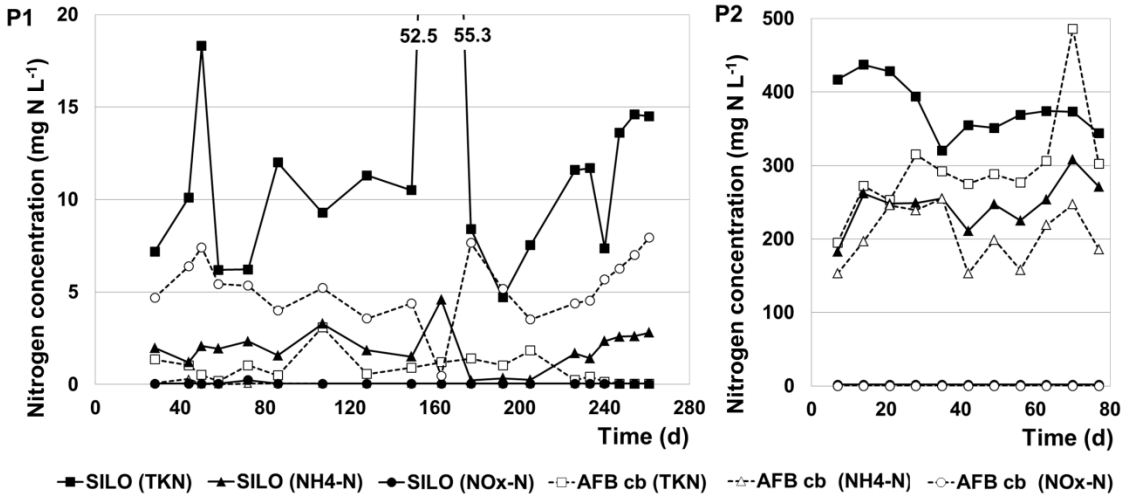

Figure 7.4 : Nitrogen removal and transformation (presented as changes in *TKN*, NH_4-*N* and NO_x-*N* concentrations) in the combined effluent of the aerated filter beds (AFB_{cb}) during Phase 1 and 2 (P1; P2)

During P2, the overall efficiency of *TKN* removal by the system was 32% of which 20%, on average, was achieved by the AFBs ($p>0.03$; Figure 7.4). The AFBs removed only 17% of ammonium and there was no increase in NO_x concentration. This can be explained by the BOD_5 concentration that was too high to allow efficient nitrification (Metcalf & Eddy, 2014). In summary, the AFB is suitable technology for sufficient pre-treatment of fish farm supernatant when appropriate loading rates are used (shown in details in Section 6.3.3).

7.3.2 Removal of total phosphorus and orthophosphate

The TP removal in the AFBs during P1 was on average 35% (effluent 2.6 mg TP L^{-1}) while the o-PO_4 concentration increased by about 10% due to hydrolysis (effluent concentration 2.4 mg L^{-1}).

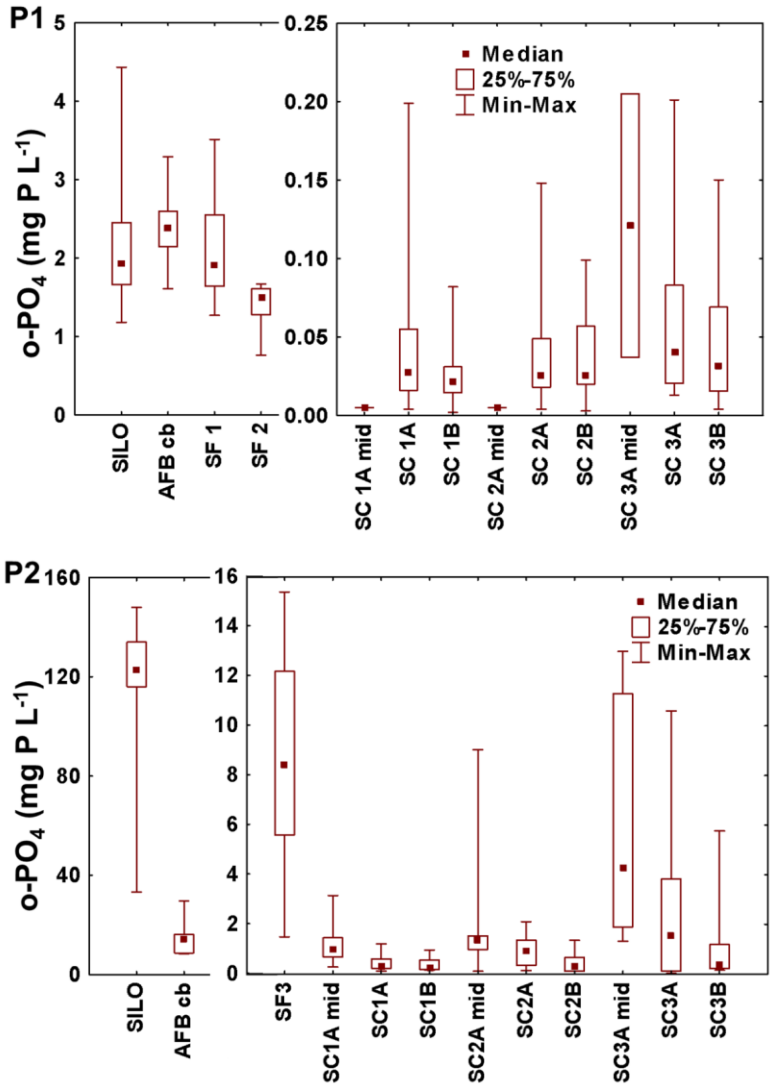

Figure 7.5 : Evolution of orthophosphate (o-PO_4) during P1 and P2 in the filter units

During P2, an average 78% of TP and 86% of o-PO_4 was removed in the AFBs (Figure 7.5). This high efficiency was unexpected and could be attributed to phosphate precipitation with calcium, iron or aluminium ions present in the sludge supernatant. In P2, sludge supernatant had a sufficiently high calcium concentration (145 mg L^{-1} soluble) to induce precipitation. Calcium leaching of the AFBs was also observed in P1.

During P1, the sacrificial slag filter showed an average o-PO_4 removal of only 17% and 34% in SF1 and SF2, respectively (Figure 7.5). During P2, the cumulative amount of TP removed and the removal efficiency in SF3 was higher than in SF1 and SF2 during P1 (Figure 7.6), with an average o-PO_4 removal of 47%. During P2, the efficiency of SF3 was comparable with SC3A – the slag column that received the highest loading rates during the whole experiment. Similarly to the constant decrease in the TP removal efficiency there was concomitant decrease in the pH value of the effluent from pH 9.0 to pH 8.0. Thus, the SF increased somewhat the pH of the treated supernatant, but contributed only slightly to phosphorus removal.

7.3.2.1 Phosphorus removal in dual-stage steel slag columns

All dual-stage slag columns (SCs) removed on average more than 96% of TP during P1 with a stable effluent concentration averaging from 0.10 to 0.17 mg P L^{-1}. During P2, a lower TP removal efficiency of 85-91% was observed. This resulted in an effluent TP of 5.4 to 7.4 mg L^{-1} but a relatively low o-PO_4 concentration of 0.3 to 1.1 mg P L^{-1} (Supplementary Table 7.5; Figure 7.5). Slag columns removed o-PO_4 by Ca-phosphate precipitation (Claveau-Mallet *et al.*, 2012) and particulate P mainly by physical filtration. Particulate P removal could be increased by increasing the HRT_V as this would slow down the water velocity inside the filter material and increase the solids filtration (Claveau-Mallet *et al.*, 2012). As particulate matter can clog slag columns, sufficient pre-treatment is needed to prevent solids accumulation (Hedström, 2006).

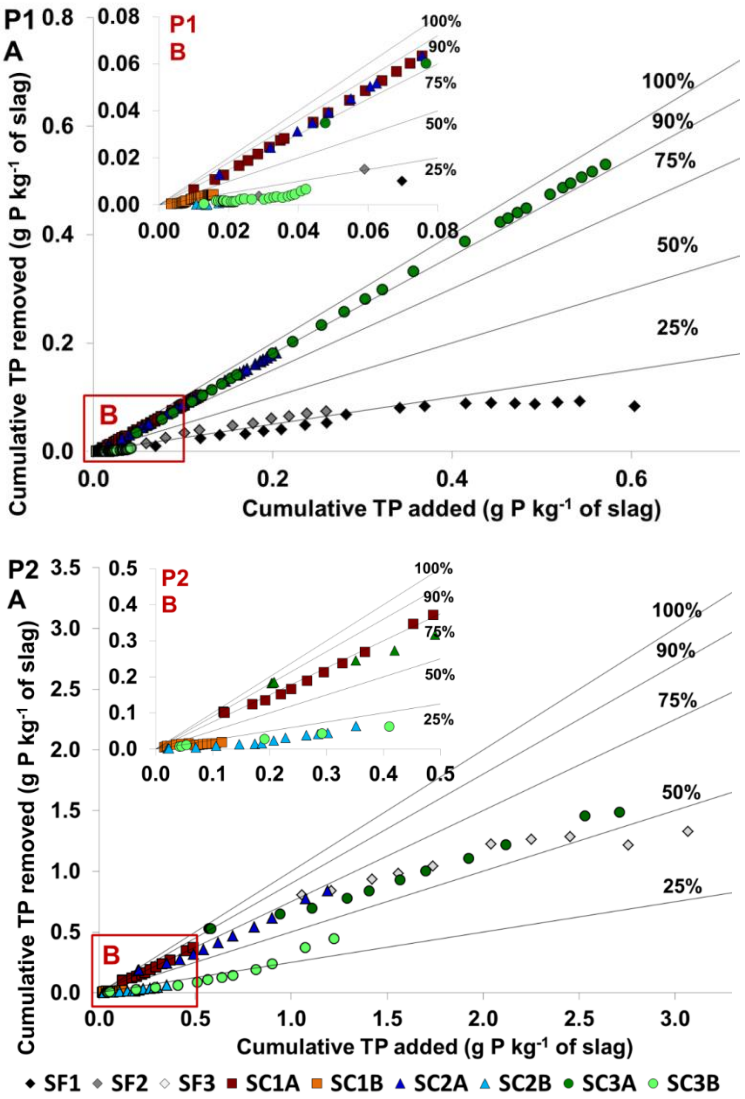

Figure 7.6 : Ratio between cumulative total phosphorus (TP) added and removed in steel slag filters (SF and SCs) during Phase 1 and 2 (P1 and P2). All SCs used during P1 continued to be used during P2, which explains why the first data points at the beginning of P2 (graph B) are not located at the origin of the graph

During P1, almost all o-PO_4 was precipitated in the first stage of the SCs (e.g. in SC1A >97%), and the final effluent o-PO_4 concentration varied from 0.03 to 0.05 mg P L^{-1} (Figure 7.4). There were only slight differences in the final TP and o-PO_4 concentration in between the SCs during P1 even though there was a tendency for the columns with longer HRT_V to remove phosphate a little more efficiently (Figure 7.5). The SC3A+SC3B with the shortest HRT_V (4.5 h + 4.5 h) and highest P loading rate had the highest orthophosphate removal efficiency during P1 (96%). Furthermore,

the SC3A started to show its first signs of saturation during the last month of operation when the effluent o-PO_4 concentration increased rapidly from 0.03 to as high as 10.6 mg P L^{-1} (see also Figure 7.8). In the downstream SC3B the average o-PO_4 removal efficiency during P2 remained above 90% (TP removal 63%), but during last two weeks of operation, the o-PO_4 removal efficiency of this column decreased to 58%.

During P2, the effect of cumulative loading on the SCs efficiency was observed (Figure 7.6). Over time, the SC3A+SC3B with higher TP loading removed less TP. During this phase, SC1A+SC1B removed up to 0.4 g P kg^{-1} and SC2A+SC2B a total of 0.9 g P kg^{-1} of slag. The first column SC3A of dual-stage slag filter which received the highest TP loading, removed a total of 1.4 g P kg^{-1} slag.

The effect of HRT_V on the average o-PO_4 removal efficiency in slag filters is shown on Figure 7.7. The SCs with longer HRT_V had high and relatively stable P removal efficiency during both phases, and an effluent o-PO_4 concentration over 2 mg L^{-1} in SC2A was only observed during the last week of operation. The only slag column that showed significantly lower o-PO_4 removal efficiency during P2 was SC3A. These results indicate that there is a clear effect of HRT_V on o-PO_4 removal especially when a high OLR is applied to the system. At a high OLR, the slag filters should be operated at a minimum HRT_V of 30 hours to ensure efficient o-PO_4 removal.

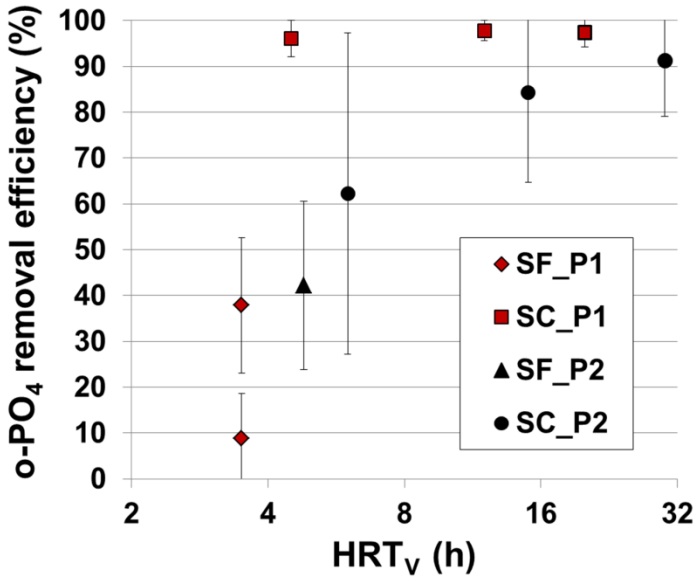

Figure 7.7 : Effect of void hydraulic retention time (HRT_V) on average orthophosphate (o-PO_4) removal efficiency during P1 (red; low o-PO_4 load) and P2 (black; high o-PO_4 load) in sacrificial slag filters (SFs) and dual-stage slag columns (SCs). Error bars denote standard deviations

The evolution of SCs effluents composition is compared to P-Hydroslag model simulation results on Figure 7.8. The experimental curves of pH were reasonably well reproduced by simulation, except for SC3A at the end of P2, where the observed pH drop was larger than that simulated. The o-PO_4 simulated curves generally reproduced experimental curves, but they were less accurate during P2. The HRT_V effect predicted by the model was observed in experimental results. The model properly predicted an o-PO_4 concentration over 1.0 mg P L^{-1} for SC3A during P2.

The model also predicted the effect of changing from P1 to P2, and showed that removing the SF did not significantly decrease the SCs performance (solid vs dotted lines on Figure 7.8). This result constitutes the first calibration of the P-Hydroslag model with a field-scale application and validates the potential of this model as a design tool. The current version of the model is intended to simulate secondary effluent containing low suspended solids content, as it considers soluble influent only. The model still needs improvement concerning some model assumptions regarding the effect of particulate matter accumulation and the refinement of the methods to measure kinetic parameters. These aspects are included in a forthcoming version of the model (Article 4 - Chapter 8).

A longer HRT_V should improve the contact between the substrate and the wastewater and increase P removal. Liira *et al.* (2009) using hydrated oil shale ash, a material with similar removal mechanisms to slag, showed that at a long HRT_V, a dense and tightly packed layer of acicular calcite crystallites forms that gradually covers the entire surface of the particles. As a result, the dissolution of Ca is inhibited, and the phosphate precipitation decreases.

From experimental results and according to numerical simulations, it was confirmed that the HRT_V plays a central role in the long-term operation of slag filters. Previous research (Shilton *et al.*, 2006; Vohla *et al.*, 2011) showed that slag filters are capable to precipitate much higher amounts of o-PO_4 than observed during this experiment (e.g. P retention capacity of EAF slag 6.4 g P kg^{-1} of slag; Claveau-Mallet *et al.*, 2012). Such high capacity was achieved in batch and lab-scale experiments with a synthetic P containing feed and there are only few studies done with onsite and full-scale systems during extended periods of time. Shilton *et al.* (2006) presented results of full-scale treatment plant with reactive steel slag filters where an average TP removal efficiency of 77% and a maximum removal level of 1.2 g TP kg^{-1} (total of 20 tons of P removed) of slag were reported during the first 5 years of operation.

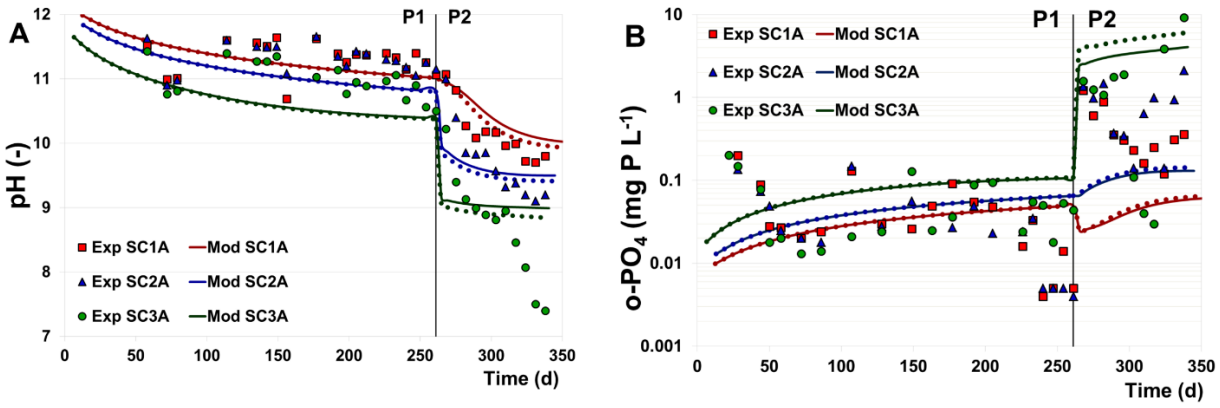

Figure 7.8 : Simulation results of the P-Hydroslag model and comparison with experimental data for A) pH and B) o-PO_4. Simulated curves with sacrificial slag filter (SF; solid lines) and without SF (dotted lines) are shown

In full-scale systems, the HRT_V of the slag filter should be chosen to favour compact crystallization (crystal growth and not formation of new crystal seeds) of Ca-phosphate and to minimize the precipitation of Ca-carbonates (Claveau-Mallet *et al.*, 2012). The minimum HRT_V required to support crystal growth and long-term operation is related to the hydroxyapatite crystal growth rate, which is related to the composition of the wastewater (Claveau-Mallet *et al.*, 2012; Article 3 - Chapter 6). Finding the optimal HRT_V according to the characteristics of wastewater is possible by using the P-Hydroslag model.

7.3.3 Preliminary design of the hybrid treatment system

Preliminary full-scale design options for the treatment of sludge settler supernatant based on the average composition of the supernatant from "Les Bobines" fish farm during P1 and P2, and experimental results of this study were proposed (see Table 7.3). For low strength supernatant (P1), the conditions were characterized by a relatively high flowrate (50 m^3 d^{-1}) but a low pollutant concentration that was similar to those of a typical low strength municipal wastewater. For high strength supernatant (P2), the conditions were for a lower flowrate (10 m^3 d^{-1}) but a higher pollutant concentration.

Table 7.3 : Preliminary full-scale design parameters for the treatment of low (P1) and high strength (P2) supernatant of a freshwater fish farm sludge settling tank, consisting of a) an aerated filter bed (AFB) and b) a reactive slag filter

Wastewater type		**P1 (low strength)**	**P2 (high strength)**
Aerated filter bed			
1) AFB influent data (see Table 7.5)			
2) Objectives			
TKN removal efficiency	%	90	10
BOD removal efficiency	%	80	50
3) AFB design criteria (results from trickling filter design, Metcalf & Eddy, 2014)			
Type of AFB		low-rate	high-rate
Specific surface area in the reactor	$m^2\ m^{-3}$	60	60
Hydraulic loading rate	$m\ d^{-1}$	3.6	1.04
Organic loading rate	$kg\ BOD_5\ m^{-3}d^{-1}$	0.13	1.57
Specific *TKN* removal rate per rock area	$g\ m^{-2}\ d^{-1}$	0.40	0.33
4) Design values			
Filter volume (empty bed)	m^3	28	19
Filter depth	m	2	2
Filter area	m^2	13.9	9.6
Particle size of material	mm	10-20	10-20
Aeration rate	$m^3\ min^{-1}$	0.83	2.92
Slag filter			
1) Slag filter influent data (see Table 7.5**)**			
2) Objectives			
P removal efficiency	%	80	80
3) Slag filter design criteria (results from numerical simulations using the P-Hydroslag model)			
Void hydraulic retention time	h	8	30
Longevity	pore volumes	5400	315
	years	5	1
P retention capacity	$g\ P\ kg^{-1}$ slag	4.5	1.7
4) Design values			
Filter volume (empty bed)	m^3	42	31
Filter depth	m	2	2
Filter area	m^2	21	15.5
Particle size of material	mm	5-10	5-10

A low-rate AFB (version P1 in Table 7.3) with nitrification was chosen for supernatant similar to the one used during P1, while a high-rate AFB with recirculation was chosen for wastewater similar to P2. Aeration was provided for BOD_5 and ammonia oxidation for P1 and P2. AFB effluent recirculation was not tested during this experiment but such a mode of operation could improve the treatment efficiency when dealing with high strength wastewater.

A potential alternative for the AFBs when treating a low concentration supernatant could be more passive and low maintenance treatment wetlands (Kadlec & Wallace, 2009). The sacrificial filter with coarse slag used in the experiment was not incorporated in this full-scale design because the SF increased somewhat the pH of the treated supernatant, but contributed only slightly to bicarbonate and phosphorus removal. Furthermore, the simulation results showed that removing the SF did not significantly decrease the SCs performance (Figure 7.8).

The reactive slag filter design was based on numerical simulations performed with the P-Hydroslag model. Using the information from this experiment and previous research (e.g. Barca *et al.*, 2012; Claveau-Mallet *et al.*, 2012; Article 2 - Chapter 5; Drizo *et al.*, 2002; Liira *et al.*, 2009; Shilton *et al.*, 2006) it was estimated that during P1, the optimal HRT_V for slag columns should be about 8 h (Table 7.3). For a more concentrated supernatant as during P2, a HRT_V of 30 h was proposed. The longevity and P retention capacity of slag filters were determined using numerical simulations as previously presented; considering that the filter longevity was reached when the effluent o-PO_4 concentration was above 1 mg P L^{-1}. A safety factor of 2 was used for longevity. The resulting longevity was 5400 pore volumes for P1 and much lower for P2 (315 pore volumes). Longevity expressed in pore volumes allows a more direct comparison of operating conditions of designs of P1 and P2, independently of the HRT_V. The longevity expressed in total time was 5 years for P1 and 1 year for P2. In the latter case, the designer could choose between frequent replacement of the media (every 1 or 2 years) or increasing the size of the slag filter.

For best performance and for preventing short-circuiting in the filter, a vertical upflow feeding mode with a uniform influent distribution system at the bottom of the slag filter is proposed. The slag filters should be built deeper than usual filter units and as airtight as possible to allow water to flow but to minimize gaseous CO_2 dissolution, thus reducing calcium carbonate precipitation and rapid pH lowering in the slag. At least two filters in series should be constructed to provide redundancy in the treatment system.

Bringing down the high effluent pH of the slag column is needed. At a fish farm, the slag filter effluent could simply be diluted in the main effluent by a ratio of at least 100:1 prior to discharge to the receiving stream, bringing the final pH value well below 9.5 which is the required pH limit in Quebec, Canada. If dilution into a larger stream is not an option, then it is possible to install a post treatment unit for pH adjustment. A peat filter installed downstream of an reactive hydrated ash filter was tested in lab-scale by Liira *et al.* (2009) for pH neutralization from > 10 to pH 7-8. An alternative option is pH neutralization with gaseous CO_2 (Sawyer *et al.*, 2003).

Once the slag filter capacity is "exhausted", an extra TCLP test (U.S. Environmental Protection Agency, 1992) should be run to determine if saturated material should be disposed of as a hazardous waste, a municipal solid waste or can be valorised by land application as a soil amendment (Bird and Drizo, 2009). However, the direct use of non-soluble phosphate such as from hydroxyapatite would require an effective and economical means of solubilisation. This problem might be solved with the use of microorganisms (e.g. phosphate-solubilizing bacteria, Richardson, 2001) and phosphate-solubilizing fungi (Whitelaw, 1999). Other research demonstrated that plant root exudates produce organic acids that are strong enough to dissolve P even from hydroxyapatite and the P-saturated filter materials could be source of slow release P (Cucarella *et al.*, 2007; Kõiv *et al.*, 2012).

Highly concentrated influents would require a more intensive biological pre-treatment upstream of the reactive slag filters and the slag would saturate faster and would need to be changed at a higher frequency. Therefore, when considering that most of freshwater fish farms produce sludge supernatant that is more similar to the characteristics of P1 it was concluded that a hybrid treatment system consisting of an aerated filter bed or a treatment wetland followed by reactive slag filters would provide efficient pollutants removal from the supernatant.

7.4 Conclusions

The goal of our study was to develop an on-site compact, cost-effective and extensive system for the treatment of fish farm sludge supernatant. The conclusions of the project regarding initial objectives are the following:

The tested system composed of a downflow AFB followed by a SF and a series of two SCs achieved a mean effluent concentration (and mean % of removal) of 6.0 mg *COD* L^{-1} (98%), 3.0 mg *TSS* L^{-}

^{1} (98%), 0.5 mg *TKN* L^{-1} (96%), 0.13 mg NH_4-*N* L^{-1} (93%), 0.10 mg TP L^{-1} (98%) and 0.05 mg o-PO_4-P L^{-1} (98%) in a low concentration supernatant and a low OLR (0.015 kg BOD_5 m^{-3} d^{-1}; Phase 1); and 1490 mg *COD* L^{-1} (67%), 200 mg *TSS* L^{-1} (37%), 256 mg *TKN* L^{-1} (32%), 188 mg NH_4-*N* L^{-1} (24%), 5.9 mg TP L^{-1} (96%) and 0.5 mg o-PO_4-P L^{-1} (99.5%) in a high concentration supernatant and a high OLR (0.5 kg BOD_5 m^{-3} d^{-1}; Phase 2). The system was especially efficient in removing o-PO_4, achieving effluent concentration below 1.0 mg P L^{-1} consistently during the whole experimental period and according to P-Hydroslag model results could have continued to do so for 5 years (when average o-PO_4 loading similar to P1).

The OLR had a substantial effect on the organic matter mineralization and nitrification efficiency of aerated filter beds. At a low OLR, the AFBs were efficient at removing *COD* (95%) and nitrifying the effluent while at a high OLR, *COD* removal was reduced to 65% and no nitrification took place.

A high HRT_V (>12 h) of SC resulted in higher o-PO_4 removal efficiency for both phases compared to SC with HRT_V < 6 h.

The P-Hydroslag model was used to predict the slag filter behaviour. Experimental pH and o-PO_4 in the effluent were reasonably well reproduced by simulated results, confirming the potential of the model as a design tool. The general effect of HRT_V and phase change was correctly predicted by the model.

Preliminary design options for a fish farm supernatant treatment system were proposed for two types of supernatant (similar to Phases 1 or 2). The suggested design included one AFB followed by a steel slag filter, without a sacrificial slag filter. The design of the AFB was based on the OLR and the design of the slag filter was based on numerical simulations with the P-Hydroslag model. The proposed AFB HRT_V was 2.4 and 96 h for P1 and P2, respectively, while the HRT_V of slag filter was 8 and 30 h for P1 and P2. The expected longevity was at least 20 years for the AFB (both phases), 5 years for the slag filter in P1, and 1 year for the slag filter during P2.

It was concluded that with proper loading rates, this compact biological and physico-chemical treatment system offers a good alternative to the high energy demand and high maintenance treatment systems for organic matter and phosphorus removal, and that this treatment system could be applicable to other agro-environmental, municipal or residential effluents.

7.5 Acknowledgements

This work was financed by the Natural Sciences and Engineering Research Council of Canada, the Société de Recherche et Développement en Aquaculture Continentale, Ressources Aquatiques Québec, EU European Social Fund, Archimedes Foundation and Estonian Research Council postdoctoral research grant no. MJD93. We thank Minéraux Harsco and ArcelorMittal for slag material, and the fish farm Les Bobines, students and staff of Polytechnique Montréal including Denis Bouchard, Edem Adiho, Marc-André Labelle and Marie Ferland for technical assistance.

7.6 Appendix A. Supplementary data

Table 7.4 : Chemical composition of EAF steel slag and quartzite gravel used in our experiment

Material	**Size**	**Chemical composition (% weight)**										
	(mm)	**SiO_2**	**Al_2O_3**	**Fe_2O_3**	**CaO**	**MgO**	**Na_2O**	**K_2O**	**MnO**	**TiO_2**	**P_2O_5**	**CrO_3**
EAF slag	5–10	14.0	5.15	38.5	27.9	11.6	0.08	0.02	2.63	0.8	0.24	0.75
	10–40	16.8	5.94	31.2	33.3	9.69	0.09	0.01	1.49	0.95	0.31	0.45
Gravel	10–15	87.0	6.61	0.45	0.11	0.07	1.10	3.51	-	-	-	-

Table 7.5 : Average composition of the fish farm sludge supernatant and the effluent concentrations of all filter units during Phases 1 and 2 (P1 and P2; units in mg L^{-1}, except for pH; SD marked with "±"). Abbreviations: SILO – fish farm sludge supernatant; AFB_{cb} – combined effluent of aerated filter beds; SF – effluents of sacrificial slag filter during different periods; SC1B, SC2B, SC3B – effluents of steel slag columns with different HRT_V

Filter unit / Parameter		***COD***	***$CBOD_5$***	***TSS***	***VSS***	***TKN***	***NH_4***	***NO_x***	***TP***	***o-PO_4***	***pH***	**Ca^{2+}**	**Alkalinity**
		mg L^{-1}	**mg L^{-1}**	**mg L^{-1}**	**mg L^{-1}**	**mg N L^{-1}**	**mg N L^{-1}**	**mg N L^{-1}**	**mg P L^{-1}**	**mg P L^{-1}**	**-**	**mg L^{-1}**	**mg $CaCO_3$ L^{-1}**
P1	**SILO**	228*	74	84*	76*	13.7	2.0	0.06	5.2	2.1	6.6	27	63
		max. 1690*	±41	max. 973*	max. 798*	±11.8	±1.1	±0.04	±4.6	±0.7	±0.2	±20	±15
	AFB_{cb}	10	2.0	3.0	2.0	0.9	0.12	5.1	2.6	2.4	7.1	24	50
		±6.0	±1.0	±4.0	±2.5	±0.7	±0.3	±1.8	±0.4	±0.4	±0.4	±2	±10
	SF1	11	< 1.0	3.0	1.8	0.7	0.16	5.2	2.3	2.1	7.9		63
		±6.0		±2.0	±1.0	±0.6	±0.35	±1.8	±0.7	±0.6	±0.6		±11
	SF2	9.0	< 1.0	3.0	1.8	0.5	< 0.05	5.6	1.7	1.4	8.6	32	72
		±5.0		±2.0	±1.0	±0.6		±1	±0.4	±0.3	±0.5	±4	±9.0
	SC1B	6.0	< 1.0	4.0	1.2	0.5	0.14	5.2	0.16	0.03	11.5	98	199
		±5.0		±2.0	±1.1	±0.5	±0.32	±1.8	±0.12	±0.02	±0.4	±16	±10
	SC2B	6.0	< 1.0	3.0	1.1	0.6	0.14	5.5	0.17	0.04	11.4	89	186
		±4.0		±2.0	±0.8	±0.6	±0.29	±1.58	±0.11	±0.03	±0.4	±14	±12
	SC3B	6.0	< 1.0	3.0	1	0.5	0.13	5.4	0.10	0.05	11.4	79	165
		±4.0		±3.0	±0.7	±0.6	±0.31	±1.72	±0.09	±0.05	±0.4	±7	±9.0

Table 7.5: Average composition of the fish farm sludge supernatant and the effluent concentrations of all filter units during Phases 1 and 2 (P1 and P2; units in mg L^{-1}, except for pH; SD marked with "±"). Abbreviations: SILO – fish farm sludge supernatant; AFB_{cb} – combined effluent of aerated filter beds; SF3 – effluents of sacrificial slag filter; SC1B, SC2B, SC3B – effluents of steel slag columns with different HRT_V (Cont'd)

Filter unit / Parameter		***COD***	***$CBOD_5$***	***TSS***	***VSS***	***TKN***	***NH_4***	***NO_x***	***TP***	***o-PO_4***	***pH***	**Ca^{2+}**	**Alkalinity**
		mg L^{-1}	**mg L^{-1}**	**mg L^{-1}**	**mg L^{-1}**	**mg N L^{-1}**	**mg N L^{-1}**	**mg N L^{-1}**	**mg P L^{-1}**	**mg P L^{-1}**	**-**	**mg L^{-1}**	**mg $CaCO_3$ L^{-1}**
P2	**SILO**	5380	3010	320	286	378	247	0.05	142	110	5.4	148	1120
		±520	±310	±74	±68	±37	±32	±0.01	±15	±39	±0.05	±61	±243
	AFB_{cb}	1713	800	340	320	296	205	< 0.05	31	14	7.6		1005
		±610	±337	±175	±145	±71	±39		±8.0	6.1	±0.3		±244
	SF3	1650**	710**	335**	270**	288	205	< 0.05	24	8.7	7.9	61	1430
		max. 2740	max. 1250	max. 1140	max. 865	±42	±35		±8.0	±4.7	±0.4	±37	±1060
	SC1B	1450	707	230	124	243	178	< 0.05	5.4	0.4	10.7	100	3300
		±530	±310	±240	±65	±62	±49		±2.5	±0.3	±0.5	±64	±1000
	SC2B	1500	755	200	155	256	188	< 0.05	5.9	0.5	10.4	68	2810
		±550	±310	±130	±92	±49	±39		±2.3	±0.4	±0.5	±51	±920
	SC3B	1520	770	250	185	273	219	< 0.05	7.4	1.1	9.6	40	2970
		±540	±335	±140	±110	±49	±55		±2.6	±1.6	±0.8	±42	±540

Note: The number of samples was 20 to 28 (12 for BOD_5; 8 for Ca^{2+}) during P1 and 11 (6 for Ca^{2+}) during P2. *COD; BOD_5; TSS and VSS values that are given as median and maximum value due to skewed distributions. **SF3 values that were corrected on the basis of a data validation analysis indicating 10% removal of particulate matter and 5% removal of filtered plus particulate matter.

7.7 References

APHA, AWWA & WEF. (2012). Standard methods for the examination of water and wastewater (22nd ed.). Washington, D. C: American Public Health Association, American Water Works Association & Water Environment Federation.

Barca, C., Gérente, C., Meyer, D., Chazarenc, F., & Andrès, Y. (2012). Phosphate removal from synthetic and real wastewater using steel slags produced in Europe. *Water Research*, 46, 2376-2384.

Bird, S. C., & Drizo, A. (2009). Investigations on phosphorus recovery and reuse as soil amendment from electric arc furnace slag filters. *Journal of Environmental Science and Health*, Part A, 44(13), 1476-1483.

Boaventura, R., Pedro, A. M., Coimbra, J., & Lencastre, E. (1997). Trout farm effluents: characterization and impact on the receiving streams. *Environmental Pollution*, 95(3), 379-387.

Brix, H., Arias, C., & Del Bubba, M. (2001). Media selection for sustainable phosphorus removal in subsurface flow constructed wetlands. *Water Science & Technology*, 44(11-12), 47-54.

Chazarenc, F., Filiatrault, M., Brisson, J. & Comeau, Y. (2010). Combination of slag, limestone and sedimentary apatite in columns for phosphorus removal from sludge fish farm effluents. Water, 2(3), 500-509.

Claveau-Mallet, D., Courcelles, B., Pasquier, P. & Comeau, Y. (2016, In preparation). P-Hydroslag model as a simulation tool for phosphorus removal prediction of slag filters.

Claveau-Mallet, D., Courcelles, B., & Comeau, Y. (2014). Phosphorus removal by steel slag filters: Modeling dissolution and precipitation kinetics to predict longevity. *Environmental Science and Technology*, *48*(13), 7486-7493.

Claveau-Mallet, D., Wallace, S., & Comeau, Y. (2012). Model of phosphorus precipitation and crystal formation in electric arc furnace steel slag filters. *Environmental Science and Technology*, *46*(3), 1465-1470. doi:10.1021/es2024884

Claveau-Mallet, D., Wallace, S., & Comeau, Y. (2013). Removal of phosphorus, fluoride and metals from a gypsum mining leachate using steel slag filters. *Water Research*, *47*(4), 1512-1520.

Comeau, Y., Brisson, J., Réville, J. P., Forget, C. & Drizo, A. (2001). Phosphorus removal from trout farm effluents by constructed wetlands. *Water Science & Technology*, 44(11-12), 55-60.

Cripps, S. J. & Bergheim, A. (2000). Solids management and removal for intensive land-based aquaculture production systes. *Aquacultural Engineering*, 22(1), 33-56.

Cucarella, V., Zaleski, T., Mazurek, R., & Renman, G. (2007). Fertilizer potential of calcium-rich substrates used for phosphorus removal from wastewater. *Polish Journal of Environmental Studies*, 16(6), 817-822.

Drizo, A., Comeau, Y., Forget, C., & Chapuis, R. P. (2002). Phosphorus saturation potential: A parameter for estimating the longevity of constructed wetland systems. *Environmental Science and Technology, 36*(21), 4642-4648.

Drizo, A., Forget, C., Chapuis, R. P., & Comeau, Y. (2006). Phosphorus removal by electric arc furnace steel slag and serpentinite. *Water Research, 40*(8), 1547-1554.

Hedström, A. (2006). Wollastonite as reactive filter medium for sorption of wastewater ammonium and phosphorus. *Environmental technology*, 27(7), 801-809.

House, C., Bergmann, B., Stomp, A., & Frederick, D. (1999). Combining constructed wetlands and aquatic and soil filters for reclamation and reuse of water. *Ecological Engineering*, 12(1), 27-38.

Kadlec, R. H., & Wallace, S. (2009). *Treatment Wetlands* (2nd ed.). Boca Raton, FL: CRC Press.

Kõiv, M., Liira, M., Mander, Ü., Mõtlep, R., Vohla, C., & Kirsimäe, K. (2010). Phosphorus removal using Ca-rich hydrated oil shale ash as filter material - The effect of different phosphorus loadings and wastewater compositions. *Water Research, 44*(18), 5232- 5239.

Kõiv, M., Ostonen, I., Vohla, C., Mõtlep, R., Liira, M., Lõhmus, K., Kirsimäe, K., & Mander, Ü. (2012). Reuse potential of phosphorus-rich filter materials from subsurface flow wastewater treatment filters for forest soil amendment. *Hydrobiologia*, 692(1), 145-156.

Lefrançois, P., Puigagut, J., Chazarenc, F., & Comeau, Y. (2010). Minimizing phosphorus discharge from aquaculture earth ponds by a novel sediment retention system. *Aquacultural Engineering*, 43(3), 94-100.

Liira, M., Kõiv, M., Mander, Ü., Mõtlep, R., Vohla, C., & Kirsimäe, K. (2009). Active filtration of phosphorus on Ca-rich hydrated oil shale ash: Does longer retention time improve the process? *Environmental Science and Technology, 43*(10), 3809-3814.

Metcalf & Eddy. (2014). *Wastewater engineering: treatment and reuse* (5th ed.). New York: McGraw-Hill.

Muñoz, P., Drizo, A., & Cully Hession, W. (2006). Flow patterns of dairy wastewater constructed wetlands in a cold climate. *Water Research*, 40(17), 3209-3218.

Nilsson, C. Renman, G., Westholm, L. J., Renman, A., & Drizo, A. (2013). Effect of organic load on phosphorus and bacteria removal from wastewater using alkaline filter materials. *Water Research*, 47(16), 6289-6297.

Nivala, J. Headley, T. Wallace, S., Bernhard, K., Brix, H., van Afferden, M., & Müller, R. A. (2013). Comparative analysis of constructed wetlands: the design and construction of the ecotechnology research facility in Langenreichenbach, Germany. *Ecological Engineering*, 61, 527-543.

Ouellet-Plamondon, C., Chazarenc, F., Comeau, Y. & Brisson, J. (2006). Artificial aeration to increase pollutant removal efficiency of constructed wetlands in cold climate. *Ecological Engineering*, 27(3), 258-264.

Pratt, C., & Shilton, A. (2010). Active slag filters-simple and sustainable phosphorus removal from wastewater using steel industry byproduct. *Water Science and Technology, 62*(8), 1713-1718.

Proctor, D. M., Fehling, K. A., Shay, E. C., Wittenborn, J. L., Green, J. J., Avent, C., Bigham, R. D., Connolly, M., Lee, B., Shepker, T. O., & Zak, M. A. (2000). Physical and chemical characteristics of blast furnace basic oxygen furnace, and electric arc furnace steel industry slags. *Environmental Science & Technology*, 34(8), 1576-1582.

Puigagut, J., Angles, H., Chazarenc, F., & Comeau, Y. (2011). Decreasing phosphorus discharge in fish farm ponds by treating the sludge generated with sludge drying beds. *Aquaculture*, 318(1), 7-14.

Richardson, A. E. (2001). Prospects for using soil microorganisms to improve the acquisition of phosphorus by plants. *Functional Plant Biology*, 28(9), 897-916.

Sawyer, C. N., McCarty, P. L., & Parkin, G. F. (2003). *Chemistry for Environmental Engineering and Science* (5th ed.). New York: McGraw-Hill.

Shilton, A. N., Elmetri, I., Drizo, A., Pratt, S., Haverkamp, R. G., & Bilby, S. C. (2006). Phosphorus removal by an 'active' slag filter-a decade of full scale experience. *Water Research, 40*(1), 113-118.

USEPA. (1992). Toxicity characteristic leaching procedure. United States Environment Protection Agency Test Method 1311, Washington (DC).

Vohla, C., Kõiv, M., Bavor, H. J., Chazarenc, F., & Mander, Ü. (2011). Filter materials for phosphorus removal from wastewater in treatment wetlands-A review. *Ecological Engineering, 37*(1), 70-89.

Vymazal, J. (Ed.), 2011. Water and nutrient management in natural and constructed wetlands. Netherlands, Dordrecht: Springer.

Whitelaw, M. A. (1999). Growth promotion of plants inoculated with phosphate-solubilizing fungi. In: Sparks, D.L. (Ed), Advances in Agronomy. Academic Press, 99-151.

CHAPTER 8 ARTICLE 4: NUMERICAL SIMULATIONS WITH THE P-HYDROSLAG MODEL TO PREDICT PHOSPHORUS REMOVAL BY STEEL SLAG FILTERS

Claveau-Mallet, D., Courcelles, B., Pasquier, P. & Comeau, Yves. Numerical simulations with the P-Hydroslag model to predict phosphorus removal by steel slag filters. Submitted to Water Research on March 9th 2017 (manuscript number WR38848).

ABSTRACT

The first version of the P-Hydroslag model for numerical simulations of steel slag filters is presented. This model main original feature is the implementation of slag exhaustion behavior, crystal growth and crystal size effect on crystal solubility, and crystal accumulation effect on slag dissolution. The model includes four mineral phases: calcite, monetite, homogeneous hydroxyapatite (constant size and solubility) and heterogeneous hydroxyapatite (increasing size and decreasing solubility). In the proposed model, slag behavior is represented by CaO dissolution kinetic rate and exhaustion equations; while slag dissolution is limited by a diffusion rate through a crystal layer. An experimental test for measurement of exhaustion equations is provided. The model was calibrated and validated with an experimental program made of three phases. Firstly, batch tests with 300g slag sample in synthetic solutions were conducted for the determination of exhaustion equation. Secondly, a slag filter column test fed with synthetic solution was run for 623 days, divided into 9 cells and sampled at the end of the experiment. Finally, the column was dismantled, sampled and analyzed with XRD, TEM and SEM. Experimental column curves for pH, oPO_4, Ca and inorganic carbon were well predicted by the model. Crystal sizes measured by XRD and TEM validated the hypothesis for homogeneous precipitation while SEM observations validated the thin crystal layer hypothesis.

Keywords: slag, phosphorus, wastewater treatment modeling, PHREEQC, hydroxyapatite, calcite, precipitation

8.1 Introduction

Steel slag filters are an effective and passive technology for phosphorus removal from wastewater, allowing typical municipal effluent o-PO_4 concentration below 0.5 mg P/L (Kõiv *et al.*, 2016).

Design tools for slag filters are not yet developed and full scale slag filters cannot be implemented without expensive pilot tests. The main issue related to steel slag filter operation relies on filter exhaustion and a relatively rapid drop of removal efficiency (Chazarenc *et al.*, 2008). A tool providing the effect of influent composition and operational conditions (type and size of slag, influent flowrate, filter geometry) on slag filter effluent o-PO_4 concentration and longevity would facilitate the design of these systems. This paper presents the P-Hydroslag model, a new model adapted for steel slag filter simulations considering influent composition and void hydraulic retention time (HRT_V) while being compatible with accepted physicochemical modeling frameworks (Lizarralde *et al.*, 2015; Mbamba, Batstone, *et al.*, 2015; Mbamba, Tait, *et al.*, 2015).

Sorption isotherms were largely proposed as a design tool for steel slag filters (Vohla *et al.*, 2011), but this method does not consider void precipitation and long-term changes in the material properties, explaining why isotherms could not yet predict correctly full-scale behavior. The kC* model traditionally used for constructed wetlands (Kadlec & Wallace, 2009) successfully predicted steel slag filter performance (Barca *et al.*, 2013). This method may be suitable for design, but it cannot estimate the lifetime of the filter. A general correlation between material CaO content and P retention capacity based on several studies was proposed by Vohla *et al.* (2011), highlighting the importance of CaO dissolution in retention mechanisms. However, such a design tool does not consider important aspects as CaO availability, HRT_V or influent composition, leading to a prediction uncertainty that is not acceptable for design purpose. Finally, a predictive model based on several material properties, HRT_V and inlet P concentration was proposed (Penn *et al.*, 2016). This model's strengths were to consider both Fe-Al and Ca based materials, propose an empiric relationship between material buffering capacity and P retention capacity, and predict P retention for both lab-scale and pilot-scale systems. This model, however, did not include direct measurement of kinetic rates, and would not be compatible with general physicochemical modeling frameworks in wastewater treatment.

Two previous modeling studies were published in the recent years. The first study (Claveau-Mallet *et al.*, 2012) qualitatively described concepts forming the basis of the model, including slag dissolution, hydroxyapatite precipitation, crystal formation and accumulation in voids, and effect of velocity on crystal accumulation. In the second study (Article 3 – Chapter 6), concepts were translated into a prototype model including mathematical equations for precipitation and slag exhaustion, and a proposition of laboratory protocol for slag characterization was presented.

Numerical simulations of a slag filter were performed on the base of this prototype model without experimental program for calibration. Results were realistic but overestimated the filter longevity. Predictions from the 2014 prototype model were compared to full-scale real data in a recent study (Kõiv *et al.*, 2016) in which longevity was overestimated.

In this paper, the first full version of the P-Hydroslag (standing for Phosphorus-hydroxyapatite-slag) model is presented. The P-Hydroslag model is similar to the 2014 prototype model, with additional features for diffusion barrier and crystal growth, a refined characterization of exhaustion equations, and a complete model equation matrix. The objectives were to calibrate the P-Hydroslag model with experimental data and evaluate the validity and realism of the model.

8.2 Material and Methods

8.2.1 Slag media

5-10 mm electric arc furnace steel slag produced by Arcelor Mittal and provided by Minéraux Harsco (Contrecoeur, Canada) was used (33% Fe_2O_3, 30% CaO, 16% SiO_2, 12% MgO. 6% Al_2O_3 and 3% other metallic oxides). Its density (3.8) and specific surface (0.308 m^2/g) were determined according to the ASTM C127-04 standard (ASTM, 2004) and the Brunauer, Emmet and Teller method (Lowell *et al.*, 2004). Slag from the same source was previously studied by the authors' research team for wastewater treatment applications (Article 1 – Chapter 3; Article 2 – Chapter 5; Kõiv *et al.*, 2016) or modeling studies (Article 3 – Chapter 6; Claveau-Mallet *et al.*, 2012).

8.2.2 Column test

A vertical filter column filled with slag was fed from its base with a synthetic wastewater in a saturated mode for a total duration of 623 days at approximatively 25ºC. The column size was 159 cm in length and 10 cm in internal diameter. The synthetic wastewater solution consisted of K_2HPO_4, KH_2PO_4, $NaHCO_3$ and $CaCl_2$ in tap water. The influent mean composition was pH of 7.80 ± 0.2, ortho-phosphates (o-PO_4) of 8.9 ± 2.0 mg P/L, total inorganic carbon (TIC) of 22 ± 2 mg C/L, Ca of 54 ± 14 mg/L and alkalinity of 102 ± 3 mg $CaCO_3$/L. The influent flowrate was 6.9 ± 1.0 mL/min for the first 517 days and 3.4 ± 0.5 mL/min for the remaining 106 days of operation.

The column was divided into 11 virtual cells for the filling step, identified #0 to #10, with #0 at bottom (inlet) and #10 at top (outlet). Cells #1 to #9 were 15 cm long and had a sampling hole in

the middle. Cells #0 and #10 were 7.5 cm long and had no sampling hole to provide a slag transition zone between the inlet/outlet tubing and sampling zones. While filling the column, two 300 g slag samples were taken from each cell using a standard sampling procedure for aggregate materials (ASTM, 2011). Slag samples were used in batch kinetic tests (presented in the next section). The total slag mass in the column was 24.24 kg, resulting in a 49.2% porosity.

The feeding barrel, column effluent and cells were sampled and analyzed periodically for pH, o-PO_4, filtered Ca, settled TIC, total P and alkalinity, using standard procedures (APHA *et al.*, 2005). A maximum of 3 cells were sampled in the same day to minimize perturbation, resulting in a monthly sampling frequency for each cell (twice a month in the second feeding phase). The feeding barrel and effluent column sampling frequency was weekly for pH and once or twice a month for the other parameters. Tracer tests were conducted after 12, 69, 82, 107, 187, 271, 376 and 558 days. Rhodamine at a concentration of 20 mg/L was used as a tracer and measured in the effluent using spectrofluorometry.

At the end of operation, feeding was stopped and the column was kept saturated for 6 days before dismantling. Upon dismantling, pore water was first sampled and analyzed, then the column was cut into 4 sections to ensure efficient solids sampling. For each cell, three samples were taken: first, several slag particles sampled before doing any major disturbance of the slag media (for scanning electron microscope (SEM) analysis); then slag was washed with water in a large pan and precipitates were sampled by sedimentation (for X-ray diffraction (XRD) and transmission electron microscope (TEM) analyses); finally, a 300 g of washed slag sample was taken for kinetic tests (described in section 8.2.3). Precipitates were air-dried for 3 days, sieved at mesh 60 and cleaned from slag dust with a strong magnet. Precipitates were analyzed with XRD using a Philipps X'Pert diffractometer operated at 50 kV and 40 mA, using the Bragg-Brentano geometry and a Cuk_{α} radiation. The Scherrer equation (Cullity, 2001) was used to estimate mean crystal sizes from diffractograms, using the ~26.1º peak for hydroxyapatite (HAP) and ~29.4º peak for calcite (CAL). Precipitates of cells 1, 2, 3 and 8 were analyzed using TEM with the bright field imaging technique (Jeol JEM-2100f field emission gun microscope, 200 kV). Before TEM analysis, samples were prepared with a 30-s ultrasound bath in methanol, and placed on a copper grid covered with Formwar lightly coated with amorphous carbon. Undisturbed slag particles of cells 1, 2, 3, 5 and 8 were analyzed with SEM using a Jeol JSM-7600F microscope (2.0 kV, LEI or SEI detector).

8.2.3 Batch kinetic tests

The batch kinetic test method is described in another reference (Article 3 – Chapter 6) and is intended to produce exhaustion equations. The batch test included 5 identical phases. In a phase, the slag sample was placed in a 1L Erlenmeyer flask containing 350 or 700 mL of a wastewater solution. The Erlenmeyer flask was placed in a gyratory shaker at 160 rpm. The flask was closed with a rubber cap that contained three airtight holes; one for a pH probe, one for a sampling tubing and one for a tubing connected to a N_2 gas balloon. The synthetic solution was composed of KH_2PO_4, K_2HPO_4, $NaHCO_3$ and $CaCl_2$ dissolved in tap or distilled water. Four solutions with different concentrations were used to test the method in a realistic range of wastewater types (pH of 6.5 to 7.9, o-PO_4 of 8 to 24 m P/L, Ca of 17 to 50 mg/L, TIC of 0.5 to 24 mg C/L and alkalinity of 3 to 107 mg $CaCO_3$/L). At time zero, slag was inserted. pH was monitored for 3 to 4 days. Three intermediary 20-mL samples were taken and analyzed for o-PO_4, filtered Ca and filtered TIC. When necessary, a linear correction against time was applied to pH measurements to account for probe drift. After this test, the slag sample was rinsed and immediately transferred to a 160 rpm shaken HNO_3 acid bath of known volume and concentration for 3 to 5 days. After the acid bath, pH was measured and the corresponding leached CaO from the slag was computed using numerical simulations (explained in section 8.2.5.2). After the acid bath, the slag sample was carefully rinsed and used again for a subsequent phase.

Each 300-g slag sample from cells 1 to 8 was used for a 5-phase kinetic test, resulting in 16 kinetic tests (2 replicates per cell). One-phase batch tests on dismantled column slag samples were performed for cells 1 to 9.

8.2.4 Model description

8.2.4.1 Precipitation

The model's Gujer matrix is presented in appendix. Three mineral phases are included: HAP typically found in slag filters (Baker *et al.*, 1998), monetite (MON) as intermediary phase and calcite (CAL). The transformation of MON into HAP (MONtoHAP) was modelled as precipitation of HAP2, an artificial phase composed of ions missing from MON before being HAP. Precipitation rates for HAP, MON and CAL were formulated with a basic expression rate = k x SI, with k being a constant normalized with slag surface and SI the saturation index. The bulk solubility constant

for HAP (K_{spHAP_bulk}) was set at 10^{-57} (Stumm & Morgan, 1996), within the 10^{-55} to 10^{-63} range reported in the literature (Lundager Madsen, 2008; Oelkers *et al.*, 2009; Parkhurst & Appelo, 1999; Stumm & Morgan, 1996). K_{spCAL} was set at $10^{-7.5}$, assuming an intermediary state between crystalline calcite ($10^{-8.48}$, PHREEQC database (Parkhurst & Appelo, 1999)) and hydrated calcium carbonate ($10^{-7.144}$, MINTEQ database (Allison, Brown, & Novo-Gradac, 1991)). K_{spMON} was set at 10^{-7} from Valsami-Jones (2001).

Two types of HAP were included to account for two types of precipitation. HAP_HO was HAP formed by homogeneous precipitation (new seeds precipitated in voids, or spontaneous precipitation) while HAP_HE was HAP formed by heterogeneous precipitation (on existing surfaces - crystal growth). HAP_HE occurred below a critical saturation index (SI_c) while HAP_HO occurred over SI_c. In homogeneous precipitation, crystal size was assumed to be constant. Using equation 8.1 for solubility of fine particles (Stumm & Morgan, 1996), K_{spHAP_HO} was set at 10^{-46}. Temperature was set at 298 K and specific surface (S_{HAP}) was calculated assuming crystal size $a_{HAP\_0} = 31.3$ nm, columnar shape for HAP and a L/D ratio (L_{HAP}) of 50. The value assumed for a_{HAP_0} is close to crystal size measured in this study (presented in a following section) and measurements made in previous studies (Claveau-Mallet *et al.*, 2012; Article 2 – Chapter 5). A value of 10^{-46} for K_{spHAP_HO} is consistent with equilibrium state generally observed in slag filters, assumed when effluent pH is over 10 with high HRT_V (Table 8.1 and Figure 8.1). In Table 8.1, Ca^{2+}, OH^- and ${PO_4}^{3-}$ activities were determined with PHREEQC and used for apparent solubility calculation. Studies conducted with hydrated oil shale ash were included in Table 8.1 as they behave in a similar way then slag. Resulting mean and median were $10^{-45,7}$ and $10^{-46,0}$ from Figure 8.1.

$$log\left(K_{spHAP_{HO}}\right) = log\left(K_{spHAP_{bulk}}\right) + \frac{\frac{2}{3}\gamma S_{HAP}}{2.3RT} \qquad (8.1)$$

Table 8.1 : Apparent HAP solubility from reported alkaline filter effluent with pH≥10, based on reported pH, Ca and o-PO_4 concentrations

Material	Size (mm)	Influent	Type of study	Apparent log K_{sp} of HAP		Ref and nb of data points	
				mean	median		
Sas	5-10	Solution	lab – column	-45.55	-45.94	(Claveau-Mallet *et al.*, 2012)	35
EAF slag	5-10	Solution	lab – column	-45.18	-45.72	(Article 2 – Chapter 5)	103
Sas	2.5-5	Solution	lab – column	-48.06	-48.17	(Forget, 2001)	6
Sas	5-10	real fishfarm WW	pilot – column	-45.23	-45.39	(Kõiv *et al.*, 2016)	46
Hydr. Oil shale ash	5-20	real domestic WW	pilot – CW	-46.32	-46.52	(Kõiv *et al.*, 2010)	62
Hydr. Oil shale ash	5-20	real landfill leachate	pilot – CW	-46.55	-46.42	(Kõiv *et al.*, 2010)	97
ladle furnace slag	0-1	reconst. fishfarm WW	lab – CW	-44.86	-45.28	(Abderraja Anjab, 2009)	9
Sas mixed with limestone	5-15	reconst. fishfarm WW	lab – CW	-46.04	-46.01	(Abderraja Anjab, 2009)	12
Sas mixed with limestone	20-40	reconst. fishfarm WW	lab – CW	-44.48	-44.56	(Abderraja Anjab, 2009)	8
Sas	10-30	reconst. domestic WW	lab – CW	-40.85	-41.01	(Stangart, 2012)	11
Sas	30-100	reconst. domestic WW	lab – CW	-45.16	-45.26	(Stangart, 2012)	8*
BOF oxide mixture	0.003-0.1	Solution	lab – column	-49.51	-49.47	(Baker *et al.*, 1998)	8*
EAF slag	20-40	real domestic WW	pilot – CW	-44.07	-	(Barca *et al.*, 2013)	* +
BOF slag	20-40	real domestic WW	pilot – CW	-43.52	-	(Barca *et al.*, 2013)	* +

*: all data below pH 10 for these studies. Data was not considered for calculation of global K_{sp}

+: single K_{sp} calculated from reported mean values for pH, o-PO_4 and Ca

Sas: same as present study; WW: wastewater; CW: constructed wetland

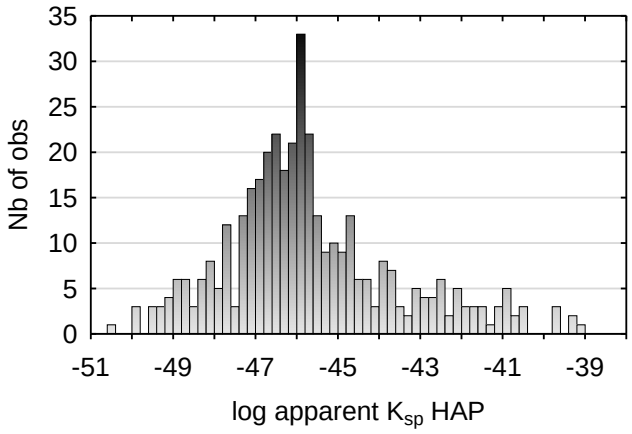

Figure 8.1 : Apparent HAP solubility distribution for all reported studies (pH≥10; 389 observations)

In heterogeneous precipitation, crystal size is a variable following crystal growth on existing seeds, assuming that all crystals have the same size. The number of seeds (se_{HAP}) increases as homogeneous precipitation takes place, assuming an initial number of seeds (se_{HAP_0}) and columnar shape. Equations for HAP_HE specific surface and solubility product are provided in equations 8.2 and 8.3.

$$log\left(K_{spHAP\_HE}\right) = log\left(K_{spHAP\_bulk}\right) + \frac{\frac{2}{3}\gamma S_{HAP}}{2.3RT} \quad (8.2)$$

$$S_{HAP} = \frac{(4L_{HAP}+2)MW_{HAP}}{a_{HAP}\rho_{HAP}} \quad (8.3)$$

8.2.4.2 Slag dissolution

Slag composition was simplified to the chemical formula CaO-0.3$CaCl_2$. Exhaustion equations were determined experimentally (described later), resulting in decreasing functions for saturation pH (pH_{sat}) and dissolution kinetic constant (k_{diss}). k_{diss} was normalized with slag surface as for precipitation constants. The proposed approach gives flexibility to the model and every specific slag has its own exhaustion parameters determined from batch tests by regression.

In this model, slag dissolution is assumed to be limited by Fick's law of diffusion (Domenico & Schwartz, 1998) through a crystal barrier that forms uniformly on the slag surface in a thin layer. The thickness of the crystal barrier (d_{barr}) increased according to CAL, HAP and MON precipitation, assuming a constant specific surface (S) for slag (equation 8.4). It was assumed that

the type of precipitation has an influence on the diffusion coefficient (D_{barr}) and that diffusion is easier in a large and organized crystals framework, compared to numerous small crystals. Mathematically, D_{barr} was defined with a step function set initially at a high value, and to a lower value when the seed concentration was doubled. As either dissolution or diffusion rate is the limiting process (the smallest), the step function was added to consider the passage from dissolution-limiting to diffusion-limiting.

$$d_{barr} = \frac{(m_{CAL}+m_{HAP}+m_{MON})\times n}{\rho_{barr} S \times 0.001(1-n)} \quad (8.4)$$

8.2.4.3 Hydraulic model

In continuous flow column simulations, the Advection-Reaction-Dispersion (ARD) equation for 1D flow was used (equation 8.5). A first-order exchange approximation was added to account for diffusion between effective and immobile porosity (equation 8.6). The hydraulic model is available in the PHREEQC software (Parkhurst & Appelo, 1999).

$$\frac{\partial C}{\partial t} = -v\frac{\partial C}{\partial x} + D^* v\frac{\partial^2 C}{\partial x^2} - \frac{\partial q}{\partial t} \quad (8.5)$$

$$\frac{db_{im}}{dt} = n_{im}\left(1+\frac{dq}{dC}\right)\frac{dC_{im}}{dt} = D_n(C_e - C_{im}) \quad (8.6)$$

8.2.5 Numerical simulations

Numerical simulations were performed using the PHREEQC software with its IPHREEQC modules for interfacing with MATLAB (Charlton & Parkhurst, 2011).

8.2.5.1 Batch tests

The initial solution was simulated with KH_2PO_4, K_2HPO_4, $CaCl_2$ and $NaHCO_3$ added to pure water. A small amount of HCl or NaOH was included to reproduce the precise pH of the experimental solution. Solutions were equilibrated with HAP and CAL (but no MON) in the EQUILIBRIUM_PHASES block prior to the simulated batch test. Simulated and experimental alkalinity were used for calibration of initial solutions. Slag exhaustion was considered to be constant, therefore, pH_{sat} and k_{diss} were constant instead of being adjusted according to exhaustion equations. pH_{sat} was set as the maximum pH value reached in the experimental batch

test. Calcite precipitation was removed from the batch test model, as surprisingly no calcite precipitation occurred in experimental batch tests (no TIC reduction).

The model constants were identified by minimizing the misfit between the simulated output and the experimental pH and oPO_4 measurements. The objective function optimization was performed on the log transformed constants k_{diss}, k_{HAP}, k_{MON}, $k_{MONtoHAP}$ and CaO_{in} with the conjugate gradient method and the golden-section search method (Press, 2007). As shown in Table 8.2, a two-step strategy was used to achieve satisfactory results and speed-up the calibration process. In the first step, the mean absolute error between the experimental and simulated pH (F_1) was minimized with large tolerances for PHREEQC (1E-11) and the optimization algorithm (1E-7 for line search and 0.01 as F stop criteria). Then, the objective function F_2 was minimized with more demanding tolerances (1E-12 for PHREEQC and line search, and 0.001 as F stop criteria). Note that CaO_{in} was a little amount of CaO instantaneously released at the water/slag contact, added for improving the calibration.

Table 8.2 : Batch test inversion parameters for conjugate gradient method

Step	Initial values (log)	Objective function
1	-7 for k_{diss} and CaO_{in} -6.5 for k_{MON} -9 for k_{HAP} and $k_{MONtoHAP}$	$F_1 = \frac{1}{n}\sum_{i=1}^{n}\left\|pH_{i,exp} - pH_{i,sim}\right\|$
2	Solution from inversion 1	$F_2 = F_1 + \frac{0.2}{m}\sum_{1}^{m}\left\|oPO_{4_{m,exp}} - oPO_{4_{m,sim}}\right\|$

8.2.5.2 Exhaustion functions

Exhaustion functions were produced by plotting pH_{sat} and k_{diss} against total leached CaO ($CaOl_{TOT}$). For a given phase i, $CaOl^i_{TOT}$ was calculated by cumulating leached CaO in preceding kinetic tests and acid bath (equation 8.7). $CaOl_{BATH}$ was determined by simulating acid bath with PHREEQC, following the final pH of the acid bath as a target value.

$$CaOl^i_{TOT} = 0.5 \times CaO^i_{KTEST} + \sum_{n=1}^{i-1}(CaO^n_{KTEST} + CaO^n_{BATH}) \qquad (8.7)$$

Exhaustion functions coefficients were determined by linear regression of pH_{sat} vs $CaOl_{TOT}$ (equation 8.8) and logistic function regression of k_{diss} vs $CaOl_{TOT}$ (equation 8.9). Mean regression coefficients were kept for k_{diss}, but coefficients following the top of the graphical data cloud were

kept for pH_{sat}, as pH_{sat} is a saturation state, and we can assume that saturation is controlled by the most reactive particles.

$$pH_{sat} = P_2 - \frac{P_2 - P_1}{\left(1 + e^{-P_3(CaOl_{TOT} - P_4)}\right)} \quad (8.8)$$

$$k_{diss} = B_1 + B_2 CaOl_{TOT} \quad (8.9)$$

In the Gujer matrix, exhaustion functions included additional terms involving porosity and slag density to account for the conversion of $CaOl_{TOT}$ (units of mol/g slag) into X_{CaO} (units of mol/L water) for filter numerical simulations.

8.2.5.3 Column test

The simulated influent was prepared according to the procedure described in the batch tests section. The column test was simulated within KINETIC and TRANSPORT blocks, with 50 numerical cells and a tolerance of 1E-6. Kinetic rates were applied to both mobile and immobile cells. Hydraulic parameters n_e, D^* and D_n were calibrated with each tracer test.

8.3 Results and discussion

8.3.1 Determination of exhaustion equations and precipitation constants

In general, batch test calibration was excellent for pH and good for o-PO_4, except for the period 0 to 100 min where the model overestimated slightly the o-PO_4 concentration. An example of a well-calibrated batch test (rank 7 out of 84 for global error function) is shown in Figure 8.2. No TIC reduction was observed. Absence of CAL precipitation in batch tests was not expected, as calcite was precipitated in column tests and is frequently observed in slag filters (Article 2 – Chapter 5; Liira *et al.*, 2009). Mean precipitation constants were $k_{HAP} = 10^{-11.03}\, mol\ HAP/s\ m^2 slag$, $k_{MON} = 10^{-8.67}\, mol\ MON/s\ m^2 slag$ and $k_{MONtoHAP} = 10^{-8.01}\, mol\ HAP2/s\ mol\ MON$.

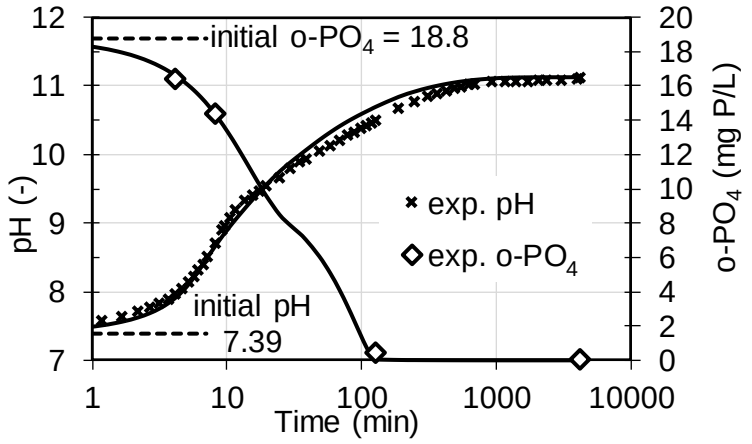

Figure 8.2 : Example of a batch test calibration. Simulated data is shown with lines. Batch test error functions: 0.09 for pH and 0.15 for o-PO_4

pH_{sat} and k_{diss} obtained from all batch tests were plotted against $CaOl_{tot}$ for the production of exhaustion functions (Figure 8.3). For k_{diss}, linear regression coefficients were used in column simulations (B_1 = -7.91 and B_2 = -1933 g/mol). pH_{sat} exhaustion function had to be slightly increased above the data cloud (discussed later) to improve the calibration (Figure 8.3B), resulting in coefficients P_1 = 9.1, P_2 = 12.1, P_3 = 6000 and P_4 = 1.2E-4.

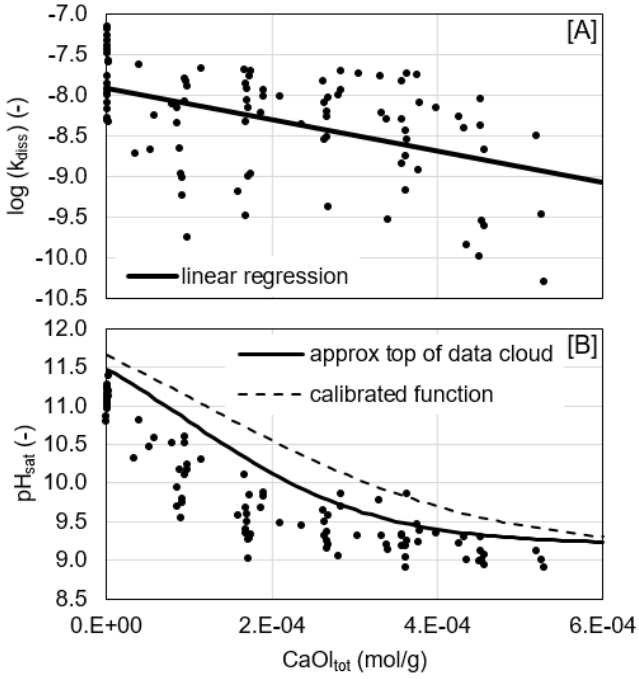

Figure 8.3 : Exhaustion functions for k_{diss} (A) and pH_{sat} (B). Regression coefficients are provided in text

8.3.2 Column test calibration

An example of tracer test calibration is shown in Section 8.4. Hydraulic parameters D^* (dispersivity) and D_n (exchange factor between mobile and immobile porosity) were roughly constant for 8 tracer tests, while effective porosity (n_e) decreased slightly following the column operation. The n_e decrease was neglected, and hydraulic parameters from tracer test at time 187 were used ($n_e = 0.359$, D^* = 5 cm and D_n=5x10^{-6} s^{-1}).

Results of numerical simulations are compared to experimental data in Figure 8.4. pH was correctly predicted for cells 1 to 6 but slightly underestimated for cells 7 to effluent. o-PO_4 was in general successfully predicted, except for cells 1 and 2 in the first 100-200 days, where the o-PO_4 rise was predicted too late. This could be explained by the close position of cells 1 and 2 relative to the influent point resulting in a non plug flow condition for these cells and in some short-circuiting. Calibration of o-PO_4 from cells 5 to 7 was less accurate for the last 100 days, as the model predicted a stable concentration while the experiment showed an increase of almost an order of magnitude. Calcium and TIC calibration were less accurate then those for pH and o-PO_4, but were considered satisfactory. The effect of the influent rate change was correctly predicted by the model.

Calibrated constants were $k_{CAL} = 10^{-9}\frac{M}{s\ m^2}$, $SI_c = 0.2$ and $\rho_{barr} = 2000\frac{kg}{m^3}$. Precipitation constants for HAP, MON and MONtoHAP were already determined in batch tests and were not changed for column simulations. SI_c was lower than reported values for calcite, which occurs in heterogeneous precipitation over $SI_c = 0.3$ and homogeneous precipitation over SI_c=1.5 (Mayes, Younger, & Aumônier, 2006). ρ_{barr} value was similar to dry density for a natural sand. k_{CAL} was 2.5 orders of magnitude higher than the reported initial value by Mbamba *et al.* (2015), and monetite constant was in the same order of magnitude as Mbamba's values. In this study, precipitation rates were function of crystal concentration, with initial crystal seeds of 1E-5 M, while the effect of crystal concentration was not considered in this model.

The column was divided in two zones for the calibration of se_{HAP_0}: cells 1 to 6 were set at 2e21 seeds/L and cells 7 to 9 (and all immobile cells) were set at 5e20 seeds/L. This refinement was necessary to achieve both o-PO_4 calibration of first cells (mainly homogeneous precipitation) and last cells (mainly heterogeneous precipitation). Attributing different se_{HAP_0} values for two zones was considered realistic because it represents a crystal behavior in which at a very low

supersaturation index, fewer but bigger crystals are formed. This behavior was confirmed during column dismantling. In cells 8 and 9, a very small amount of precipitates was observed and sampled, with fresh- and unused-looking slag. Several well-formed crystals could be seen by naked eyes only in cells 8 and 9 (3-4 mm in length).

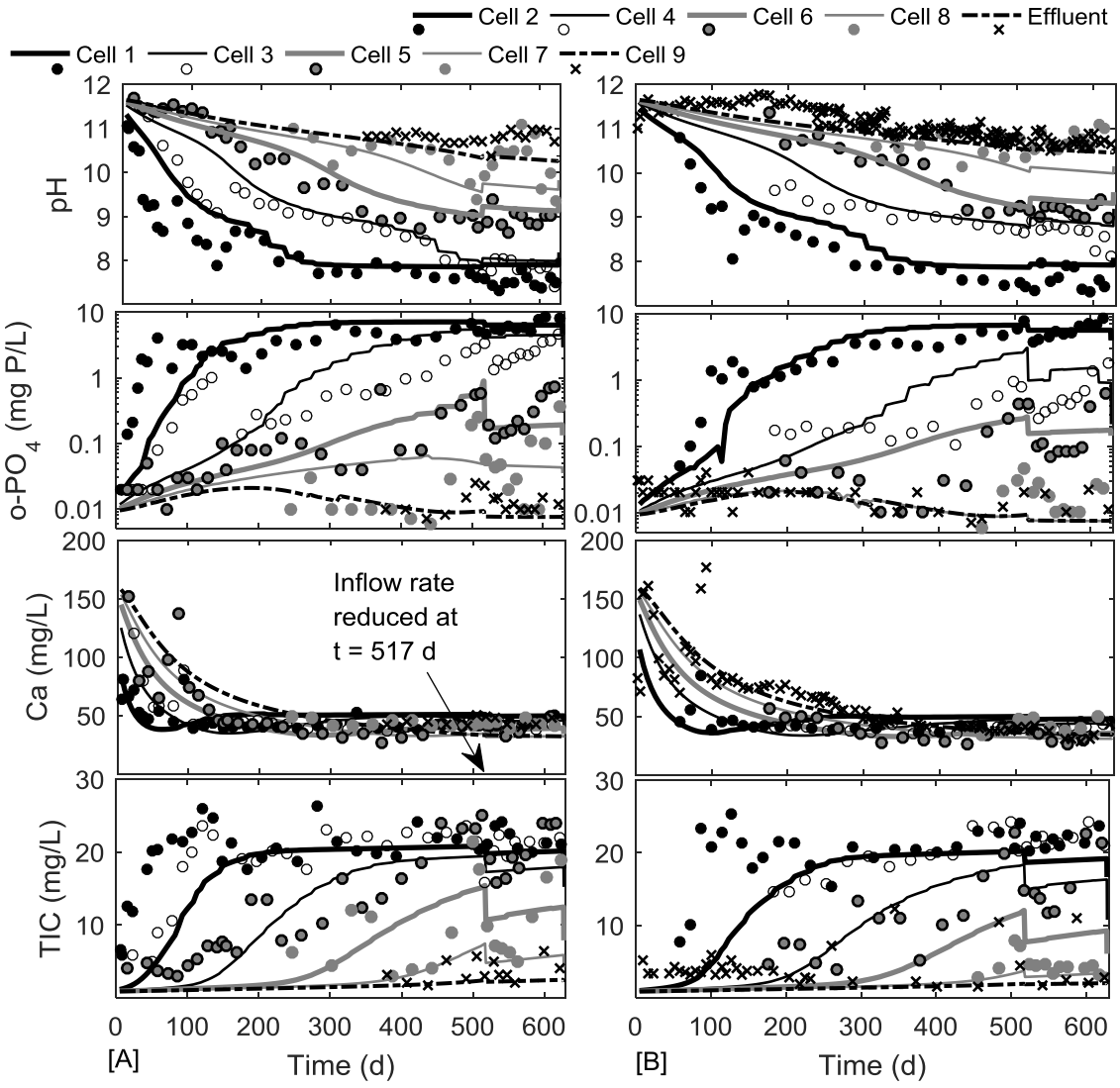

Figure 8.4 : Water composition in a column test for cells 1 to 9 (A) and cells 2 to effluent (B). Experimental data is shown with dots or x and simulated data with lines

The implementation of the diffusion equation is considered a major improvement compared to previous prototype versions of the model. Without the diffusion equation, CaO would always be leached at its maximum capacity (pH_{sat}) and longevity would be highly overestimated. D_{barr} calibration was 1E-10 m^2/s at first and was decreased to 5E-16 m^2/s when the seed concentration

was doubled. Calibrated values of D_{barr} for the two steps are similar to diffusion coefficients observed for clays. A large range was reported for radioactive waste storage applications: from 10^{-17} to > 10^{-13} m^2/s in consolidated clay (Alonso *et al.*, 2009) and 10^{-11} to 10^{-10} m^2/s in altered bentonite (Manjanna, Kozaki, & Sato, 2009).

8.3.3 Validation of model hypothesis

The diffusion equation can be validated by the robustness of the model regarding pH. The model could predict pH at the end of operation, pH after the 6-day rest and pH_{sat} (Figure 8.5). pH was slightly underestimated for pH_{sat} and pH after rest, but relative trends for pH and pH_{sat} were properly predicted, as well as the pH increase induced by the 6-day rest. The crystal layer was realistic as uniform crystal deposits were observed by SEM (Figure 8.6). The presence of cracks induced by air-drying was also suggesting that a crystal suspension layer was present onto the slag surface. Uniformity of crystal composition was confirmed by TEM-EDS as CAL and HAP were frequently found in the same crystal at nanometric scale.

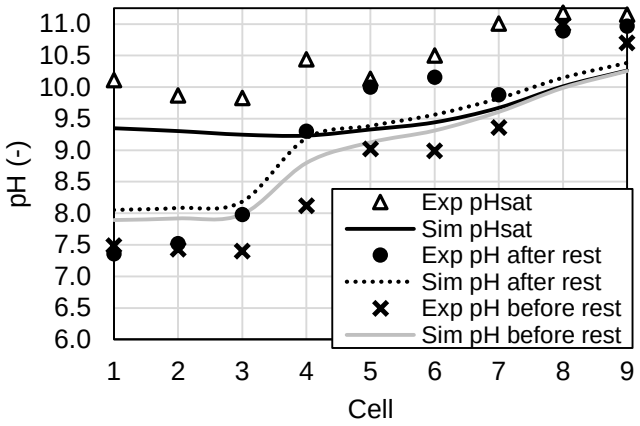

Figure 8.5 : pH distribution within column at the end of operation (623 days of feeding followed by 6 days of rest)

Cristal size in homogeneous precipitation was confirmed by microscope observations. In cells 1 to 3, where the amount of precipitated HAP was sufficient for measurements, isolated crystals in TEM pictures were measured, resulting in a 35 nm mean value for 505 measurements. A similar value of 24 nm was calculated from XRD diffractograms of cells 1 to 3. No specific increase was observed in crystal size from cells 1 to 3, validating the constant crystal size hypothesis for homogeneous precipitation. HAP composition was confirmed by XRD patterns (provided in

Section 8.4). HAP composition for individual crystals from TEM was confirmed by P and Ca presence with EDS. No monetite was detected by XRD and no monetite precipitation occurred in the column simulations while monetite was precipitated in batch test simulations, suggesting that pH rise in column was too fast for monetite formation.

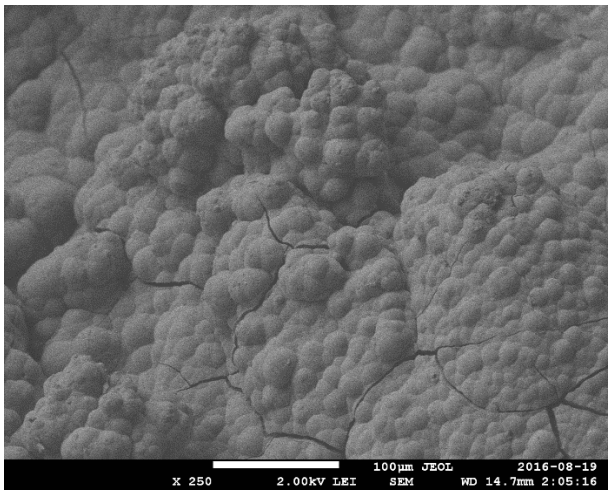

Figure 8.6 : SEM picture of slag grain surface from cell 2 at dismantling

The relative small amount of formed HAP in heterogeneous precipitation made impossible XRD or TEM crystal size analysis for heterogeneous HAP. However, it was possible to analyse the progression of calcite crystal size within the column using XRD. Its size was around 200 nm in cells 1 to 3, increased to 900 nm in cell 5, and was over the limit of Scherrer equation in cells 6 and higher. This suggests homogeneous precipitation and constant size in the first cells and heterogeneous precipitation and crystal growth in last cells.

Even if a distinction between homogeneous and heterogeneous precipitation was made for calcite, its solubility was kept constant for both conditions. Assuming homogeneous precipitation at 200 nm (as measured in cells 1 to 3) and spherical crystals, the computed solubility product from equation 8.1 is very close to bulk solubility. While HAP growth decreases its solubility, CAL homogeneous crystals are large enough to neglect this effect.

8.3.4 Model limits and recommendations

The main issue regarding the model is the number of batch kinetic tests needed to provide exhaustion equations. The hypothesis of most reactive grains in batch tests conditioning column tests should also be examined, because even if pH_{sat} exhaustion equation was overestimating

experimental data, pH in the last cells of columns were underestimated. Work should be done using statistical analysis and theory of artificial granular material sampling (Gy, 1979) for reducing the number of batch tests and transposing correctly batch to column conditions.

Calibration of heterogeneous precipitation was limited by experimental data, as last cells did not reach their longevity. Additional studies involving long-term operation of slag filters and breakthrough of last sections of filters, in which heterogeneous precipitation occurred for a while, would be needed for accurate calibration and in-depth study of seeds concentration and type of precipitation. In this paper, two layers of different seeds concentration were proposed, but other formulations would be possible including step functions for seeds VS saturation index, increasing the number of layers or adding a third type of HAP.

Further work should be conducted regarding need for refinement of the model. Additional features such as interaction with atmospheric CO_2 or porosity reduction (Courcelles *et al.*, 2011) may be needed in some cases as constructed wetlands. The model could be improved with additional P species (Mbamba, Tait, *et al.*, 2015) or consideration of crystal surface in rate equations. Crystal surface is obviously increasing in this type of process, with long operation time without extraction, but kinetic parameters may be less important than saturation parameters (pH_{sat} and K_{spHAP_HE}). Sensitivity analyses would be needed to assess which aspect should be studied further, slag dissolution kinetics, crystal equilibrium parameters or crystal kinetic parameters.

8.4 Appendix

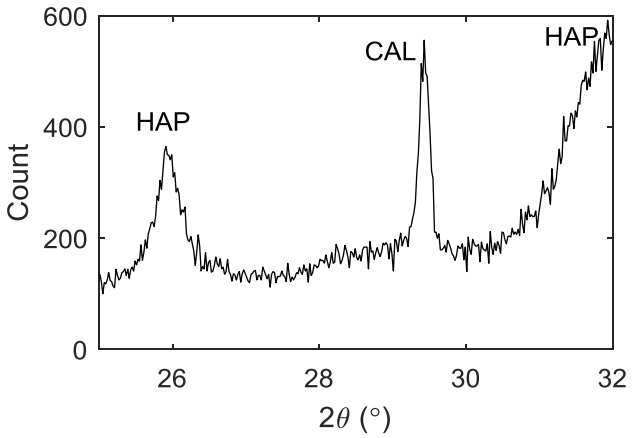

Figure 8.7 : XRD pattern of precipitates sampled in cell #2. Main peaks of HAP and CAL diffractograms are indicated in the figure

Table 8.3 : P-Hydroslag model matrix

Phase	Stoichiometry - aqueous						Stoichiometry – mineral phases				Rate equation	Equilibrium constants
	H^+	OH^-	Ca^{2+}	${CO_3}^{2-}$	${PO_4}^{3-}$	Cl^-	HAP	MON	CAL	HAP2		
Primary homogenous hydroxyapatite (HAP_HO)		-1	-5		-3		+1				$r_{HAP\_HO} = 0.001 k_{HAP} S \frac{(1-n)}{n} \times SI_{HAP\_HO} \times SF_{HAP\_HO}$ $SI_{HAP\_HO} = log\left(\frac{\{Ca^{2+}\}^5\{{PO_4}^{3-}\}^3\{OH^-\}}{K_{spHAP\_HO}}\right)$ $SF_{HAP\_HO} = \frac{1}{1+e^{-50\left(log(SI_{HAP\_HO})-log(SI_c)\right)}}$	$pK_{spHAP\_HO} = 46$
Primary heterogeneous hydroxyapatite (HAP_HE)		-1	-5		-3		+1				$r_{HAP\_HE} = 0.001 k_{HAP} S \frac{(1-n)}{n} \times SI_{HAP\_HE} \times SF_{HAP\_HE}$ $SI_{HAP\_HE} = log\left(\frac{\{Ca^{2+}\}^5\{{PO_4}^{3-}\}^3\{OH^-\}}{K_{spHAP\_HE}}\right)$ $SF_{HAP\_HE} = 1 - \frac{1}{1+e^{-50\left(log(SI_{HAP\_HO})-log(SI_c)\right)}}$	$log(K_{spHAP\_HE}) = log(K_{spHAP\_bulk} + \frac{\frac{2}{3}\gamma S_{HAP}}{2.3RT}$
Monetite (MON)	-1		-1		-1			+1			$r_{MON} = 0.001 k_{MON} S \frac{(1-n)}{n} \times log\left(\frac{\{Ca^{2+}\}\{{HPO_4}^{2-}\}}{K_{spMON}}\right)$	$pK_{spMON} = 7$
Calcite (CAL)			-1	-1					+1		$r_{CAL} = 0.001 k_{CAL} S \frac{(1-n)}{n} \times log\left(\frac{\{Ca^{2+}\}\{{CO_3}^{2-}\}}{K_{spCAL}}\right)$	$pK_{spCAL} = 6.8$
Secondary hydroxyapatite * (HAP2)		-2	-4		-2					+1	$r_{MONtoHAP} = k_{MONtoHAP} \times SI_{HAP\_HO}[MON]$	$pK_{spHAP\_HO} = 46$

*: transformation of monetite into hydroxyapatite

Table 8.3 : P-Hydroslag model matrix (Cont'd)

Slag dissolution		+2	+1.3			+0.3					$r_{diss} = A \times SF_{diss}$ $A = 0.001 k_{diss} S \frac{(1-n)}{n} \left(\frac{pH_{sat} - pH}{pH_{sat}}\right)$ $SF_{diss} = 1 - \frac{1}{1 + e^{-50(A-B)}}$	N/A
CaO diffusion through crystal barrier		+2	+1								$r_{diff} = B \times SF_{diff}$ $B = \frac{0.5 \times D_{barr} \times (10^{pH_{sat}-14} - \{OH^-\})}{d_{barr}} \times \frac{S \times 0.001(1-n)}{n}$ $SF_{diff} = \frac{1}{1 + e^{-50(A-B)}}$ $log(D_{barr}) = -10 - 5.3 \times \frac{1}{1 + e^{-50\left(\frac{se_{HAP}}{se_{HAP\_0}} - 2\right)}}$	N/A

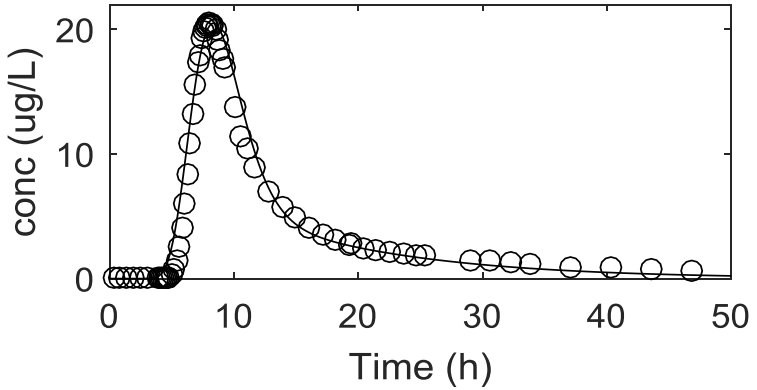

Figure 8.8 : Tracer test experimental data (circles) and numerical calibration (line) (started at Time = 187 d of filter operation)

Detailed equations to complement the model matrix

Advection-reaction-dispersion (ARD) equation for 1D transport and First-order exchange approximation between effective and immobile porosity:

$$\frac{\partial C}{\partial t} = -v\frac{\partial C}{\partial x} + D^* v\frac{\partial^2 C}{\partial x^2} - \frac{\partial q}{\partial t} \tag{8.10}$$

$$\frac{db_{im}}{dt} = n_{im}\left(1 + \frac{dq}{dC}\right)\frac{dC_{im}}{dt} = D_n(C_e - C_{im}) \tag{8.11}$$

Detailed equations for HAP_HE:

$$S_{HAP} = \frac{(4L_{HAP}+2)MW_{HAP}}{a_{HAP}\rho_{HAP}} \tag{8.12}$$

$$a_{HAP} = \frac{[HAP\_HE]MW_{HAP}{L_{HAP}}^2}{\rho_{HAP}\sqrt[3]{se_{HAP}}} + \sqrt[3]{{se_{HAP}}^2}{a_{HAP\_0}}^3 \tag{8.13}$$

$$se_{HAP} = se_{HAP\_0} + \frac{[HAP\_HO]MW_{HAP}{L_{HAP}}^2}{\rho_{HAP}{a_{HAP\_0}}^3} \tag{8.14}$$

Detailed equations for diffusion through crystal barrier:

$$d_{barr} = \frac{(100[CAL]+502[HAP]+136[MON]+366[HAP2])\times n}{\rho_{barr}S(n-1)} \tag{8.15}$$

Detailed equations for exhaustion functions:

$$pH_{sat} = P_2 - \frac{P_2 - P_1}{\left(1+e^{-\frac{P_3}{F}(CaOl_{TOT}-F\times P_4)}\right)} \tag{8.16}$$

$$log(k_{diss}) = B_1 + \frac{1}{F}B_2X_{CaO} + log\left(0.001S\frac{(1-n)}{n}\right) \tag{8.17}$$

$$F = \frac{1000\rho_{slag}(1-n)}{n} \tag{8.18}$$

8.5 Acknowledgment

The authors warmly thank Denis Bouchard, Manon Leduc, Simon Allaire, Simon Amiot and Patricia Bove from Polytechnique Montreal for chemical analyses and technical assistance. They also thank Margit Kõiv-Vainik, from University of Tartu, for providing constructive comments on the manuscript. A special thank is given to Jean-Philippe Massé and Philippe Plamondon, from

Polytechnique Montreal CM^2 lab, for their assistance with TEM, XRD and SEM analysis. Slag material was provided by Philippe Bouchard, from Minéraux Harsco.

8.6 Abbreviations

Symbol	Description
General abbreviations	
BOF	Basic oxygen furnace
CW	Constructed wetands
EAF	Electric arc furnace
HRT_V	Hydraulic retention time of voids
MONtoHAP	Transformation of MON into HAP
o-PO_4	Ortho-phosphates
SEM	Scanning electron microscope
TEM	Transmission electron microscope
TIC	Total inorganic carbon
WW	Wastewater
XRD	X-Ray diffraction

Abbreviations for mineral phases		
CAL	Calcite	$CaCO_3$
HAP	Hydroxyapatite	$Ca_5OH(PO_4)_3$
HAP_HO	Primary hydroxyapatite via homogeneous precipitation	$Ca_5OH(PO_4)_3$
HAP_HE	Primary hydroxyapatite via heterogeneous precipitation	$Ca_5OH(PO_4)_3$
HAP2	Secondary hydroxyapatite via monetite transformation	$Ca_4OH_2(PO_4)_2$
MON	Monetite	$CaHPO_4$

Symbol	Description	Units (value)
Constants		
a_{HAP_0}	HAP crystal size in homogeneous precipitation	[m]
B_1 and B_2	Regression coefficients in k_{diss} exhaustion function	
D^*	Dispersivity (transport model)	[cm]
D_n	Exchange factor between effective and immobile porosity (transport model)	[s^{-1}]
k_{CAL}	CAL precipitation constant	[mol CAL/s m^2 slag]
k_{HAP}	HAP precipitation constant	[mol HAP/s m^2 slag]
k_{MON}	MON precipitation constant	[mol MON/s m^2 slag]
$k_{MONtoHAP}$	MONtoHAP precipitation constant	[M HAP2/(M MON s)]
K_{spCAL}	Solubility product for CAL	[M^2]
K_{spHAP_bulk}	Bulk solubility product for HAP	[10^{-57} M^9]
K_{spHAP_HO}	Solubility product for HAP_HO	[M^9]
K_{spMON}	Solubility product for MON	[M^2]
L_{HAP}	L/D ratio for columnar HAP crystals	[-]
mv_{exp}	Slag mass to water volume ratio in a batch test	[g/mL]
MW_{HAP}	HAP Molecular weight	[502 g/mol]
n	Total porosity in the slag filter	[-]
n_e	Effective porosity in the slag filter	[-]
n_{im}	Immobile porosity in the slag filter	[-]
P_1, P_2, P_3 and P_4	Regression coefficients in pH_{sat} exhaustion function	
R	Ideal gas constant	[8.31 J mol^{-1} K^{-1}]
S	Slag specific surface	[m^2/m^3]
se_{HAP_0}	initial HAP seeds concentration	[seeds/L]

SI_c	Critical saturation index between HAP_HE and HAP_HO	[-]
T	Temperature	[K]
γ	HAP mean free surface energy	[87 mJ/m^3]
ρ_{barr}	Crystal concentration in the crystal barrier	[g crystal/m^3]
ρ_{HAP}	HAP crystal density	[3 600 000 g/m^3]
ρ_{slag}	Slag grain density	[3.8 g/mL]

Rates, functions and variables

a_{HAP}	Mean HAP crystal size	[m]
b_{im}	Moles of an element in immobile porosity (transport model)	[mol]
C	Total dissolved concentration for an element (transport model)	[mol/kgw]
C_e	C in effective porosity (transport model)	[mol/kgw]
C_{im}	C in immobile porosity (transport model)	[mol/kgw]
$CaOl_{BATH}$	Leached CaO in a acid bath	[mol/g]
CaO_{KTEST}	Leached CaO in a batch test	[mol/g]
$CaOl_{TOT}$	Cumulative leached CaO in a batch test	[mol/g]
D_{barr}	Diffusion coefficient in the crystal barrier	[m^2/s]
d_{barr}	Thickness of the crystal barrier	[m]
k_{diss}	Slag dissolution constant	[mol CaO/m^2 slag]
K_{spHAP_HE}	Solubility product for HAP_HE	[M^9]
pH_{sat}	Saturation pH in the slag filter	[-]
q	Concentration in the solid phase for an element (transport model)	[mol/kgw]
r_{CAL}	CAL precipitation rate	[M CAL/s]
r_{diff}	CaO diffusion rate through crystal barrier	[M CaO/s]

r_{diss}	Slag dissolution rate	[M CaO/s]
r_{HAP_HE}	Primary heterogeneous HAP precipitation rate	[M HAP/s]
r_{HAP_HO}	Primary homogenous HAP precipitation rate	[M HAP/s]
r_{MON}	MON precipitation rate	[M MON/s]
$r_{MONtoHAP}$	Secondary HAP precipitation rate	[M HAP2/s]
S_{HAP}	HAP molar specific surface	[m^2/mol]
se_{HAP}	HAP seeds concentration	[units/L]
SF_{diff}	Step function in diffusion rate	[-]
SF_{diss}	Step function in dissolution rate	[-]
SF_{HAP_HE}	Step function in HAP_HE rate	[-]
SF_{HAP_HO}	Step function in HAP_HO rate	[-]
SI_{HAP_HE}	Saturation index for HAP_HE	[-]
SI_{HAP_HO}	Saturation index for HAP_HO	[-]
t	Time (transport model)	[s]
v	Pore water flow velocity (transport model)	[m/s]
x	1D distance (transport model)	[m]
X_{CaO}	Total leached CaO in the slag filter	[M]

8.7 References

Abderraja Anjab, Z. (2009). *Development of a steel slag bed for phosphorus removal from fishfarm wastewater (In French).* (M.A.Sc. thesis, Polytechnique Montreal, Canada).

Allison, J. D., Brown, D. S., & Novo-Gradac, K. J. (1991). *MINTEQA2/PRODEFA2, a geochemical assessment model for environmental systems: version 3.0 user's manual*. Athens, GA: Environmental Research Laboratory, United States Environment Protection Agency.

Alonso, U., Missana, T., García-Gutiérrez, M., Patelli, A., Siitari-Kauppi, M., & Rigato, V. (2009). Diffusion coefficient measurements in consolidated clay by RBS micro-scale profiling. *Applied Clay Science, 43*, 477-484.

APHA, AWWA & WEF. (2012). Standard methods for the examination of water and wastewater (22nd ed.). Washington, D. C: American Public Health Association, American Water Works Association & Water Environment Federation.

ASTM. (2004). *Standard Test Method for Density, Relative Density (Specific Gravity), and Absorption of Coarse Aggregate*. ASTM C127-04. West Conshohocken, PA: American Society for Testing Materals.

ASTM. (2011). *Standard Practice for Reducing Samples of Aggregate to Testing Size*. ASTM C 702 / C 702 M−11. West Conshohocken, PA: American Society for Testing Materals.

Baker, M. J., Blowes, D. W., & Ptacek, C. J. (1998). Laboratory development of permeable reactive mixtures for the removal of phosphorus from onsite wastewater disposal systems. *Environmental Science and Technology, 32*(15), 2308-2316.

Barca, C., Troesch, S., Meyer, D., Drissen, P., Andrès, Y., & Chazarenc, F. (2013). Steel slag filters to upgrade phosphorus removal in constructed wetlands: two years of field experiments. *Environmental Science and Technology, 47*(1), 549-556. doi:10.1021/es303778t

Charlton, S. R., & Parkhurst, D. L. (2011). Modules based on the geochemical model PHREEQC for use in scripting and programming languages. *Computers & Geosciences, 37*(10), 1653-1663.

Chazarenc, F., Kacem, M., Gérente, C., & Andrès, Y. (2008). *'Active' filters: a mini-review on the use of industrial by-products for upgrading phosphorus removal from treatment wetlands.* Paper presented at the 11th Int. Conf. on Wetland Systems for Water Pollution Control, Indore, India, November 1 – November 7.

Claveau-Mallet, D., Courcelles, B., & Comeau, Y. (2014). Phosphorus removal by steel slag filters: Modeling dissolution and precipitation kinetics to predict longevity. *Environmental Science and Technology, 48*(13), 7486-7493.

Claveau-Mallet, D., Lida, F., & Comeau, Y. (2015). Improving phosphorus removal of conventional septic tanks by a recirculating steel slag filter. *Water Quality Research Journal of Canada, 50*(3), 211-218.

Claveau-Mallet, D., Wallace, S., & Comeau, Y. (2012). Model of phosphorus precipitation and crystal formation in electric arc furnace steel slag filters. *Environmental Science and Technology, 46*(3), 1465-1470. doi:10.1021/es2024884

Claveau-Mallet, D., Wallace, S., & Comeau, Y. (2013). Removal of phosphorus, fluoride and metals from a gypsum mining leachate using steel slag filters. *Water Research, 47*(4), 1512-1520.

Courcelles, B., Modaressi-Farahmand-Razavi, A., Gouvenot, D., & Esnault-Filet, A. (2011). Influence of precipitates on hydraulic performance of permeable reactive barrier filters. *International Journal of Geomechanics, 11*(2), 142-151.

Cullity, B. D. (2001). *Elements of x-ray diffaction* (3rd ed.). Upper Saddle River, NJ: Prentice Hall.

Domenico, P. A., & Schwartz, F. W. (1998). *Physical and Chemical Hydrogeology* (2nd ed.). New York: John Wiley & sons.

Forget, C. (2001). *Dissolved phosphorus removal from fish farm effluents by reactive granular media (In French).* (M.A.Sc. thesis, Polytechnique Montreal, Montreal, Canada).

Gy, P. (1979). *Developments in geomathematics. theory and practive 4, Sampling of particulate materials*. New York: Elsevier Scientific Publications.

Kadlec, R. H., & Wallace, S. (2009). *Treatment Wetlands* (2nd ed.). Boca Raton, FL: CRC Press.

Kim, E.-H., Yim, S.-B., Jung, H.-C., & Lee, E.-J. (2006). Hydroxyapatite crystallization from a highly concentrated phosphate solution using powdered converter slag as a seed material. *Journal of Hazardous Materials, 136*(3), 690-697. doi:10.1016/j.jhazmat.2005.12.051

Kõiv, M., Liira, M., Mander, Ü., Mõtlep, R., Vohla, C., & Kirsimäe, K. (2010). Phosphorus removal using Ca-rich hydrated oil shale ash as filter material - The effect of different phosphorus loadings and wastewater compositions. *Water Research, 44*(18), 5232- 5239.

Kõiv, M., Mahadeo, K., Brient, S., Claveau-Mallet, D., & Comeau, Y. (2016). Treatment of fish farm sludge supernatant by aerated filter beds and steel slag filters - effect of organic loading rate. *Ecological Engineering, 94*, 190-199.

Liira, M., Kõiv, M., Mander, Ü., Mõtlep, R., Vohla, C., & Kirsimäe, K. (2009). Active filtration of phosphorus on Ca-rich hydrated oil shale ash: Does longer retention time improve the process? *Environmental Science and Technology, 43*(10), 3809-3814.

Lizarralde, I., Fernández-Arévalo, T., Brouckaert, C., Vanrolleghem, P., Ikumi, D. S., Ekama, G. A., Ayesa, E., & Grau, P. (2015). A new methodology for incorporating physico-chemical transformations into multi-phase wastewater treatment process models. *Water Research, 74*, 239-256.

Lowell, S., Shields, J. E., Thomas, M. A., & Thommes, M. (2004). *Characterization of Porous Solids and Powders: Surface Area, Pore Size and Density*. New York: Springer.

Lundager Madsen, H. E. (2008). Influence of foreign metal ions on crystal growth and morphology of brushite (CaHPO4, 2H2O) and its transformation to octacalcium phosphate and apatite. *Journal of Crystal Growth, 310*(10), 2602-2612.

Manjanna, J., Kozaki, T., & Sato, S. (2009). Fe(III)-montmorillonite: basic properties and diffusion of tracers relevant to alteration of bentonite in deep geological disposal. *Applied Clay Science, 43*, 208-217.

Mayes, W. M., Younger, P. L., & Aumônier, J. (2006). Buffering of Alkaline Steel Slag Leachate across a Natural Weland. *Environmental Science and Technology, 40*, 1237-1243.

Mbamba, C. K., Batstone, D. J., Flores-Alsina, X., & Tait, S. (2015). A generalised chemical precipitation modelling approach in wastewater treatment applied to calcite. *Water Research, 68*, 342-353.

Mbamba, C. K., Tait, S., Flores-Alsina, X., & Batstone, D. J. (2015). A systematic study of multiple minerals precipitation modelling in wastewater treatment. *Water Research, 85*, 359-370.

Oelkers, E. H., Bénézeth, P., & Pokrovski, G. S. (2009). Thermodynamic Databases for Water-Rock Interaction. In Mineralogical Society of America & Geochemical Society (Eds.), *Thermodynamics and kinetics of water-rock interaction* (Vol. 70, pp. 1-46). Chantilly, VA.

Parkhurst, D. L., & Appelo, C. A. J. (1999). *User's guide to PHREEQC (Version 2) - A computer program for speciation, batch-reaction, one-dimensional transport, and inverse geochemical calculations*. (Water-Resources Investigations Report 99-4259). Denver: United States Geological Survey.

Penn, C., Bowen, J., McGrath, J., Nairn, R., Fox, G., Brown, G., Wilson, S., & Gill, C. (2016). Evaluation of a universal flow-through model for predicting and designing phosphorus removal structures. *Chemosphere, 151*, 345-355.

Press, W. H. (2007). *Numerical recipes: the art of scientific computing* (3rd ed.). Cambridge: Cambridge University Press.

Stangart, A. (2012). Phosphorus removal fromp septic tank effluents by coarse steel slag (In French). (M.Eng. thesis, Polytechnique Montreal, Canada).

Stumm, W., & Morgan, J. J. (1996). *Aquatic Chemistry: Chemical Equilibria and Rates in Natural Waters* (3rd ed.). New York: John Wiley & Sons.

Valsami-Jones, E. (2001). Mineralogical controls on phosphorus recovery from wastewaters. *Mineralogical Magazine, 65*(5), 611-620.

Vohla, C., Kõiv, M., Bavor, H. J., Chazarenc, F., & Mander, Ü. (2011). Filter materials for phosphorus removal from wastewater in treatment wetlands-A review. *Ecological Engineering, 37*(1), 70-89.

CHAPTER 9 GENERAL DISCUSSION AND RECOMMENDATIONS REGARDING THE P-HYDROSLAG MODEL

The second objective of this thesis was to propose a removal mechanisms model for steel slag filters that would be usable for the prediction of efficiency and longevity by numerical simulations. While papers #2 to 3 and complementary paper presented intermediary results regarding this objective, paper #4 fulfilled the objective, with the presentation of the P-Hydroslag model calibrated with experimental results. Consequently, paper #4 represents the main achievement of this thesis.

This chapter composed of five sections presents a critical overview of the modeling work accomplished in this thesis. In the first section, a discussion regarding main model development steps in provided, followed by a general modeling strategy in the second section. Complementary modeling works are presented in sections 9.3 (modeling for industrial needs) and 9.4 (modeling applied to neutralization processes). The last section presents research needs for further development of the P-Hydroslag model.

9.1 Main steps of model development

Modeling work published in papers is presented first as a model including equations followed by results from simulation experiments. In reality, the research path followed a reverse progression, working from results to model development by iterations. The following section is intended to present the logical succession of papers #2 to #4 that makes them coherent for this thesis project progression. Six challenges that were met in the development of the P-Hydroslag model will be presented in a logical order.

9.1.1 What are the involved phenomena in steel slag filters?

When this project was started, it appeared from the literature, that slag was leaching CaO, resulting in a pH rise in the filter. It was also reported that phosphorus was mainly removed by hydroxyapatite precipitation in steel slag filters following pH rise. These two observations, quite simple ones, remained the basis of the model. The challenge was to model correctly these two phenomena.

The first try for CaO slag leaching modeling was to understand slag composition. Major compounds composition (as Ca content (%), Fe content (%), etc) would not be appropriate for defining the leaching behavior, as calcium oxides may be present as various complex oxides with various properties. Real slag calcium oxide is therefore not well represented by CaO as it is divided into several long-name complex calcium oxides, with different solubility. The incidence of this for wastewater treatment modeling was clear in an excellent study of Kostura *et al.* (2005), who associated the buffering capacity of slag with its mineralogical composition via acid neutralization capacity curves. One possibility was to model accurately every mineralogical calcium oxide, with its individual properties (as solubility or kinetic dissolution rate). This strategy would reproduce the exhaustion behavior of slag, as fast and readily soluble oxides would dissolve first, then slower oxides would follow. This avenue appeared too complex and risky (experimental data would not easily follow predicted behavior). A second avenue was the intra-particle diffusion model (Kostura *et al.*, 2005), interesting because it considered slow release of deep oxides from grain core, but it did not consider slag exhaustion, which is a crucial aspect of slag filters.

Following these observations and literature review, the hypothesis that readily soluble oxides are leached first, followed by slower-release oxides, was proposed. The objective was to develop an empirical approach for representing the oxide complexity of slag, without needing accurate measurement of slag oxide mineralogical composition. This approach would involve kinetic rates like those used for biological wastewater treatment modeling (Metcalf & Eddy *et al.*, 2014). Saturation functions used for biomass growth were especially interesting as a starting point, because slag is leaching until a saturation state is reached. The turning point came with the first batch test simulations (paper #3), when a methodology was proposed for simulating and controlling slag aging with acid baths, then repeating the CaO leaching parameter measurements. This principle was the basis of the experimental protocol for exhaustion function measurements, proposed in paper #3, and validated in paper #4. Exhaustion functions of the P-Hydroslag model are an empirical (and easily measurable) manner of representing slag calcium oxide complexity, and exhaustion behavior. Note that slag mineralogical analysis was performed in paper #2, while readings and findings related to slag mineralogy were still going on. When the method for exhaustion functions was developed, mineralogical analysis of slag was abandoned, explaining why this analysis is not part of papers #3 to #4.

The first literature review work for hydroxyapatite precipitation was reading a master thesis of a former project related to steel slag filters (Forget, 2001). This work described adsorption isotherms (Fetter, 1999) and possible surface removal mechanisms. From the beginning, it was clear that adsorption isotherms would not be suitable for steel slag filters modeling, because hydroxyapatite precipitation is a volume-based and not surface-based phenomenon. P removal mechanisms were roughly sorted into sorption for neutral-pH materials, and precipitation for alkaline pH materials (Baker *et al.*, 1998).

Three important features were developed for hydroxyapatite precipitation: solubility of fine particles, crystal growth and hydroxyapatite structures. The equation of fine particles solubility was found while reading about precipitation in Stumm and Morgan (1996) for a literature review of hydroxyapatite solubility. After studying more deeply this equation, it was found that considering the small hydroxyapatite size in steel slag filters, this equation would explain alone the apparent supersaturation observed in previous studies (Baker *et al.*, 1998), and also in data from paper #2. It was concluded that steel slag filters are not supersaturated with hydroxyapatite, they are equilibrated with a hydroxyapatite phase much more soluble then tabulated (bulk) hydroxyapatite, because of crystal smallness.

In the former master work of the candidate, crystal growth was observed in steel slag filters with limited XRD crystal size measurements (Claveau-Mallet *et al.*, 2012). XRD was preferred to sequential extraction (Audette *et al.*, 2016) for crystal characterization as it is possible to measure crystal size with this method. Following this work, a more exhaustive crystal sampling campaign was performed in this Ph.D. work (paper #2), with the objective to confirm crystal growth as a removal mechanism. In this project (paper #2), the effect of influent water composition on crystal growth was also confirmed, as two different wastewater influents were used. These observations led to the use of precipitation rates from the mineralogy science (Oelkers *et al.*, 2009), as they were defined using the saturation index (therefore water composition). The project resulting in paper #2 also helped to understand connected precipitation issues involving metals and fluoride. Metal precipitation more especially helped to understand the critical role of pH in a precipitation process. Development steps for fine-particle solubility and crystal growth were completed at the end of the first year, and were included in paper #3 and complementary paper.

At the beginning of this Ph.D. project, it was already outlined that hydroxyapatite structures played a role in phosphorus removal mechanisms, as an effect of crystal organization on efficient volume use in the filter was indirectly observed in a former project (Claveau-Mallet *et al.*, 2012). This work resulted in this hypothesis: water velocity affects crystal organization, and crystal organization affects the efficient use of the slag filter volume by clogging. Later, in 2012, a crystal precipitation study conducted by the candidate (not presented in the thesis) confirmed this hypothesis with SEM observations of crystal structures on used slag grains. This work resulted in a qualitative schematic showing the effect of water velocity on crystal structures (Figure 9.1). An important step for understanding of HAP structures was a review of literature on implant biocompatibility, where a lot of information related to HAP precipitation is present, including crystal shape and organization under various organic or inorganic conditions. This research branch showed that HAP is extremely versatile in shapes and structures. It would be therefore wiser to find a way to represent it in a macroscopic way instead of modeling crystal structures at small scale. This observation led to the development of the diffusion through a uniform thin crystal layer approximation. The first development on this thin crystal layer approximation was done early in the Ph.D. project, but it was included only in paper #4, because full mathematical development was completed in the third year, and it involved calibration work that was not possible in paper #3 and complementary paper.

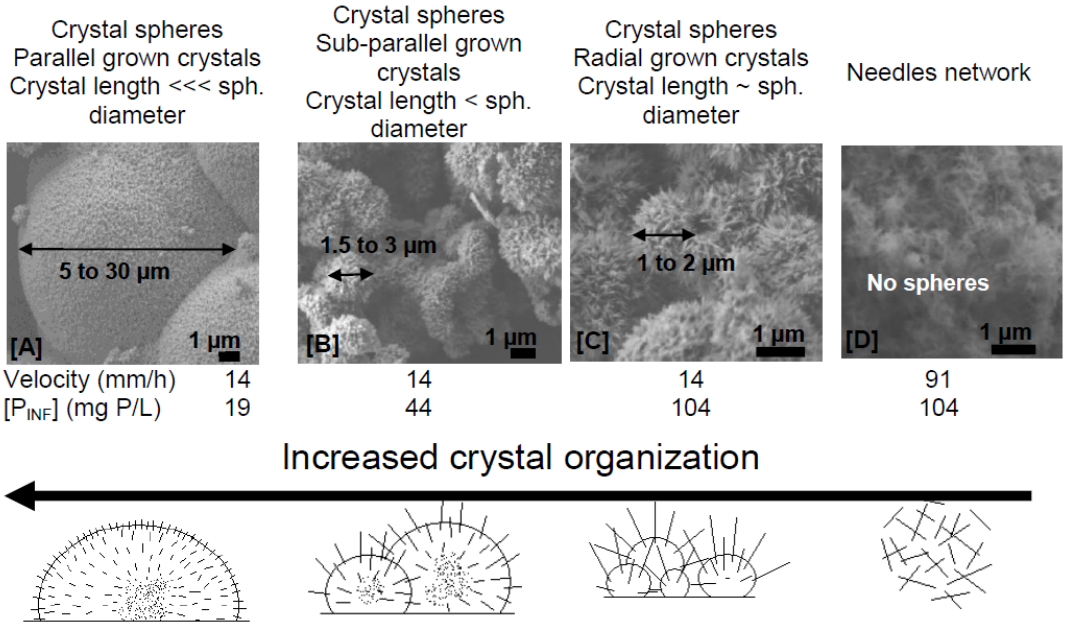

Figure 9.1 : Representative SEM photography and schematic representation of different organization levels in filters (unpublished work)

9.1.2 How could phosphorus removal mechanisms in slag filters be transposed into a mathematical model?

One important challenge in this project was to integrate qualitative observations into mathematical equations that would make numerical simulations possible. Several features of this model were found directly in the literature, as standard precipitation rates for mineral phases (Oelkers *et al.*, 2009). Other features were also already described in the geochemistry literature, but the application for wastewater treatment or slag filters was not so obvious (equation for fine particles solubility, Fick's law diffusion through a thin film, critical supersaturation index for homogeneous precipitation, transformation of MON into HAP). Finally, features for slag exhaustion behavior (exhaustion functions) were completely new and had to be developed from zero.

The first step for solving this challenge was the understanding of the PHREEQC software. PHREEQC was understood before understanding how a formal model should be implemented. Kinetic rates concepts were acquired while reading the user's guide examples, and trials were done for reproducing these examples with CaO and saturation functions in simple batch tests. These first modeling trials help to learn PHREEQC as a tool, but also learn what a kinetic model is.

The second important step was during the candidate's predoctoral examination, which included a modeling problem for a geothermal application. Geochemical 2D isocontour maps in a geothermal well surrounding had to be produced, considering the pressure and temperature dependence of carbonate system constants. This problem was formulated for scaling management in geothermal systems. This problem helped to understand how a hydraulic model could be coupled with a geochemical model.

The last two steps were accomplished almost simultaneously, just after the predoctoral examination, and led to significant and fast development, in such way that the preliminary model and resulting paper #3 were completed within four months. The PHREEQC batch model was combined to a simple 1D flow model, also available in PHREEQC. The key concept that made possible 1D column simulation with the model was the fact that dissolution constants did not remain constant, as slag was exhausting. The lab procedure that would made possible the measurement of exhaustion behavior was developed at this point.

9.1.3 Now there is a numerical model. Will it work?

The model developed in paper #3 was realistic from a theoretical point of view, but there was no insurance that real measured exhaustion functions would lead to realistic and accurate predictions. The model's simulations needed to be compared to real data. An experimental program including a slag filter column test and numerous batch tests for the measurement of exhaustion functions was initiated. This part of model development was critical, and risky, as a whole year of experiments had to be conducted, before having any indication of success or failure of the experimental method. The column test was started at first in November 2014, and a year of batch tests followed. The multi-variable calibration of batch tests by conjugate gradient was developed and used in parallel to batch tests for the whole duration of these experiments. A great amount of calibrated batch tests was needed for the production of exhaustion equations before conducting any column simulations. Even with column simulations, a relatively long experimental column operation time (and exhaustion of first cells) was needed before comparing simulated and experimental results.

The very first column simulation was performed after one year of waiting, in October 2015. Results from this simulation was probably the most important result of the thesis, as they showed pH and o-PO_4 curves that were realistic and close to experimental results. These curves were not perfect, but it was clear that it was a calibration issue, and not a fundamental problem with the approach. In the middle of this year of experiment, modeling work performed in complementary paper was considered as an intermediate guarantee that the model principle was correct. In this paper, simulations using the preliminary model without diffusion barrier led to overestimating but still realistic longevity predictions. These simulations also showed that the model was correctly sensitive to influent composition.

9.1.4 How much more complex should the model be?

The refinement of the model took place from October 2015 to November 2016. The modeling strategy was to calibrate the model with experimental data, and if not possible add a layer of complexity. The diffusion barrier was implemented at the beginning of this simulation phase. The diffusion barrier was necessary, otherwise longevity would be largely overestimated. The first significant increase in complexity was to include two distinct phases for HAP, one for homogeneous HAP and one for heterogeneous HAP. This was necessary because of stable or even

decreasing o-PO_4 concentration in the last cells. The second element of complexity was the addition of step functions for diffusion coefficient that was justified by crystal structures (Figure 9.1). This step function would associate two different diffusion coefficient values for homogeneous (disorganized) or heterogeneous (organized) precipitation. This step was made because it was impossible to calibrate both the first and last cells for pH.

The last element of complexity added to the model was the implementation of different initial seed numbers in cells. This step was necessary to achieve accurate o-PO_4 calibration in both the first and last cells. It was justified by the growth behavior of crystals at a very low saturation index on few big crystals instead of numerous smaller ones. This feature was arbitrarily chosen to represent this phenomenon, but other approaches would have been possible, such as defining a third HAP phase occurring at very low saturation index. The one-year calibration phase was ended when it was felt that additional efforts would overcalibrate the model. More accurate calibration of seeding and crystal growth would have needed an extended operational period of the filter.

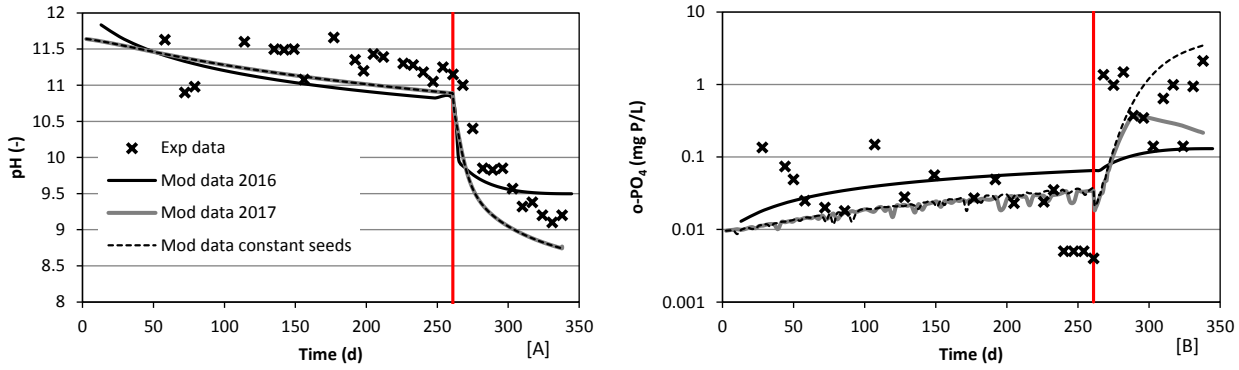

Figure 9.2 : Comparison of simulation results from different model versions for the Bobines project, column CS2A (see Chapter 7 for complete description). Mod data 2016: as published using preliminary model (complementary paper). Mod data 2017: using complete model from paper #5. Mod data constant seeds: using complete model from paper #4 with 2e21 seed concentration for all cells

The effect of model complexity is shown in Figure 9.2, where simulations of the Bobines project are shown. Experimental data of slag filter from this project where compared to numerical simulations in complementary paper using a preliminary model (model presented in paper #3). Results presented in complementary paper roughly predicted pH at effluent, but underestimated o-PO_4 concentrations. The importance of considering the diffusion barrier is seen in simulations with

the 2017 model (Figure 9.2): prediction of o-PO_4 rise at the beginning of phase 2 was more accurate. The pH curve from 2016 and 2017 models were similar, except for the last 50 days, where a plateau is seen in the 2016 model. The o-PO_4 concentration from the 2017 model slowly decreases after 275 d, which is not in accordance with experimental data. A third simulation using a constant seed concentration of 2e21 was performed (the 2017 model had seed concentration of 1e20 in last cells). This simulation was more accurate than the 2017 one, showing that seeding calibration as presented in Paper #4 still needs refinement before being applied to other cases.

9.1.5 How model hypotheses could be validated?

This Ph.D. challenge was to develop simple hypotheses, and find a way to measure them, considering that crystals are difficult to sample without disturbance with acceptable representativity. Moreover, a critical part of the model (heterogeneous precipitation and crystal growth) would have needed sampling of trace HAP in the last cells of the column, which represents a real challenge.

Crystal sampling is possible only at dismantling: it needs a long operation time for sufficient crystal mass for sampling and analyzing, and involves careful attention. In this Ph.D. project, the sampling and analyze procedure was developed and refined through five long-term column experiments. At first dismantling in a former project (Claveau-Mallet *et al.*, 2012), first trials of crystal analysis with XRD were done. At second dismantling (paper #2), more analyses of crystals were performed using a similar protocol, and at third dismantling (this work is not presented in the thesis) crystal properties were related to the position in columns, and SEM was experienced for the first time. At fourth dismantling (complementary paper), experience was gained on utilization of the developed sampling methods in real wastewater conditions at a pilot scale, and a P mass balance was attempted. At the last dismantling (paper #4), the method was again refined and focused on the validation of hypotheses. Each column dismantling contributed to the improvement of the sampling and characterization methods for the next experiment.

A semi-quantitative approach was chosen for validation of crystal hypotheses. It is true that an accurate measurement of crystal size in a steel slag filter is not easy, but it is possible to indirectly measure a mean crystal size with XRD, or measure directly the length of disturbed crystals from a very small sample. This approach involves quantitative measurements, with such incertitude that it is preferable to call them semi-quantitative. Consequently, resulting size measurements were

considered satisfactory if they were in the same order of magnitude as postulated values in the model. Visual observations of crystal structures at SEM, or at naked eyes in the columns, also followed this approach. Conducting kinetic tests on dismantled slag sample was also a strong validation of the model, as it was possible to separate the exhaustion effect from the crystal barrier effect by slag washing (Figure 8.5).

9.1.6 How should the model be integrated to the existing wastewater modeling community?

Modeling works in papers #2 to #3 and complementary paper were presented in such way that it would be difficult to use it by the general scientific community, and it was not expressed in a conventional language for the modeling community. The objective of linking the P-Hydroslag model with other models commonly used in wastewater and physicochemical treatments was stated in paper #4. A critical step for reaching this objective was the participation of the candidate at the WWTmod 2016 conference on wastewater treatment modeling in April 2016 as a workshop chair (Claveau-Mallet, 2016). Other physicochemical modelers were met and a serious literature review on their recent work (mainly anaerobic digestion or nutrient recovery) was realised. Modeling issues common to steel slag filters and other physicochemical processes were outlined, as precipitation seeding or pH prediction. Recent works on a generalized physicochemical modeling framework was the basis for the P-Hydroslag model expression into a matrix format commonly used in wastewater treatment (Mbamba, Batstone, *et al.*, 2015). This matrix is included in paper #4. Nucleation features in the P-Hydroslag model are considered an improvement compared to previous work: consideration of both homogeneous and heterogeneous precipitation eliminates the need of assuming artefact initial seed concentration for self seeding (Mbamba, Batstone, *et al.*, 2015).

9.2 Development of a modeling strategy

The experience gained through this project resulted in a general modeling strategy that is not clearly stated in papers #2 to #4. This modeling strategy is presented in this section.

9.2.1 Step 1: chemical model

This step involves understanding of chemical phenomena, and the definition of their kinetic reaction rates. The P-Hydroslag model involves several equations for precipitation and CaO dissolution, as stated in Table 8.3. An important issue related to this model is the unavoidable implementation of equilibrium reactions associated with acid/base systems for o-PO_4 and carbonates. Lack of equilibrium reaction consideration was identified as a major problem for several wastewater treatment models (Claveau-Mallet, 2016). In this project, the chemical model was implemented in the PHREEQC software, which already includes a wide database for equilibrium reactions, and only kinetic reactions were added.

9.2.2 Step 2: hydraulic model

A chemical model cannot be used without an accurate knowledge of the reactor hydraulics. The chemical model should thus be complemented with a hydraulic model. The hydraulic model should be calibrated with tracer tests, and the selected software for numerical simulations should include both chemical and hydraulic models. In this project, the hydraulic model was implemented in PHREEQC with the ADR equations, resulting in good tracer test calibration (Figure 8.8).

PHREEQC is an interesting tool because it already handles equilibrium reactions, but its disadvantage relies on its limited capacities for hydraulics (1D column with diffusion). It is still possible, however, to consider complex tracer curve response as tails by adding an immobile porosity, as done is this project. It is also possible to simulate batch feeding conditions, completely mixed reactors or intermediary feeding mode via the 1D ARD (see section 9.4.3).

9.2.3 Step 3: calibration of influent

The influent calibration is a critical step of steel slag numerical simulations as influent composition greatly affects simulation results. Experimental measured parameters Ca, TIC and o-PO_4 were used as input in PHREEQC for the preparation of influent using salts. After this step, a small amount NaOH or HCl was added to the solution until reaching the measured experimental pH, using the Newton method. The numerical solution was equilibrated with involved phases (HAP and CAL) prior to modeling. Equilibrium with MON was done at beginning, but it was removed from the calibration step, as metastable state was possible for MON. This detail was especially important

for batch test calibration. Finally, the computed alkalinity was compared to the experimental one as a validation step. The validation step for the column test influent was successful, as shown in Table 9.1. Note that mean values were used for column test, resulting in a constant composition for influent. For batch tests, the mean error between measured and simulated alkalinity for individual batch tests was 14%, which is considered to be an acceptable error.

Table 9.1 : MATLAB output for the influent calibration step of the column test

Parameters	Units	Exp	Mod
pH	-	7.8	7.8
o-PO_4	mg P/L	8.87	8.87
Ca	mg/L	53.8	53.8
TIC	mg C/L	21.9	21.9
Alk	mg $CaCO_3$/L	102	102

If alkalinity is not well reproduced by the simulated influent, the modeller should consider to modify experimental TIC in order to reproduce the experimental alkalinity. This strategy was used in a secondary modeling work for neutralization processes (see section 9.4). In this case, the influent was a steel slag filter, and TIC analysis in steel slag effluents has higher uncertainty then alkalinity because of rapid CO_2 transfer with the atmosphere. Consequently, alkalinity remains a more reliable parameter for calibration, and alkalinity has a major influence on simulation results (see section 9.3.1). For neutralization processes, if little data is available for influent calibration, it is possible to include both steel slag influent and effluent in the calibration process (done for project presented in section 9.4.6). In this case, CaO is simply added to the influent until the target pH value is met, and a validation is performed for both influent and effluent of steel slag filter.

It is important to note the potential contribution of organic matter in alkalinity. In the Bobines project, the measured alkalinity was around 1000 mg $CaCO_3$/L, and numerical calibration of influent never reached such a high alkalinity (Table 7.2). Volatile fatty acids formed in anaerobic digestion, if present, could explain the missing alkalinity. Simulations with the 2017 model presented in section 9.1.4 included an acetic acid buffer that increased alkalinity to 950 mg $CaCO_3$/L. Note that alkalinity computed by PHREEQC is not accurate if the organic compounds concentration is too high, because of alkalinity computation assumptions. In that case, it is

preferable to compute alkalinity by doing a numerical titration until pH 4.5 using the Newton method.

9.2.4 Step 4: Simulate

The last step consists in simulating the addressed problem, using the chemical model, as well as calibrated hydraulic model and influent. Note that a high incertitude is inherent to steel slag filter modeling because of high pH. pH measurement uncertainty increases with increased pH values. Moreover, as pH is a logarithmic parameter, small changes in high pH values results in great OH^- concentration changes.

A lot of what was presented in the proposed methodology could not easily be done by PHREEQC alone. The MATLAB modules were needed for better interfacing with input data, and solving problems that involved iterations (calibration using Newton method or completely mixed reactor operation).

9.3 Modeling steel slag filters for industrial needs

Simultaneously to the P-Hydroslag model development, a close collaboration was held with *Bionest*, a wastewater treatment technology developer (see section 2.1.3.1). While the modeling work conducted in this thesis helped *Bionest* to orient their R&D efforts, *Bionest* R&D needs contributed to the model development and understanding of involved phenomena. Modeling studies conducted for *Bionest* are summarized in this section.

9.3.1 Longevity prediction and effect of alkalinity

This project, realized at the beginning of 2015, was intended to produce an estimate of a slag filter longevity fed with a typical domestic secondary treatment effluent. The preliminary model and exhaustion functions from paper #3 were used, HRT_V of the filter was set at 12 h and the o-PO_4 influent concentration was 3.1 mg P/L. Two simulations were realized with different alkalinities. Simulation results are shown in Figure 9.3. The results were not intended to be accurate, but they gave a range of possible longevity. Longevity was assumed to be overestimated, as the diffusion barrier feature was not yet implemented in the model, and total phosphorus was not considered in this study. The main outcome of this study was to highlight the importance of low influent alkalinity for a longer filter longevity. This outcome helped *Bionest* to comfort his choice of placing

the slag filter after the secondary treatment process and not before, as alkalinity is reduced in the secondary treatment process by nitrification.

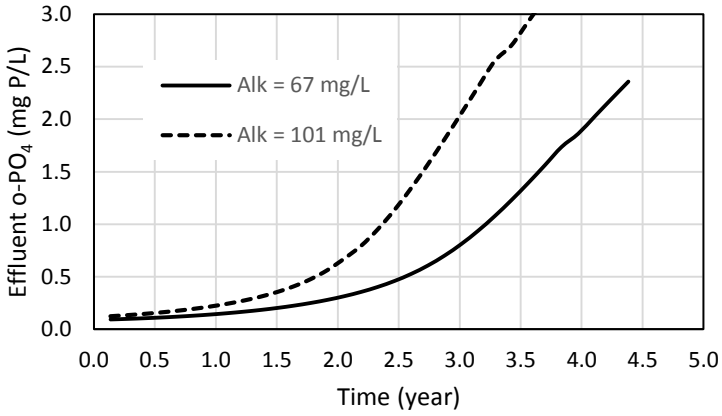

Figure 9.3 : Effect of alkalinity on longevity prediction of a slag filter operated at HRT_V = 12 h, using the preliminary model from paper #3

9.3.2 Effect of atmospheric CO_2

This project was realized in November 2015 and was intended to optimize the *Bionest* R&D slag filter. This slag filter's efficiency was suspected to be reduced by an atmospheric CO_2 input. In projects presented in this thesis, CO_2 has never been a concern because filters were implemented in tightly sealed columns, with no or minimal contact with atmosphere. In the case of *Bionest* project, the slag filter was installed in the first compartment of a conventional septic tank, fed from the bottom by a batch feeding mode (morning, noon and late afternoon) using a low-pressure distribution system for drainfield similar to those used in infiltration beds (Figure 9.4). The slag filer outlet involved a 5-cm water layer over-flowing to the second compartment, in which a neutralization process by CO_2- enriched air was running. The slag filter effluent was over-flowing through sealed pipes to avoid direct contact between the slag filter and the neutralization reactor. The outlet of the filter was in contact with the septic tank air that was suspected to be continuously fed with atmospheric CO_2 (weak sealing of the cover) or CO_2 from the neutralization process.

Intuitively, it was assumed that CO_2 input would reduce pH in the filter, because CO_2 is an acid. It was not possible, however, to assess quantitatively the amount of CO_2 entering in the filter, and how this would CO_2 affect the longevity of the filter, without conducting additional studies. The objective of this project was to answer these two questions. The project was done in two steps.

First, the CO_2 transfer rate was calibrated using *Bionest* slag filter experimental data and second, simulations were conducted to assess the effect of this CO_2 transfer on filter longevity.

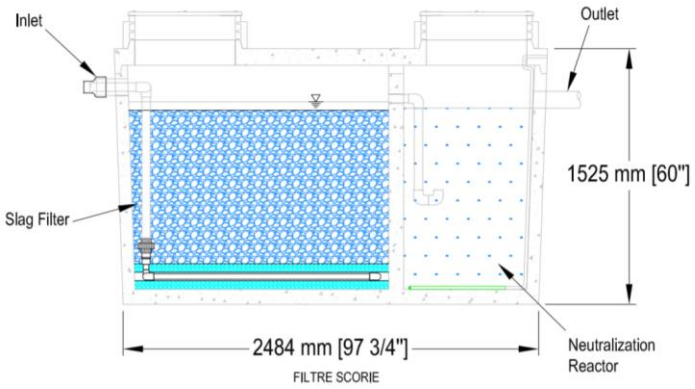

Figure 9.4 : R&D slag filter test conducted at *Bionest* (schematic provided by *Bionest*)

9.3.2.1 Calibration of the CO_2 transfer model

The slag filter was simulated with plug-flow continuous feeding, assuming hydraulic parameters similar to those observed in the column test conducted at Polytechnique and presented in paper #4 (n = 49%, n_e = 36% and D^* = 5.5 cm). The column had 20 numerical cells and an HRT_V of 15.4 h. An equation for CO_2 transfer was added to the P-Hydroslag model (Table 9.2). CO_2 was transferred only in the last 25% of the column, with a decreasing rate while going deeper in the filter. Calibration was performed on the transfer constant k_{CO2} as seen in Figure 9.5. In this figure, both steel slag filter and neutralization unit effluent are shown for o-PO_4, as either of them were measured. O-PO_4 at the effluent of the neutralization unit was assumed to be representative of the steel slag effluent.

Table 9.2 : CO_2 transfer equations added to the model

Numerical cell	Rate
1 to 15	
16	$r_{CO2} = 0.2k_{CO2}pH$
17	$r_{CO2} = 0.4k_{CO2}pH$
18	$r_{CO2} = 0.6k_{CO2}pH$
19	$r_{CO2} = 0.8k_{CO2}pH$
20	$r_{CO2} = k_{CO2}pH$

The addition of the CO_2 transfer rate improved the pH calibration, but o-PO_4 calibration remained poor (this issue was solved in the following simulation project). It was possible to see, however, that CO_2 transfer in the filter decreased its longevity by shifting the o-PO_4 curve to the left. $log(k_{CO2}) = -8$ was kept for following simulations. The chosen model for CO_2 transfer (linear progression in last 25% of the filter) was probably not perfect, but the calibrated constant was in accordance with experimental CO_2 transfer batch tests conducted for neutralization applications (see section 9.4.5). The proportion of affected column (25%) was chosen because of the presence of sampling port at 25% depth, which could have contributed to CO_2 contacting. Note that the CO_2 transfer model was improved and refined later in a neutralization modeling work (presented in section 9.4).

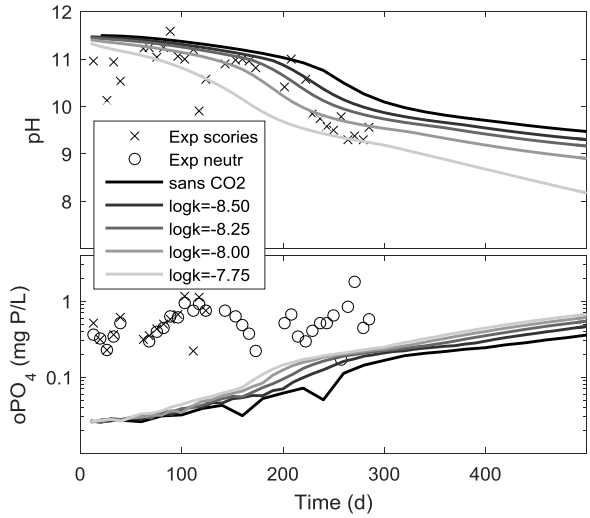

Figure 9.5 : *Bionest* R&D slag filter effluent composition compared to simulations

9.3.2.2 Effect of CO_2 input and HRT_V on filter longevity

Simulations with or without CO_2 input were performed, using HRT_V from 8 to 24 hours, which correspond to realistic operation conditions for a slag filter. Simulations with CO_2 input included $log(k_{CO2}) = -8$, as calibrated in the last step. Two longevity criteria were defined; the first at 1 mg P/L reach (as required by tertiary treatment target), the second at 0.5 mg P/L considering an arbitrary safety factor for total phosphorus (regulation is for TP and not o-PO_4) and a potentially noisy behavior of the slag filter. Results of simulations are shown in Table 9.3. Contact with CO_2 reduced the slag filter longevity, for example, the 0.5 mg P/L longevity is reduced by 260 days at HRT_V = 24 h.

Table 9.3 : Influence of HRT_V and CO_2 contact on longevity prediction of a slag filter

		With CO_2 contact					Without CO_2 contact				
HRT_V	h	8	12	16	18	24	8	12	16	18	24
Longevity at 1 mg P/L	d	246	396	575	800	1050	300	525	835	1184	1600
Longevity at 0.5 mg P/L	d	184	295	400	550	700	220	375	550	736	960

Following these results, it was recommended to *Bionest* to limit the presence of any air reservoir above the slag filter in their product configuration development. If not possible, the cover must be sealed, and CO_2 concentration in the air should be monitored in a validation step. If CO_2 concentration in this air reservoir is not close to zero, then there is a continuous CO_2 input in the filter and sealing should be improved.

The batch-feeding mode was not considered in this work, as continuous flow was assumed. At that time, it was suspected that bad hydraulics would maybe explain bad o-PO_4 calibration obtained in this study. This suspicion was confirmed in a later study in which hydraulic feeding mode was considered (presented in section 9.3.3).

Note that simulations were done with an ‘under progress’ version of the P-Hydroslag model. The diffusion barrier was there, leading to reduced longevity prediction compared to first simulation work (section 9.3.1), but homogeneous and heterogeneous precipitation as well as nucleation refinement were not yet implemented.

9.3.3 Effect of short-circuiting

The objective of this study realized in January 2016 was to evaluate the hydraulic efficiency of the R&D *Bionest* slag filter (the same that was described in section 9.3.2), using a tracer test that was conducted by *Bionest*. The project included two steps: hydraulic calibration and numerical simulations.

9.3.3.1 Calibration of Bionest R&D slag filter tracer test

The PHREEQC code used for numerical simulations had to be improved to consider batch feeding. This was made possible by iterative uses of the TRANSPORT datablock for representing each feeding phases, and assumption that rest periods could be represented by a single shift in the TRANSPORT datablock. Considering three feedings phases and three rest periods in a day, the

code resulted into six TRANSPORT datablock reproduced in an iterative way for the desired duration of the simulation. The tracer test was calibrated using the PHREEQC double porosity feature, as described in section 8.2.5.3. Calibration of the tracer test resulted in hydraulic parameters n_e = 0.288, D^* = 20 cm and D_n = 10^{-4} s^{-1}. The tracer test was well calibrated (Figure 9.6), PHREEQC could reproduce correctly rest periods. The tail was slightly underestimated, but the peak was recovered. Note that the first peak observed at t = 1.5 h was not modelled in the tracer test simulation; this peak was considered as short-circuiting not following the regular pathway of the slag filter. It was calculated from the tracer response curve that 8.8% of the tracer mass passed in this short-circuit.

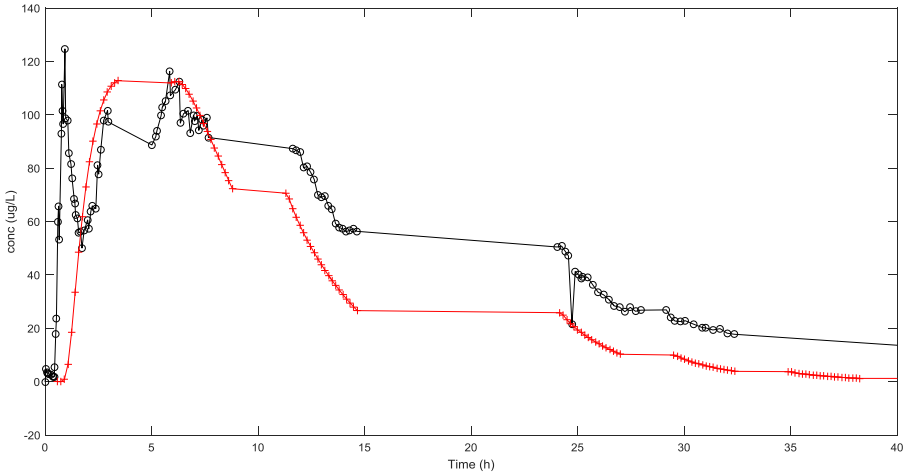

Figure 9.6 : Tracer test calibration for the R&D *Bionest* slag filter. black: experimental data, red: simulated data

9.3.3.2 Simulations of short-circuiting

Simulation of a short-circuited filter was performed by mixing the simulated effluent from a regular slag filter with 8.4% influent, assuming that short-circuited effluent passed the filter without any treatment. Simulation results for o-PO_4 of non-short-circuited and short-circuited filters are shown in Figure 9.7. In this figure, a sensitivity analysis on hydraulic parameters was performed, explaining why there are two curves for short-circuiting and two curves for regular filter.

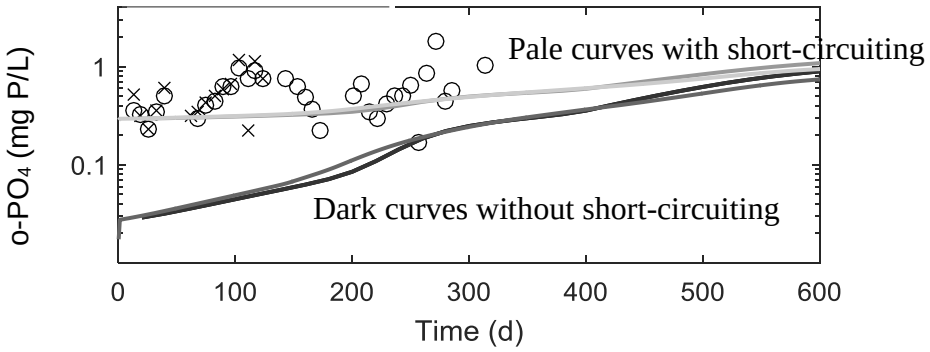

Figure 9.7 : Effect of short-circuiting on o-PO_4 effluent of the R&D *Bionest* slag filter

Results indicate that short-circuiting affected the effluent quality, mostly at the beginning of operation (first 250 days). The consideration of short-circuiting in simulations increased the model's accuracy in predicting o-PO_4 experimental results. This study led to recommendation for filter configuration. Continuous feeding mode was recommended, as batch feeding mode induces fast instantaneous water velocity that increases short-circuiting risks. As batch feeding mode is effective in autonomous and decentralized treatment, and also in product normalization protocol (BNQ, 2009), it was recommended to keep a filter geometry closer to plug-flow, as a column or several tanks in series, to reduce the risk of short-circuiting.

These simulations assumed that the model was valid for any water velocity. It is not sure, however, that D_{barr} remains the same if the water velocity is too high, as shown in Figure 9.1. These simulations were useful because they showed the great impact of short-circuiting, using tracer test interpretation and assumption of dilution with untreated influent. They would not be useful for comparing directly continuous and batch feeding mode (assuming that there is not short-circuiting) because of the unknown relationship between D_{barr} and water velocity.

9.4 Model development applied to neutralization processes

The model development strategy developed in this project was used in a related project, in which steel slag filter effluent neutralization was studied. Steel slag effluent must be neutralized before being discharged to the environment, as effluent pH (10-11) is higher than the maximum value acceptable of 9.5. A master's project was developed for optimization of a neutralization process by enriched-CO_2 air. This project was conducted by Patricia Bove, a master's student. The project initial objective was to assess the influence of feeding mode (saturated or percolating), type of media (none, gravel, K3 or *Bionest* media) and type of air (natural or CO_2-enriched air) on the

process performance. The candidate was involved in this project to better answer the objective with modeling work. An additional objective was added with the implementation of the model: propose a neutralization model as a design tool for process optimization.

The proposed CO_2 neutralization model was based on kinetic CO_2 transfer and kinetic calcite precipitation. This project is a good example of application of knowledge acquired in this Ph. D. project, as it followed more clearly steps defined in section 9.2. This model development was fast, the whole modeling project was realized within five months, excluding experimental work (September 2016 to January 2017).

9.4.1 Description of the neutralization unit experimental setup

Two column neutralization units (D= 6.3 cm and L = 152 cm) were continuously fed with steel slag effluents at an *HRT* of about 10 h. Air was injected at the bottom of the columns with a fine-bubble diffuser. Column 1 was fed with a synthetic inorganic solution, while column 2 was fed with a synthetic solution containing an acetic acid buffer. Each feeding mode-media-air type combination was tested during several days in both columns. Influent and effluent of the neutralization units were sampled and analyzed for pH, TIC, Ca and alkalinity. A tracer test using rhodamine was conducted on each media-feeding-mode configuration.

9.4.2 Chemical model for the neutralization process

The neutralization model was simpler than the P-Hydroslag model, as shown in Table 9.4. Only two kinetic equations were considered, one for CO_2 transfer and one for calcite precipitation. The calcite precipitation equation was identical to the one included in the P-Hydroslag model. The CO_2 transfer rate was chosen according to readings from the PHREEQC manual. In the implementation work, this model was compared to a more standard aeration model using $r_{CO2} = k_{CO2} \times (K_{H\_CO2} p_{CO2} - \{CO_2\})$, but the rate formulation presented in Table 9.4 resulted in more realistic results. The standard aeration model was defined following oxygen transfer model from wastewater treatment (Metcalf & Eddy *et al.*, 2014). In Table 9.4, the CO_2 transfer coefficient k_{CO2} includes both transfer from bubbles and from air-water surface. The model also included standard acid/base equilibrium reactions from the PHREEQC database.

Table 9.4 : Neutralization model equations

Process	Formula	Rate	K
CO_2 transfer	CO_2	$r_{CO2} = -k_{CO2} log\left(\frac{\{CO_2\}}{K_{H\_CO2} p_{CO2}}\right)$	$K_{H\_CO2} = 10^{-1.468}\, M/_{atm}$
Calcite precipitation	$CaCO_3$	$r_{CAL} = -k_{CAL} log\left(\frac{\{Ca^{2+}\}\{CO_3{}^{2-}\}}{K_{spCAL}}\right)$	$K_{spCAL} = 10^{-8.48} M^2$

9.4.3 Hydraulic calibration of neutralization reactors

Tracer tests showed that neutralization units had a hybrid hydraulic behavior, between completely mixed and plug flow. The exact hydraulic pattern changed following media and feeding mode. Most of tracer tests were calibrated using the ADR model from PHREEQC, in a similar way than what was done in preceding works (sections 8.2.5.3 and 9.3.3.1). An example of calibration following this methodology is shown in Figure 9.8. When the tracer response curve was very close to a completely mixed behavior, the reactor was assumed to be completely mixed. In that case, completely mixed numerical tracer tests were performed and compared to experimental data for validation (Figure 9.9). Only two configurations (saturated with no media and saturated with *Bionest* media) were modeled as completely mixed reactors.

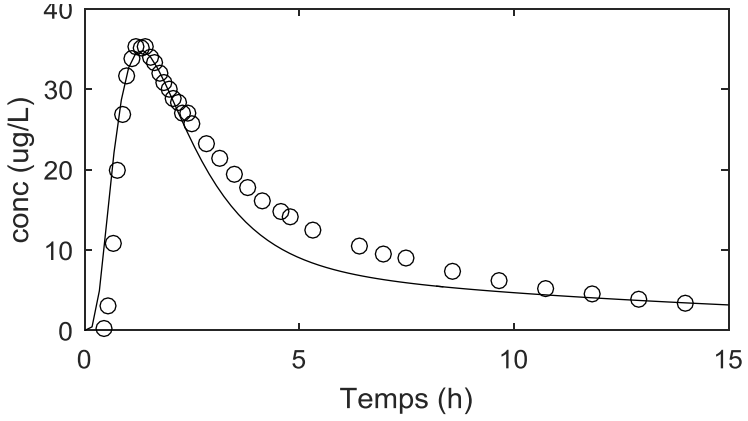

Figure 9.8 : Tracer test calibration of a neutralization unit (saturated with *Bionest* media) using the ARD equation. Line: simulated, o: experimental data

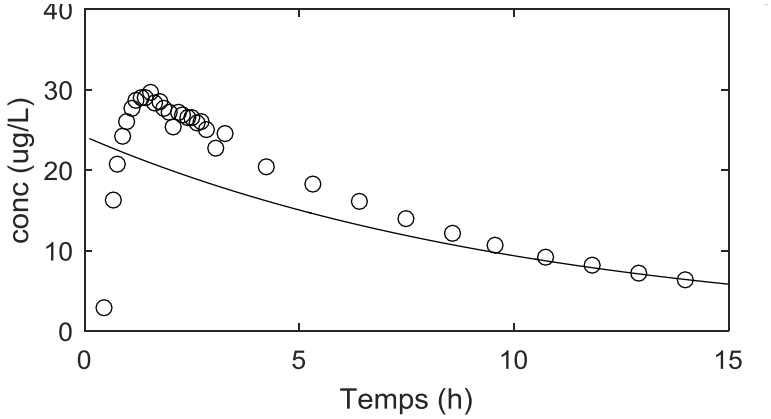

Figure 9.9 : Tracer test validation of a neutralization unit (saturated with no media) using a completely mixed reactor. Line: simulated, o: experimental data

9.4.4 Calibration of the neutralization model

Calibration of the neutralization model was performed individually for each neutralization unit configuration by iterative changes of k_{CO2} and k_{CAL}, until pH and CIT experimental data were accurately reproduced. Ca experimental data was not used in the calibration process, it was used as a validation indicator. An example of calibration is shown in Figure 9.10. pH and CIT were accurately reproduced, while calcium was approximatively well reproduced.

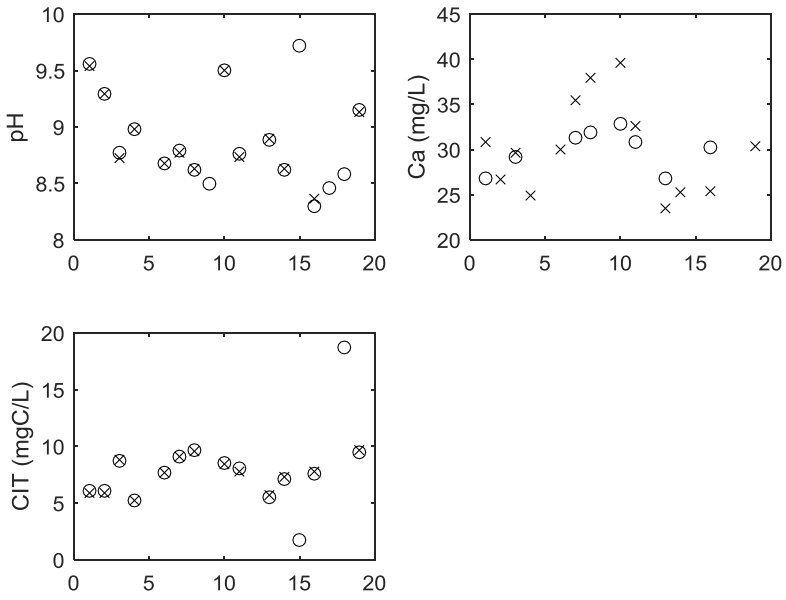

Figure 9.10 : Calibration of the neutralization model (configuration saturated, no media). O: experimental data, x: simulated data

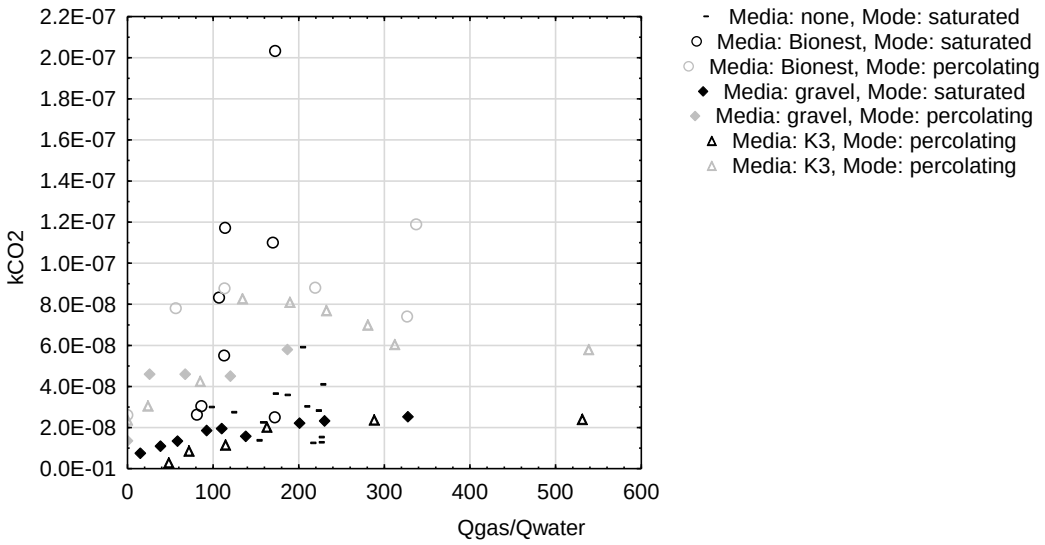

Figure 9.11 : Effect of media type and feeding mode on CO_2 transfer coefficient

Resulting calibrated CO_2 transfer coefficient for all tested configurations are shown in Figure 9.11. These results indicate that CO_2 transfer coefficient is mainly affected by feeding mode. Transfer coefficient for percolating mode were approximately 3-4 times higher then transfer coefficients for saturated mode. Note that coefficient transfer rates higher then 4e-8 for *Bionest* saturated mode were discarded because of CIT analysis incertitude leading to modeling artefact.

Calibrated calcite precipitation coefficient k_{CAL} is shown in Figure 9.12. Saturated and percolating conditions showed different behavior. While saturated reactors had a constant k_{CAL}, k_{CAL} from percolating reactors increased with time. This indicates that calcite precipitation rate increased following calcite precipitation on media in percolating reactors. In other words, the calcite precipitation rate should include an additional term for calcite specific surface, as suggested in standard geochemical precipitation models (Oelkers *et al.*, 2009) or recent physicochemical models for wastewater (Mbamba *et al.*, 2015). In saturated reactors, however, calcite seems to precipitate within liquid and be evacuated from the reactor with the main outflow, as the precipitation coefficient increase was not observed. Precipitation of calcite could thus be interpreted as homogenous in saturated conditions, and heterogeneous in percolating conditions. There is also an effect of media type on heterogeneous precipitation as media with greater specific surface (*Bionest* and K3) had a higher k_{CAL} increase then media with smaller specific surface (gravel).

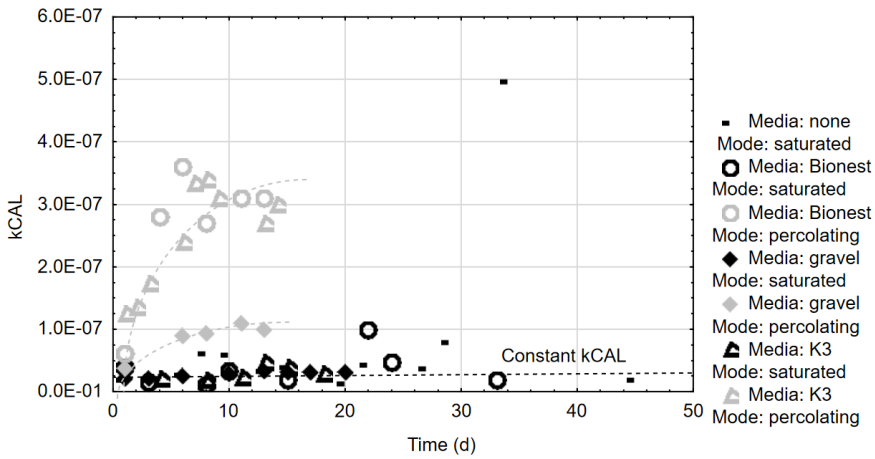

Figure 9.12 : Effect of media type and feeding mode on calcite precipitation coefficient. Dashed curves represent approximate tendendy

9.4.5 Impact of the neutralization process modeling study

The objective of this project was to assess the influence of media type and feeding mode on the efficiency of a neutralization process. It was possible to partly answer the objective by direct comparison of experimental pH results, without conducting simulations. The modeling study refined the interpretation by isolating four factors affecting experimental pH results: influent composition, CO_2 air concentration, hydraulics and media type. For example, all percolating conditions showed higher CO_2 transfer coefficient then saturated ones, but the final result on effluent pH was not so good for percolating conditions, because hydraulics was not very good for *Bionest* and K3 media. For percolating conditions, only the gravel media showed a sufficient hydraulic efficiency for resulting in acceptable pH decrease.

The calcite precipitation study was important for precipitation processes in general. It showed that either homogeneous or heterogeneous precipitation of a single phase occurs in a process, and it affects the rate formulation (consider mineral specific surface or not). In this study, the feeding mode was the factor determining precipitation type, but other factors as turbulence, mixing or water composition may have an impact in other processes. In the P-Hydroslag model HAP precipitation equations, only the water composition was considered to influence the precipitation type. Specific surface of heterogeneous crystal was neglected in equations, as equilibrium slag parameter (pH_{sat}) was more influent than kinetic parameter (k_{HAP}). In calcite precipitation for neutralization processes, the presented study showed that specific surface should be added to the model.

Table 9.5 : Scale effect on CO_2 transfer coefficient in saturated neutralization reactors

Scale	Aeration device	CO_2 in air	CO_2 transfer via	Water surface	Surface to volume	Side to volume	kCO_2
-	-	ppm	-	-	m^2/m^3	m/m^3	M/s
Batch	no	450	S only	flat	20.43	-	1e-8
Column	fine bubbles	450	S and A	Bubbles	0.8	152	2e-8
Pilot	fine bubbles	5000	S and A	Bubbles	0.9	6.4	20e-8

S: surface; A: aeration with fine bubbles

The calibration step realised in this project was extended to a multi-scale study. The calibration was performed on both small lab-scale neutralization batch tests conducted by the candidate (not presented in details) and on a full-scale neutralization test conducted by *Bionest* on their R&D slag filter (described in section 9.3.2). Resulting CO_2 transfer coefficient are shown in Table 9.5. A significant increase in kCO_2 was observed from batch to pilot conditions. This scale effect could be explained by the high contribution of transfer from water interface compared to transfer from bubbles. Considering this, the turbulence at the water interface may have an effect on gas transfer (more turbulence increases transfer). High side surface area (m^2) to volume (m^3) ratio in a column configuration may have reduced the turbulence at the water interface, resulting in decreased kCO_2.

9.4.6 Validation of the CO_2 neutralization model

The neutralization model was validated using a second neutralization test conducted by *Bionest* on their R&D slag filter. The validation simulation is compared to real data in Figure 9.13. The model showed accuracy in reproducing data. This model could consequently be used for useful design criteria for neutralization processes (minimum CO_2 concentration in air, minimum *HRT* in feeding phases, lowering electricity consumption by shutting the pump in rest periods, etc.)

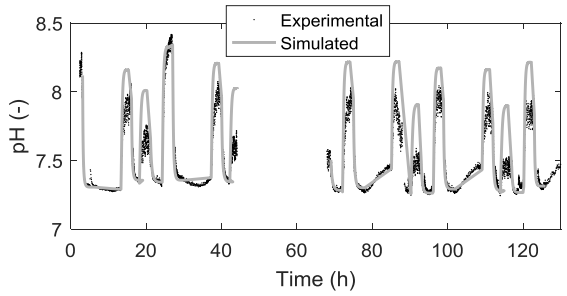

Figure 9.13 : Validation of the neutralization model on a neutralization test conducted by *Bionest*

At time of writing this thesis, an article presenting the neutralization modeling study was under preparation in collaboration with Patricia Bove.

9.5 Research needs for the P-Hydroslag model

During this project, the P-Hydroslag model has gone through three important model development steps, 1) qualitative description of involved phenomena (Claveau-Mallet *et al.*, 2012), 2) translation of phenomena into mathematical equations that make possible numerical simulations (paper #3) and 3) presentation of a first model version sufficiently mature for reproduction of real data (paper #4). A number of subsequent steps are necessary, however, before allowing the regular use of the model by wastewater modeling professionals. A list of research needs related to the development of this model are proposed.

One challenge related to use of by-products is their great heterogeneity. Slag composition is highly variable between different slag types (Vohla *et al.*, 2011), while storage and aging conditions affect their reactivity (Chazarenc *et al.*, 2007). The development of the P-Hydroslag model has needed eighty 3-day slag dissolution kinetic tests, which is much too long for practical applications. It would be more reasonable to complete the experimental characterization within five or six 3-day tests. Reducing the number of tests is a real challenge considering the large heterogeneity of slag. If reducing the number of tests is not possible, a validity range of already produced exhaustion functions should be defined. Can we use these functions in applications with the same material from a different production batch? Two solutions are possible for answering this, refinement of sampling methods and statistical analysis.

For the production of exhaustion equations, a very small sample representative of the whole slag batch used for filter has to be taken. Slag is friable, it is easily broken during transport, producing small and highly reactive particles that fall at the bottom of the slag lot. These small particles may not be sampled for the dissolution kinetic test, and it would underestimate exhaustion functions. Sampling challenges in the mining industry are similar, with friable and heavy minerals that are concentrated in metals. This issue was studied and sampling methods already exist (Gy, 1979). The application of these theories would contribute to the accurate characterization of exhaustion functions. It would also bring the water treatment modeling community thoughts regarding the utilization of synthetic materials in processes.

Statistical analysis is the second indispensable tool for accurate characterization of heterogeneity of reactive media and success in test number reduction. The model independence should be evaluated regarding water composition; and several model hypotheses should be validated, as influence of slag surface (essential hypothesis for translation of batch test conditions to filter conditions) and regression choice for definition of exhaustion equations. Slag heterogeneity could be validated with sensitivity analysis.

The P-Hydroslag model was calibrated with a specific type of reactive media: 5-10 mm electric arc furnace steel slag provided by Les Minéraux Harsco, Contrecoeur. The model principle involves that it would be possible to use the model with other reactive media as long as its exhaustion equations are measured experimentally. It would be interesting to measure exhaustion functions for other alkaline materials as hydrated oil slag ash (Kõiv *et al.*, 2010), and validate the use of the model for these materials.

The actual model was developed for a simple geometry reactor, namely a one-dimension plug-flow reactor. Yet, real steel slag filters are not always designed this way as they may be implemented in two-dimension constructed wetlands or percolation beds (Barca *et al.*, 2013; Kõiv *et al.*, 2010). The two-dimension geometry, including position of inlet and outlet of the filter, induces a complexification of flow as the filter clogs progressively following precipitation and organic matter input. Filter surface may be exposed to atmosphere, inducing a continuous atmospheric CO_2 input that prematurely exhausts the filter, as discussed in section 9.3.2. Moreover, the model was developed with a completely inorganic synthetic influent while real life effluents contain organic matter. All these questions should be addressed in a research program, with utilization in real-life cases as a target.

CHAPTER 10 CONCLUSION

The first objective of this thesis was to propose a phosphorus treatment system based on a steel slag filter integrated to a septic-tank-infiltration-bed system. The objective was achieved with the proposal of a recirculating steel slag filter (presented in paper #1). A recirculating filter within the second compartment of a septic tank at 50% recirculation ratio achieved 4.2 and 1.9 mg P/L at the effluent for TP and o-PO_4, respectively. The 1 mg P/L TP goal was not reached, but a significant P retention increase was observed with the addition of the steel slag filter. The o-PO_4-pH relationship found in the septic tank was similar to the one generally observed in steel slag filter, which facilitates future design of such systems. The theoretical needed pH in infiltration water for reaching 1 mg/L o-PO_4, assuming equilibrium with small-size hydroxyapatite, was between 8.4 and 9.0. Several recommendations were proposed for the development of recirculating slag filters in septic tanks: evaluate the effect of influent characteristics, determine the needed slag filter HRT_V for ensuring a two-year longevity, validate the utilization of the P-Hydroslag model as a design tool and test the proposed system in a pilot-scale study, including testing of higher recirculation ratio (50 to 75%) and monitoring infiltration water quality.

The second objective of this thesis was to propose a phosphorus removal mechanisms model for steel slag filters that must be usable for prediction of removal efficiency and longevity by numerical simulations. The objective was fulfilled by the presentation of the P-Hydroslag model, which involved several development steps presented in four papers. Hydroxyapatite precipitation and crystal growth were outlined as removal mechanisms in steel slag filters (paper #2). An effect of solution composition on growth rate was observed, and secondary treatment mechanisms as coprecipitation of fluoroapatite and metal precipitation were observed. A batch test experimental procedure was proposed for the characterization of exhaustion behavior (paper #3), resulting in exhaustion functions that can be used in a preliminary model for slag filter numerical simulations. The preliminary model was validated by reproducing approximately real experimental data of steel slag filters treating fish farm effluents (complementary paper). The P-Hydroslag model including equations for hydroxyapatite precipitation into homogeneous or heterogeneous nucleation, crystal growth, slag leaching, slag exhaustion and barrier effect caused by precipitates, was presented in paper #4. This model was calibrated with batch tests and a column test. Recommendations for further developments of this model were proposed: refinement of the exhaustion functions

measurement methodology by sampling and statistical analysis, utilisation of the model with other reactive materials, implementation in 2D geometry, consideration of biological reactions, reduction of available volume following clogging and consideration of atmosphere interactions.

A general model development methodology was proposed, including definition of the chemical model, definition of the hydraulic model, calibration of influent and simulations. Specific issues related to influent calibration for physicochemical processes were addressed (equilibrium of influent and calibration of alkalinity).

Three steel slag filter modeling works for industrial needs were presented. Modeling works were conducted in collaboration with *Bionest*, who operated a demonstration scale steel slag filter. In the first project, the effect of alkalinity on the *Bionest* steel slag filter longevity was assessed. The importance of low alkalinity for extending longevity was confirmed, and it was recommended to keep the steel slag filter downstream of secondary treatment units which would ideally nitrify, in order to reduce influent alkalinity of the slag filter. In the second project, it was shown that contact with atmospheric CO_2 in the *Bionest* steel slag filter decreased its longevity. It was recommended to limit or avoid the presence of an air reservoir above the slag filter, to limit CO_2 input. In the third project, it was shown that batch feeding mode in the *Bionest* slag filter combined to its geometry induced short-circuiting and reduced the filter removal efficiency. To reduce short-circuiting, it was recommended to implement slag filters in a geometry as close as possible to plug-flow conditions by using multiple tanks in series.

A physicochemical model for neutralization of steel slag effluents was proposed. The model included equations for CO_2 transfer and calcite precipitation and it was calibrated on lab-scale neutralization tests. Feeding mode (saturated or percolating) had a significant impact on CO_2 transfer rate while the influence of type of media in the reactor (none, gravel, Bionest or K3) was low. The calcite precipitation constant increased in percolating reactors but remained constant in saturated reactors, indicating that a precipitation rate equation should include specific surface only in the percolating mode. A scale effect was observed for CO_2 transfer rate: CO_2 transfer coefficient was ten times higher in pilot conditions compared to lab scale conditions. The scale effect was explained by important side area to reactor volume in column geometry.

REFERENCES

Abderraja Anjab, Z. (2009). *Development of a steel slag bed for phosphorus removal from fishfarm wastewater (In French).* (M.A.Sc. thesis, Polytechnique Montreal, Canada).

Aldaco, R., Irabien, A., & Luis, P. (2005). Fluidized bed reactor for fluoride removal. *Chemical Engineering Journal, 107*(1-3), 113-117.

Allison, J. D., Brown, D. S., & Novo-Gradac, K. J. (1991). *MINTEQA2/PRODEFA2, a geochemical assessment model for environmental systems: version 3.0 user's manual*. Athens, GA: Environmental Research Laboratory, United States Environment Protection Agency.

Alonso, U., Missana, T., García-Gutiérrez, M., Patelli, A., Siitari-Kauppi, M., & Rigato, V. (2009). Diffusion coefficient measurements in consolidated clay by RBS micro-scale profiling. *Applied Clay Science, 43*, 477-484.

APHA, AWWA & WEF. (2005). Standard methods for the examination of water and wastewater (21st ed.). Washington, D. C: American Public Health Association, American Water Works Association & Water Environment Federation.

APHA, AWWA & WEF. (2012). Standard methods for the examination of water and wastewater (22nd ed.). Washington, D. C: American Public Health Association, American Water Works Association & Water Environment Federation.

ASTM. (2004). *Standard Test Method for Density, Relative Density (Specific Gravity), and Absorption of Coarse Aggregate*. ASTM C127-04. West Conshohocken, PA: American Society for Testing Materals.

ASTM. (2006). *Standard test method for permeability of granular soils (constant head).* ASTM D2434-68. West Conshohocken, PA: American Society for Testing Materals.

ASTM. (2011). *Standard Practice for Reducing Samples of Aggregate to Testing Size*. ASTM C 702 / C 702 M−11. West Conshohocken, PA: American Society for Testing Materals.

Audette, Y., O'Halloran, I. P., Evans, L. J, & Voroney, R. P. (2016). Preliminary validation of a sequential fractionation method to study phosphorus chemistry in a calcareous soil. *Chemosphere, 152*, 369-375.

Baker, M. J., Blowes, D. W., & Ptacek, C. J. (1998). Laboratory development of permeable reactive mixtures for the removal of phosphorus from onsite wastewater disposal systems. *Environmental Science and Technology, 32*(15), 2308-2316.

Bankole, L. K., Rezan, S. A., & Sharif, N. M. (2011). Thermodynamic modeling of mineral phases formation in EAF slag system and its application as agricultural fertilizer. *SEAISI Quarterly (South East Asia Iron and Steel Institute), 40*(4), 26-32.

Barca, C., Gérente, C., Meyer, D., Chazarenc, F., & Andrès, Y. (2012). Phosphate removal from synthetic and real wastewater using steel slags produced in Europe. *Water Research*, 46, 2376-2384.

Barca, C., Troesch, S., Meyer, D., Drissen, P., Andrès, Y., & Chazarenc, F. (2013). Steel slag filters to upgrade phosphorus removal in constructed wetlands: two years of field experiments. *Environmental Science and Technology, 47*(1), 549-556. doi:10.1021/es303778t

Bernier, B. (2001). *Guide pour l'étude des technologies conventionnelles de traitement des eaux usées d'origine domestique.* Direction des politiques du secteur municipal – Service de l'expertise technique en eau, Québec: Ministère du développement durable, de l'environnement et des parcs.

Bird, S. C., & Drizo, A. (2009). Investigations on phosphorus recovery and reuse as soil amendment from electric arc furnace slag filters. *Journal of Environmental Science and Health*, Part A, 44(13), 1476-1483.

Blais, S. (2008). *Guide d'identification des fleurs d'eau de cyanobactéries. Comment les distinguer des végétaux observés dans nos lacs et nos rivières*. Ministère du développement durable, de l'environnement et des parcs, Retrieved from http://www.mddep.gouv.qc.ca/eau/eco_aqua/cyanobacteries/guide-identif.pdf.

BNQ. (2009). *Onsite Residential Wastewater Treatment Technologies*. CAN/BNQ 3680-600/2009. Bureau de Normalisation du Québec (BNQ).

Boaventura, R., Pedro, A. M., Coimbra, J., & Lencastre, E. (1997). Trout farm effluents: characterization and impact on the receiving streams. *Environmental Pollution*, 95(3), 379-387.

Boutet, E., Baillargeon, S., Allaire, F., Lida, F., Claveau-Mallet, D. & Comeau, Y. (2017). Apparatus and method for wastewater treatment, US Provisional Patent Application No. 62/450,210, filed January 25, 2017.

Bowden, L. I., Jarvis, A. P., Younger, P. L., & Johnson, K. L. (2009). Phosphorus removal from waste waters using basic oxygen steel slag. *Environmental Science and Technology, 43*(7), 2476-2481.

Brient, S. (2012). *Dephosphatation of a fish farm wastewater with extensive steel slag fiters (in French).* (M.A.Sc. thesis, Polytechnique Montreal, Canada).

Brix, H., Arias, C., & Del Bubba, M. (2001). Media selection for sustainable phosphorus removal in subsurface flow constructed wetlands. *Water Science & Technology*, 44(11-12), 47-54.

Chambers, P. A., Guy, M., Roberts, E. S., Charlton, M. N., Kent, R., Gagnon, C., Grove, G., & Foster, N. (2001). *Les éléments nutritifs et leurs effets sur l'environnement au Canada*. Ottawa: Agriculture et Agroalimentaire Canada, Environnement Canada, Pêches et Océans Canada, Santé Canada & Ressources naturelles Canada.

Chapuis, R. P., Baass, K., & Davenne, L. (1989). Granular soils in rigid-wall permeameters. Method for determining the degree of saturation. *Canadian Geotechnical Journal, 26*(1), 71-79.

Charlton, S. R., & Parkhurst, D. L. (2011). Modules based on the geochemical model PHREEQC for use in scripting and programming languages. *Computers & Geosciences, 37*(10), 1653-1663.

Chazarenc, F., Brisson, J., & Comeau, Y. (2007). Slag columns for upgrading phosphorus removal from constructed wetland effluents. *Water Science and Technology, 56*, 109-115.

Chazarenc, F., Kacem, M., Gérente, C., & Andrès, Y. (2008). *'Active' filters: a mini-review on the use of industrial by-products for upgrading phosphorus removal from treatment wetlands.* Paper presented at the 11th Int. Conf. on Wetland Systems for Water Pollution Control, Indore, India, November 1 – November 7.

Chazarenc, F., Filiatrault, M., Brisson, J. & Comeau, Y. (2010). Combination of slag, limestone and sedimentary apatite in columns for phosphorus removal from sludge fish farm effluents. Water, 2(3), 500-509.

Claveau-Mallet, D., Courcelles, B., Pasquier, P. & Comeau, Y. (2016, In preparation). P-Hydroslag model as a simulation tool for phosphorus removal prediction of slag filters.

Claveau-Mallet, D. (2016). *Physicochemical modeling of phosphorus removal and recovery from wastewater*. Workshop held at the 5th IWA/WEF Wastewater Treatment Modelling Seminar WWTmod2016, Annecy, France, April 2-6.

Claveau-Mallet, D., Courcelles, B., & Comeau, Y. (2014). Phosphorus removal by steel slag filters: Modeling dissolution and precipitation kinetics to predict longevity. *Environmental Science and Technology, 48*(13), 7486-7493.

Claveau-Mallet, D., Lida, F., & Comeau, Y. (2015). Improving phosphorus removal of conventional septic tanks by a recirculating steel slag filter. *Water Quality Research Journal of Canada, 50*(3), 211-218.

Claveau-Mallet, D., Wallace, S., & Comeau, Y. (2012). Model of phosphorus precipitation and crystal formation in electric arc furnace steel slag filters. *Environmental Science and Technology, 46*(3), 1465-1470. doi:10.1021/es2024884

Claveau-Mallet, D., Wallace, S., & Comeau, Y. (2013). Removal of phosphorus, fluoride and metals from a gypsum mining leachate using steel slag filters. *Water Research, 47*(4), 1512-1520.

Comeau, Y., Brisson, J., Réville, J. P., Forget, C. & Drizo, A. (2001). Phosphorus removal from trout farm effluents by constructed wetlands. *Water Science & Technology*, 44(11-12), 55-60.

COMSOL. (2014). Retrieved from http://www.comsol.com/, accessed on May 9, 2014.

Corominas, L., Rieger, L., Takács, I., Ekama, G., Hauduc, H., Vanrolleghem, P., Oehmen, A., Gernaey, K. V., van Loosdrecht, M. C. M., & Comeau, Y. (2010). New framework for standardized notation in wastewater treatment modelling. *Water Science and Technology, 61*(4), 841-857.

Courcelles, B., Modaressi-Farahmand-Razavi, A., Gouvenot, D., & Esnault-Filet, A. (2011). Influence of precipitates on hydraulic performance of permeable reactive barrier filters. *International Journal of Geomechanics, 11*(2), 142-151.

Cripps, S. J. & Bergheim, A. (2000). Solids management and removal for intensive land-based aquaculture production systes. *Aquacultural Engineering*, 22(1), 33-56.

Cucarella, V., & Renman, G. (2009). Phosphorus sorption capacity of filter materials used for on-site wastewater treatment determined in batch experiments - a comparative study. *Journal of Environmental Quality, 38*(2), 381-392.

Cucarella, V., Zaleski, T., Mazurek, R., & Renman, G. (2007). Fertilizer potential of calcium-rich substrates used for phosphorus removal from wastewater. *Polish Journal of Environmental Studies*, 16(6), 817-822.

Cullity, B. D. (2001). *Elements of x-ray diffaction* (3rd ed.). Upper Saddle River, NJ: Prentice Hall.

de Repentigny, C., & Courcelles, B. (2014). A simplified model to predict clogging of reactive barriers. *Environmental Geotechnics, 3*(3), 166-177.

Delgado, J. M. P. Q. (2006). A critical review of dispersion in packed beds. *Heat Mass Transfer, 42*(4), 279-310.

Domenico, P. A., & Schwartz, F. W. (1998). *Physical and Chemical Hydrogeology* (2nd ed.). New York: John Wiley & Sons.

Drizo, A., Comeau, Y., Forget, C., & Chapuis, R. P. (2002). Phosphorus saturation potential: A parameter for estimating the longevity of constructed wetland systems. *Environmental Science and Technology, 36*(21), 4642-4648.

Drizo, A., Forget, C., Chapuis, R. P., & Comeau, Y. (2006). Phosphorus removal by electric arc furnace steel slag and serpentinite. *Water Research, 40*(8), 1547-1554.

Environmental Health and Safety Online. (2008). The EPA TCLP: Toxicity Characteristic Leaching Procedure and Characteristic Wastes (D-codes). Retrieved from http://ehso.com/cssepa/TCLP.htm, accessed on April 19, 2012.

Eppner, F., Pasquier, P., & Baudron, P. (2015). *Development of a thermo-hydro-geochemical model for low temperature geoexchange.* Paper presented at the COMSOL Conference, Boston, October 5-7.

Evoqua Water Technologies. (2014). Biomag system for enhanced secondary treatment. Retrieved from www.evoqua.com/en/products/separation_clarification/ballasted-clarifiers/Pages/biomag-system.aspx, accessed on December 26, 2014.

Fetter, G. W. (1999). *Contaminant Hydrogeology* (2nd ed.). Long Grove, IL: Waveland Press.

Flores-Alsina, X., Mbamba, C. K., Solon, K., Vrecko, D., Tait, S., Batstone, D. J., Jeppsson, U., & Gernaey, K. V. (2015). A plant-wide aqueous phase chemistry module describing pH variations and ion speciation/pairing in wastewater treatment process models. *Water Research, 85*, 255-265.

Forget, C. (2001). *Dissolved phosphorus removal from fish farm effluents by reactive granular media (In French).* (M.A.Sc. thesis, Polytechnique Montreal, Canada).

Grzmil, B., & Wronkowski, J. (2006). Removal of phosphates and fluorides from industrial wastewater. *Desalination, 189*(1-3 SPEC. ISS.), 261-268.

Gy, P. (1979). *Developments in geomathematics. theory and practive 4, Sampling of particulate materials*. New York: Elsevier Scientific Publications.

Hauduc, H., Takács, I., Smith, S., Szabó, A., Murthy, S., Daigger, G. T., & Spérandio, M. (2015). A dynamic physicochemical model for chemical phosphorus removal. *Water Research, 73*, 157-170.

Hedström, A. (2006). Wollastonite as reactive filter medium for sorption of wastewater ammonium and phosphorus. *Environmental Technology*, 27(7), 801-809.

Henze, M., Gujer, W., Mino, Takashi., & van Loosdrecht, M. (2000). Activated sludge models ASM1, ASM2, ASM2d and ASM3. Scientific and Technical Report Series, London (U.K.): IWA Publishing.

House, C., Bergmann, B., Stomp, A., & Frederick, D. (1999). Combining constructed wetlands and aquatic and soil filters for reclamation and reuse of water. *Ecological Engineering*, 12(1), 27-38.

Huang, Y. H., Shih, Y. J., & Chang, C. C. (2011). Adsorption of fluoride by waste iron oxide: The effects of solution pH, major coexisting anions, and adsorbent calcination temperature. *Journal of Hazardous Materials, 186*(2-3), 1355-1359.

Ito, H., Oaki, Y., & Imai, H. (2008). Selective synthesis of various nanoscale morphologies of hydroxyapatite via an intermediate phase. *Crystal Growth & Design, 8*(3), 1055-1059.

IWA. (2017). Generalized Physicochemical Framework. Retrieved from http://www.iwa-network.org/groups/generalized-physicochemical-framework/, accessed on February 20, 2017.

Jaffer, Y., Clark, T. A., Pearce, P., & Parsons, S. A. (2002). Potential phosphorus recovey by struvite formation. *Water Research, 36*(7), 1834-1842.

Jourak, A., Frishfelds, V., Hellström, J. G., Lundström, T. S., Herrmann, I., & Hedström, A. (2013). Longitudinal dispersion coefficient: effects of particle-size distribution. *Transport in Porous Media, 99*(1), 1-16.

Kadlec, R. H., & Wallace, S. (2009). *Treatment Wetlands* (2nd ed.). Boca Raton, FL: CRC Press.

Kim, E.-H., Yim, S.-B., Jung, H.-C., & Lee, E.-J. (2006). Hydroxyapatite crystallization from a highly concentrated phosphate solution using powdered converter slag as a seed material. *Journal of Hazardous Materials, 136*(3), 690-697. doi:10.1016/j.jhazmat.2005.12.051

Kõiv, M., Liira, M., Mander, Ü., Mõtlep, R., Vohla, C., & Kirsimäe, K. (2010). Phosphorus removal using Ca-rich hydrated oil shale ash as filter material - The effect of different phosphorus loadings and wastewater compositions. *Water Research, 44*(18), 5232- 5239.

Kõiv, M., Ostonen, I., Vohla, C., Mõtlep, R., Liira, M., Lõhmus, K., Kirsimäe, K., & Mander, Ü. (2012). Reuse potential of phosphorus-rich filter materials from subsurface flow wastewater treatment filters for forest soil amendment. *Hydrobiologia*, 692(1), 145-156.

Kõiv, M., Mahadeo, K., Brient, S., Claveau-Mallet, D., & Comeau, Y. (2016). Treatment of fish farm sludge supernatant by aerated filter beds and steel slag filters - effect of organic loading rate. *Ecological Engineering, 94*, 190-199.

Kostura, B., Kulveitová, H., & Leško, J. (2005). Blast furnace slags as sorbents of phosphate from water solutions. *Water Research, 39*(9), 1795-1802.

Lasaga, A. C. (1981). Rate laws of chemical reactions, In *Kinetics of Geochemical Processes* (Vol. 8, pp. 1-68). Chelsea, MI: Mineralogical Society of America.

Lefrançois, P., Puigagut, J., Chazarenc, F., & Comeau, Y. (2010). Minimizing phosphorus discharge from aquaculture earth ponds by a novel sediment retention system. *Aquacultural Engineering*, 43(3), 94-100.

Le, H. R., Chen, K. Y., & Wang, C. A. (2012). Effect of pH and temperature on the morphology and phases of co-precipitated hydroxyapatite. *Journal of Sol-Gel Science and Technology, 61*(3), 592-599. doi:10.1007/s10971-011-2665-7

Liira, M., Kõiv, M., Mander, Ü., Mõtlep, R., Vohla, C., & Kirsimäe, K. (2009). Active filtration of phosphorus on Ca-rich hydrated oil shale ash: Does longer retention time improve the process? *Environmental Science and Technology, 43*(10), 3809-3814.

Lizarralde, I., Fernández-Arévalo, T., Brouckaert, C., Vanrolleghem, P., Ikumi, D. S., Ekama, G. A., Ayesa, E., & Grau, P. (2015). A new methodology for incorporating physico-chemical transformations into multi-phase wastewater treatment process models. *Water Research, 74*, 239-256.

Lospied, C. (2003). *Evaluation of steel slag capacity and removal conditions for dissolved phosphorus (In French).* (M.A.Sc. thesis, Polytechnique Montreal, Canada).

Lowell, S., Shields, J. E., Thomas, M. A., & Thommes, M. (2004). *Characterization of Porous Solids and Powders: Surface Area, Pore Size and Density*. New York: Springer.

Lundager Madsen, H. E. (2008). Influence of foreign metal ions on crystal growth and morphology of brushite ($CaHPO_4$, $2H_2O$) and its transformation to octacalcium phosphate and apatite. *Journal of Crystal Growth, 310*(10), 2602-2612.

Mahadeo, K. (2013). *Treatment of fish farm sludge supernatant with aerated filter beds and steel slag filters - Effect of organic matter and nutrient loading rates.* (M.Eng. thesis, Polytechnique Montreal, Canada).

Maher, C., Neethling, J. B., Murthy, S., & Pagilla, K. (2015). Kinetics and capacities of phosphorus sorption to tertiary stage wastewater alum solids, and process implications for achieving low-level phosphorus effluents. *Water Research, 85*, 226-234.

Manjanna, J., Kozaki, T., & Sato, S. (2009). Fe(III)-montmorillonite: basic properties and diffusion of tracers relevant to alteration of bentonite in deep geological disposal. *Applied Clay Science, 43*, 208-217.

Mayes, W. M., Younger, P. L., & Aumônier, J. (2006). Buffering of alkaline steel slag leachate across a natural weland. *Environmental Science and Technology, 40*, 1237-1243.

Mbamba, C. K., Batstone, D. J., Flores-Alsina, X., & Tait, S. (2015). A generalised chemical precipitation modelling approach in wastewater treatment applied to calcite. *Water Research, 68*, 342-353.

Mbamba, C. K., Tait, S., Flores-Alsina, X., & Batstone, D. J. (2015). A systematic study of multiple minerals precipitation modelling in wastewater treatment. *Water Research, 85*, 359-370.

MDDEP. (2006). Metals determination: method by mass spectrometry with argon plasma ionizing source (in French) (3rd ed.): Centre d'expertise en analyse environnementale, Ministère du développement durable, de l'environnement et des parcs. MA. 200 – Mét 1.1.

MDDEP. (2009a). *Guide technique - traitement des eaux usées des résidences isolées*. Québec: Ministère du développement durable, de l'environnement et des parcs.

MDDEP. (2009b). *Réduction du phosphore dans les rejets d'eaux usées d'origine domestique - Position du ministère du Développement durable, de l'Environnement et des Parcs (MDDEP)*. Québec: Ministère du développement durable, de l'environnement et des Parcs

Retrieved from http://www.mddep.gouv.qc.ca/eau/eaux-usees/reduc-phosphore/index.htm.

Metcalf & Eddy. (2003). *Wastewater Engineering: Treatment and Reuse* (4th ed.). New York: McGraw-Hill.

Metcalf & Eddy. (2014). *Wastewater Engineering: Treatment and Reuse* (5th ed.). New York: McGraw-Hill.

Muñoz, P., Drizo, A., & Cully Hession, W. (2006). Flow patterns of dairy wastewater constructed wetlands in a cold climate. *Water Research*, 40(17), 3209-3218.

National Slag Association. (2009). General Information about National Slag Association (NSA). Retrieved from http://www.nationalslag.org/nsageneral.htm, accessed on March 16, 2012.

Nilsson, C. Renman, G., Westholm, L. J., Renman, A., & Drizo, A. (2013). Effect of organic load on phosphorus and bacteria removal from wastewater using alkaline filter materials. *Water Research*, 47(16), 6289-6297.

Nivala, J. Headley, T. Wallace, S., Bernhard, K., Brix, H., van Afferden, M., & Müller, R. A. (2013). Comparative analysis of constructed wetlands: the design and construction of the ecotechnology research facility in Langenreichenbach, Germany. *Ecological Engineering*, 61, 527-543.

Oelkers, E. H., Bénézeth, P., & Pokrovski, G. S. (2009). Thermodynamic Databases for Water-Rock Interaction. In Mineralogical Society of America & Geochemical Society (Eds.), *Thermodynamics and Kinetics of Water-Rock Interaction* (Vol. 70, pp. 1-46). Chantilly, VA.

Ouellet-Plamondon, C., Chazarenc, F., Comeau, Y. & Brisson, J. (2006). Artificial aeration to increase pollutant removal efficiency of constructed wetlands in cold climate. *Ecological Engineering*, 27(3), 258-264.

Parkhurst, D. L., & Appelo, C. A. J. (1999). *User's guide to PHREEQC (Version 2) - A computer program for speciation, batch-reaction, one-dimensional transport, and inverse geochemical calculations*. (Water-Resources Investigations Report 99-4259). Denver: United States Geological Survey.

PC Progress. (2014). Hydrus-1D for Windows, Version 4.xx. Retrieved from PC Progress website, http://www.pc-progress.com/en/Default.aspx?hydrus-1d, accessed on May 9, 2014.

Penn, C., Bowen, J., McGrath, J., Nairn, R., Fox, G., Brown, G., Wilson, S., & Gill, C. (2016). Evaluation of a universal flow-through model for predicting and designing phosphorus removal structures. *Chemosphere, 151*, 345-355.

Ping, Q., Li, Y., Wu, X., Yang, L., & Wang, L. (2016). Characterization of morphology and component of struvite pellets crystallized from sludge dewatering liquor: effects of total suspended solid and phosphate concentrations. *Journal of Hazardous Materials, 310*, 261-269.

Pratt, C., & Shilton, A. (2010). Active slag filters-simple and sustainable phosphorus removal from wastewater using steel industry byproduct. *Water Science and Technology, 62*(8), 1713-1718.

Premier Tech Aqua. (2014). Premier Tech Aqua products. Retrieved from http://premiertechaqua.com/assainissement-traitement-eaux-usees/biofiltre-entrepreneur-desinfection#1389, accessed December 26, 2014.

Press, W. H. (2007). *Numerical recipes: the art of scientific computing* (3rd ed.). Cambridge: Cambridge University Press.

Proctor, D. M., Fehling, K. A., Shay, E. C., Wittenborn, J. L., Green, J. J., Avent, C., Bigham, R. D., Connolly, M., Lee, B., Shepker, T. O., & Zak, M. A. (2000). Physical and chemical characteristics of blast furnace basic oxygen furnace, and electric arc furnace steel industry slags. *Environmental Science & Technology*, 34(8), 1576-1582.

Puigagut, J., Angles, H., Chazarenc, F., & Comeau, Y. (2011). Decreasing phosphorus discharge in fish farm ponds by treating the sludge generated with sludge drying beds. *Aquaculture*, 318(1), 7-14.

Radio-Canada. (2002). Champ d'épuration: les tests de percolation, indispensables! Retrieved from http://www.radio-canada.ca/actualite/lafacture/224/rept.html, accessed on April 26, 2013.

Rehman, U., De Mulder, C., Amerlinck, Y., Arnaldos, M., Weijers, S. R., Potier, O., & Nopens, I. (2016). *Towards better models for describing mixing using compartmental modelling: a full-scale case demonstration.* Paper presented at the 5th IWA/WEF Wastewater Treatment Modelling Seminar WWTmod2016, Annecy, France, April 2-6.

Renman, A., Renman, G., Gustafsson, J. P., & Hylander, L. (2009). Metal removal by bed filter materials used in domestic wastewater treatment. *Journal of Hazardous Materials, 166*(2-3), 734-739.

Richardson, A. E. (2001). Prospects for using soil microorganisms to improve the acquisition of phosphorus by plants. *Functional Plant Biology*, 28(9), 897-916.

Robertson, W. D., Schiff, S. L., & Ptacek, C. J. (1998). Review of phosphate mobility and persistence in 10 septic system plumes. *Groundwater, 36*(6), 1000-1010.

Samsó, R., García, J., Molle, P., & Forquet, N. (2015). Modelling bioclogging in variably saturated porous media and the interactions between surface/subsurface flows: Application to Constructed Wetlands. *Journal of Environmental Management, 165*, 271-279.

Sawyer, C. N., McCarty, P. L., & Parkin, G. F. (2003). *Chemistry for Environmental Engineering and Science* (5th ed.). New York: McGraw-Hill.

Seckler, M. M., Bruinsma, O. S. L., & van Rosmalen, G. M. (1991). Crystallization of calcium and magnesium phosphates in a fluidized bed. *Crystal Properties and Preparation, 36*(38), 263-272.

Shilton, A., Pratt, S., Drizo, A., Mahmood, B., Banker, S., Billings, L., Glenny, S., & Luo, D. (2005). 'Active' filters for upgrading phosphorus removal from pond systems. *Water Science and Technology, 51*(12), 111-116.

Shilton, A. N., Elmetri, I., Drizo, A., Pratt, S., Haverkamp, R. G., & Bilby, S. C. (2006). Phosphorus removal by an 'active' slag filter-a decade of full scale experience. *Water Research, 40*(1), 113-118.

Smyth, D. J. A., Blowes, D. W., Ptacek, C. J., Baker, M. J., & McRae, C. W. T. (2002). *Steel production wastes for use in permeable reactive barriers (PRBs).* Paper presented at the

Third International Conference on Remediation of Chlorinated and Recalcitrant Compounds, Monterey, CA., May 20-23.

Solon, K., Flores-Alsina, X., Mbamba, C. K., Volcke, E. I. P., Tait, S., Batstone, D. J., Gernaey, K. V., & Jeppsson, U. (2015). Effects of ionic strength and ion pairing on (plant-wide) modelling of anaerobic digestion. *Water Research, 70*, 235-245.

Stangart, A. (2012). Phosphorus removal fromp septic tank effluents by coarse steel slag (In French). (M.Eng. thesis, Polytechnique Montreal, Canada).

Stumm, W., & Morgan, J. J. (1996). *Aquatic Chemistry: Chemical Equilibria and Rates in Natural Waters* (3rd ed.). New York: John Wiley & Sons.

Szabó, A., Takács, I., Murthy, S., Daigger, G. T., Licskó, I., & Smith, S. (2008). Significance of design and operational variables in chemical phosphorus removal. *Water Environment Research, 80*(5), 407- 416.

Terashima, M., Goel, R., Komatsu, K., Yasui, H., Takahashi, H., Li, Y. Y., & Noike, T. (2009). CFD simulation of mixing in anaerobic digesters. *Bioresource Technology, 100*, 2228-2233.

Tsuru, K., Kubo, M., Hayakawa, S., Ohtsuki, C., & Osaka, A. (2001). Kinetics of apatite deposition of silica gel dependent on the inorganic ion composition of simulated body fluids. *Nippon Seramikkusu Kyokai Gakujutsu Ronbunshi/Journal of the Ceramic Society of Japan, 109*(1269), 412-418.

USEPA. (1992). Toxicity characteristic leaching procedure. United States Environment Protection Agency Test Method 1311, Washington, (DC).

Vallet, B. (2001). *Phosphorus removal of the Montreal Biodome marine Saint-Lawrence basin by steel slag (In French)*. Internal Report, Polytechnique Montreal, Montreal.

Valsami-Jones, E. (2001). Mineralogical controls on phosphorus recovery from wastewaters. *Mineralogical Magazine, 65*(5), 611-620.

Vohla, C., Kõiv, M., Bavor, H. J., Chazarenc, F., & Mander, Ü. (2011). Filter materials for phosphorus removal from wastewater in treatment wetlands-A review. *Ecological Engineering, 37*(1), 70-89.

Vymazal, J. (Ed.), 2011. Water and nutrient management in natural and constructed wetlands. Netherlands, Dordrecht: Springer.

Warmadewanthi, & Liu, J. C. (2009). Selective precipitation of phosphate from semiconductor wastewater. *Journal of Environmental Engineering, 135*(10), 1063-1070.

Whitelaw, M. A. (1999). Growth promotion of plants inoculated with phosphate-solubilizing fungi. In: Sparks, D.L., Advances in Agronomy. Academic Press, 99-151.

Xu, X., Li, Q., Cui, H., Pang, J., Sun, L., An, H., & Zhai, J. (2011). Adsorption of fluoride from aqueous solution on magnesia-loaded fly ash cenospheres. *Desalination, 272*(1-3), 233-239.

Yamada, H., Kayama, M., Saito, K., & Hara, M. (1986). A fundamental research on phosphate removal by using slag. *Water Research, 20*(5), 547-557.

Yang, M., Zhang, Y., Shao, B., Qi, R., & Myoga, H. (2001). Precipitative removal of fluoride from electronics wastewater. *Journal of Environmental Engineering, 127*(10), 902-907.

Yehia, A., & Ezzat, K. (2009). Fluoride ion uptake by synthetic apatites. *Adsorption Science and Technology, 27*(3), 337-347.

Zhou, Y. F., & Haynes, R. J. (2010). Sorption of heavy metals by inorganic and organic components of solid wastes: Significance to use of wastes as low-cost adsorbents and immobilizing agents. *Critical Reviews in Environmental Science and Technology, 40*(11), 909-977.